

SYNTHESIS AND PHYSICO-CHEMICAL
CHARACTERIZATION OF pH-SENSITIVE HYDROGELS
AND THEIR APPLICATIONS IN DRUG DELIVERY

SHAHID BASHIR

FACULTY OF SCIENCE
UNIVERSITY OF MALAYA
KUALA LUMPUR

2017

**SYNTHESIS AND PHYSICO-CHEMICAL
CHARACTERIZATION OF pH-SENSITIVE
HYDROGELS AND THEIR APPLICATIONS IN DRUG
DELIVERY**

SHAHID BASHIR

**THESIS SUBMITTED IN FULFILMENT OF THE
REQUIREMENTS FOR THE DEGREE OF
PHILOSOPHY**

**DEPARTMENT OF CHEMISTRY
FACULTY OF SCIENCE
UNIVERSITY OF MALAYA
KUALA LUMPUR**

2017

UNIVERSITY OF MALAYA

ORIGINAL LITERARY WORK DECLARATION

Name of Candidate: Shahid Bashir

Registration/Matric No: SHC130112

Name of Degree: DOCTOR OF PHILOSOPHY

Title of Project "Thesis": Synthesis and Physico-chemical characterization of pH-sensitive hydrogels and their applications in drug delivery

Field of Study: Physical Chemistry

I do solemnly and sincerely declare that:

- (1) I am the sole author/writer of this Work;
- (2) This Work is original;
- (3) Any use of any work in which copyright exists was done by way of fair dealing and for permitted purposes and any excerpt or extract from, or reference to or reproduction of any copyright work has been disclosed expressly and sufficiently and the title of the Work and its authorship have been acknowledged in this Work;
- (4) I do not have any actual knowledge nor do I ought reasonably to know that the making of this work constitutes an infringement of any copyright work;
- (5) I hereby assign all and every rights in the copyright to this Work to the University of Malaya ("UM"), who henceforth shall be owner of the copyright in this Work and that any reproduction or use in any form or by any means whatsoever is prohibited without the written consent of UM having been first had and obtained;
- (6) I am fully aware that if in the course of making this Work I have infringed any copyright whether intentionally or otherwise, I may be subject to legal action or any other action as may be determined by UM.

Candidate's Signature

Date:

Subscribed and solemnly declared before,

Witness's Signature

Date:

Name:

Designation:

ABSTRACT

Environmentally sensitive hydrogels have been investigated as smart drug delivery systems capable to release drug at the appropriate time and site of action. In the present work, N-succinyl chitosan was prepared by modification of chitosan using succinic anhydride in acetic acid/methanol solution. Then, pH-sensitive semi-interpenetrating network hydrogels of N-succinyl chitosan/ poly (acrylamide-co-acrylic acid) were prepared by crosslinking of N-succinyl-chitosan and poly (acrylamide-co-acrylic acid) via Schiff base mechanism using glutaraldehyde as a crosslinking agent. On the other hand, N-succinyl chitosan-g-poly (acrylamide-co-acrylic acid), N-succinyl chitosan-g-poly (acrylic acid), N-succinyl chitosan-g-poly (methacrylic acid), and Karaya gum-g-poly (acrylic acid) hydrogels were prepared using ammonium persulfate as an initiator and N, N'-methylenebisacrylamide as a crosslinking agent, through free radical mechanism. The successful of the synthesis of hydrogels were confirmed by their physico-chemical characterization using Fourier transform infrared analysis, X-ray diffraction analysis, and differential scanning calorimetric analysis. The surface morphology of hydrogels was observed under field emission scanning electron microscope and suggests the highly porous network structures of the synthesized hydrogels. The yield (%), gel contents (%), and gel time was observed which was dependent on the hydrogels composition. The rheology study was performed to measure the mechanical strength. Moreover, swelling study revealed that hydrogels were highly swellable and depended on the hydrogel composition, pH, type and concentration of salt solutions. Swelling kinetics was evaluated and swelling ratio of hydrogels followed non-linear second order rate equation. Encapsulation efficiency of the hydrophilic 5-fluorouracil (5-FU) in N-succinyl chitosan/ poly (acrylamide-co- acrylic acid) and theophylline in N-succinyl chitosan-g-poly (acrylamide-co- acrylic acid), N-succinyl chitosan-g-poly (acrylic acid), N-succinyl chitosan-g-poly (methacrylic acid) hydrogels

was found to be 72.45 ± 0.06 %, 88.0 ± 0.2 %, 0.88 ± 0.3 and 90.0 ± 0.2 %, respectively. Moreover, the maximum encapsulation efficiency of quercetin was found to be 88.0 ± 0.03 %. The maximum in vitro release of drugs from these hydrogels was found to be 86.0 ± 0.2 %, 93.0 ± 0.03 %, 87.3 ± 0.09 %, 89.5 ± 0.15 %, and 83.0 ± 0.14 %, respectively at pH 7.4. The drug release from the hydrogels at pH 1.2 was found to be 18.3 ± 0.06 %, 24.0 ± 0.1 %, 12.5 ± 0.09 %, 13.2 ± 0.1 %, and 19.0 ± 0.14 %, respectively. Furthermore, the drug release kinetics followed non-Fickian to non-Fickian anomalous (case-II) transport. The chemical activity of the pure drugs and after in vitro release was found and results revealed that drugs maintained their chemical activity after in vitro release. According to the observed facts, synthesized hydrogels can be adapted for their prospective exploitation in targeted drug delivery applications.

ABSTRAK

Hidrogel sensitif alam sekitar telah disiasat sebagai sistem penyampaian ubat pintar yang mampu untuk melepaskan ubat pada masa dan tapak tindakan yang sesuai. Dalam kajian ini, N-suksinil kitosan telah disediakan dengan oleh pengubahsuaian kitosan menggunakan asetik succinic dalam larutan asid / metanol asetik. Kemudian, hidrogel sensitif terhadap pH jaringan separuh salingtembus N-suksinil kitosan/ poli (asid akrilamid-co-akrilik) telah disediakan oleh ikatan silang daripada (asid akrilamid-co-akrilik) N-suksinil-kitosan dan poli melalui mekanisme asas Schiff menggunakan glutaraldehid sebagai ejen ikatan silang. Sebaliknya, hidrogel N-suksinil kitosan-g-poli (asid akrilamid-co-akrilik), hidrogel N-suksinil kitosan-g-poli (asid akrilik), hidrogel N-suksinil kitosan-g-poli (asid metakrilik), dan hidrogel gam Karaya-g-poli (asid akrilik) telah disediakan dengan menggunakan ammonium persulfat sebagai pemula dan N, n'-methylenebisakrilamid sebagai ejen ikatan silang, melalui mekanisme radikal bebas. Kejayaan sintesis hidrogel-hidrogel telah disahkan melalui oleh pencirian fiziko-kimia menggunakan analisis jelmaan fourier inframerah, analisis pembelauan sinar-X, analisis, dan analisis imbasan pengkamiran kalorimetri. Morfologi permukaan hidrogel-hidrogel telah diperhatikan di bawah bidang imbasan pancaran elektron mikroskop dan mencadangkan hidrogel-hidrogel tersebut mempunyai struktur jaringan yang sangat berliang. hasil (%), jumlah gel (%), dan masa gel diperhatikan yang bergantung kepada komposisi hidrogel-hidrogel tersebut. Kajian reologi telah dilakukan untuk mengukur kekuatan mekanikal. Lebih-lebih lagi, kajian pembengkakan mendedahkan bahawa hidrogel-hidrogel adalah sangat membengkak dan bergantung kepada komposisi hidrogel, pH, jenis dan kepekatan larutan garam. Kinetik bengkak telah dinilai dan nisbah bengkak hidrogel-hidrogel mengikuti persamaan bukan lurus kadar tertib kedua. Kecekapan pengkapsulan daripada hidrofilik 5-fluorouracil (5-FU) dalam N-suksinil kitosan/ Poli (akrilamida -bersama asid akrilik) dan teofilin dalam hidrogel N-suksinil kitosan-g-poli (akrilamid-co-asid akrilik), hidrogel N-succinyl kitosan-

g-poli (asid akrilik), dan hidrogel N-suksinil kitosan-g-poli (asid metakrilik) masing-masing didapati sebanyak $72.45 \pm 0.06 \%$, $88.0 \pm 0.2 \%$, $0.88 \pm 0.3 \%$, dan $90.0 \pm 0.2 \%$. Selain itu, kecekapan pengkapsulan maksimum quercetin didapati sebanyak $88.0 \pm 0.03 \%$. Maksimum ubat-ubatan perlepasan di dalam kaca daripada hidrogel-hidrogel pada pH 7.4 didapati masing-masing sebanyak $86.0 \pm 0.2 \%$, $93.0 \pm 0.03 \%$, $87.3 \pm 0.09 \%$, $89.5 \pm 0.15 \%$, dan $83.0 \pm 0.14 \%$. Perlepasan ubat-ubatan daripada hidrogel-hidrogel pada pH 1.2 masing-masing didapati $18.3 \pm 0.06 \%$, $24.0 \pm 0.1 \%$, $12.5 \pm 0.09 \%$, $13.2 \pm 0.1 \%$, dan $19.0 \pm 0.14 \%$. Tambahan pula, kinetik pelepasan ubat mengikuti pengangkutan bukan Fickian kepada bukan Fickian ganjil (kes II). Aktiviti kimia ubat-ubatan tulen dan selepas pelepasan di dalam kaca ditemui dan keputusan mendedahkan bahawa ubat-ubatan selepas pelepasan di dalam kaca mengekalkan aktiviti kimia mereka. Merujuk kepada fakta yang telah didapati, hidrogel-hidrogel yang telah disintesis boleh disesuaikan untuk pengeksploitasian dalam aplikasi penyampaian ubat yang disasarkan.

ACKNOWLEDGEMENTS

All praises to **ALLAH almighty**, the creator, sustainer, merciful and beneficent, who granted me with knowledge, courage and strength to accomplish this task. All the respects and dorood for **Prophet Muhammad (ﷺ)**, whose teachings enlightened me with the light of true believe in **ALLAH**.

I would like to pay humble gratitude to my respected supervisors **Professor Dr. Ramesh T. Subramaniam, Dr. Teo Yin Yin, Associate Professor Dr. Ramesh Kasi, and Professor Dr. Amir Azam Khan** for nourishing me with innovative ideas and guidance throughout the project. They provided me with the right balance of freedom and direction to make the project well defined, yet flexible enough to allow for a free ranging, interdisciplinary body of work to evolve. I extend my heartfelt respect for their unflagging encouragement and diligent supervision. Their co-operative amiable nature is indeed exemplary.

My special thanks are also to Head and all the Faculty of Department of Chemistry and Physics, especially **Professor Misni Misran** for providing lab facilities.

I have many thanks for my lab fellows and friends for cooperation and providing enjoyable moments especially **Prema, Farhanim, Nurshafiq, Dr. Muhammad Adil Mansoor, Dr Javed Iqbal, Dr. Yugal Kishor Mahipal, Muhammad Rizwan, Numan Arshid, Fatin, Sumaira Naeem, Lim, Ms Chong, Syed Tawab Shah, Shahid Mehmood, Saif UR Rehman, Raja Sehrab Bashir, Raja Wasim Ahmad, and Umar Draz**.

I gratefully acknowledge the funding sources, High Impact Research (**HIR**) grant and University of Malaya Research Grant (**UMRG**) that made my Ph.D work possible.

Finally would pay my heartiest gratitude to the most precious and divine relations of life, my ideal my father **Bashir Ahmad (Late)**, my beloved and kind mother, my sweet brothers and kind sisters, their husbands, and all their pretty kids for their unflagging love, numerous sacrifices and support throughout my life and their thoughts and prayers gave me strength and motivation with positive energy to prosper myself in the life. In the end, I acknowledge the role of those important characters whose names could not be displayed in the words but will always remain in my memories.

Shahid Bashir

May 01, 2017

TABLE OF CONTENTS

ABSTRACT.....	iii
ABSTRAK.....	v
ACKNOWLEDGEMENTS.....	vii
TABLE OF CONTENTS.....	viii
LIST OF FIGURES.....	xviii
LIST OF TABLES.....	xxv
LIST OF SYMBOLS AND ABBREVIATIONS.....	xxvii
CHAPTER 1: INTRODUCTION.....	1
1.1 Introduction of Hydrogels	1
1.2 Composition of Hydrogels.....	2
1.3 Types of Hydrogels	3
1.4 Properties of Hydrogels	4
1.5 Biomedical Applications	5
1.5.1 Hydrogels in Contact lens Applications	5
1.5.2 Hydrogels in Drug Delivery Applications	6
1.5.3 Hydrogels in Conductive Biomedical Applications	7
1.5.4 Hydrogels in Tissue Engineering Applications	8

1.6	Objectives	8
1.7	Thesis Outlines	8
CHAPTER 2: LITERATURE REVIEW.....		10
2.1	Natural Polymer Hydrogels	10
2.1.1	Polysaccharide Hydrogels.....	10
2.1.2	Chitosan	11
2.1.2.1	Chitosan Based Hydrogels	12
2.1.2.2	Limitations of Chitosan.....	12
2.1.2.3	Modification of Chitosan	13
2.1.2.4	Acylation.....	16
2.1.2.5	N-Succinyl chitosan.....	18
2.1.2.6	N-Succinyl chitosan Based Hydrogel	19
2.1.3	Karaya gum Hydrogels	23
2.1.4	Synthetic Polymer Hydrogels	24
2.1.4.1	Hydrogels Based on Poly (acrylic acid) derivatives.....	25
2.1.4.2	Hydrogels Based on Poly (acrylamide) derivatives.....	26
2.1.5	Natural Polymers in Combination with Synthetic Polymer Hydrogels.....	28
2.1.6	Types of Hydrogels.....	30
2.1.6.1	Physical Hydrogels	30
2.1.6.2	Chemical Hydrogels.....	32

(a)	Crosslinking by Small molecules	32
(b)	Crosslinking through Ionizing radiation.....	33
(c)	Crosslinking through Free radical Mechanism.....	38
2.1.6.3	Interpenetrating Network (IPN) Hydrogel	41
(a)	Semi-Interpenetrating Network (semi-IPN) Hydrogels	42
(b)	Full-Interpenetrating Network (Full-IPN) Hydrogels	45
2.1.7	Properties of Hydrogels	48
2.1.7.1	Mechanical Properties.....	48
2.1.7.2	Biocompatibility.....	52
2.1.7.3	Biodegradability.....	54
2.1.7.4	Swelling Behavior of Hydrogel	56
(a)	Swelling Kinetics.....	57
2.1.7.5	Stimuli sensitive Hydrogels	58
(a)	pH-sensitive Hydrogels	59
(b)	Thermosensitive Hydrogels.....	60
2.1.8	Drug Loading and Encapsulation Efficiency	62
2.1.9	Drug Release and Release Kinetics	63
(a)	Swelling Controlled Systems.....	65
(b)	Empirical Model.....	66
(c)	Mechanistic Models.....	67
2.1.10	Model Drugs	68

CHAPTER 3: MATERIALS AND METHODS	73
3.1 Introduction to Materials and Methods	73
3.2 Materials	73
3.3 Methods	74
3.3.1 Synthesis of N-succinyl chitosan.....	74
3.3.1.1 Degree of Substitution (DS).....	74
3.3.2 Synthesis of N-succinyl chitosan/ poly (acrylamide-co-acrylic acid) Hydrogels via Schiff base Mechanism	75
3.3.3 Synthesis of N-succinyl chitosan-g-poly (acrylamide-co-acrylic acid) Hydrogels via Free radical Mechanism	76
3.3.4 Synthesis of N-succinyl chitosan-g-poly (acrylic acid) Hydrogels via Free radical Mechanism	76
3.3.5 Synthesis of N-succinyl chitosan-g-poly (methacrylic acid) Hydrogels via Free radical Mechanism	77
3.3.6 Synthesis of Karaya gum-g-poly (acrylic acid) Hydrogels via Free radical Mechanism.....	78
3.4 Characterization of the Hydrogels	79
3.4.1 Fourier Transform Infrared (FTIR) Analysis.....	79
3.4.2 X-ray Diffraction (XRD) Analysis	80
3.4.3 Differential Scanning Calorimetry (DSC) Analysis	81

3.4.4	Field Emission Scanning Electron Microscopy (FESEM) Analysis	83
3.4.5	Determination of Yield (%), Gel contents (%), and Gel time of the Hydrogels.....	84
3.5	Properties of Hydrogels	85
3.5.1	Mechanical Properties.....	85
3.5.2	Swelling Ratio.....	86
3.5.2.1	Swelling Kinetics	87
3.5.2.2	Salinity and Swelling Ratio.....	87
3.6	Encapsulation Efficiency.....	88
3.7	In Vitro Drug Release.....	89
3.7.1	Drug Release Kinetics	90
3.7.2	Chemical Activity of the Drugs	90
CHAPTER 4: RESULTS AND DISCUSSION		91
4.1	Synthesis.....	91
4.1.1	Synthesis of N-succinyl chitosan and Degree of Substitution.....	91
4.1.2	Synthesis of N-succinyl chitosan/ poly (acrylamide-co-acrylic acid) Hydrogels.....	91
4.1.3	Synthesis of N-succinyl chitosan-g-poly (acrylamide-co-acrylic acid) Hydrogels.....	92

4.1.4	Synthesis of N-succinyl chitosan-g-poly (acrylic acid)	
	Hydrogels.....	93
4.1.5	Synthesis of N-succinyl chitosan-g-poly (methacrylic acid)	
	Hydrogels.....	96
4.1.6	Synthesis of Karaya gum-g-poly (acrylic acid) Hydrogels	96
4.2	Characterization.....	99
4.2.1	Fourier Transform Infrared Analysis	99
4.2.1.1	Starting Materials.....	99
4.2.1.2	Hydrogels	104
	(a) N-succinyl chitosan/ poly (acrylamide-co-acrylic acid)	
	Hydrogel	104
	(b) N-succinyl chitosan-g-poly (acrylamide-co-acrylic acid) Hydrogel.....	106
	(c) N-succinyl chitosan-g-poly (acrylic acid) Hydrogel	107
	(d) N-succinyl chitosan-g-poly (methacrylic acid) Hydrogel	108
	(e) Karaya gum-g-poly (acrylic acid) Hydrogel	109
4.2.2	X-ray Diffraction Analysis	111
4.2.2.1	Chitosan and N-succinyl chitosan.....	111
4.2.2.2	N-succinyl chitosan/ poly (acrylamide-co-acrylic acid) Hydrogel	112

4.2.2.3 N-succinyl chitosan-g-poly (acrylamide-co-acrylic acid)	
Hydrogel	112
4.2.2.4 N-succinyl chitosan-g-poly (acrylic acid) Hydrogel.....	113
4.2.2.5 N-succinyl chitosan-g-poly (methacrylic acid) Hydrogel.....	113
4.2.2.6 Karaya gum-g-poly (acrylic acid) Hydrogel.....	115
4.2.3 Differential Scanning Calorimetry Analysis.....	116
4.2.3.1 Chitosan and N-succinyl chitosan.....	116
4.2.3.2 N-succinyl chitosan/ poly (acrylamide-co-acrylic acid)	
Hydrogel	117
4.2.3.3 N-succinyl chitosan-g-poly (acrylamide-co-acrylic acid)	
Hydrogel	118
4.2.3.4 N-succinyl chitosan-g-poly (acrylic acid) Hydrogel.....	118
4.2.3.5 N-succinyl chitosan-g-poly (methacrylic acid) Hydrogel.....	119
4.2.3.6 Karaya gum-g-poly (acrylic acid) Hydrogel	120
4.2.4 Morphology	122
4.2.4.1 N-succinyl chitosan/ poly (acrylamide-co-acrylic acid)	
Hydrogels	122
4.2.4.2 N-succinyl chitosan-g-poly (acrylamide-co-acrylic acid)	
Hydrogels	123
4.2.4.3 N-succinyl chitosan-g-poly (acrylic acid) Hydrogels	124
4.2.4.4 N-succinyl chitosan-g-poly (methacrylic acid) Hydrogels	125
4.2.4.5 Karaya gum-g-poly (acrylic acid) Hydrogels	126

4.2.5	Yield (%), Gel contents (%), and Gel time of the Hydrogels	127
4.3	Properties of Hydrogels	131
4.3.1	Mechanical Properties.....	131
4.3.1.1	Mechanical Properties of N-succinyl chitosan/ poly (acrylamide-co-acrylic acid) Hydrogels.....	131
(a)	Strain Amplitude Test.....	131
(b)	Frequency Sweep Test.....	133
4.3.2	Mechanical Properties of Hydrogels Formed through Free radical Mechanism.....	134
(a)	Amplitude Sweep Test.....	134
(b)	Frequency Sweep Test.....	136
4.3.3	Swelling Ratio.....	142
4.3.3.1	Swelling Ratio of N-succinyl chitosan/ poly (acrylamide-co- acrylic acid) Hydrogels	142
4.3.3.2	Swelling Ratio of Hydrogels Formed through Free radical Mechanism.....	144
(a)	Swelling Ratio of Hydrogels in Water	144
(b)	Swelling Ratio of Hydrogels in Buffer Solutions.....	146
4.3.3.3	Swelling Ratio of Hydrogels in Salt Solutions	151
4.3.3.4	Swelling Kinetics	154
(a)	Swelling Kinetics of N-succinyl chitosan/ poly (acrylamide-co-acrylic acid) Hydrogels.....	154

(b)	Swelling Kinetics of Hydrogels Formed through Free radical Mechanism.....	157
4.4	Drug Encapsulation Efficiency of Hydrogels.....	160
4.4.1	Encapsulation Efficiency of N-succinyl chitosan/ poly (acrylamide-co-acrylic acid) Hydrogels	160
4.4.2	Encapsulation Efficiency of Hydrogels Formed through Free radical Mechanism.....	161
4.5	In Vitro Drug Release.....	163
4.5.1	In Vitro Drug Release from N-succinyl chitosan/ poly (acrylamide-co-acrylic acid) Hydrogels	163
4.5.2	In Vitro Drug Release from Hydrogels Formed through Free radical Mechanism.....	165
4.5.3	Drug Release Kinetics	172
4.5.3.1	Drug Release Kinetics of N-succinyl chitosan/ poly (acrylamide-co-acrylic acid) Hydrogels.....	172
4.5.3.2	Drug Release Kinetics of Hydrogels Formed through Free radical Mechanism.....	173
4.5.4	Chemical Activity of Drugs.....	177
CHAPTER 5: CONCLUSION AND FUTURE WORK		181
5.1	Conclusion.....	181
5.2	Future Work.....	184

REFERENCES..... 186

LIST OF PUBLICATIONS AND PAPERS PRESENTED 210

University of Malaya

LIST OF FIGURES

Figure 2.1: Structure of Chitin and chitosan.....	12
Figure 2.2: Various modifications of chitosan.....	14
Figure 2.3: N-acylation of chitosan	17
Figure 2.4: Synthesis of N-Succinyl chitosan (Yan et al., 2006).....	19
Figure 2.5: Synthetic scheme of NSC/OCMC (Lü et al., 2010).....	20
Figure 2.6: The plausible mechanism of carboxymethyl cellulose-g-poly (acrylamide-co-acrylic acid-co-2-acrylamido-2-methyl-1-propanesulfonic acid (AMPS)/montmorillonite (MMT)) hydrogel synthesis (Bao et al., 2011).....	40
Figure 2.7: Proposed reaction mechanism of IPN formation a) simultaneous strategy; b) sequential strategy; c) selective crosslinking of a linear polymer entrapped in semi-IPN (Dragan, 2014)	42
Figure 2.8: The proposed reaction mechanism of semi-IPN hydrogel of chitosan/ acrylamide-g-hydroxyethyl cellulose (Angadi et al., 2010)	43
Figure 2.9: Structure of drugs a) 5-fluorouracil, b) theophylline, and c) quercetin.....	71
Figure 4.1: Synthesis of N-succinyl chitosan from chitosan	91
Figure 4.2: The proposed reaction mechanism of Schiff base crosslinking of N-succinyl chitosan and formation of semi-IPN through embedding of poly (acrylamide-co-acrylic acid) in N-succinyl chitosan network	92

Figure 4.3: The proposed reaction mechanism of N-succinyl chitosan-g-poly (acrylamide-co-acrylic acid).....	94
Figure 4.4: The proposed reaction mechanism of synthesis of N-succinyl chitosan-g-poly (acrylic acid).....	95
Figure 4.5: The proposed reaction mechanism of synthesis of N-succinyl chitosan-g-poly (methacrylic acid).....	97
Figure 4.6: The proposed reaction mechanism of karaya gum-g-poly (acrylic acid).....	98
Figure 4.7: FTIR spectra of a) Chitosan, b) N-succinyl chitosan	100
Figure 4.8: FTIR spectra of a) poly (acrylamide-co-acrylic acid), b) acrylic acid, c) acrylamide, and d) methacrylic acid	102
Figure 4.9: FTIR spectrum of karaya gum.....	103
Figure 4.10: FTIR spectra of a) 5-Fluorouracil, b) theophylline, and c) quercetin	104
Figure 4.11: FTIR spectra of a) Chitosan, b) N-succinyl chitosan, c) poly (acrylamide-co-acrylic acid), d) SP2 formulation of N-succinyl chitosan/ poly (acrylamide-co-acrylic acid) hydrogel, e) 5-FU, and f) 5-FU loaded N-succinyl chitosan/ poly (acrylamide-co-acrylic acid) hydrogel	105
Figure 4.12: FTIR spectra of a) Chitosan, b) N-succinyl chitosan, c) NAA1 formulation of N-succinyl chitosan-g-poly (acrylamide-co-acrylic acid) hydrogel, d) theophylline, and e) theophylline loaded N-succinyl chitosan-g-poly (acrylamide-co-acrylic acid) hydrogel	106

Figure 4.13: FTIR spectra of a) Chitosan, b) N-succinyl chitosan, c) acrylic acid, d) NSA1 formulation of N-succinyl chitosan-g-poly (acrylic acid) hydrogel, e) theophylline, and f) theophylline loaded N-succinyl chitosan-g-poly (acrylic acid) hydrogel	107
Figure 4.14: FTIR spectra of a) Chitosan, b) N-succinyl chitosan, c) methacrylic acid, d) NSM1 formulation of N-succinyl chitosan-g-poly (methacrylic acid) hydrogel, e) theophylline, and f) theophylline loaded N-succinyl chitosan-g-poly (methacrylic acid) hydrogel	109
Figure 4.15: FTIR spectra of a) karaya gum, b) acrylic acid, c) KGA1 formulation of karaya gum-g-poly (acrylic acid) hydrogel, d) quercetin, and e) quercetin loaded karaya gum-g-poly (acrylic acid) hydrogel	110
Figure 4.16: XRD spectra of a) Chitosan, b) N-succinyl chitosan	112
Figure 4.17: XRD spectra of a) SP2 formulation of N-succinyl chitosan/ poly (acrylamide-co-acrylic acid) hydrogel, b) NAA1 formulation of N-succinyl chitosan-g-poly (acrylamide-co-acrylic acid) hydrogel, c) NSA1 formulation of N-succinyl chitosan-g-poly (acrylic acid) hydrogel, and d) NSM1 formulation of N-succinyl chitosan-g-poly (methacrylic acid) hydrogel	114
Figure 4.18: XRD spectra of a) karaya gum, b) KGA1 formulation of karaya gum-g-poly (acrylic acid) hydrogel	115
Figure 4.19: DSC thermograms of a) Chitosan and b) N-succinyl chitosan	117
Figure 4.20: DSC thermograms of a) SP2 formulation of N-succinyl chitosan/ poly (acrylamide-co-acrylic acid), b) NAA1 formulation of N-succinyl	

chitosan-g-poly (acrylamide-co-acrylic acid), c) NSA1 formulation of N-succinyl chitosan-g-poly (acrylic acid), d) NSM1 formulation of N-succinyl chitosan-g-poly (methacrylic acid) hydrogels	119
Figure 4.21: DSC thermograms of a) karaya gum, and b) KGA1 formulation of karaya gum-g-poly (acrylic acid) hydrogel.....	121
Figure 4.22: Micrographs of a) SP1, b) SP2, c) SP3, and d) SP7 hydrogel.....	123
Figure 4.23: Micrographs of a) NAA1 and b) NAA3 hydrogels.....	124
Figure 4.24: Micrographs of a) NSA1) and b) NSA3 hydrogels.....	125
Figure 4.25: Micrographs of a) NSM1 and b) NSM3 hydrogels.....	126
Figure 4.26: Micrographs of a) KGA1 and b) KGA3 hydrogels.....	127
Figure 4.27: Yield (%), gel contents (%), and gel time of synthesized N-succinyl chitosan-g-poly (acrylamide-co-acrylic acid) hydrogels	129
Figure 4.28: Yield (%), gel contents (%), and gel time of synthesized N-succinyl chitosan-g-poly (acrylic acid) hydrogels.....	129
Figure 4.29: Yield (%), gel contents (%), and gel time of synthesized N-succinyl chitosan-g-poly (methacrylic acid) hydrogels.....	130
Figure 4.30: Yield (%), gel contents (%), and gel time of synthesized karaya gum-g-poly (acrylic acid) hydrogels.....	130
Figure 4.31: Strain amplitude test of all SP hydrogels (N-succinyl chitosan/ poly (acrylamide-co-acrylic acid) hydrogels).....	132

Figure 4.32: Frequency sweep test of all SP hydrogels (N-succinyl chitosan/ poly (acrylamide-co-acrylic acid) hydrogels).....	132
Figure 4.33: Strain amplitude test of N-succinyl chitosan-g-poly (acrylamide-co-acrylic acid) hydrogels	135
Figure 4.34: Strain amplitude test of N-succinyl chitosan-g-poly (acrylic acid) hydrogels.....	135
Figure 4.35: Strain amplitude test of N-succinyl chitosan-g-poly (methacrylic acid) hydrogels.....	136
Figure 4.36: Strain amplitude test of karaya gum-g-poly (acrylic acid) hydrogels	136
Figure 4.37: Frequency sweep test of N-succinyl chitosan-g-poly (acrylamide-co-acrylic acid) hydrogels.....	140
Figure 4.38: Frequency sweep test of N-succinyl chitosan-g-poly (acrylic acid) hydrogels.....	141
Figure 4.39: Frequency sweep test of N-succinyl chitosan-g-poly (methacrylic acid) hydrogels.....	141
Figure 4.40: Frequency sweep test of karaya gum-g-poly (acrylic acid) hydrogels.....	142
Figure 4.41: Swelling ratios of N-succinyl chitosan/ poly (acrylamide-co-acrylic acid) hydrogels at a) pH 7.4, b) pH 1.2.....	144
Figure 4.42: Swelling ratio of N-succinyl chitosan-g-poly (acrylamide-co-acrylic acid) hydrogels in a) water, b) pH 7.4, and c) pH 1.2.....	149

Figure 4.43: Swelling ratio of N-succinyl chitosan-g-poly (acrylic acid) hydrogels in a) water, b) pH 7.4, and c) pH 1.2.....	149
Figure 4.44: Swelling ratio of N-succinyl chitosan-g-poly (methacrylic acid) hydrogels in a) water, b) pH 7.4, and c) pH 1.2.....	150
Figure 4.45: Swelling ratio of karaya gum-g-poly (acrylic acid) hydrogels in a) water, b) pH 7.4, and c) pH 1.2.....	150
Figure 4.46: Effect of ionic strength of salt solutions on swelling ratio of SP1 (N-succinyl chitosan/ poly (acrylamide-co-acrylic acid) hydrogel).....	152
Figure 4.47: Effect of ionic strength of salt solutions on swelling ratio of NAA1 (N-succinyl chitosan-g-poly (acrylamide-co-acrylic acid) hydrogel)	152
Figure 4.48: Effect of ionic strength of salt solutions on swelling ratio of NSA1 (N-succinyl chitosan-g-poly (acrylic acid) hydrogel)	153
Figure 4.49: Effect of ionic strength of salt solutions on swelling ratio of NSM1 (N-succinyl chitosan-g-poly (methacrylic acid) hydrogel)	153
Figure 4.50: Effect of ionic strength of salt solutions on swelling ratio of KGA1 (Karaya gum-g-poly (acrylic acid) hydrogel)	154
Figure 4.51: Drug release of 5-Fu from N-succinyl chitosan/ poly (acrylamide-co-acrylic acid) hydrogels at pH 7.4 and pH 1.2.....	165
Figure 4.52: In vitro release of theophylline from N-succinyl chitosan-g-poly (acrylamide-co-acrylic acid) hydrogels at pH 7.4 and pH 1.2	170

Figure 4.53: In vitro release of theophylline from N-succinyl chitosan-g-poly (acrylic acid) hydrogels at pH 7.4 and pH 1.2	170
Figure 4.54: In vitro release of theophylline from N-succinyl chitosan-g-poly (methacrylic acid) hydrogels at pH 7.4 and pH 1.2	171
Figure 4.55: In vitro release of quercetin from karaya gum-g-poly (acrylic acid) hydrogels at pH 7.4 and pH 1.2	171
Figure 4.56: Chemical activity of pure 5-FU and 5-FU after release from N-succinyl chitosan/ poly (acrylamide-co-acrylic acid) hydrogel	178
Figure 4.57: Chemical activity of pure theophylline and theophylline after release from N-succinyl chitosan-g-poly (acrylamide-co-acrylic acid) hydrogel	179
Figure 4.58: Chemical activity of pure theophylline and theophylline after release from N-succinyl chitosan-g-poly (acrylic acid) hydrogel.....	179
Figure 4.59: Chemical activity of pure theophylline and theophylline after release from N-succinyl chitosan-g-poly (methacrylic acid) hydrogel.....	180
Figure 4.60: Chemical activity of pure quercetin and quercetin after release from karaya gum-g-poly (acrylic acid) hydrogel.....	180

LIST OF TABLES

Table 2.1: Chitosan modification methods and examples of each modified chitosan	15
Table 2.2: NSC-based hydrogel formulations and preparation techniques.....	21
Table 2.3: Crosslinking of polymers through small molecules and light sensitive functional groups.....	35
Table 2.4: Crosslinking of polymers through reactive functional groups.....	37
Table 3.1: Synthesis scheme of formulations of N-succinyl chitosan/ poly (acrylamide-co-acrylic acid) hydrogels	75
Table 3.2: Synthesis scheme of formulations of N-succinyl chitosan-g-poly (acrylamide-co-acrylic acid) of hydrogels	76
Table 3.3: Synthesis scheme of formulations of N-succinyl chitosan-g-poly (acrylic acid) of hydrogels.....	77
Table 3.4: Synthesis scheme of formulations of N-succinyl chitosan-g-poly (methacrylic acid) of hydrogels.....	78
Table 3.5: Synthesis scheme of formulations of karaya gum-g-poly (acrylic acid) of hydrogels.....	79
Table 4.1: Crystalline melting temperature (T_m) of endothermic curves, peak temperature (T_p) of exothermic curves, and enthalpy change (ΔH) of chitosan, N-succinyl chitosan, karaya gum and N-succinyl chitosan-g-poly (acrylamide-co-acrylic acid), N-succinyl chitosan-g-poly (acrylic acid), N-	

succinyl chitosan-g-poly (methacrylic acid), and karaya gum-g-poly (acrylic acid) hydrogels	120
Table 4.2: Swelling kinetics at pH 7.4 and pH 1.2 ((N-succinyl chitosan/ poly (acrylamide-co-acrylic acid) hydrogels)	156
Table 4.3: Swelling kinetics in water, pH 7.4 and pH 1.2 (N-succinyl chitosan-g-poly (acrylamide-co-acrylic acid) hydrogels)	158
Table 4.4: Swelling kinetics in water, pH 7.4 and pH 1.2 (N-succinyl chitosan-g-poly (acrylic acid) hydrogels).....	158
Table 4.5: Swelling kinetics in water, pH 7.4 and pH 1.2 (N-succinyl chitosan-g-poly (methacrylic acid) hydrogels).....	159
Table 4.6: 5-FU encapsulation efficiency of N-succinyl chitosan/ poly (acrylamide-co-acrylic acid) hydrogels	160
Table 4.7: 5-FU release kinetics at pH 7.4/ pH 1.2	173
Table 4.8: Theophylline release kinetics at pH 7.4 and pH 1.2 (N-succinyl chitosan-g-poly (acrylamide-co-acrylic acid) hydrogels)	176
Table 4.9: Theophylline release kinetics at pH 7.4 and pH 1.2 (N-succinyl chitosan-g-poly (acrylic acid) hydrogels)	176
Table 4.10: Theophylline release kinetics at pH 7.4/pH 1.2 (N-succinyl chitosan-g-poly (methacrylic acid) hydrogels).....	176
Table 4.11: Quercetin release kinetics in pH 7.4/pH 1.2 (Karaya gum-g-poly (acrylic acid) hydrogels).....	177

LIST OF SYMBOLS AND ABBREVIATIONS

5-ASA	5-Aminosalicylic acid
AAM	Acrylamide
AA	Acrylic acid
APS	Ammonium persulfate
AIBN	2,2'-Azobisisobutyronitrile
BMA	Butyl methacrylate
EPA	Environmental protection agency
ESR	Equilibrium swelling ratio
DMSO	Dimethyl sulfoxide
EGDMA	Ethylene glycol dimethacrylate
FDA	Food and drug administration
HPN	Hybrid polymeric networks
IPN	Interpenetrating polymer network
LCST	Lower critical solution temperature
LVR	Linear viscoelastic region
GI	Gastrointestinal
GA	Glutaraldehyde

g	graft
MBA	N, N'-methylene bisacrylamide
NSC	N-succinyl chitosan
OCMC	O-carboxymethyl cellulose
PAAm	Poly (acrylamide)
PAA	Poly (acrylic acid)
PEG	Poly (ethylene glycol)
PEO	Poly (ethylene oxide)
PHEMA	Poly(2-hydroxethyl methacrylate)
PLA	Poly (lactic acid)
PMAA	Poly (methacrylic acid)
PNDEAM	Poly (N,N'-diethyl acrylamide)
PNIPAM	Poly (N-isopropyl acrylamide)
PVA	Poly vinyl alcohol
PVP	Poly (vinyl pyrrolidone)
KPS	Potassium persulfate
SEM	Scanning electron microscope

SR_t	Swelling ratio at time 't'
Full-IPN	Full-Interpenetrating network
Semi-IPN	Semi-Interpenetrating network
UCST	Upper critical solution temperature

University of Malaya

CHAPTER 1: INTRODUCTION

1.1 Introduction of Hydrogels

The first hydrogels for practical use in biomedical field was coined by the synthesis of poly(2-hydroxyethyl methacrylate) (PHEMA) by Wichterle and Lim for contact lens applications in 1960 (Nguyen et al., 2015). PHEMA can absorb plenty of water while maintaining its network structure representing the modern hydrogels. Hydrogels are three dimensionally crosslinked polymer network that can absorb lots of water in the interstices and can hold it without losing the network structure in the swollen state (Islam et al., 2012). This is owing to the presence of some strongly polar hydrophilic groups such as NH_2 , OH , COOH , CONH_2 , SO_3H etc. along the polymer chains as pendant groups. The swelling of hydrogels as a result of water absorption is controlled by the nature of hydrophilic groups, crosslinking density and swelling media. Crosslinking controls water absorption as well as help in maintaining the network structure in the swollen state (Abad et al., 2003; Ahmed, 2015; Ali & Zaidi, 2005; Bhattarai et al., 2010). Apart from the contribution of hydrophilic groups to water uptake, it is also responsible for secondary interactions with biological tissues (Prabaharan, 2011).

Hydrogels are especially important in biomedical field because of their unique properties such as biocompatibility, biodegradability, softness, superabsorbancy, hydrophilicity and viscoelasticity in swollen state. Besides, hydrogels also responses to different stimuli. These stimuli are pH, temperature, electric field, magnetic field, biological molecules, and ionic strength (Miyata et al., 2002; Juergen et al., 2011). Many hydrogels are bioadhesive and mucoadhesive. Hydrogels enhance the residence time of drugs which make them more attractive candidate as a drug carrier (Bhattarai et al., 2010).

1.2 Composition of Hydrogels

Hydrogels compose mainly crosslinked polymers regardless natural or synthetic grafted polymer derivatives or combination of both natural and synthetic polymers. Natural hydrogels comprise of natural polymers which are abundantly available in the market, cheap, and non-toxic. Natural polymers can be categorized into various classes according to their chemical structure. These belong to variety of classes based on their chemical structure: i) polysaccharides (Chitin, chitosan, cellulose, starch, gums, alginate, carrageenan), ii) biological polymers (nucleic acid, DNA), iii) polyamides (Collagen) iv) polyphenols (lignin), v) organic polyesters, vi) inorganic polyesters (polyphosphazene), vii) polyanhydrides (poly sebacic acid) (Pillai & Panchagnula, 2001). Hydrogels formed from natural polymers especially polysaccharides and proteins are similar to extra cellular matrix due to their natural origin and can easily be identified by the cells, hence appear to be biocompatible (Kirschner & Anseth, 2013). However, hydrogels formulated from natural polymers especially chitosan and other polysaccharides are fragile and poor in mechanical strength. In order to improve their mechanical properties, natural polymers are crosslinked, grafted with monomers or blended with synthetic polymers (Islam et al., 2012). For example, synthetic polymer poly (vinyl alcohol) is used as blending agent to improve the mechanical strength and flexibility of natural polymers (Kirschner & Anseth, 2013).

Synthetic hydrogels contain synthetic polymers which offer more flexibility to tune the mechanical properties of hydrogels. The most commonly used synthetic polymers are polycaprolactone (Gong et al., 2007), poly (vinyl pyrrolidone) (PVP) (Sohail et al., 2014), poly (lactic acid) (PLA) (Pawar et al., 2014), poly (ethylene glycol) (PEG) (Atta et al., 2015), and poly (vinyl alcohol) (PVA) (Kirschner & Anseth, 2013; Rafique et al., 2016). PEG is water soluble, biocompatible, and biodegradable and is especially important as it can conjugate with peptides, proteins and some other drugs. PEG is also utilized to graft

with some natural polymers to induce typical properties required for specific application. Bhattarai *et al.* synthesized PEG-graft-chitosan as injectable thermo-responsive hydrogels that are liquid at low temperature but solidify as solid at body temperature (Bhattarai *et al.*, 2005).

1.3 Types of Hydrogels

Based on the type of crosslinking (the type of forces) between the polymer chains, hydrogels may be categorized as physical and chemical hydrogels. If the crosslinking interactions between the polymer chains are the non-covalent forces (secondary forces) such as hydrogen bonding, ionic forces, Van der Waals interactions, polyelectrolyte complexation, stereocomplexation, and hydrophobic forces, the hydrogels form through these interaction are classified as physical hydrogels. Physical hydrogels show reversible response to environmental changes because of the secondary interactions between the polymer chains are not very strong. They are disordered, fragile and mechanically weak when exposed to the external stimuli. Due to weak interactions, physical hydrogels usually dissolve in organic solvents and water upon heating (Boucard *et al.*, 2005; Hennink & Nostrum, 2012). Whereas, the formation of chemical hydrogels and also known as permanent hydrogels involve covalent bonding between the polymer chains. These hydrogels do not dissolve in surrounding medium and hence do not show reversible response (sol-gel transition) similar to physical hydrogels due to the presence of strong covalent bonding between the macromolecular chains (Juergen Siepmann *et al.*, 2011). Chemical crosslinking takes place through numerous ways by using small molecules (formaldehyde, glutaraldehyde (GA), genipin, diglycidyl ether, and N, N'-methylene bisacrylamide. These small molecules form covalent bond with the polymers to stabilize the network formed through condensation reaction or free radical mechanism. In the case of condensation reactions, crosslinker should contain two functional groups normally (GA) (Reddy *et al.*, 2008) but mono functional group containing crosslinker

(formaldehyde) can also be used (Magami et al., 2015). In free radical mechanism, the crosslinker must contain at least two double bonds to bind with the polymer chains on its either side. Chemical crosslinking imparts characteristics like excellent thermal, mechanical, chemical and surface properties to the prepared hydrogels as well as it is responsible for maintaining network structure of hydrogels in fully swollen state (Costa-Júnior et al., 2009).

1.4 Properties of Hydrogels

The use of polymers (natural or synthetic) containing hydrophilic pendant groups to synthesize hydrogels for biomedical applications is greatly advantageous because these hydrophilic groups not only facilitate ample water absorption but also assist in the interaction with biological tissues (epithelial tissues, mucous membrane) (Prabaharan, 2011). Normally, hydrogels in the fully swollen state are nearly viscoelastic, soft, rubbery and low in interfacial angle with biological fluids that decreases the chances of negative immune response. All these contribute to biocompatibility of hydrogels (Islam et al., 2012). The hydrogels are also normally degradable to different extent depending upon the type of crosslinker involved (McBath & Shipp, 2010).

Furthermore, hydrogels have swelling property which is the most significant in their existence. The swelling of hydrogels takes place in three steps: i) diffusion of water into hydrogel network (water moving in called primary bound water), ii) relaxation of polymer chains (more water moving in called secondary bound water) followed by iii) expansion of hydrogel network (additional water moving in is termed as free water) (Ferreira et al., 2000). According to Flory-Reihner theory, swelling is a function of elastic nature of the polymer chains and their compatibility with water molecules (Buenger et al., 2012).

Hydrogels show different responses to the change in environmental stimulus which may generally categorized into i) physical (temperature, light etc.), ii) chemical (pH, ionic

strength) and iii) biological (enzymes). Chemical and biological stimuli are internal whereas physical stimuli are external except for temperature which may be external or internal (Karimi et al., 2016). Besides all this, there is a special type of stimuli responsive smart hydrogels called shape memory hydrogel with two characteristics i) permanent shape and ii) a chemical or physical code that can help restore original shape (Guo et al., 2015).

Covalently crosslinked hydrogels that contains ionic pendants groups show a response to change in pH and are referred to as pH responsive hydrogels. Hydrogels with anionic groups swell at higher pH due to ionization of pendant groups that causes electrostatic repulsion. However, hydrogels containing cationic groups swell at low pH. Some hydrogels show swelling/deswelling behavior in response to temperature changes as a result of change in polymer-polymer or water-polymer interactions and are known as temperature sensitive hydrogels. Poly (N-isopropyl acrylamide) (PNIPAM) hydrogel is an example of temperature sensitive hydrogel (Jiali et al., 2012). They may be positive temperature sensitive which show swelling at higher temperature than upper critical solution temperature (UCST) (Kim et al., 2003), negative temperature sensitive which show swelling at lower temperature than lower critical solution temperature (LCST), and thermally reversible hydrogels that show sol-gel transition above and below a characteristic temperature. Ploxamer hydrogels are known as thermally reversible hydrogels (Wu et al., 2010).

1.5 Biomedical Applications

1.5.1 Hydrogels in Contact lens Applications

Revolution in the field of hydrogels was begun after the synthesis of poly (2-hydroxyethyl methacrylate) (PHEMA) for contact lens applications in 1960 and got an approval from food and drug administration (FDA) in 1971. Based on elasticity, contact lenses can be

classified as hard lenses which composed of poly (hexa-fluoroisopropyl methacrylate) or poly(methylmethacrylate)] and soft lenses (usually comprised of hydrogels) (Caló & Khutoryanskiy, 2015).

1.5.2 Hydrogels in Drug Delivery Applications

Hydrogels are gaining exceptional raise as biomaterials in targeted drug and protein delivery applications due to their unique properties such as biocompatibility, biodegradability, distinctive configurations and stimuli responsive swelling characteristic. Targeted and controlled drug release mechanism may be through diffusion, osmosis, dissolution and/or ion exchange (Kim et al., 2002). Biocompatible hydrogels have been synthesized by many researchers for controlled drug delivery, tissue engineering and some other biomedical applications (Costa-Júnior et al., 2009). There are different dosage ways for drugs to be delivered into the body. These numerous ways of drug delivery are: oral implants, parental, subcutaneous, nasal, ocular, epidermal, transdermal, injectable forms, and wound dressing etc. (Peppas et al., 2000). The detection and growth of new drug are facilitated by hydrogels (Ritschel, 1989) via peroral delivery and it is used to target oral cavity, stomach, small intestine and colon in the body. Moreover, researchers have explored drug incorporated bioadhesive hydrogels as a carrier for site specific drug delivery in buccal cavity. The drugs used for the buccal site may be in the form of pills (Madgulkar et al., 2009), patches (Vamshi Vishnu et al., 2007) and hydrogels (Petelin et al., 1998). A wide range of pH variation along the gastrointestinal tract (GI) is a motive for the use of biodegradable stimuli sensitive hydrogels for the targeted delivery of drugs. Tablet form of hydrogels formulations are used for oral intake and passing through the GI tract with most of the drug is released on the target area and hydrogels disintegrates in lower part of GI (Brannon-Peppas, 1997).

In early 1980's, controlled release technology (Kim, 1996) emerged as a hot cake in the pharmaceutical field for the release of any drug or protein to extend the period of time the drug can be released at predetermined rate (Bhattarai et al., 2010). As the stomach and intestine have different pH, hydrogels used for the controlled release must be pH sensitive. Remunan-Lopez *et al.* prepared fluorescein isothiocyanate-bovine serum albumin for the controlled release of diclofenac sodium (Remuñán-López et al., 1998). To avoid the drug wreck in the GI and cause systematic side effects, skin can be an alternate route for the drug delivery, called transdermal delivery and have several attributes. Easy access, easy delivery, steady drug release and non-invasive are the significant attributes of transdermal drug delivery. Mi *et al.* synthesized bilayer of chitosan filled with antibiotic to control wound infection. Drug molecules can penetrate via outer most layer of epidermis and intra cellular lipids (Mi et al., 2002). Ocular drug delivery has some shielding barriers such as effectual tear drainage, low porosity of cornea and flashing of eye which results in less retention time and quick drainage of drug from eye. To increase the dwelling time of the drugs, investigators used hydrogels for ocular drug delivery (Mashkevich, 2007). Hui *et al.* prepared crosslinked poly (acrylic acid) (PAA) for ocular delivery of progesterone in rabbits (Hui & Robinson, 1985).

1.5.3 Hydrogels in Conductive Biomedical Applications

Polyelectrolyte hydrogels based on biopolymers are conductive to ions and are electrochemically stable and hence can be used to design electrochemical devices for biomedical applications such as electrode coatings, bio-electrodes, biosensors, and gas sensors. These electrical devices are pH sensitive, low cost of production, solvent resistant and good in mechanical properties (Green et al., 2010; Guimard et al., 2007). These biopolymer based electrochemical devices are used as drug delivery systems, electrochemical biosensors, adhesives, separation membranes, soft tissue replacement

implants and artificial cornea (Oliveira et al., 2009; Green et al., 2010; Guimard et al., 2007; Pauliukaite et al., 2010; Rodriguesm et al., 2007).

1.5.4 Hydrogels in Tissue Engineering Applications

One of the recent and advanced applications of hydrogels is for tissue engineering. Hydrogels may be used as three dimensional structures that act as stimuli to organize cells and ensures the proper development of specific tissue, as a carrier for delivery of bioactive agents or as space filling agents. Hydrogels as space filling agents so called scaffolds are usually applied in encapsulation of secretory cells, promotion of angiogenesis, to transplant cells and to engineer many tissues such as smooth muscles, cartilage and bone (Drury & Mooney, 2003). Harris *et al.* introduced self-assembling peptides to design nanoporous and nanofibrous hydrogels for microporous and nanoporous scaffolds in tissue engineering applications. These hydrogel scaffolds are beneficial because they are capable of interacting with cells, stimulate tissue ingrowth, vascularization, biodegradable, non-immunogenic and most importantly can manage slow diffusion of drugs (Harris et al., 2011).

1.6 Objectives

The research will include the following objectives:

- a) To modify chitosan as N-succinyl chitosan
- b) To synthesize and characterize pH-sensitive N-succinyl chitosan hydrogels.
- c) To synthesize and characterize pH-sensitive karaya gum hydrogels.
- d) To study the application of hydrogels as drug carriers.

1.7 Thesis Outlines

This thesis presents the scope of pH-sensitive hydrogels as hydrophilic as well as hydrophobic drug carriers. This work covers the fabrication of hydrogels through Schiff

base and free radical mechanism, characterization of fabricated hydrogels, properties of hydrogels, and applications in drug delivery. The thesis outlines are presented below.

Chapter 1 emphasizes the basic introduction of hydrogels, materials involve in the synthesis of hydrogels, types, properties, and applications of hydrogel. Chapter 2 presents the detailed literature review of hydrogels, natural, synthetic polymers, and polymerizable monomers used to synthesize hydrogels. This chapter also describes the methods of preparation of hydrogels, crosslinking agents used in the synthesis of hydrogels, and types of hydrogels formed as final product. Moreover, properties and applications of hydrogels have been briefly discussed in this chapter.

Chapter 3 introduces the materials used and methodology adopted for the synthesis of N-succinyl chitosan, hydrogels, physico-chemical characterization, ways of evaluation of properties and their utilization in the drug delivery.

Chapter 4 is further divided into 4 major sections. These sections are comprehensive discussion on synthesis of N-succinyl chitosan and hydrogels, characterization of hydrogels, properties of hydrogels, and applications of hydrogels in the drug delivery.

At the end of thesis, conclusions based on our findings from this research work and future directions are given in chapter 5.

CHAPTER 2: LITERATURE REVIEW

2.1 Natural Polymer Hydrogels

Hydrogels can be categorized as natural, synthetic or combination of natural and synthetic polymers. Hydrogels obtained from natural polymers are classified as natural polymer hydrogels. These natural polymers include polysaccharides, polynucleotides, and polypeptides. The natural polymers can be obtained from diverse natural sources and classified as neutral, cationic and anionic in nature. These polymers are easy to access, abundant, inexpensive, non-toxic, biodegradable, and possess attractive biological properties. There has always been a great interest in the relationship of structure and function especially in natural biologically active compounds. The advances in structural and functional substances over the few decades made an increasing number of developments in materials to be used in biomedical technology. The natural polymers have well defined larger structure formed by covalently bonded monomeric units. The natural polymer hydrogels can be used for numerous biomedical applications such as controlled and targeted release of drugs, tissue engineering, and wound healing (Islam et al., 2012; Omidian & Park, 2008; Tang et al., 2016).

2.1.1 Polysaccharide Hydrogels

Polysaccharides are distinctive class of naturally occurring polymers that acquire massive variety of structural characteristics (Bhattarai et al., 2010). Polysaccharides can be used as renewable biomaterials due to their exceptional biological properties. They are formed from long chain carbohydrate molecules of repeated monomeric units held by glycosidic bonds. These act as promising biomaterials and carry special physiological functions and biological activities and are helpful for a variety of applications (Matricardi et al., 2013). Naturally available polysaccharides such as cellulose, starch, chitin, chitosan,

carrageenan, alginates, dextran, pullulan, and pectin are studied extensively for industrial, medical, pharmaceutical, and tissue engineering applications.

There has been a great interest in the growth and development of polysaccharide hydrogels during the past few years for the biomedical applications. Hydrogel loaded with drug can sustain its level in blood and can be controlled subcutaneously, orally, and/or intramuscularly. (Piyakulawat et al., 2007; Reis et al., 2008). Although, synthetically developed biocompatible and biodegradable polymers hydrogels are also useful for biomedical applications but polysaccharides remain smart and attractive due to abundance availability, non-toxicity, good biocompatibility and biodegradability, ease of modification and preparation, low cost, renewable physicochemical properties and hence have been used by the mankind in different forms (Berger et al., 2004).

2.1.2 Chitosan

Chitosan is obtained by the thermochemical deacetylation of chitin in the presence of alkaline condition (Pillai et al., 2009). Several approaches have been reported for the synthesis of chitosan. Chitin is a second most abundant natural polysaccharide and is acquired from the exoskeleton of crustaceans, insects, and certain fungi. Chitin has limited applications due to its poor solubility in organic and aqueous solutions. Chitosan is formed from chitin through alkaline hydrolysis. Chitosan is a suitable alternative due to its solubility in acidic media (below pH 6.0) and its vast range of practical applications as a biomaterial (Mima et al., 1983). The properties of chitosan depend on the degree of deacetylation and the molecular weight. The molecular structures of chitin and chitosan are shown in Figure 2.1.

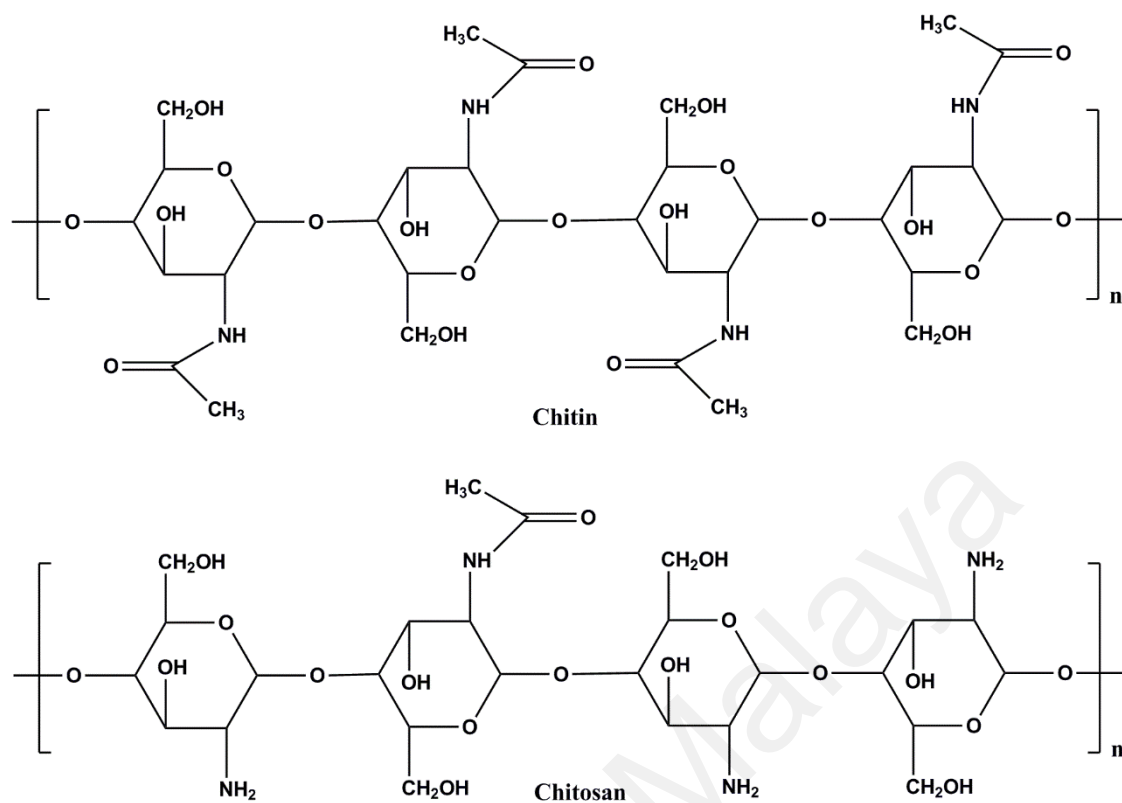


Figure 2.1: Structure of Chitin and chitosan

2.1.2.1 Chitosan Based Hydrogels

The ability of chitosan to form hydrogel is one of the most important developments in medical and polymer science. It is greatly helpful for understanding the functions of biological molecules from renewable sources and make us realize the important function of hydrogels in biological systems. Chitosan contains various functional groups which can be modified to obtain the desired properties of hydrogel. Chitosan has been used to prepare hydrogels with low toxicity due to their similarities with extracellular matrix. The inherent properties of chitosan to form hydrogels make it an important material particularly useful as biomaterials (Muzzarelli, 2009; Singh et al., 2006).

2.1.2.2 Limitations of Chitosan

Chitosan with the nature of mucoadhesiveness enable it to enhance drug absorption properties have been highly cited in the literature. However, effectiveness of drug absorption by chitosan decreases at high pH due to its poor solubility at a pH greater than

6.0. Chitosan is soluble in dilute acidic solution. Acids used for the dissolution of chitosan include inorganic acid hydrochloric acid (HCl) and organic acids methanoic acid, ethanoic acid, oxalic acid, and lactic acid. The mechanism of solubilization involves protonation of the amino functional group at the C-2 position of the glucosamine units. The acetyl groups distributed over the chitosan chain are also a factor responsible for changes in solubility. Chitosan with a deacetylation degree of 86 % is partially soluble up to pH 6.5. Furthermore, the ionization degree depends on the strength of the acid and the pH, which has been experimentally confirmed during the protonation of chitosan in the presence of aqueous acids during solubilization (Fan et al., 2009).

It should be highlighted that the pH of the small intestine is 4.5 and the pH of the ileum is 7.4; the pH varies gradually from the small intestine to the terminal ileum, so chitosan is not soluble in the lower part of the intestine. Therefore, chitosan cannot be used to deliver a drug in the lower part of the intestine. In order to enhance oral bioavailability of a drug using chitosan as a drug carrier, its dissolution in lower part of the intestine is required. Thus, researchers have made impressive contributions but much work is still required to improve drug bioavailability. This can only be achieved through modification of chitosan which enhances its water solubility at higher pH. It can be done through derivatization of the amino and hydroxyl groups of chitosan. After modification of the amino and hydroxyl groups, they are quaternized (Polnok et al., 2004) with carboxyalkyl (Wongpanit et al., 2005), hydroxyalkyl (Richardson & Gorton, 2003), and acyl derivatives. Among these derivatives, acyl derivatives have substantial importance in biomedical applications.

2.1.2.3 Modification of Chitosan

The abovementioned significant disadvantages of chitosan have motivated researchers to design further modification of chitosan. Modification of the amino and hydroxyl groups

of chitosan improves its solubility in acidic as well as in alkaline environments, improves its biodegradability and biocompatibility, enhances transfection efficiency, while decreases toxicity. Figure 2.2 shows several modification methods, while some examples of chitosan derivatives are listed in Table 2.1.

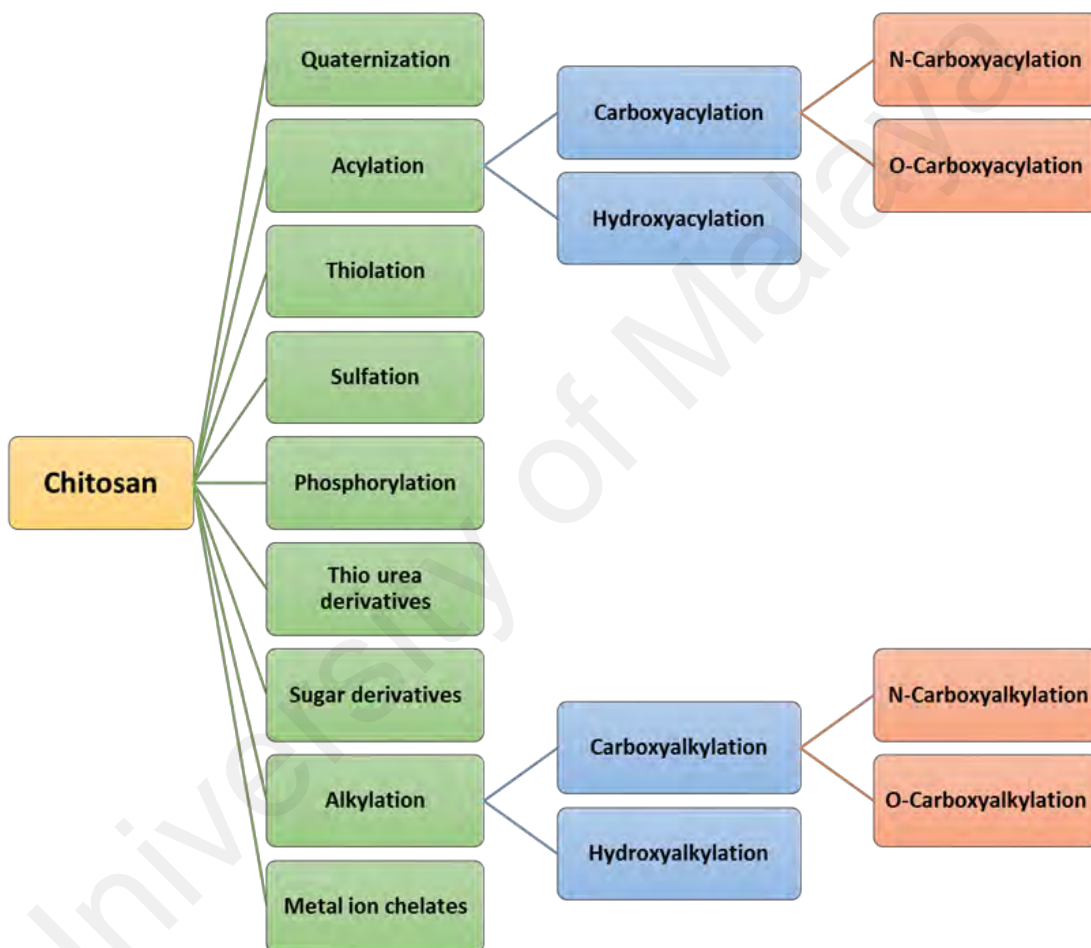


Figure 2.2: Various modifications of chitosan

Table 2.1: Chitosan modification methods and examples of each modified chitosan

Methods	Examples
Quaternization	N,N,N-trimethyl chitosan chloride (Thanou et al., 2000), N,N,N-trimethyl chitosan iodide, quaternized derivatives of N,N,N-trimethyl carboxymethyl chitosan, N-ethyl-N,N-dimethyl carboxymethyl chitosan, N-propyl-N,N-dimethyl carboxymethyl chitosan, N-butyl-N,N-dimethyl carboxymethyl chitosan, N-isobutyl-N,N-dimethyl carboxymethyl chitosan.
Alkylation	N-furfuryl- N, N-dimethyl chitosan, N-propoyl-N, N-dimethyl chitosan, N-diethylmethylamino chitosan.
Carboxyalkylation	N-carboxymethyl chitosan, N, N, N-trimethyl carboxymethyl chitosan, N-ethyl-N,N-dimethyl carboxymethyl chitosan, N-carboxylpropyl chitosan, N-propyl-N,N-dimethyl carboxymethyl chitosan, N-butyl-N,N-dimethyl carboxymethyl chitosan, N-isobutyl-N,N-dimethyl carboxymethyl chitosan, N-carboxybenoyl chitosan
Hydroxyalkylation	Hydroxyethylchitosan, hydroxypropyl chitosan, 3-trimethylammonium-2-hydroxypropyl-N-chitosan, N-hydroxyethyl-O-benzyl, N-hydroxypropyl-O-benzyl, N-hydroxybutyl-O-benzyl chitosan.
Thiolation	Chitosan-thioglycolic acid, chitosan-2-iminothiolane, chitosan-cysteine conjugate.
Thiolated urea derivatives	Thiourea chitosan, acetyl and chloroacetyl thiourea chitosan, benzoyl thiourea (Zhong et al., 2008), thiourea chitosan(antibacterial), benzoyl thiourea chitosan (Eweis, Elkholy, & Elsabee, 2006)
Sulfation or sulphonation	Chitosan sulfate, N-sulfofurfuryl chitosan, O-sulfated chitosan, N-sulfated O-carboxymethyl chitosan (Jayakumar, Nwe, Tokura, & Tamura, 2007), N-sulphonato-N,O-carboxymethyl chitosan, (N,O)-sulfated chitosan (Karadeniz et al., 2011)
Phosphorylation	Phosphorylcholine and N-Methylenephosphonic chitosan, N-phosphonomethyl chitosan, chitosan phosphite (Matevosyan et al., 2003)
Sugar derivatives	Lactosaminated N-succinyl chitosan (Jain et al., 2014), galactosyl conjugated N-succinyl chitosan (Lu et al., 2010), Galactosylated chitosan

2.1.2.4 Acylation

The chemical reaction between chitosan and acyl halides or aliphatic carboxylic anhydrides is called acylation. There are numerous acid anhydrides, lactones, and acyl halides, which form a variety of acylated outcomes. The acylation of chitosan takes place at the amino and hydroxyl groups of chitosan. Acylation in which substitution takes place at an amino group is called N-acylation and substitution of a hydroxyl group is known as O-acylation. N-acylation is the most extensively studied chitosan modification. It proceeds through the addition or elimination mechanisms in acetic acid/methanol, methanol/ethanol, pyridine, dichloroethane/trichloroacetic acid or formamide/methanol (Kurita, 1986). N-acylation typically proceeds toward the formation of amide functional groups because amides are more stable.

Acid anhydrides are extensively used for the N-acylation of chitosan, but anhydrides have very low solubility in aqueous media. Therefore, this reaction takes place under heterogeneous conditions, and methanol is used to solvate anhydride in the medium. The presence of aqueous acetic acid in methanol also leads to selective acylation at an amino functional group. Diverse N-acyl derivatives have been synthesized by researchers. For example, Hirano *et al.* (Hirano *et al.*, 2002a) reported N-saturated fatty acyl derivatives. These derivatives were synthesized through the reaction of chitosan with short and long chain anhydrides. These anhydrides are propionic, butyric, pentanoic, succinic, lauric, itaconic, palmitic, stearic, and myristic anhydrides. Short-chain acyl derivatives show greater water solubility while longer chain derivatives are water insoluble regardless of the degree of substitution. The reaction of chitosan with cyclic anhydride usually forms carboxyacyl chitosan. These derivatives exhibit water solubility in the degree of substitution range of 0.45-0.8 and in the pH range of 4.0-7.0. The introduction of lactones to the amino group of chitosan forms hydroxyacyl derivatives with improved water solubility, lactones are much less reactive and more stable. For these reasons, few N-

hydroxyacyl derivatives have been prepared (Champagne, 2008; Hirano et al., 2002b; Wu et al., 2006). Figure 2.3 shows N-acylation of chitosan.

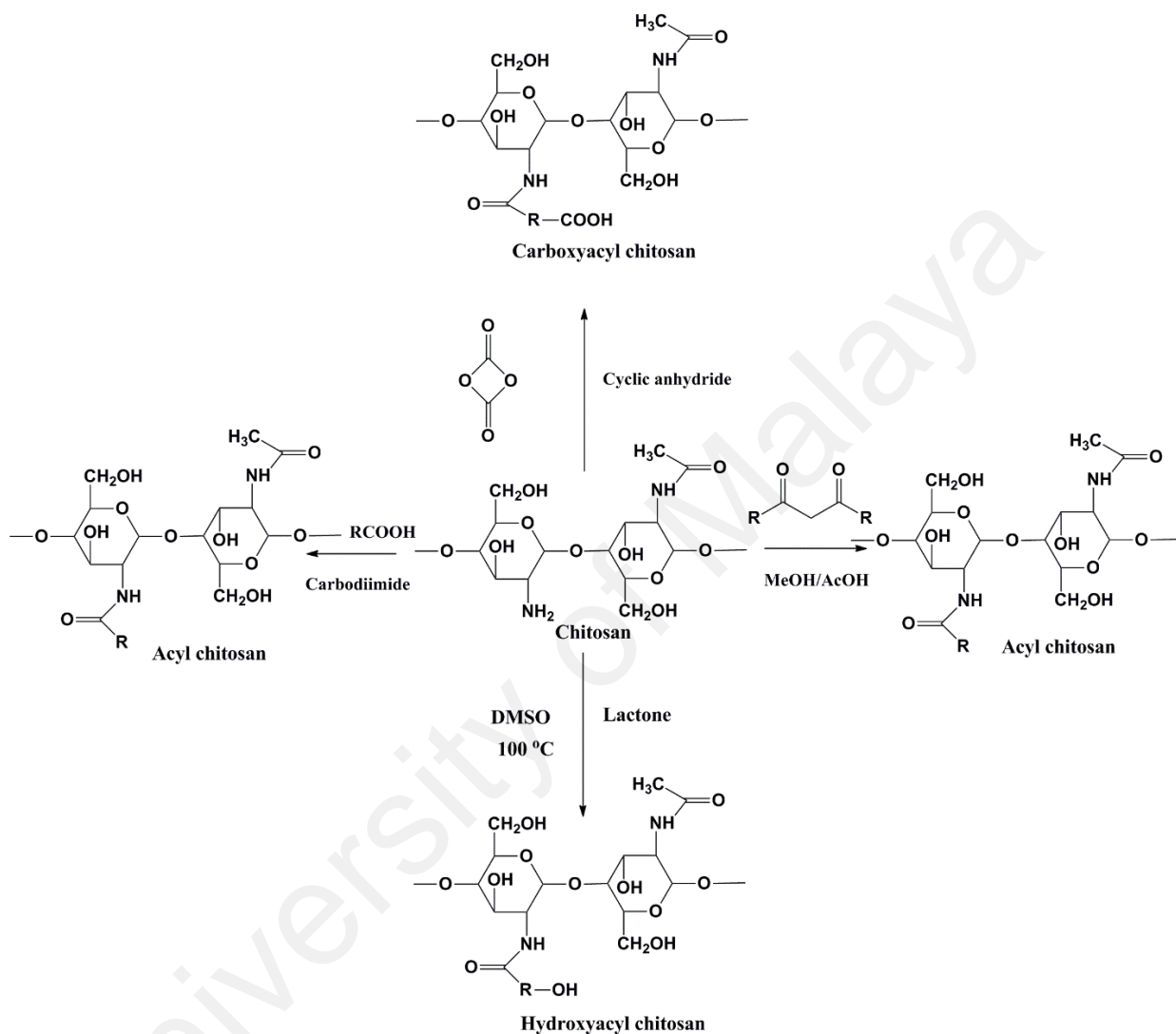


Figure 2.3: N-acylation of chitosan

Chitosan is a multi-nucleophilic polymer, as can be seen from its molecular structure.

Substitution can occur at an amino or hydroxyl group, but substitution at an amino group is given the priority due to the greater reactivity of this group. However, O-acylation can be accomplished by the protection of N-amino groups and controlling the experimental conditions. Amino groups can be protected by N-phthaloyl groups; this allows O-acylation in dimethylformamide (DMF) at a high temperature. In addition,

methanesulfonic acid at a low temperature and H_2SO_4 can also be used for the O-acylation of chitosan without additional protection of the amino group.

2.1.2.5 N-Succinyl chitosan

N-acylation of chitosan has already been discussed in section 2.1.2.4. Carboxyacyl formation takes place upon the introduction of cyclic anhydrides to chitosan. Among these anhydrides, the reaction of succinic anhydride with chitosan in dimethyl sulfoxide (DMSO) or acetic acid/methanol mediums produces N-succinyl chitosan (NSC) with a specific degree of succinylation. The mechanism of NSC synthesis is shown in Figure 2.4. The degree of succinylation can be measured by numerous ways (ninhydrin assay, titrimetry, elemental analysis, and ^1H NMR). The degree of succinylation depends on the reaction conditions. N-succinyl chitosan has excellent solubility at neutral pH compared to chitosan that only soluble in acidic media and precipitates above pH 6.5. Its solubility in the basic environment is due to the formation of carboxylate ions ($-\text{COO}^-$). The advantages of N-succinyl chitosan are that it is biocompatible, biodegradable, bioadhesive, and possesses long-term retention properties both in vitro and in vivo (Kato et al., 2000). Due to the abovementioned properties, it has considerable applications in the medical field as a drug carrier to prepare conjugates with anticancer drugs and has exhibited excellent antitumor activity. Other applications include wound dressings, tissue engineering, growth factor delivery, gene delivery, and cosmetic applications. It has been applied in wound healing for arthritis treatment in Japan (patent 06107551) and recently investigated as a wound dressing material (Tang et al., 2016).

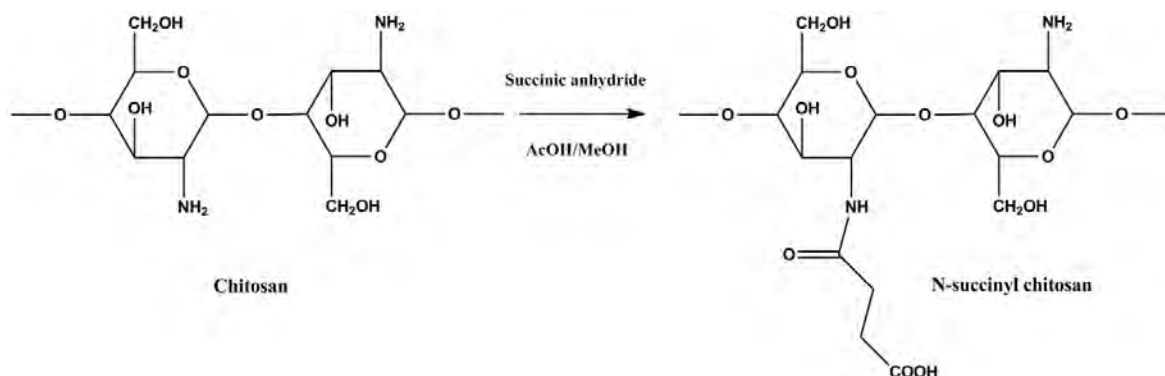


Figure 2.4: Synthesis of N-Succinyl chitosan (Yan et al., 2006)

2.1.2.6 N-Succinyl chitosan Based Hydrogel

Different formulations of NSC such as hydrogels, beads, blends, matrices, microparticles, nanoparticles, and nanospheres using distinct methods have been developed for biomedical applications. Researchers prepared hydrogels using various methods based on the requirements of the host organ/tissue. NSC molecules are either physically associated or chemically crosslinked with other materials in the formation of hydrogel. The major mechanisms of physical association leading to gel formation with NSC are ionic interactions, hydrophobic associations, hydrogen bonding, van der Waals forces, and inter-polymer complexes. Physically associated hydrogels are advantageous due to the absence of toxic crosslinking agents. However, there are also certain limitations as well. These limitations include difficulties in maintaining pore size, dissolution, and degradation of the gel. Physically associated hydrogels show unpredictable performance *in vivo*. On the other hand, chemically crosslinked hydrogels are formed through covalent bonding with the help of certain crosslinking agents. These hydrogels possess excellent mechanical properties and controlled biodegradation. These properties of hydrogels play a vital role in tissue engineering. Chemically crosslinked hydrogels have one major limitation that is arose from the toxicity of the crosslinking agent. Lu *et al.* (Lü et al., 2010) synthesized N-succinyl chitosan/ O-carboxymethyl cellulose (NSC/OCMC) hydrogel using Schiff base mechanism, which is chemical crosslinking. In this method,

NSC and OCMC solutions were prepared separately in phosphate-buffered saline. The reaction mechanism is shown in Figure 2.5. Dai *et al.* (Dai *et al.*, 2008) prepared NSC/sodium alginate hydrogel beads through chemical crosslinking. NSC and alginate solutions were dropped into a CaCl_2 solution. NSC and alginate crosslinked with Ca^{2+} ions to form hydrogel beads. Tan *et al.* (Tan *et al.*, 2013) synthesized physically crosslinked NSC/PEG hydrogels. First of all, methacrylic acid was grafted onto NSC and dimethacrylate onto PEG. Then, methacrylated NSC was irradiated with UV to sterilize it and dissolved in phosphate saline buffer. Dimethacrylate was sterilized by filtration through a syringe and dissolved in a buffer solution. In order to prepare the gel, photoinitiator, Irgacure was added into the starting material and irradiated by UV light at 365 nm for 15 minutes at 37 °C. NSC-based reported hydrogel formulations and preparation techniques are given in Table 2.2. Other formulations included microparticles, matrices, beads, blends, and nanospheres. The preparation of microparticles, matrices, beads, and nanospheres involves different methods such as spray drying, freeze drying, ionic gelation, and emulsion crosslinking.

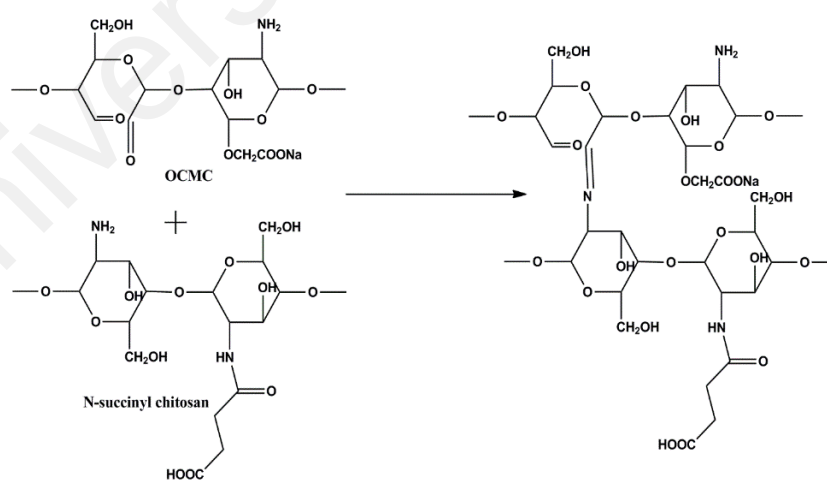


Figure 2.5: Synthetic scheme of NSC/OCMC (Lü *et al.*, 2010)

Table 2.2: NSC-based hydrogel formulations and preparation techniques

NSC based Formulation	Composition	Method of preparation	Reference
Hydrogel	NSC/oxidized carboxymethyl cellulose	Schiff's base mechanism	(Lü et al., 2010)
Hydrogel	NSC/polyethylene glycol	Radiation crosslinking	(Tan et al., 2013)
Hydrogel	NSC/sodium alginate	Ionic gelation	(Rogalsky et al., 2011)
Hydrogel	NSC/RGD grafted sodium alginate	Schiff's base mechanism	(Liu et al., 2013)
Hydrogel	NSC/oxidized hyaluronic acid	Schiff's base mechanism	(Tan et al., 2009a)
Hydrogel	Dexamethasone grafted NSC/aldehyde hyaluronic acid	Schiff's base mechanism	(Jinchen Sun et al., 2013)
Hydrogel	NSC/RGD grafted sodium alginate/LIPUS	Schiff's base mechanism	(Wang et al., 2014)
Hydrogel	NSC/dextran aldehyde	Hemiacetal formation	(Aziz et al., 2012)
Microparticles	NSC	TPP crosslinking	(Mura et al., 2012)

Table 2.2: NSC-based hydrogel formulations and preparation techniques (Continued)

NSC based Formulation	Composition	Method of preparation	Reference
Microparticles	NSC	Spray drying	(Rekha & Sharma, 2008)
Microparticles	NSC-MMC	Ionic crosslinking	(Onishi et al., 2001)
Microparticles	NSC/PVA	Emulsion technique	(Kajjari et al., 2013)
Microsphere	NSC/sodium alginate	Ionic gelation	(Duan et al., 2016)
Beads	NSC	Ionic gelation	(Li et al., 2012)
Beads	NSC/oxidized alginate	Ionic gelation	(Straccia et al., 2014)
Blend	NSC/oxidized alginate	Ionic gelation	(Fan et al., 2010)
Matrix	NSC	×	(Tang et al., 2016)

2.1.3 Karaya gum Hydrogels

Karaya gum is an acidic polysaccharide attained from the *Sterculia* trees. It is a branched polysaccharide comprised of D-galacturonic acid, L-rhamnose, D-galactose, and D-glucuronic acid. The carbohydrate structure has rhamnogalacturonan main chain consisting of α -(1 \rightarrow 4)-linked-L-rhamnosyl residues. However, the side chains comprised of (1 \rightarrow 3)-linked β -D-glucuronic acid or (1 \rightarrow 2)-linked β -D-galactose on the galacturonic acid unit where half of the rhamnose is substituted by (1 \rightarrow 4)-linked β -D-galactose. This natural polymer has stabilizing, thickening and emulsifying characteristics. Therefore, it has a significance potential in food and pharmaceutical sector. However, it has very low water solubility. It swells up many times when immersed in water, ultimately dispersed after sometime. The dispersion of karaya gum can be achieved by immersing in water at high temperature and sonication. However, its solubility can be increased by adding aqueous solution of ammonia. Ammonia causes deacetylation and increases the solubility in water.

Karaya gum is newly introduced polysaccharide applied in the biomedical field for drug delivery and act as adsorbent to remove pollutant. Baljit Singh *et al.* reported karaya gum modified with methacrylic acid and acrylamide through free radical crosslinking and swelling studies were investigated in water and at pH 2.2 and at pH 7.4. The hydrogels showed higher swelling in water and at pH 7.4 while lower swelling at pH 2.2. The anti-ulcer drug delivery such as ranitidine hydrochloride release study revealed drug release in water and followed Fickian diffusion mechanism at pH 2.2 and non-Fickian at pH 7.4 (B. Singh & Sharma, 2008a, 2008b). In another study, Baljit Singh *et al.* synthesized hydrogels of karaya gum modified with acrylic acid and 2-hydroxyethylmethacrylate through gamma radiation crosslinking polymerization. The anti-diarrhea drug ornidazole release results revealed the higher drug release at initial stage and slow drug release at later stage. Moreover, the drug release in water and buffer solutions of pH 2.2 and pH 7.4

followed non-Fickian diffusion mechanism (Singh & Vashishtha, 2008). Moreover, Baljit Singh *et al.* prepared hydrogels of karaya gum crosslinked with PVA through glutaraldehyde and gamma radiation for the wound dressing applications. The antimicrobial agent tetracycline hydrochloride was loaded and release trend was observed in simulated wound fluid. The drug release showed non-Fickian diffusion mechanism in water, buffer solutions and simulated wound fluid (Singh & Pal, 2008) (Singh *et al.*, 2011).

Tremendous increase in population and industrial growth increase the demand for water. However, pure water available for human consumption remained the same. Moreover, improper water management at industrial level created problems for the availability of clean water. The industries use toxic chemicals on large scale and pollute the water. The process of cleaning the contaminated water becomes a major challenge in the world. Polymer materials have become popular interest to clean the water because of easy availability, low cost and environmental friendly nature. Mittal *et al.* used copolymer grafted karaya gum and silica hydrogel nanocomposite as an adsorbent for the removal of toxic methylene blue dye. Copolymer grafted karaya gum/silica hydrogel nanocomposite has excellent adsorption properties for the removal of toxic dye (Mittal *et al.*, 2015).

2.1.4 Synthetic Polymer Hydrogels

Synthetic polymers are attractive for the synthesis of hydrogels as these have highly controllable physical and chemical properties than natural polymers. Synthetic polymers can be produced with long chain structure and high molecular weight. Unfortunately, synthetic polymer hydrogels have low biological activity than natural hydrogels. Synthetic polymer hydrogels can be synthesized via numerous ways employing polymerizable vinyl monomers or chemical crosslinking of polymers. Synthetic polymers

used in the synthesis of hydrogels are poly (vinyl alcohol) (PVA), poly (ethylene glycol) (PEG), poly (ethylene oxide) (PEO), poly (2-hydroxyethyl methacrylate) (PHEMA), poly (acrylic acid) (PAA), and poly (acrylamide) (PAAm) etc. Some of synthetic polymer hydrogels are discussed in the section below.

2.1.4.1 Hydrogels Based on Poly (acrylic acid) derivatives

Acrylic acid based hydrogels are pH-sensitive due to the presence of anionic carboxyl groups and show higher swelling at basic pH while low swelling at acidic pH compared to hydrogels containing nonionic or neutral pendant groups. The high swelling at basic pH might be owing to electrostatic repulsion of carboxylate ions formed at basic pH as a result of deprotonation of carboxylic groups. Acrylic acid based hydrogels have been extensively prepared and used in numerous fields specifically in the biomedical field due to excellent adhesive properties. Poly (acrylic acid) and glycidyl methacrylate dextran copolymer hydrogels were prepared using UV irradiation. Synthesized hydrogels exhibited pH-sensitive swelling in the presence of dextranase at pH 7.4 (Kim & Oh, 2005). Lee *et al.* reported glycerol crosslinked poly (acrylic acid) hydrogel by polymerizing acrylic acid in the presence of benzoyl peroxide and novozym 435. This hydrogel showed 100 % higher swelling in neutral, acidic, and basic pH (Lee et al., 2011). Furthermore, poly (acrylic acid) hydrogel was prepared by free radical copolymerization using N, N'-methylenebisacrylamide as a crosslinking agent (Amin et al., 2012). Nho *et al.* synthesized acrylic acid hydrogels by irradiating the acrylic acid solution using electron beam of maximum 75 kGy and physical properties such as swelling ratio, mucoadhesion and gel contents were investigated (Nho et al., 2014).

Methacrylic acid is a derivative of acrylic acid and it has also significant attraction in the biomedical field. Kou *et al.* synthesized poly (2-hydroxyethyl methacrylate-co-methacrylic acid) hydrogel slabs and cylinders using free radical polymerization.

Hydrogel slabs were synthesized using redox couple ammonium persulfate and sodium metabisulfite as an initiator while tetraethyleneglycol dimethacrylate (TEGDMA) as a crosslinker. Hydrogel cylinders were synthesized using 2, 2'-azobisisobutyronitrile (AIBN) and TEGDMA as an initiator and crosslinking agent, respectively. Furthermore, phenylpropanolamine drug release was studied at different pH via desorption method (Kou et al., 1988). In another study, Park *et al.* synthesized pH-sensitive poly (vinyl alcohol-co-acrylic acid) and poly (vinyl alcohol-co-methacrylic acid) hydrogels via grafting of acrylic acid and methacrylic acid on PVA hydrogels in two steps using gamma irradiation. Initially, PVA hydrogels were prepared using gamma rays of 50 kGy and then acrylic acid and methacrylic acid were grafted onto PVA hydrogels with irradiation of 5-20 kGy. Grafted hydrogels showed pH sensitive swelling properties and pH-controlled insulin release behavior (Park et al., 2004). Moreover, interpenetrating network (IPN) of methacrylic acid and PVA hydrogels has been prepared using glutaraldehyde as crosslinking agent via water-in-oil emulsion method. The synthesized hydrogels showed pH-sensitive swelling property and release of ibuprofen (Mundargi et al., 2008).

2.1.4.2 Hydrogels Based on Poly (acrylamide) derivatives

Many acrylamide hydrogels have been prepared and utilized in numerous fields. Poly (acrylamide) hydrogels are hydrophilic, neutral and possess significant valuable physical and chemical properties for potential applications as biomaterial, immobilization of cell and biocatalyst, drug delivery systems, heavy metal ions absorption and bio separator. Saraydin *et al.* synthesized poly (acrylamide) hydrogels using chemical free radical initiation and gamma ray irradiation (0.72 kGy hr^{-1}) method in the presence of three different crosslinking agents. The synthesized gel displayed different swelling ratio ranged from 255 % to 1450 % depending upon the synthesis method, crosslinking agent type and concentration. Poly (acrylamide) hydrogels are weak in hydrolytic stability and mechanical strength. Attempts have been made to improve their properties by

copolymerization with other monomers (Saraydın et al., 2004). Poly (acrylamide-co-acrylic acid) hydrogel has been synthesized by free radical polymerization. The rheological study of the hydrogels revealed the increase in mechanical strength of copolymer hydrogels (Nesrinne & Djamel, 2013). In another study, poly (acrylamide-co-acrylic acid)/poly (acrylamide) super porous and IPN hydrogels were prepared by prepolymerization, synchronous polymerization and frothing process. The swelling property was observed to be high while low in compressive strength. Furthermore, the IPN hydrogels showed decrease in water absorption whereas increase in water retention and compression strength (Ao et al., 2009). However, poly (alkylacrylamide) hydrogels are thermosensitive although most of the hydrogels show negative temperature sensitivity. These hydrogels have lower critical solution temperature (LCST) and show contraction upon heating above lower critical solution temperature (LCST) (Hirotsu et al., 1987). Poly (N-isopropyl acrylamide) (PNIPAM) is the most important thermosensitive polymer and its hydrogels have been extensively studied in the numerous fields. Matzelle *et al.* prepared PNIPAM and poly (acrylamide) hydrogels to investigate the effect of temperature on elastic properties. Elastic properties of PNIPAM hydrogel was temperature dependent while poly (acrylamide) hydrogel had very slight response to change in temperature (Matzelle et al., 2003). PNIPAM copolymer hydrogels have been extensively observed as biomaterial for the pulsatile delivery of thrombolytic and antithrombotic streptokinase and heparin (Brazel & Peppas, 1996). Panayiotou *et al.* prepared poly (N, N'-diethyl acrylamide) (PNDEAM) and poly (N-isopropyl acrylamide) hydrogels through free radical polymerization and compared the swelling-deswelling-reswelling, insulin storage, and controlled release ability. The results revealed the stronger dependency of PNDEAM hydrogel swelling over crosslinking agent, slower reswelling kinetics and faster insulin release as compared to PNIPAM hydrogel (Panayiotou & Freitag, 2005).

2.1.5 Natural Polymers in Combination with Synthetic Polymer Hydrogels

Natural polymers have very weak mechanical strength which limits its applications in the biomedical field. In contrast, synthetic polymers are gaining more and more attraction and can be used in variety of fields because of their easy availability, low cost, and convenient modification of properties according to their applications. Moreover, synthetic polymers have excellent mechanical properties (Hu et al., 2014). Nevertheless, synthetic polymers produce lots of non-degradable solid waste which causes environmental pollution.

Chitosan based hydrogel formulations involving formaldehyde as a crosslinking agent release the drug at acidic pH which is a pH of stomach (Chen et al., 2004). Chen *et al.* synthesized semi-interpenetrating networks (semi-IPN) of chitosan-graft-poly (methacrylic acid) via free radical mechanism using formaldehyde as a crosslinker and 2, 2'-azo bis-isobutyronitrile as an initiator (Chen et al., 2005). Chitosan-graft-poly (acrylic acid-co-hydroxyethyl methacrylate) hydrogel membranes were synthesized using cerium ammonium nitrate chemical initiator. The grafting of copolymer on chitosan was further characterized using different techniques (Dos Santos et al., 2006). Agnihotri *et al.* fabricated semi-IPN chitosan-poly (acrylamide-co-ethylene oxide) hydrogel microspheres. In the first step, poly (acrylamide-co-ethylene oxide) was prepared by free radical mechanism and embedded it in the glutaraldehyde (GA) crosslinked chitosan. These hydrogel microspheres were used to encapsulate and delivery of anticancer drug (Agnihotri & Aminabhavi, 2006). On the other hand, novel pH sensitive IPN of acrylamide-grafted-PVA crosslinked with chitosan using glutaraldehyde was used to deliver antibiotic drug. The hydrogel demonstrated prolonged release of the drug up to 10 hours (Rao et al., 2006). Stimuli sensitive chitosan grafted poly (acrylic acid), poly (hydroxy propyl methacrylate), PVA, and gelatin hydrogels were prepared using gamma rays. (Sokker et al., 2009). Lejardi *et al.* reported hydrogel blends of chitosan and

modified PVA-graft- glycolic acid by mixing chitosan solution with modified PVA under constant agitation. These hydrogels showed enhanced rheological properties (Lejardi et al., 2014). A pH responsive semi-IPN of N-carboxyethyl chitosan and PHEMA hydrogels were synthesized through photo polymerization. This hydrogel exhibited good mechanical properties and sustained release of 5-fluorouracil (Zhou et al., 2008). Hydrogel films of pectin grafted acrylamide which crosslinked with glutaraldehyde were also reported elsewhere. This formulation showed better film forming, gelling and mechanical properties as compared to pure pectin (Sutar et al., 2008). Cellulose supported synthetic polymerizable monomers hydrogels were prepared by using chemical, photo, and gamma ray initiation. Some disadvantages of these techniques are due to non-availability and expensive equipments are required and difficulties in homopolymerization (Karlsson & Gatenholm, 1997). Interpenetrating network of guar gum and PVA were reported using glutaraldehyde as a crosslinking agent. These IPN hydrogels were used in drug delivery systems (Soppimath et al., 2000). In other study, grafted copolymer of guar gum and acrylamide hydrogel microspheres were prepared using GA as a crosslinking agent. These hydrogels were further characterized and tested as an antihypertensive drug delivery (Soppirnath & Aminabhavi, 2002). Hydrogel microparticles of hydroxyethyl starch-grafted- PHEMA were prepared by free radical polymerization and protein release was studied. Results showed that protein release was dependent upon hydrogel network density, and size of entrapped protein (Schwoerer et al., 2009). Other hydrogel formulations including alginate, carrageenan, alginic acid, gum arabic, and xanthan gum modified with synthetic polymers as well as synthetic polymerizable monomers through different methods have been reported. In our work, we synthesized hydrogels comprised of natural and synthetic polymers using different crosslinking agents for anti-cancer, anti-asthma and anti-inflammatory drug delivery at various pH.

2.1.6 Types of Hydrogels

Hydrogels may perhaps chemically stable or may degrade and ultimately disintegrate and dissolve. Chemically stable hydrogels most often formed by crosslinking of polymers through covalent bond. These gels are called permanent or irreversible hydrogels. However, physical gels form when their networks are detained together by secondary forces including hydrogen bonding, ionic or hydrophobic forces and molecular entanglements (Hoffman, 2012). Both types of hydrogels can be synthesized from natural and synthetic polymers with heterogeneous association of autonomous domains and possess different molecular associations (Bordi et al., 2002).

2.1.6.1 Physical Hydrogels

Polymer networks should gratify the following conditions to form hydrogels: a) strong inter-chain interactions in order to form stable junction points in the molecular network, and b) polymer network must encourage the access and residence of water within the hydrogel. Hydrogels fulfill these demands may perhaps be formed by non-covalent approaches such as electrostatic, hydrogen bonding, and hydrophobic forces among polymer chains. The hydrogels form by these interactions are solely physical gels and have high water sensitivity and thermo-reversibility (Berger et al., 2004). These gels have a short life time in physiological media, ranging from a few days to a month. Therefore, physical gels are good for short-term drug release applications. Because the gelation does not require any toxic covalent crosslinker molecules, it is always safe for clinical applications. Polysaccharide-based physical hydrogels can be synthesized by mixing the polymers in suitable circumstances. For example, ionic complexation of chitosan with small anionic molecules i.e., sulfates, phosphates, and citrates or anions of Pt (II), Pd (II), and Mo (VI) can form physical hydrogels. Anions bind to the chitosan via protonated amino group of chitosan. Properties of the formed hydrogels depend on the charge and size of anions as well as concentration and degree of deacetylation of chitosan. However,

chitosan has slight or no charge above pH 6, this results in reduction of ability in chitosan to form ionic complexes and its applications in physiological media (Brack et al., 1997). Chitosan derivatives also form physical hydrogels through ionic interaction. N-succinyl chitosan formed hydrogel beads and blends with alginate in the presence of Ca^{2+} , and Zn^{2+} ions (Fan et al., 2010). For example, alginate is a well-known polysaccharide that can be crosslinked with Ca^{+2} ions (Gacesa, 1988) via ionic interaction. Carrageenan comprised of α -D galactose and β -D-galactose with different fraction of sulfate ions can form hydrogel in the presence of K^+ ions. Although it may also form hydrogels in the absence of salt solutions, the hydrogels without metal ions are relatively weaker than hydrogels formed in the presence of metal ions (Hossain et al., 2001).

Furthermore, polyelectrolyte hydrogels can also be prepared by complex formation of polycations with polyanions. Chitosan as a polycationic polysaccharide formed complex with polyanions such as dextran sulfate or polyphosphoric acid (Janes et al., 2001). Other natural type anionic polysaccharides such as alginate, carrageenan, carboxymethyl cellulose, pectin, and xanthan also form complex with the chitosan. Chitosan can also form polyelectrolyte complexes with synthetic type anionic polymer such as poly (acrylic acid). The stability of these complexes depends on the charge density, pH, solvent, ionic strength and temperature.

Physical hydrogels can also be prepared by physically blending of non-ionic polymers. These polymers form intersection points in the form of crystallites after freeze dried or freeze-thaw cycles. Hydrogel formation is most likely formed by crystallization due to association of chains via hydrogen bonding. For example, aqueous solution of PVA formed gel having weak mechanical strength when kept at room temperature. After the process of freeze-thaw, aqueous solution PVA formed hydrogel. Mechanical strength of this hydrogel became stronger than before the process of freeze-thaw. The properties of

hydrogels depended on the PVA concentration, time and number of freeze-thawing cycles (Yokoyama et al., 1986). Moreover, addition of polysaccharides such as chitosan reduced the crystallinity of PVA hydrogels, dextran increased the process of crystallization of PVA hydrogels, and alginate increased the mechanical strength of the PVA hydrogels (Cascone et al., 1999; Takamura et al., 1992).

2.1.6.2 Chemical Hydrogels

Formation of the physical gels through clustering of molecules cause formation of free chain loops and thus inhomogeneity that signify short-lived network imperfection (Campoccia et al., 1998). Chemical crosslinked hydrogel networks are easy to be controlled as compared to physical hydrogels because their synthesis and applications are not only dependent on pH. Chemical crosslinking can be used to transform the physical properties of the hydrogels. Usually, the swelling behavior, biodegradability, and mechanical strength have been modulated via covalent crosslinking. Covalent crosslinking can be done through numerous approaches. These are discussed below:

(a) Crosslinking by Small molecules

Polymers can be crosslinked using mono and bi-functional small molecules such as formaldehyde, glutaraldehyde, genipin, diethyl squarate, ethyleneglycol diglycidyl ether (EGDE), and blocked diisocyanate as revealed in Table 2.3. Crosslinking of polymers using these small molecules have been reported and reviewed extensively. Covalent crosslinked polymers have improved mechanical strength than physically crosslinked polymers. In spite of offering many attractive properties, the biocompatibility of some crosslinkers is still unknown. In order to avoid the introduction of crosslinking agents, polymers have been functionalized with desired reactive functional groups for synthesize hydrogels in situ. Numerous hydrogels have been prepared based on the selective functional groups as shown in Table 2.4. Chitosan hydrogels have been synthesized

through Schiff bases with other pre-functionalized polysaccharides such as oxidized dextran and aldehyde hyaluronic acid (Weng et al., 2007). Tan *et al.* prepared N-succinyl chitosan/aldehyde functionalized hyaluronic acid injectable composite hydrogels through a Schiff base mechanism. It was observed that the compressive modulus, which is an important factor for cartilage tissue engineering, improved with an increasing amount of NSC in the hybrid hydrogel (Tan et al., 2009b). Similarly, other hydrogels of cellulose and alginate have also been prepared (Ito et al., 2007; Lee et al., 2001). Furthermore, amino group containing polymers such as chitosan and its derivatives form hydrogels via Michael addition reactions. The amino groups react with the vinyl group of other polymers. Metters *et al.* prepared chitosan-polyethylene oxide (PEO) hydrogels through Michael addition reactions. In the first step, chitosan treated with 2-carboxyethyl acrylate to form acrylated chitosan and then processed with thiolated PEO through Michael addition reaction. This method is very popular due to short reaction time and comparatively compassionate reactivity towards biomolecules. Hydrogels prepared through this method have also enhanced mucoadhesive properties (Kim et al., 2007). In spite of many advantages of this method, several disadvantages also exist. Hydrogel preparation using this method involves multi-step preparation and purification. Moreover, polymers might become cytotoxic after functionalization with the reactive groups.

(b) Crosslinking through Ionizing radiation

Hydrogels have been prepared through light sensitive functional groups. This technique has significant advantages such as ease and speedy preparation, low cost of production compared to chemical crosslinking methods. Ono et al. reported UV light irradiated chitosan hydrogels by introducing azide and lactose as light sensitive moieties. Azide group converted into nitrene group after UV irradiation that bound to amino groups of chitosan to form hydrogel in short time (Ono et al., 2000). Other UV irradiated chitosan

hydrogels were prepared by pre-functionalization with photo-sensitive acrylates of chitosan and pluronic acid (Yoo, 2007).

Light sensitive polymers form hydrogels in situ. Hydrogels formation via this method has some serious drawbacks. Irradiation crosslinking requires light sensitizer and delayed irradiation which causes increase in local temperature and damage of cells and tissues. The functional groups and proposed mechanism of UV light sensitive are shown in Table 2.3.

University of Malaya

Table 2.3: Crosslinking of polymers through small molecules and light sensitive functional groups

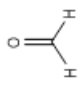
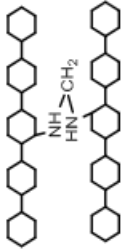
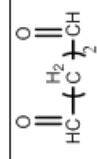
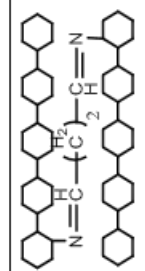
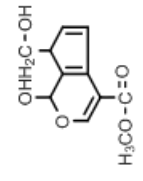
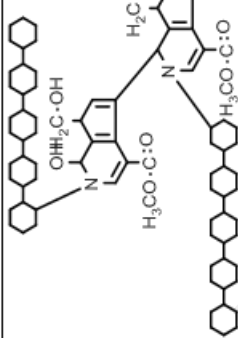
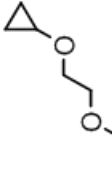
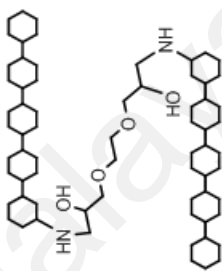
Agent	Target functional group	Reaction conditions	Crosslinkage	Comments
 Formaldehyde	Primary amines and aldehydes	Reaction favors basic and neutral pH		Reaction takes one hour to complete. Difficult to remove trace formaldehyde
 Glutaraldehyde	Primary amines and aldehydes	Reaction favors basic and neutral pH		Reaction takes one hour to complete.
 Genipin	Primary amines and aldehydes	Independent pH		Nontoxic crosslinker and can undergo self-polymerization
 EGDMA	Primary amines and oxiranes	Basic pH and at high temperature		Weak base, reaction takes one hour. Hydrogels beads form

Table 2.3: Crosslinking of polymers through small molecules and light sensitive functional groups (Continued)

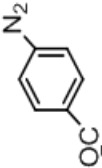
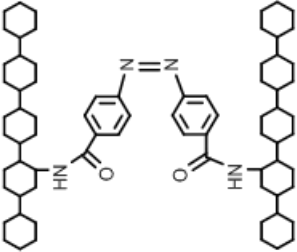
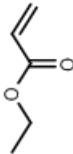
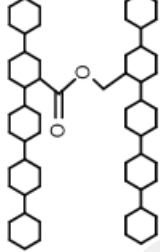
	Agent	Target functional group	Reaction conditions	Crosslinkage	Comments
Light sensitive groups	 <p>Functional azides</p>	<p>Primary amines</p>	<p>pH Independent</p>		<p>Multi step crosslinker. Suitable for injectable hydrogel synthesis</p>
	 <p>Functional acrylates</p>	<p>Other acrylic acids</p>	<p>pH Independent</p>		<p>Multi step crosslinker. Suitable for injectable hydrogel synthesis</p>

Table 2.4: Crosslinking of polymers through reactive functional groups

Reaction	Reaction conditions	Reactive polymer groups	Crosslinkage	Comments
Schiff base mechanism	Neutral pH			Good candidate for in situ gel formation. Reaction takes minimum 10 minutes
Disulfide bonding	Neutral pH			Good candidate for in situ gel formation and hydrogels have good mucoadhesivity
Michael addition	Weak base and in presence of catalyst			Good candidate for in situ gel formation and hydrogels have good mucoadhesivity

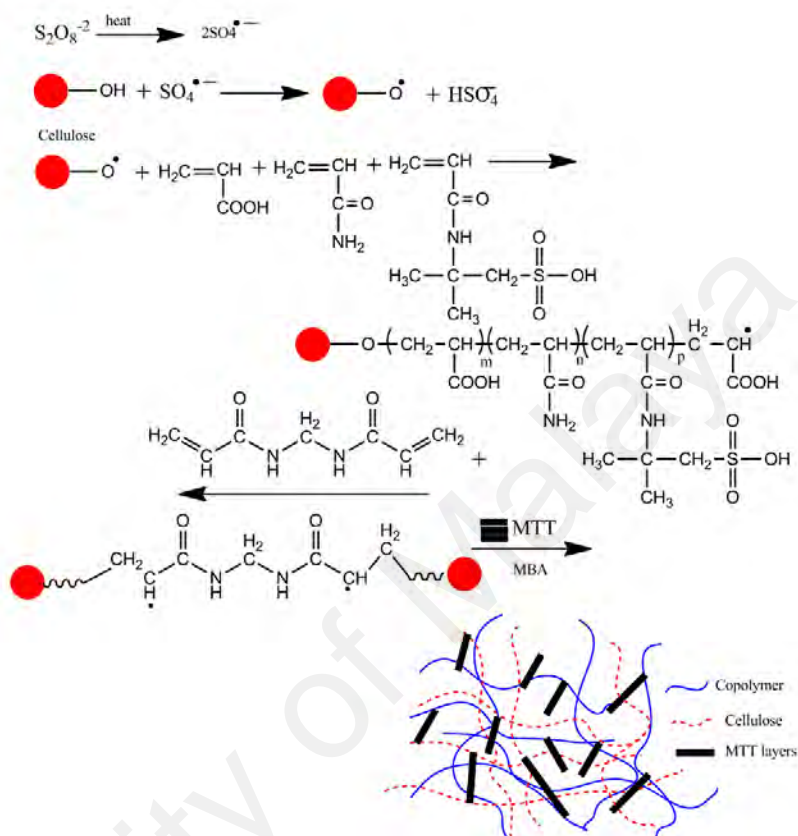
(c) Crosslinking through Free radical Mechanism

The free radical polymerization of low molecular weight monomers in the presence of crosslinking agent results in the development of chemically crosslinked hydrogels. The initiation reactions start by using initiator such as potassium persulfate (KPS), ammonium persulfate (APS), ceric ammonium nitrate, ferrous ammonium sulfate, 2,2'-azobisisobutyronitrile (AIBN), and benzoyl peroxide. In this mechanism, vinyl monomers radically polymerize in the presence of crosslinker to form chemically crosslinked hydrogels. Vinyl monomers including acrylic acid, acrylamide, vinyl chloride, styrene, epoxide, N-vinyl-2-pyrrolidone, and 2-hydroxyethyl methacrylate. The crosslinking agents used in the free radical mechanism are N, N'-methylene bisacrylamide (MBA), ethyleneglycol dimethacrylate (EGDMA), melamine trimethylacrylamide and melamine triacrylamide. The crosslinked homopolymers such as poly (2-hydroxyethyl methacrylate) (PHEMA), polyvinylpyrrolidone (PVP) and copolymers of N-vinyl-2-pyrrolidone and 2-hydroxyethyl methacrylate (HEMA) are synthesized by free radical polymerization using melamine trimethylacrylamide and melamine triacrylamide as crosslinkers and AIBN as initiator (Atta & Arndt, 2004).

Moreover, free radical mechanism is used to graft synthetic monomers over natural polysaccharides. Grafting is a general way to improve the properties of polysaccharides such as complexation, chelating and absorption enhancing properties, and solubility in water as well as in organic solvents. Grafting also improve some interesting properties related to biomedical applications such as biodegradability, biocompatibility, mucoadhesivity, and mechanical strength. Numerous hydrogels have been reported in literature in which natural polymers such as chitosan, cellulose, starch, pectin, alginate, hyaluronic acid, dextran, carrageenan, and gums have been grafted by synthetic monomers in the presence of crosslinking agent to improve their intrinsic properties. Hydrogels of chitosan and its derivatives have been prepared by grafting of synthetic

monomers and their properties are extensively investigated. The pH sensitive chitosan-graft-poly (acrylamide) hydrogels have been prepared by Pourjavadi *et al.* using APS and MBA as an initiator and crosslinker, respectively. The results revealed that swelling ratio is dependent on the acrylamide contents, MBA and alkaline hydrolysis of hydrogels further increased the swelling ratio. The swelling kinetics was observed to be the second order kinetics (Ali Pourjavadi & Mahdavinia, 2006). In another study, Mahdivinia *et al.* prepared chitosan-graft- poly (acrylamide-co-acrylic acid) hydrogels using KPS as an initiator and MBA as a crosslinker, they studied the effect of pH and salt solution on the swelling properties of hydrogels. The alkaline hydrolysis was also done to observe the swelling properties and found that alkaline hydrolyzed hydrogels having greater amount of acrylamide showed higher swelling ratio and non-hydrolyzed hydrogels having greater amount of acrylic acid showed greater swelling. This study was in good agreement with the previous one (Mahdavinia *et al.*, 2004). Moreover, free radical mechanism is used to prepare carboxymethyl chitosan/acrylic acid hydrogels by copolymerization in the presence of vinyltriethoxysilane as a crosslinker using KPS as an initiator (Yasin *et al.*, 2008). Pourjavadi *et al.* synthesized super porous kappa-carrageenan-g-poly (acrylic acid) in air via free radical initiator, APS in the presence of MBA. The synthesis of hydrogel was optimized by varying the composition of reaction. Appreciable swelling capacity was reported in different salt solutions, especially in sodium chloride solution due to anti-salt characteristics of the sulfate groups in carrageenan of the super absorbing hydrogels. Moreover, the results revealed that the presence of air had no significant effect on hydrogels and swelling behavior (Pourjavadi *et al.*, 2004). The copolymerization and crosslinking of acrylic acid and kappa carrageenan using vinyltriethoxysilane as silane crosslinker and KPS as an initiator synthesized a hydrogel network structure. (Rasool *et al.*, 2010). Elvira *et al.* prepared novel biodegradable hydrogels of acrylamide and acrylic acid in the presence of starch using free radical mechanism. The hydrogels showed

desirable characteristics such as pH sensitivity, biodegradability, and swelling properties (Elvira et al., 2002).



2.6: The plausible mechanism of carboxymethyl cellulose-g-poly (acrylamide-co-acrylic acid-co-2-acrylamido-2-methyl-1-propanesulfonic acid (AMPS)/montmorillonite (MMT)) hydrogel synthesis (Bao et al., 2011)

Bao *et al.* reported superabsorbent hydrogels of sodium carboxymethyl cellulose-graft-poly (acrylamide-co-acrylic acid-co-2-acrylamido-2-methyl-1-propanesulfonic acid (AMPS))/ montmorillonite (MMT)) using KPS and MBA as an initiator and crosslinking agent, respectively. These super porous hydrogels contained porous networks owing to MMT and carboxymethyl cellulose with side chains carrying carboxamide, carboxylate and sulfate. The swelling ratio of hydrogels exhibited high external pH sensitivity. The hydrogels showed swelling ratio in the following order in the presence of salt solutions $K^+ > Na^+ > Ca^{2+} > Mg^{2+}$. The plausible mechanism of hydrogel synthesis is shown in Figure 2.6 (Bao et al., 2011).

2.1.6.3 Interpenetrating Network (IPN) Hydrogel

Crosslinked polymer networks can be supplementary reinforced through interlocking secondary polymers within the entangled networks. A polymer comprising of two or more networks which are at least partially interlaced on a molecular scale but not covalently bonded to each other and cannot be separated unless chemical bonds are broken is known as interpenetrating polymer network (IPN). In other words, when the entangled polymer networks are allowed to swell in an aqueous solution in the presence of polymerizable monomers and these monomers polymerize to form physically associated networks are called interpenetrating polymer network (IPN). There are two different possibilities of IPN formation, if one polymer network is crosslinked while the other polymer physically associated with the crosslinked polymer the network formed is called semi- interpenetrating polymer network (semi-IPN). However, if the second polymer is also crosslinked with the already crosslinked polymer network, then the network formed is called full-interpenetrating polymer network (full-IPN). Numerous polymers form these types of networks in order to balance the deficiency of other polymer. These polymers may be natural polysaccharides, proteins or synthetic hydrophilic polymers containing CONH_2 , OH , SO_3H , COOH , NH_2 , and quaternary ammonium groups. IPN hydrogels can be prepared via three different routes by

combining of natural polymers as well as synthetic polymers. These routes are presented in Figure 2.7.

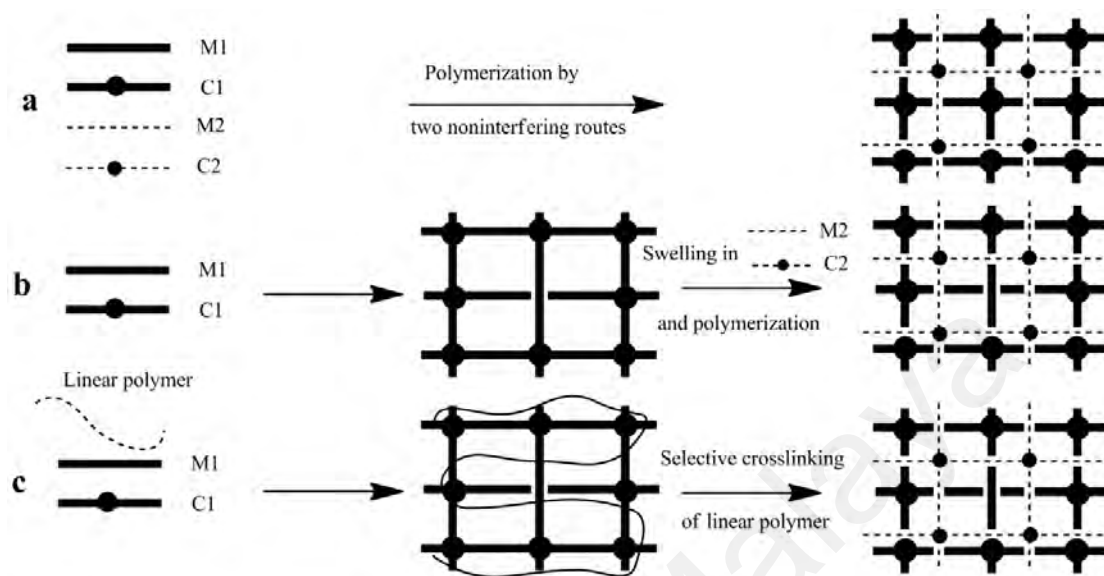


Figure 2.7: Proposed reaction mechanism of IPN formation a) simultaneous strategy; b) sequential strategy; c) selective crosslinking of a linear polymer entrapped in semi-IPN (Dragan, 2014)

According to the chemistry of preparation, IPN hydrogels can be classified in: (i) simultaneous IPN, when the precursors (M1, C1, M2, and C2) of both networks are mixed and the two networks are synthesized at the same time by independent, noninterfering routes such as chain and stepwise polymerization (Figure 2.7(a)), and (ii) sequential IPN, typically performed by swelling of a single-network hydrogel into a solution containing the mixture of monomer, initiator and activator, with or without a crosslinker (Figure 2.7(b)). If a crosslinker is present, fully-IPN result, while in the absence of a crosslinker, a network having linear polymers embedded within the first network is formed (semi-IPN). When a linear polymer, either synthetic or biopolymer, is entrapped in a matrix, forming thus a semi-IPN hydrogel, fully-IPN can be prepared after that by a selective crosslinking of the linear polymer chains (Figure 2.7 (c)) (Dragan, 2014).

(a) *Semi-Interpenetrating Network (semi-IPN) Hydrogels*

Numerous attempts have been performed to synthesize semi-IPN hydrogels of polysaccharides and synthetic polymers for the efficient biomedical applications. Semi-

IPN chitosan based hydrogels have been reported by several researchers. In these hydrogels, cellulose and its derivatives and acrylamide-graft-dextran have been blended with chitosan followed by selective chitosan crosslinking through glutaraldehyde (Ahmed et al., 2009; Angadi et al., 2010; Cai & Kim, 2009; Rokhade et al., 2007; Rokhade et al., 2007). Diclofenac sodium was loaded in the semi-IPN hydrogels of crosslinked chitosan entrapped with acrylamide-graft-hydroxyethyl cellulose. The drug loading efficiency was found to be ranging from 50 % to 66 %. The schematic representation of crosslinked chitosan entrapped with acrylamide-g-hydroxyethyl cellulose is shown in Figure 2.8.

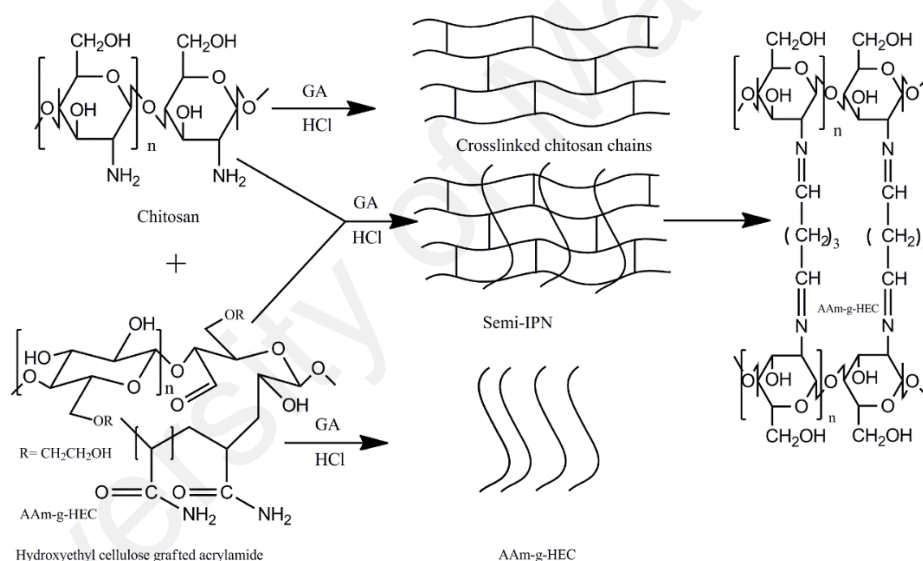


Figure 2.8: The proposed reaction mechanism of semi-IPN hydrogel of chitosan/ acrylamide-g-hydroxyethyl cellulose (Angadi et al., 2010)

Yang *et al.* prepared semi-IPN hydrogels comprised of poly (ethylene glycol) grafted on alginate and carboxymethyl chitosan for the oral delivery of protein in the intestine. They found that the hydrogels were promising in protein delivery (Yang et al., 2013). Semi-IPN hydrogels of chitosan and its derivatives with numerous ionic polymers including cationic groups such as amine and quaternary ammonium groups and anionic group like carboxylic group were synthesized. These hydrogels were synthesized by selective crosslinking of polyelectrolytes in the presence of chitosan or crosslinking of chitosan in

the presence of pre-formed polyelectrolytes. The studies revealed that ionic interaction of COO^- ions of polyelectrolytes and NH_3^+ from chitosan resulted in an increase in mechanical strength of the hydrogels while decrease in swelling ratio of the gels. These interactions increased the crosslinking intensity of the hydrogels. These hydrogels showed reversible response to solutions of various pH and strength of salt. These hydrogel systems were found to be more efficient for the controlled release of drugs. All these improvements attracted researchers towards such systems (Chen et al., 2005; El-Sherbiny et al., 2005; Guo et al., 2007; Kim et al., 2005; Kim et al., 2004; Milosavljević et al., 2011; Povea et al., 2011; Pulat & Asil, 2009; Sharma, 2006; Yin et al., 2008). Various semi-IPN hydrogels based on chitosan and non-ionic polymers have also been reported. These semi-IPN hydrogels were synthesized through either crosslinking of chitosan in the presence of uncrosslinked nonionic monomers or nonionic monomers were crosslinked in the presence of chitosan solution. The nonionic monomers were mostly consists of acrylamide and its derivatives and 2-hydroxyethyl methacrylate. The swelling kinetics studies revealed that all gels followed Fickian diffusion mechanism for water transport (Babu et al., 2008; Han et al., 2008; Kim et al., 2004; Martinez-Ruvalcaba et al., 2009; Xia et al., 2005). The modulation in mechanical strength and water contents were investigated in all these hydrogels. The mechanical strength and water contents were dependent on the composition of hydrogels. The other factors might be the use as controlled release carrier and scaffolds in tissue engineering.

Several semi-IPN hydrogels comprised of alginate and synthetic polymers have been investigated. These hydrogels had novel properties such as outstanding porosity, sustained drug delivery, multi-responsive and electrical sensitivity. Alginate and methacrylic acid based semi-IPN revealed significant response to electrical field. Therefore, it was suggested that the hydrogels should be used in artificial organ component, sensors, and electrical sensitive drug delivery systems (Kim et al., 2004).

Amphoteric semi-IPN hydrogels have been prepared through graft copolymerization of acrylic acid on cationic starch in the presence of poly (methacryloyloxyethyl ammonium chloride) (PDMC). The salt link between quaternary ammonium groups of PDMC and COO^- ions of starch-graft-poly (acrylic acid) were investigated by FTIR analysis. PDMC was entrapped within the starch-graft-poly (acrylic acid) hydrogel and was not washed away during washing process. The hydrogels were highly sensitive to pH but with the increase in concentration of PDMC, the swelling ratios were decreased in the basic medium due to unavailability of carboxylic groups (Li et al., 2009). Other polysaccharides like cellulose, kappa carrageenan, hyaluronic acid, guar gum, and xanthan also form semi-IPN hydrogels. Semi-IPN hydrogels of kappa carrageenan and poly (N, N-diethylacrylamide) were reported. These hydrogels were highly temperature sensitive (Chen et al., 2008).

(b) Full-Interpenetrating Network (Full-IPN) Hydrogels

When a linear polymer either natural or synthetic polymer is entrapped in the other matrix to form semi-IPN hydrogel, fully IPN may be formed by selective crosslinking of second polymer which is not already crosslinked. Formation of full-IPN can prevail over the thermodynamic incompatibility due to stable network formation and limited phase separation can be attained. The interlocked components of crosslinked network structures ensure the stability of full IPN polymer in the bulk and surface morphology. The major advantages of full-IPN are relatively compact hydrogels structure with improved mechanical strength, tunable physical properties and enhanced drug loading efficiency as compared to conventional hydrogels. The surface chemistry and pore size of full-IPN can be controlled to adjust the drug release rate, interaction between hydrogels and tissues of the body. Numerous natural and synthetic polymers can form full-IPN such as chitosan and PVA etc. The particular characteristics of this new material can be investigated by mechanical strength and resistance to wear. Fang *et al.* synthesized full-IPN hydrogel

composed of chitosan/PNIPAM. In these hydrogels, NIPAM was crosslinked with N, N'-methylenebisacrylamide while chitosan crosslinked with formaldehyde. They studied the properties of hydrogels including extraction of PNIPAM from crosslinked chitosan networks, phase transition behavior, and the swelling ratio measurements in water and in ethanol/water mixtures. The results obtained revealed dissimilarities from semi-IPN of chitosan/PNIPAM hydrogel. However, this hydrogel was found thermo sensitive as semi-IPN chitosan/PNIPAM hydrogel and showed transparency at 30 °C but became opaque above this temperature (Wang et al., 2001). Poly (vinyl alcohol) is hydrophilic polymer, having potential applications in the biomedical field, absorption of heavy metal ions, and removal of toxic dyes from the waste water. Kim *et al.* prepared and measured free water contents as well as swelling ratio of full-IPN hydrogel- based on chitosan/ PVA using UV irradiation. The results revealed fast swelling of the prepared hydrogel that reached equilibrium within one hour. The free water contents and swelling ratio were increasing with increase in the concentration of chitosan. The hydrogels also exhibited pH and temperature sensitive swelling behavior which revealed the significant applications in the biomedical field (Kim et al., 2003). Usually, nonporous hydrogels swell very slowly in the aqueous phase and also show low drug loading efficiencies. These drawbacks of such hydrogels limit their exploitation in the biomedical field. Therefore, super porous hydrogels restraining carboxymethyl chitosan/ poly (acrylamide-co-acrylic acid) hydrogels were prepared to improve mechanical strength, mucoadhesive force, and drug loading efficiency of the hydrogels. Swelling ratio of the hydrogels decreased with increasing the concentration of carboxymethyl chitosan, glutaraldehyde amount, and crosslinking time. However, by the formation of full-IPN structure, mechanical strength, mucoadhesive force, and drug loading efficiency of hydrogels were considerably enhanced. These full-IPN hydrogels were biocompatible. These characteristic of

hydrogels suggested the potential exploitation in mucosal drug delivery system (Yin et al., 2007).

Dragan *et al.* prepared semi-IPN hydrogels of chitosan/ polyacrylamide in which chitosan was entrapped in the polyacrylamide matrix. Moreover, full-IPN hydrogels were synthesized by selective crosslinking of chitosan with epichlorohydrin (ECH). This crosslinking was performed in alkaline medium and simultaneously amide group of polyacrylamide matrix was partially hydrolyzed to generate anionic sites. FTIR analysis demonstrated the partial hydrolysis of amide group and confirms the formation of full-IPN structure (Dragan et al., 2012).

Yin *et al.* prepared super porous IPN composed of acrylamide, sodium acrylate and sodium alginate. Acrylamide and sodium acrylate were crosslinked in the presence of sodium alginate. The CaCl_2 was added to crosslink sodium alginate in the semi-IPN hydrogels and sodium bicarbonate was used as blowing agent. These super porous hydrogels showed fast water uptake, high swelling ratio and pH sensitivity, biocompatible and had good mechanical properties (Yin et al., 2007). Other full-IPN alginate hydrogels have also been reported in the literature (Lee et al., 2006; Zdražil & Štěpánek, 2010). Anionic and cationic groups containing IPN hydrogels are not only stabilized by covalent linkages but also by ionic interaction of these groups as well. These ionic interactions improve the mechanical strength, promote the reversible pH and ionic strength responsive in hydrogels. These hydrogels form polyion complex due to presence of opposite charges. These types of hydrogels are very interesting category having significant potential applications as biomaterials.

2.1.7 Properties of Hydrogels

2.1.7.1 Mechanical Properties

Mechanical strength of hydrogels is incredibly imperative for pharmaceutical and biomedical applications. The assessment of mechanical strength of the hydrogels is necessary and significant for suitable physiological function in various perspectives such as for biomedical applications, tendon and ligament repair, replacement of cartilage, tissue engineering, wound dressing and drug delivery matrix. It is significant for the hydrogel to sustain its physical texture during release of therapeutic agents for specific time period.

The preferred mechanical properties of hydrogels may be attained by incorporating specific polymer, co-monomers, crosslinkers, and by changing the crosslinking degree. The strong gel network can be obtained with increasing the degree of crosslinking. However, too high in the degree of crosslink will result in low elongation and elasticity with greater brittleness. Elasticity is very significant to give increased flexibility to the crosslinked network and to assist in the movement of incorporated therapeutic moieties. Therefore, optimum degree of crosslinking for the hydrogels is essential in order to retain the compromise between mechanical strength and elasticity (Das, 2013).

The evaluation of mechanical properties of hydrogels can be done through numerous techniques such as compression and tension analysis which can be done by confined or unconfined, local indentation with a probe or frequency based tests using rheometry and dynamic mechanical analysis. Frequency based sinusoidal testing is usually done using rheometer. The sample is loaded on a specified geometry instrument and different type of sweep measurements can be performed (Oyen, 2014).

The viscoelastic properties of hydrogels can be investigated by rheometer. Rheology may be defined as “the science of deformability and flow of matter under stress or strain. It

comes from the Greek words “rheo” means flow and “-ology” for study of (Goodwin & Hughes, 2008). This definition was acknowledged by the American Rheology Society in 1929. Since past 3 centuries, ideal liquid and solid behaviors were characterized mathematically by Newton’s and Hooke’s law respectively. However, many materials possess transitional behavior between perfect liquids and solids. These behaviors cannot be explained by these classical theories. Scientists felt doubt after non-ideal behavior of fluids and silk thread described by Maxwell and Wilhelm Weber respectively. According to Maxwell, fluids showed elastic properties which were verified mathematically. Moreover, Wilhelm Weber found non-ideal elastic behavior of silk thread. These materials were typically classified as viscoelastic and non-Newtonian materials. The viscoelastic materials can be recovered after small deformation while the viscosity of non-Newtonian materials is stress and time dependent (Barnes et al., 1989).

The variable of shear stress and strain are important parameters in rheology. The shear stress is defined as “the ratio of force per unit area to cause disorder in the materials between plates”. The strain is “the ratio of deviation in displacement (x) of material to the height of the material (h) or more simply is $\tan \alpha$ ”. After applying force, the velocity of the movement is controlled by the internal force acting within the material. The mechanical properties of the hydrogels can be found by small deformation rheology experiments. When the hydrogel is deformed by applying force, the material particles are displaced relative to each other causing strain. Moreover, it is a well-known that elastic materials undergo change in shape on applying force resulting in elastic strain and return to their original shape when the force is removed. In contrast, the external force applied on the viscous materials causes’ irreversible strain. This input force causes the viscous materials to flow. However, hydrogels are neither fully viscous, nor completely elastic but show viscoelastic nature. The rheological experiments are conducted within the linear viscoelastic region (LVR) of the investigated materials. The LVR ensuring the

mechanical properties of hydrogels are not affected by the magnitude of imposed stress or strain. Moreover, deformation in viscoelastic materials by applying slow external force is still very small. This is owing to molecular arrangements in the polymers are still close to equilibrium. The mechanical behavior is then just a reflection of dynamic processes at the molecular level, which go on constant, even for a system at equilibrium.

For controlled-strain rheometers, the shear strain is defined as sinusoidal function of time (t) which can be expressed as in

$$\gamma(t) = \gamma_0 (\sin \omega t) \quad (\text{Equation 2.1})$$

Where γ_0 is magnitude of applied strain and ω is angular frequency of oscillation. It is measured in rad/s. The relation between angular frequency and frequency measured, f , in Hertz is $\omega = 2 \pi f$. Furthermore, the sinusoidal strain causes the sinusoidal stress which can be illustrated in Equation 2.2.

$$\tau(t) = \tau_0 (\sin \omega t + \delta) \quad (\text{Equation 2.2})$$

Where, τ_0 is the stress amplitude and δ is the difference in phase between two waves.

For controlled-stress rheometers, the shear stress is defined as sinusoidal function of time (t) which can be expressed in Equation 2.3.

$$\tau(t) = \tau_0 (\sin \omega t) \quad (\text{Equation 2.3})$$

The sinusoidal stress causes the sinusoidal strain which can be illustrated in Equation 2.4.

$$\gamma(t) = \gamma_0 (\sin \omega t + \delta) \quad (\text{Equation 2.4})$$

Purely elastic materials follow Hooke's law which states that stress and strain are always in phase. So phase angle is 0 ($\delta = 0^\circ$). On the other hand, pure viscous materials have two

different waves having phase angle 90° ($\delta = 90^\circ$). However, viscoelastic materials have phase angle somewhere in between $0-90^\circ$.

In small amplitude oscillatory measurements, the shear storage modulus (G'), loss modulus (G''), and loss factor, $\tan \delta$ are significant properties of hydrogels. The storage modulus evaluates the deformation energy stored during the process of shearing of a material which expresses its rigidity. The loss modulus measures the energy dissipated during shearing which attributes to flow behavior of material. The loss factor, $\tan \delta$ is the ratio of G'' and G' (G''/G'). When $\tan \delta$ is greater than 1 ($G'' > G'$), materials have more viscous characteristics. On the other hand, $\tan \delta < 1$ ($G' > G''$) means materials possess more elastic solid characteristics. The storage modulus and loss modulus are examined as a function of strain, time, and frequency. The gelation process can be investigated by observing the temporal assessment of storage and loss modulus. The LVR within which both moduli are independent of strain can be determined by observing these moduli of the material as a function of strain.

The behavior of hydrogel at different time scales can be investigated by measuring the moduli against frequency. When $G' \gg G''$ at high frequency for short time, the material have quite solid characteristics and $G'' > G'$ at low frequency for long time then material has dominant liquid behavior. Moreover, gelation kinetics and gel rigidity are very important factors which have significant influence on the material's application.

The mechanical properties of viscoelastic materials are independent of strain up to certain value known as critical strain. When strain increases above this value, storage modulus declines and a non-linear behavior is observed. The strain dependent G' and G'' measurement are the first step to investigate the LVR of a material at a frequency of 1 Hz. Further, the structure of material can be investigated at constant strain below the critical level. These observations provide more information about the effect of colloidal

forces and interactions among particles. Below the critical strain, G' is independent of frequency which shows the characteristics of solid materials. Conversely, frequency dependent G'' represents the fluid-like material. Jeong *et al.* observed the sol gel behavior of thermogelling chitosan-graft-(PEG- PAF). The storage and loss moduli were examined against frequency at 10 °C and 37 °C. It was observed that G'' higher than G' (sol behavior) at 10 °C while G' higher than G'' (gel behavior) at 37 °C. However, the storage modulus was independent of frequency (Kang *et al.*, 2012). The gelation mechanism and the stability of the gel material during the testing time and for significant exploitation at commercial level is another aspect. For this purpose, time sweep profile of the materials at critical strain and at frequency of 1 Hz can be carried out. Moura *et al.* investigated the gel kinetics and gel properties upon crosslinking of chitosan through genipin. The moduli results revealed the dominant of viscous behavior when the chitosan was in solution state. Upon addition of crosslinker (genipin), the elastic modulus increased due to the crosslinked gel network. It was also observed that gelation time decreased owing to increase in crosslinker concentration (Moura *et al.*, 2007).

2.1.7.2 Biocompatibility

The cytotoxicity of a biomaterial is very important in order to make it applicable in the biomedical field. Similarly, hydrogels should be biocompatible and non-toxic. Basically, the biocompatibility is the property of material to work efficiently with the host tissues and respond properly in an explicit environment. The bio-safety and bio-functionality are two basic elements of biocompatibility. If the hydrogels cannot fulfill these conditions, then they can be fouled. Toxic chemical used in the preparation of hydrogel formulations often cause challenge for *in vivo* biocompatibility. However, polysaccharides are widely regarded as being non-toxic, biologically compatible polymer and approved for dietary applications. Tokura *et al.* reported the *in vivo* cytotoxicity studies of different biodegradable polysaccharides. No acute toxicity was noticed in rat blood system (Yang

et al., 2012). Chan *et al.* investigated the cytotoxicity of chitosan, chitosan-PEG, and folic acid conjugated chitosan-PEG/DNA complexes. The results revealed the average cell viability of 90 % (Chan et al., 2007). In another study, in vitro cytotoxicity profile of chitosan, O-carboxymethyl chitosan, and N, O-carboxymethyl chitosan to breast cancer cells MCF-7. The results showed that these are very less toxic and cells had 98 % viability (Anitha et al., 2009). NSC is a well-known biocompatible material and, like chitosan, can be used in the preparation of hydrogels, microparticles, nanoparticles, and Nano spheres. Lu *et al.* observed the cytotoxicity of a NSC/carboxymethyl cellulose hydrogel on the proliferation of HEK 293T cells. The results demonstrated 93% cell viability after 48 hours (Lü et al., 2010). Moreover, cytotoxicity of NSC hydrogel formulations in 293T, CHO, HepG2, and HeLa cells have been investigated and found nontoxic nature of NSC (Lu et al., 2009; Lu et al., 2010). Chitosan is non-toxic and tissue compatible, but NSC is a synthesized derivative, and is known to significantly promote cell proliferation. Zhu *et al.* assessed in vitro cell toxicity and found that NSC had no negative effects on 3T3 fibroblasts up to 0.25 mg/ml (Aiping et al., 2006). Furthermore, Mishra *et al.* did the MTT assay of pectin/poly (vinyl pyrrolidone) (PVP) hydrogel membranes on B16 melanoma cells. The results showed that the hydrogel membranes did not induce significant cytotoxic effect even at high concentration of polymer solution. This indicates the biocompatibility of the hydrogel membranes (Mishra et al., 2008). Some synthetic polymers are non-toxic and biocompatible to living cells. Cytotoxicity of poly glutamic acid, poly (acrylic acid), poly (methacrylic acid), poly (ethacrylic acid), and poly (propacrylic acid) hydrogels was studied on HeLa cells and these hydrogels showed 90 % cell viability. Wang *et al.* investigated the cytotoxicity of methoxyl poly (ethylene glycol)-poly (caprolactone)-acryloyl chloride (PEC-AC) on HEK 293 cells and found that cell viability was decreased with the increase in concentration of PCE-AC. The minimum viability was found to be 60 % when the concentration of PEC-AC copolymer was 200

$\mu\text{g/ml}$ (Wang et al., 2010). Therefore, most of the polysaccharides are biocompatible and can be used as biomaterials. Moreover, the synthetic polymers are also non-toxic to some extent but less cytocompatible as compared to natural polysaccharides.

2.1.7.3 Biodegradability

The exploitation of biodegradable hydrogels is essential in the biomedical field. Biodegradability means breakdown of hydrogels into harmless end products by the living organism. The biodegradability of hydrogels depends on the moieties present in the systems and method of preparation. The processes of degradation include hydrolysis and solubilization of biological entities of hydrogels into end products. The hydrogels may degrade and eliminate from the body through bio absorption and bio erosion.

Numerous hydrophilic natural and synthetic polymers can be classified as biodegradable polymers. These polymers absorb water due to diffusion and swell up to large extent and eventually dissolve into water upon auxiliary water absorption. The degradation of these polymers depends on the several factors such as hydrophilicity, molecular weight, and polymer-water interaction. Other environmental factors being pH and temperature may also control the degradation through simple solubilization. However, this class of polymer is very limited. There is a range of polymers which cannot be degraded by simple hydrolysis but can be degraded through chemical hydrolysis. These polymers do not form hydrogels but combine with hydrogel forming hydrophilic monomers or polymers to form biodegradable hydrogels. These hydrogel systems usually undergo degradation through chemical hydrolysis of ester linkages. Moreover, hydrogels can also be degraded through enzyme hydrolysis and this class of hydrogels includes polymers for instance polysaccharides, proteins, and synthetic polypeptides. Due to significant advantage of enzymatic degradation, these polymers can be used in drug delivery systems. Enzyme hydrolysis occurs through the group of hydrolases which catalyze the hydrolysis of C-C,

C-O, and C-N bonds. Hydrolases that degrade the protein and polypeptide hydrogels are proteinases and peptidases, respectively. Furthermore, the biodegradation of polysaccharide hydrogels only occurs through glycosidase. Specifically, chitosan can be degraded by enzymes hydrolysis of glucosamine-glucosamine, glucosamine-N-acetyl-glucosamine and N-acetyl-glucosamine-N-acetyl-glucosamine. However, the degradation of chitosan also occurs through free radical and redox reaction. Lysozyme had been used to study the in vitro degradation of chitosan. It was found that 50 % acetylated chitosan showed 66 % viscosity loss in first 4 hours of incubation in buffer solution of pH 5.5 (Onishi & Machida, 1999). Modification of chitosan has no significant change in the rate of degradation. Trimethylchitosan showed degradation at the similar rate as chitosan but the rate of degradation was not sensitive to pH (Verheul et al., 2009). In vitro degradation of tripolyphosphate and glutaraldehyde crosslinked chitosan films were investigated by McConnell et al. where porcine pancreatic enzymes were used to investigate the degradation rate. The results revealed that glutaraldehyde crosslinked films showed higher rate of degradation than tripolyphosphate crosslinked hydrogels. Furthermore, NSC has considerable biodegradability in vitro as well as in vivo. Normally, the degradability of a hydrogel depends upon the pH, temperature, oxygen content, water potential, structure of the polymer network, crystalline nature of the polymer, and the type of linkages. Degradability is observed by a change in weight over a specific period of time. The biodegradability of NSC was confirmed using an NSC/OCMC hydrogel in phosphate buffer solution at 37 °C. In this hydrogel, Schiff-base linkages were hydrolytically susceptible and not stable, resulting in an enlarged lattice size of the network. This phenomenon led to disintegration of the hydrogel (Ito et al., 2007). Tan *et al.* also studied biodegradation of an NSC/PEG hybrid hydrogel in phosphate buffer solution at 37 °C. The results revealed that the hydrogel was biodegradable. Other polysaccharides like starch (Das et al., 2012), cellulose, dextran (Dijk-Wolthuis et al.,

1997), alginate, pectin (Majzoob et al., 2006), and natural gums hydrogels (Rana et al., 2011) are also biodegradable as chitosan and its derivatives. Some synthetic polymers are also biodegradable but the rate of degradation is very low as compared to natural polymers (Tan & Marra, 2010). Gao *et al.* studied the in vitro biodegradation of poly (acrylic acid) and its derivatives and poly (glutamic acid) in buffer solutions of pH 1.2 and 7.4 in the presence of proteinase. The results revealed the higher degradation rate at pH 7.4, while lower degradation at pH 1.2. This might be due to higher hydrophilicity at pH 7.4 and higher hydrophobicity at pH 1.2 (Gao et al., 2013).

2.1.7.4 Swelling Behavior of Hydrogel

The swelling response in different matrix environment such as water, pH and ionic strength is the characteristic of hydrogel to be used in different fields. The hydrogel respond to its biological and environmental media such as pH, ionic media, solvent, electric field, exposure to light and temperature (Angadi et al., 2010). The swelling kinetics and equilibrium are affected by different factors such as crosslinking ratio, chemical nature of polymers, ionic media, synthesis state (Ali Pourjavadi & Mahdavinia, 2006). Swelling is measured in terms of swelling ratio which is the weight swelling ratio of swollen gel to the dry gel. Crosslinking affects the swelling ratio of the hydrogel as highly crosslinked structures have less swelling ratio and vice versa. Chemical structure has also a significant function to the swelling property due to the hydrophilic and hydrophobic groups present on the polymer chains. Hydrogels containing more hydrophilic groups swells more as compared to the hydrophobic groups. The swelling of hydrogel is also affected by temperature and pH. The pH sensitive hydrogels swell due to the ionization of hydrophilic groups with variation in pH. Ionization produces electrostatic repulsion between like charges on the polymer and breaks the secondary bonding between the polymer chains. Swelling of hydrogel involves three steps: First is the diffusion of water into the hydrogel network, second is the loosening up of polymer

chains and third is the expansion of hydrogel network. The hydrogel in dehydrated state is referred as glassy state and in swollen form as rubbery state. The free spaces in the chains permit the solvent molecules to find the spaces when glassy or dry hydrogel make contact with the aqueous medium. When enough water is entered into the hydrogel matrix, the glassy state turns into the rubbery state named as swelling. The diffusion process is responsible for entrance and removal of the water from hydrogel matrix.

(a) Swelling Kinetics

Practically, swelling of the hydrogels follows first-order and second order kinetics, depends on the rate of swelling with respect to time, swelling capacity of the hydrogels, size distribution of the particles, and the polymer gel composition. The diffusion controlled system follows first-order kinetics. According to this, rate of swelling at any time is directly proportional to swelling medium contents before reaching the equilibrium absorbed water (W_e). The swelling of hydrogels is given in the equation 2.5.

$$\frac{dW}{dt} = k_f (W_e - W_t) \quad (\text{Equation 2.5})$$

Where, k_f is the rate constant for first-order kinetics, W_e is the amount of absorbate at equilibrium, and W_t is the absorbate at time t . Abovementioned equation expresses the swelling of hydrogels in the solvent and shrinkage on drying. The integration of this equation gives the following illustration in equation 2.6.

$$\ln \frac{W_e}{W_e - W} = k_f t \quad (\text{Equation 2.6})$$

The swelling process follows first-order if the graph between $\ln \frac{W_e}{W_e - W}$ and time t is a straight line. Moreover, polymer systems having limited swelling obey first-order kinetics under these two conditions: the swelling must be diffusion controlled and obeyed Fick's laws. However, the divergence from first-order kinetics is also possible, specifically at

longer swelling times and for extensive swelling of the hydrogel. It is very difficult to follow first-order swelling kinetics throughout the swelling process especially the process of polymer relaxation controlled over the swelling rather than diffusion. The second order swelling kinetics equation in terms of swelling rate is described in equation 2.7.

$$\frac{dW}{dt} = k_s (W_e - W_t)^2 \quad (\text{Equation 2.7})$$

Rearranging and Integrating the equation 2.7 between the limits when $t = 0$ to t , $W_t = 0$ to W_t which can be expressed as equation 2.8.

$$\int_0^{W_t} \frac{dW}{(W_e - W_t)^2} = k_s \int_0^t dt \quad (\text{Equation 2.8})$$

The equation 2.8 becomes:

$$\frac{t}{W_t} = \frac{1}{W_e} t + \frac{1}{W_e^2 k_s} \quad (\text{Equation 2.9})$$

Equation 2.9 may be written as:

$$W = \frac{k_s W_e^2 t}{1 + W_e k_s t} = \frac{r_o t}{1 + W_e k_s t} \quad (\text{Equation 2.10})$$

Where r_o is the initial rate of swelling.

$$r_o = k_s W_e^2.$$

According to equation 2.9, profile of $\frac{t}{W_t}$ versus t should give a straight line with a slope

of $\frac{1}{W_e}$ and an ordinate of $\frac{1}{W_e^2 k_s}$.

2.1.7.5 Stimuli sensitive Hydrogels

Recently, stimuli polymer hydrogels attract striking attention in numerous fields. These hydrogels respond to environmental changes such as pH, light, temperature, ionic

strength, electric and magnetic fields. Some of these stimuli sensitive properties are discussed in this section.

(a) pH-sensitive Hydrogels

The pH-sensitive polymer hydrogels restrain pendant acidic and basic groups. Polymers containing acidic groups such as carboxylic acid and sulfonic acid are known as anionic polymers while polymers consist of basic group like amine are known as cationic polymers. These groups accept or release protons and become ionize with the change in pH. The polymers including large number of such groups are recognized as polyelectrolytes. Further, three dimensional crosslinked polyelectrolytes show change in swelling behavior with the change in pH. The ionization of pendants in polyelectrolytes have tendency to make difference in apparent dissociation constants (K_a) from the corresponding acid or base. The swelling property of crosslinked polyelectrolytes are mainly caused by electrostatic repulsion of the ionized groups. This property is exceedingly influenced by variation in pH, ionic strength, and electrostatic repulsion. The pH-sensitive hydrogels have been exploited for targeted and controlled oral drug release formulations. This is due to the difference of pH in the body parts like stomach ($\text{pH} < 3$) and the intestine ($\text{pH} > 7$). The difference in pH is sufficient to exploit the use of hydrogels via oral administration. The swelling behavior is maximum and drug release occurs at low pH for hydrogels comprised of polycationic polymers due to ionization of pendant groups. Cationic hydrogels are usually used as stomach specific drug delivery carriers. The swelling ratio of N, N'-dimethylaminoethylmethacrylate (DMAEM) and methylmethacrylate copolymer hydrogel were found low at neutral pH while high at acidic pH. Caffeine was loaded in the hydrogel, it was not released at neutral pH but release significantly at pH 3 (Siegel et al., 1988). Moreover, crosslinked chitosan and polyethylene oxide (PEO) semi-IPN hydrogels demonstrated high swelling at pH 1.2. These hydrogels would be best for stomach specific delivery of metronidazole and

amoxicillin for the *Helicobacter pylori* treatment as these drugs were released in large amount at pH 1.2 (Patel & Amiji, 1996). However, the pendant groups of anionic hydrogels ionize at neutral pH and the hydrogels show maximum swelling at this pH. Moreover, this type of hydrogels can be used in intestine specific drug delivery. Anionic polymers are poly acrylic acid, methacrylic acid, pectin, anionic chitosan derivatives, and karaya gum etc. The pH-sensitive semi-IPN hydrogels of poly (acrylic acid) and PEO displayed pH-dependent swelling which was high at neutral pH and low at acidic pH (stomach pH 1.2). The release behavior of some drugs having different water solubility (including nicotinamide, prednisolone, salicylamide, and clonidine HCl) was also tested. The release patterns were significantly correlated with the swelling behavior of the hydrogels. The greater amount of drug was released at neutral pH and small amount of drug was released at pH 1.2 (Bilia et al., 1996). Moreover, carboxymethyl chitosan crosslinked with glutaraldehyde hydrogels were pH dependent and promising carrier for colon specific drugs administration (Vaghani et al., 2012). Mura *et al.* studied colon targeted delivery of 5-aminosalicylic acid (5-ASA) using chitosan and NSC. They investigated drug release from different matrices of chitosan and NSC. The release rate of 5-ASA from chitosan matrices was fast in acidic medium while the release rate from NSC was rapid in alkaline medium in vitro (Carla Mura et al., 2011).

(b) Thermosensitive Hydrogels

The temperature is highly extensively exploited stimulus in environmentally sensitive hydrogels. Temperature sensitive polymer hydrogels experience volume phase transformation upon change in temperature. The effect of temperature on the polymer hydrogels can be recognized through direct heating. The polymers increase or decrease their solubility in water with the temperature change. The polymers whose water solubility decreases with increase in temperature show lower critical solution temperature (LCST). However, the polymers whose water solubility increases with increase in

temperature possess upper critical solution temperature (UCST). The LCST polymer hydrogels swell at low temperature and shrink at high temperature exceeding LCST. This category of hydrogels is known as negative temperature responsive systems. Negative temperature sensitive hydrogels have been used in pulsatile drug release systems. Poly (N-isopropylacrylamide-co-butyl methacrylate) (poly (NIPAM-co-BMA) hydrogels were synthesized to study pulsatile drug release. The BMA contents caused the increase in mechanical strength. The pulsatile indomethacin delivery was obtained with continued at low temperature while stopped at high temperature. This release behavior followed the swelling trend of the hydrogels. In other study, poly (N-isopropylacrylamide-co-acrylic acid) hydrogels have been synthesized and the thermosensitive property of these hydrogels was shown to be manipulated by changing the molar ratio of the two monomers. 5-FU was loaded with an entrapment efficiency of 4 %. The release results clearly investigated the pH and temperature dependency of release rates (Chen et al., 2007). However, the UCST polymer hydrogels display higher swelling with increase in temperature and shrinking at low temperature and classified as positive temperature sensitive systems. IPN hydrogels of poly (acrylic acid) and poly (AAm-co-BMA) and crosslinked poly (AAm-co-BMA) and poly (AAm-co-AA-co-BMA) showed positive temperature responsive swelling behavior. The study revealed the increase in hydrophobic butyl methacrylate concentration shifted the transition temperature to higher temperature. The swelling and drug (ketoprofen) release rates demonstrated reversible temperature dependence trends (Katono et al., 1991). Other type of temperature sensitive hydrogels is known as thermoreversible gels. The most common thermoreversible gels are Poloxamer (Pluronics) and Tetronics. Food and drug administration (FDA) and environmental protection agency (EPA) approved some of these gels to be use in food, pharmaceutical, and agricultural applications. Pluronic F127 20 wt % solution behaves as free flowing liquid at temperature less than 25 °C but turns into semi-solid gel at a

temperature of 27 °C. Cytotoxicity studies revealed the non-toxic nature of Pluronic. Early studies evaluated Pluronic F127 thermosensitive solutions for the treatment of burns, topical administration of anticancer agents, and sustained delivery of drugs after extravascular parenteral injection (Schmolka, 1972). After parenteral injection, poloxamer gels can prolong drug release compared to solutions, but the delivery period rarely exceeds a few days. This characteristic makes poloxamer gels interesting for short-term therapies like pain management, infection treatment, and fertility control. Moreover, poloxamer-graft-PAA hydrogel has been reported by Hoffman *et al.* (Hoffman *et al.*, 1997).

2.1.8 Drug Loading and Encapsulation Efficiency

There are two general methods of drug loading in the hydrogels. In the first method, drug either hydrophilic or hydrophobic is added during the hydrogels preparation. In this method, fixed volume of drug solution is mixed with the hydrogel components and stirred continuously in order to mix the drug uniformly. After that, the hydrogels may synthesize in some specific conditions such as pH, temperature, and pressure. This method of drug loading or entrapment is known as direct drug loading method. In another method, preformed hydrogel allows to swell in the drug solution for some time. During hydrogels swelling, drug absorb and interact with active sites. This method is known as indirect or swelling method. This method has some advantages over direct method. Hydrogels synthesis is a polymerization process requires critical conditions which may cause harmful effect on the properties of drug and sometimes cause drug denaturation. Moreover, there are difficulties in the purification of drug loaded hydrogels. However, direct drug loading method is suitable for loading of hydrophobic drug. Hydrophobic drugs have very low solubility in water or buffer media therefore, drug loading via indirect method seems almost impossible. Furthermore, solubility of hydrophobic drugs requires organic media while swelling of hydrogels does not occur in the organic solvent.

Hence, swelling method is only applicable for the hydrophilic drugs. Moreover, drug loading efficiency of hydrogels for hydrophilic drugs is higher than hydrophobic drugs. This is owing to presence of hydrophilic groups in the hydrogels which may act as surface sites where hydrophilic drug interact with these active sites and absorb or adsorb in the hydrogels. However, hydrophobic sites are also present in the hydrogels but they are not actively interact with the hydrophobic drugs. Hence the drug loading efficiency of hydrophobic drug is low. The drug loading and encapsulation efficiency can be calculated using the equations 2.11 and 2.12, respectively.

$$\text{Drug loading efficiency (\%)} = \frac{\text{Amount of drug in the hydrogel}}{\text{Total amount of the hydrogel}} \times 100 \quad (\text{Equation 2.11})$$

$$\text{Encapsulation Efficiency (\%)} = \frac{\text{Amount of drug in the hydrogel}}{\text{Amount of drug in the solution and in the hydrogel}} \times 100$$

(Equation 2.12)

2.1.9 Drug Release and Release Kinetics

The drug release mechanism is very crucial in the drug delivery system. Drug release from hydrogels depends on the hydrogel composition, extent of crosslinking, nature of drug, and the existence of adjuvants. The drug release in vitro depends on the nature of dissolution medium such as polarity and pH. The release of drug from hydrogels involves several steps. The researchers spent many years to predict the release mechanism of drugs as a function of time by exploiting the mathematical models. These models explain the effect of various factors on the release mechanism such as mass transport, the effect of design constraints, apparatus geometry, and loading of drug. Mostly, the study on release mechanism can be found in the literature based on the diffusion equations. Controlled release systems can be classified as follows:

- a) Diffusion controlled (drug diffusion from non-degradable polymers)
- b) Swelling controlled (drug diffusion owing to swelling of polymers)
- c) Chemically controlled (drug diffusion based on degradation and erosion of polymers)

Mainly, the knowledge about the basics of diffusion and interrelated mathematical models are vital elements to realize the drug release mechanism through the drug release systems. Moreover, the drug release from non-biodegradable polymers takes place through swelling of matrix or diffusion owing to concentration gradient. However, the drug release from biodegradable polymers is controlled by hydrolytic cleavage of the polymers that ultimately causes erosion (Peppas et al., 2000). Researchers have developed very simple and easy equations to study the release mechanism from different polymer systems using diffusion principles. The diffusion coefficients can be described in numerous ways depending upon the nature of pores in the systems. This diffusion can be Fickian, anomalous, or Case-II type. Fick's law helps us to illustrate the Fickian diffusion of drug which is only effective for first 60 % release. Furthermore, the mathematical models reveal the drug release from non- swellable polymers hydrogels, but are also reasonably accurate for swellable polymer hydrogels. The elucidation of the diffusion equations changes rather than the alteration in mathematics of the diffusion equations.

Diffusion controlled is the most exploited to describe the controlled drug release. Fick's law might be used to explain the drug release mechanism. The diffusion coefficients are either constant or varied during the analysis. For diffusion controlled systems, drug release profile is attained by resolving Fick's second law with proper boundary conditions. Moreover, the boundary conditions can be obtained by mass transfer process at the surface and the volume of the surrounding medium. The diffusion controlled systems are further classified as matrix and reservoir systems. In the matrix systems, the

drug is incorporated (dissolved or dispersed) in the matrix, while surrounded by the matrix in the reservoir systems (Arifin et al., 2006).

(a) Swelling Controlled Systems

Hydrophilic polymer matrices immersed in the solvent, the inward pull of solvent molecules within the polymers causes swelling of the polymer matrices is regarded as swelling controlled systems. The incorporated drug release is controlled by inward flux of the solvent is known as swelling controlled release. The momentum behind the polymer swelling is to grant further control over the drug release when diffusivity in the matrix is low. The diffusion of drug from some polymers is very low. Therefore, swellable polymers are exploited, which absorb large quantity of water and result in subsequent disentanglement. The imbibing of water in the polymers reduces the polymer concentration and alters the chain disentanglement. This phenomenon directs the polymer matrix swelling, results in enhance rubbery region with increased diffusion permitting frequent movement of drug out of the matrix. This drug release can also be expressed by Fick's law. Though, the deviation from Fickian diffusion is expected when the drug release is not only controlled by diffusion but also by polymer disentanglement and dissolution.

The degree of swelling of the hydrophilic polymers depends on the composition of polymers and geometry of the gel. The mathematical models developed for swelling controlled systems are mostly for cylindrical geometry, although other models can be developed by transformation of coordinates (Narasimhan, 2001). NSC, pectin, karaya gum, dextran, poly (acrylamide), poly (acrylic acid), and PVA are examples of hydrophilic polymers. Peppas and Lee derived a model that illustrates matrix swelling. According to this model, when the polymer networks interact with the aqueous medium, the swelling takes place to attain thermodynamic equilibrium owing to water

concentration gradient. The absorption of water reduces the glass transition temperature, results in transformation of polymer from glassy to rubbery state. The drug diffusion is very high from rubbery state of polymer. If water penetration is insignificant, polymer swelling or relaxation is negligible. The drug release occurs through Fickian diffusion (Arifin et al., 2006). The polymer relaxation is dominant when the swelling is high. The drug release follows case-II transport (Kwei & Zupko, 1969). Numerous polymers show anomalous transport which is an intermediate characteristic to the already mentioned two cases. Two models have been derived to demonstrate drug release kinetics from the hydrogels. These models are described in the following sections.

(b) Empirical Model

A simple power law expression explains the relationship between drug release and time. It is most extensively used to interpret release data for non-swelling devices. The equation 2.13 is as follows:

$$F_D = \frac{M_t}{M_\infty} = kt^n \quad (\text{Equation 2.13})$$

$\frac{M_t}{M_\infty}$ is a ratio of drug release at time “t” to the equilibrium state. k is a constant to measure velocity of drug release and geometrical parameters analogous to drug-polymer system. It also describes the effect of chemical functionality of carrier on drug release system, while n is a diffusional exponent and explains the drug release mechanism. If $n < 0.45$, diffusion of solvent into the carrier is diffusion controlled (Fickian process) and penetration of solvent into the carrier is much faster than polymer chain relaxation. However, if $n > 0.89$, drug diffusion and release occurs in a complete non-Fickian or case II transport type mechanism. The drug diffusion and release follow swelling or relaxation of system. When, $0.45 < n < 0.89$ diffusion and release of drug occur in non-Fickian manner (Guilherme et al., 2010).

Equation 2.13 is also used to illustrate the drug release mechanism from swellable polymer systems. Though, the rate of solvent penetration into the system is different and significantly affects the drug release behavior. This power law expression is used to explain drug release mechanism in swellable systems, as long as they swell only moderately in the presence of solvent. Hence, the drug diffusion from swellable polymer system is a combination of diffusion and polymer relaxation. However, these polymer systems should not swell more than 25 % of its original volume. Moreover, the diffusional exponent is significantly affected by polymer geometry.

(c) Mechanistic Models

Mostly, these empirical equations are not capable to explain the effect of swelling on drug release behavior. Therefore, mechanistic models have been derived to describe the effect of swelling on controlled release. These equations are based on moving fronts of the glassy and rubbery regions. Lee et al. derived first model for swellable polymer systems without drug loading (two component systems). According to this model, drug release is dependent on rational thermodynamics, viscoelastic description of the polymer, and concentration dependent drug diffusion coefficient (Lee & Peppas, 1987). Furthermore, Siepmann *et al.* derived a model for drug release from hydroxypropylmethyl cellulose by combining diffusion, swelling, and dissolution mechanisms into Fujita-type exponential concentration dependent diffusivities. According to this model, the concentration of polymer highly affected the water and drug diffusion owing to viscosity inducing abilities. Moreover, the transport analysis is two dimensional which is integrated with the swelling as well as dissolution of the polymer (Siepmann et al., 1999). Siepmann *et al.* further modified their models by employing Fick's second law with cylindrical coordinates and Fujita-type exponential dependence of diffusion coefficients into sequential layer model. According to this model, swelling occur layer by layer in which outer layer first then inner layer, accordingly. This development was significant progress

in the model. We can determine the volume changes which give precise idea of the changes in concentration of all species and the mobility of the species (Siepmann & Peppas, 2000).

2.1.10 Model Drugs

Recently, there has been increased attention in hydrogels to exploit in smart drug delivery systems. The basic purpose of the hydrogels utilization is to improve the bioavailability of the hydrophilic as well as hydrophobic drugs, to attain the prolonged release of drugs, and to develop the method of drug administration. In our work, we investigated the in vitro release of three model drugs from hydrogel systems.

i. 5-Fluorouracil

5-Fluorouracil (5-FU) is an anti-tumor and anti-metabolite drug that has been used for few decades (Sagara et al., 2016; Sastre et al., 2007). The chemical structure of the 5-FU is shown in Figure 2.9 (a). It is usually used in the treatment of stomach cancer, gastrointestinal tract pancreas, colon, ovarian, breast, and head (Babu et al., 2006). However, direct or intravenous administration of 5-FU has several side effects such as diarrhea, nausea, vomiting, soreness of the mouth, stomach pain, anemia, decrease in platelets, and white blood cells (Slamon et al., 2001). Cardiac, hematological, neural, and dermatological toxic side effects are also severe via intravenous administration. However, oral administration using controlled formulations significantly reduced side effects (Fournier et al., 2003; Rama et al., 2015). Many polymer materials have been reported for the encapsulation and in vitro release of 5-FU. In those studies, natural, synthetic as well as combination of both polymers were investigated. However, amount of 5-FU released from these carriers at acidic pH (stomach pH, 1.2) was higher as compared to intestine pH (pH 7.4) (Abdelaal et al., 2007; Ravichandran et al., 1997; Shantha & Harding, 2000; Zhang et al., 2002). Ravichandran *et al.* synthesized pH-sensitive poly

(N-vinyl pyrrolidone-acrylic acid)-polyethylene glycol hydrogels. These hydrogels released 62 % 5-FU at pH 1.2. 43 % drug was released rapidly within 2 hours (Ravichandran et al., 1997). Shantha *et al.* synthesized pH-sensitive interpolymeric hydrogels of chitosan, N-vinyl pyrrolidone, and polyethylene glycol acrylate. These hydrogels were highly swelled in acidic pH (pH 1.2) as compared to pH 7.4. More than 60 % 5-FU was released at pH 1.2 in first two hours and 98 % drug was released in 5 hours (Shantha & Harding, 2000). The pH-responsive hydrogels of chitosan-poly (acrylic acid) and chitosan-poly (vinyl alcohol) using gamma irradiation for the 5-FU delivery. More than 90 % 5-FU was released at pH 7.4 within 1 hour in case of chitosan-poly (acrylic acid), while higher 5-FU release occurred from chitosan-poly (vinyl alcohol) at acidic pH. However, drug was released in a short time and synthesis method involved gamma radiation which is very difficult to handle (Abdelaal et al., 2007; Shim & Nho, 2003). Other pH-sensitive interpenetrating hydrogel networks of poly (N-acryloylglycine-chitosan) were reported for the 5-FU release. The 5-FU release results revealed higher release of drug at pH 2.1 (El-Sherbiny et al., 2005). However, our synthesized hydrogels showed lower drug release at pH 1.2 while higher drug release at pH 7.4 which is a significant advantage over reported formulations.

ii. Theophylline

Theophylline is a methylxanthine drug used in therapy for respiratory diseases such as asthma and chronic obstructive pulmonary disease under variety of brand names. It is naturally found in cocoa beans and brewed tea. Theophylline was first extracted from tea leaves and chemically identified around 1888 by the German biologist Albrecht Kossel. The chemical structure of theophylline is shown in Figure 2.9 (b). Numerous formulations have been reported as theophylline carriers. Aiedeh *et al.* synthesized iron crosslinked hydroxamated chitosan succinate hydrogels and theophylline was loaded. The release

results suggested the higher drug release in the acidic pH and lower at basic pH (Aiedeh & Taha, 2001). Rokhade *et al.* reported IPN microspheres of chitosan and methylcellulose crosslinked through emulsion method in the presence of GA. Encapsulation efficiency was found to be 82 % maximum. The in vitro release study was done in 0.1N HCl and pH 7.4. Theophylline release was observed for first 2 hours in 0.1N HCl, then at pH 7.4 up to 12 hours. The release results indicate more than 40 % release in first 2 hours in 0.1N HCl (Rokhade *et al.*, 2007). Thermosensitive physical blend hydrogels of agar, carrageenan, and gelatin were used as theophylline carrier. Theophylline released in short time at high temperature while for long time at low temperature (Liu *et al.*, 2005). From all the reported literature, it can be observed that theophylline release to a greater extent in acidic medium from the carriers or temperature sensitive blend hydrogels. Blend hydrogels were formed through physical interaction of polymers. Usually, physical hydrogels are not stable. We synthesized stable hydrogels through chemical crosslinking and investigated the in vitro release of theophylline at pH 1.2 and pH 7.4. The results revealed that small amount of drug released at pH 1.2 while large amount at pH 7.4.

iii. Quercetin

Quercetin is a dietary flavonoid found in many fruits, tea leaves, vegetables, grains, and red wine. Quercetin is a flavonoid widely distributed in nature. The name has been used since 1857, and is derived from quercetum (oak forest), after *Quercus*. The chemical structure of quercetin is shown in Figure 2.9 (c). It is a naturally occurring polar auxin transport inhibitor (Fischer *et al.*, 1997). Quercetin is one of the most abundant dietary flavonoids with an average daily consumption of 25–50 milligrams (Formica & Regelson, 1995). It is used as an ingredient in foods, beverages, and supplements. Quercetin is nowadays under investigation for prevention and treatment of cancer. Quercetin supplements have also been promoted for the treatment of a wide spectrum of other

diseases. The main limitation of quercetin is its poor solubility in water and instability in physiological medium which restricts the use of this flavonoid to administration. Several attempts were made by different researchers to increase the stability and bioavailability of quercetin through different drug release systems. Lee *et al.* reported polymethyl methacrylate microcapsules to study the stability of quercetin. They stored free quercetin and encapsulated quercetin in the microcapsules for 28 days. 82 % free quercetin was oxidized and 18 % contents were found. However, encapsulated quercetin only degraded 18 % and 82 % residual contents of pure contents were found. In vitro release results revealed 44 % drug release after 36 hours at pH 7.4 (Lee et al., 2007). Kumara *et al.* synthesized poly-lactide (PLA) nanoparticles through solvent evaporation method. The encapsulation efficiency of nanoparticles was found to be 96.7 %. The in vitro release revealed 87.6 % release at pH 7.4 in 96 hours (Kumari et al., 2010). Gelatin and carrageenan hydrogels were reported as quercetin carrier and 96 % release was found at pH 7.4 in 24 hours (Varghese et al., 2014).

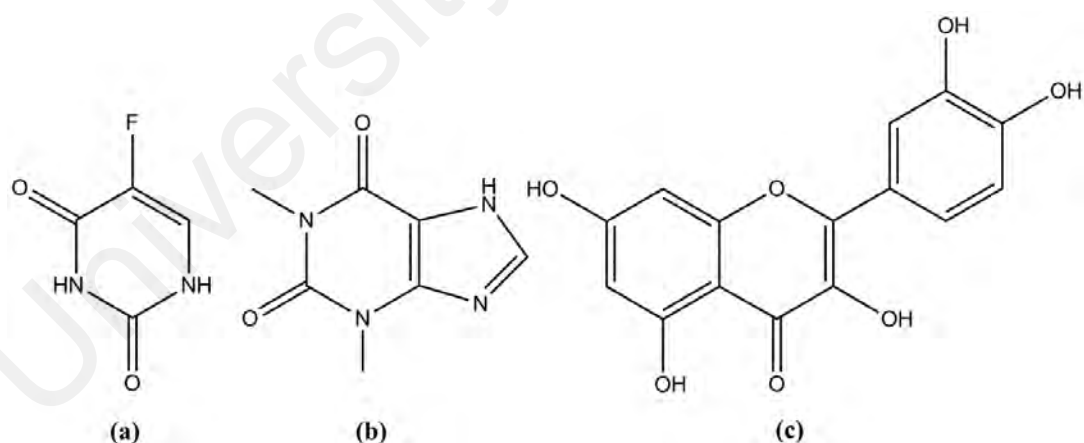


Figure 2.9: Structure of drugs a) 5-fluorouracil, b) theophylline, and c) quercetin

All these studies investigated the quercetin stability and in vitro release at pH 7.4. Our work describes the encapsulation of quercetin in karaya gum-g-poly (acrylic acid) hydrogels and in vitro release of quercetin at pH 1.2 and pH 7.4. Small amount of drug

release at pH 1.2 and large release at pH 7.4 suggests the successful drug carrier synthesis for the oral drug delivery.

University of Malaya

CHAPTER 3: MATERIALS AND METHODS

3.1 Introduction to Materials and Methods

The first section of this chapter describes the materials involved during the synthesis, characterization, and applications of hydrogels. The second section briefly elaborates the methods of fabrication of materials as well as hydrogels. The third section gives brief overview of techniques involved in characterization of fabricated materials and conditions of the instruments during analysis. The fourth section describes yield (%), gel contents (%) and gel time of the hydrogels. The fifth section illustrates the protocols to measure the properties of synthesized hydrogels. The last section winds up the hydrophilic and hydrophobic drug loading, drug release and release kinetics as well as the chemical activity of the model drugs.

3.2 Materials

Chitosan medium molecular weight (M_w 190-310 kDa), degree of deacetylation 75-85 %, viscosity = 200 - 800 centipoise), karaya gum, poly (acrylamide-co-acrylic acid), succinic anhydride, acrylic acid, methacrylic acid (MAA), N, N'-methylenebisacrylamide (MBA), N, N, N', N'- tetramethylethylenediamine (TEMED), 5-fluorouracil, quercetin, and theophylline were obtained from Sigma Aldrich. Acetic acid, sodium hydroxide, methanol, and acetone were purchased from Friendemann Schmidt. Acrylamide and redox pair of initiator (ammonium persulfate and sodium metabisulfite) were obtained from Merck. Glutaraldehyde, ethanol (John Koillin chemicals), phenolphthalein, sodium chloride, calcium chloride, oxalic acid, potassium chloride, and potassium dihydrogen phosphate were purchased from Univar. All chemicals were used as obtained.

3.3 Methods

3.3.1 Synthesis of N-succinyl chitosan

N-succinyl chitosan was synthesized according to the reported method with slight modification (Liu et al., 2013). 0.6 g chitosan was dissolved in 150 ml of 5 % acetic acid solution and stirred for 45 min at 60 °C. Then, 50 ml methanol was added to dilute the solution followed by dropwise addition of already prepared 2.5 g succinic anhydride solution in 50 ml acetone. The reaction mixture was stirred at 1400 rpm at 60 °C for 48 hours to form gel followed by dilution with excess 1M NaOH solution until clear solution was formed. The clear solution was kept under stirring for 24 hours at 50 °C. Then, ethanol was added to precipitate the product. Filtration was performed to separate the precipitate. The precipitate was dispersed in ethanol for 24 hours and washed several times with ethanol and acetone to remove the excess of reactants and to purify the product. Pure product was dried in vacuum oven for 3 hours at 50 °C.

3.3.1.1 Degree of Substitution (DS)

The DS of N-succinyl chitosan was determined according to the reported method (Mukhopadhyay et al., 2013). 0.1g of N-succinyl chitosan was dissolved in 20 ml distilled water, pH of this solution was adjusted to 2 using HCl. Then, it was titrated against 0.1M NaOH solution. The DS was calculated as stated in equation 3.1:

$$DS = \frac{177 \times A}{m_{NSC} - 101 \times A} \quad (\text{Equation 3.1})$$

$$A = V_{NaOH} \times C_{NaOH}$$

Where, V_{NaOH} and C_{NaOH} are volume and concentration of NaOH, respectively. m_{NSC} is the mass of N-succinyl chitosan. 177 and 101 are molecular weights of glucosamine unit and succinyl group, respectively.

3.3.2 Synthesis of N-succinyl chitosan/ poly (acrylamide-co-acrylic acid) Hydrogels via Schiff base Mechanism

N-succinyl chitosan and poly (acrylamide-co-acrylic acid) were dissolved in distilled water at 25 °C. These reactants were mixed with amounts of glutaraldehyde as a crosslinking agent in the presence of 0.01M HCl solution to crosslink N-succinyl chitosan through Schiff base mechanism. Numerous hydrogels were synthesized using different amounts of N-succinyl chitosan and poly (acrylamide-co-acrylic acid) with different crosslinking agent concentration. The mixtures were stirred at 60 °C for 3-6 hours by magnetic stirrer. The resulting hydrogels were washed with distilled water and dried in vacuum oven at 60 °C followed by physical properties characterization. Usually, the washing and drying of hydrogels can be done through different methods. First simple method is to immerse the hydrogels in distilled water in order to remove unreacted species. Then, dry it in the vacuum oven. In another method, hydrogels can be immersed in the water for washing and then in the methanol. The purpose of hydrogels immersion in methanol is the rapid water removal from hydrogels. Composition of the synthesized hydrogels is given in Table 3.1.

Table 3.1: Synthesis scheme of formulations of N-succinyl chitosan/ poly (acrylamide-co-acrylic acid) hydrogels

Hydrogel	N-succinyl chitosan (mg)	Poly (acrylamide-co-acrylic acid) (mg)	GA (mg)
SP1	10	5	1
SP2	10	10	1
SP3	5	10	1
SP4	10	5	2
SP5	10	10	2
SP6	5	10	2
SP7	10	5	3
SP8	10	10	3
SP9	5	10	3

3.3.3 Synthesis of N-succinyl chitosan-g-poly (acrylamide-co-acrylic acid)

Hydrogels via Free radical Mechanism

N-succinyl chitosan-g-poly (acrylamide-co-acrylic acid) hydrogel was synthesized through free radical mechanism. Initially, N-succinyl chitosan (50 mg dissolved in deionized water), acrylamide (50 mg dissolved in deionized water), and acrylic acid (50 mg) were mixed in a vial. Then, 0.75 ml (7.5 mg) ammonium persulfate solution was added as an initiator and allowed to stir for 15 min at 60 °C. After this, 1 ml MBA (10 mg) and 0.2 ml TEMED (0.2 mg) were added as crosslinking agent and accelerator, respectively. Then, this mixture was kept on heating at 70 °C until hydrogel was formed and gelation time was noted. Hydrogel formed was taken out from vial and washed with distilled water to remove unreacted species. Then, hydrogel was dried in vacuum oven at 50 °C. Similarly, numerous hydrogels with varying amount of monomers, initiator, and crosslinking agent were prepared using the similar method. The synthesis scheme of hydrogels is given in Table 3.2.

Table 3.2: Synthesis scheme of formulations of N-succinyl chitosan-g-poly (acrylamide-co-acrylic acid) hydrogels

Formulation	NSC (mg)	Acrylamide (mg)	Acrylic acid (mg)	APS (mg)	MBA (mg)	TEMED (mg)
NAA1	50	50	50	7.5	10	0.2
NAA2	50	50	50	15	10	0.2
NAA3	50	50	50	7.5	20	0.2
NAA4	65	65	65	7.5	10	0.2

3.3.4 Synthesis of N-succinyl chitosan-g-poly (acrylic acid) Hydrogels via Free radical Mechanism

N-succinyl chitosan-g-poly (acrylic acid) hydrogel was prepared by free radical copolymerization of N-succinyl chitosan with acrylic acid in the presence of crosslinking agent (MBA). For this, N-succinyl chitosan was dissolved in 5 ml distilled water at 50 °C

under magnetic stirring. Then, acrylic acid was added into N-succinyl chitosan solution. The dissolved oxygen was removed by purging N₂ gas in the reaction mixture for 30 min before adding initiator. Then, aqueous solution of initiator was added into the mixture and stirred for 5 minutes at 60 °C for process of polymerization. MBA and TEMED were added in the free radical generated mixture and stirring was continued for 10 minutes at 60 °C. The mixture was cooled to room temperature and the resulting hydrogel was kept in distilled water to remove unreacted monomers, crosslinking agent, and initiator. Then, hydrogel was cut into pieces to be taken out from vial and kept in methanol to remove water followed by drying in vacuum oven to completely remove the water. By following the above procedure, different formulations of hydrogels were prepared by varying the amount of N-succinyl chitosan, acrylic acid, MBA, and initiator. The hydrogels formation scheme is shown in Table 3.3.

Table 3.3: Synthesis scheme of formulations of N-succinyl chitosan-g-poly (acrylic acid) hydrogels

Formulation	NSC (mg)	Acrylic acid (mg)	APS (mg)	MBA (mg)	TEMED (mg)
NSA1	60	60	5	10	0.3
NSA2	60	60	10	10	0.3
NSA3	60	60	5	20	0.3
NSA4	90	90	5	10	0.3

3.3.5 Synthesis of N-succinyl chitosan-g-poly (methacrylic acid) Hydrogels via Free radical Mechanism

N-succinyl chitosan-g-poly (methacrylic acid) hydrogels were synthesized by free radical polymerization method. In order to prepare hydrogels, various weight ratios of N-succinyl chitosan, methacrylic acid, MBA, and initiator were used. The hydrogels were prepared with the addition of catalyst TEMED. During the preparation of hydrogels, sodium metabisulfite was used (Hassan et al., 1997). Sodium metabisulfite also acts as initiator

as well as preservative. The mixture of N-succinyl chitosan, methacrylic acid, APS, and sodium metabisulfite was stirred to homogenize for 30 minutes. Then, the solution was deoxygenated by bubbling through N₂ gas for 30 minutes. This deoxygenated mixture was stirred at 60 °C. Then, MBA and TEMED were added as crosslinking agent and accelerator, respectively. The stirring was continued for 10 minutes. After that stirring was stopped and mixture was kept at 60 °C until completion of gelation. The dried gel was immersed in water to remove unreacted monomers. The swollen hydrogel was immersed in methanol to remove water and dried completely in vacuum oven. Numerous formulations of hydrogel were synthesized by varying the concentration of monomers, initiator, and MBA. The synthesis scheme of formulations of hydrogels is given in Table 3.4.

Table 3.4: Synthesis scheme of formulations of N-succinyl chitosan-g-poly (methacrylic acid) hydrogels

Formulation	NSC (mg)	Methacrylic acid (mg)	APS (mg)	MBA (mg)	TEMED (mg)
NSM1	60	100	10	10	0.3
NSM2	60	100	20	10	0.3
NSM3	60	100	10	20	0.3
NSM4	90	150	10	10	0.3

3.3.6 Synthesis of Karaya gum-g-poly (acrylic acid) Hydrogels via Free radical Mechanism

Karaya gum (2 %) aqueous solution was prepared by adding 2 gram in distilled water and mixed thoroughly in order to form homogeneous solution. Karaya gum aqueous solution was placed for 24 hours. After that, this mixture was stirred at 800 rpm for 4 hours at 50 °C. Then, this mixture was sonicated for 15 minutes. Specific amount of karaya gum was mixed with ammonium persulfate. This mixture was stirred for one hour at 70 °C. After that fixed volume of acrylic acid was added and polymerization reaction was carried out

using aqueous solutions of MBA and TEMED as a crosslinking agent and catalyst, respectively. The reaction mixture was stirred for 1 hour at 70 °C and thick gel was formed once the stirring was stopped after the specific time. After this, the gel was immersed in distilled water for 12 hours to remove unreacted soluble fractions and then cut into pieces in order to take out from vial and kept in vacuum oven at 50 °C. Similarly, other formulations of hydrogels were prepared using different amounts of karaya gum, acrylic acid, initiator, and MBA by adopting the same procedure. The synthesis scheme of formulations of hydrogels is given in Table 3.5.

Table 3.5: Synthesis scheme of formulations of karaya gum-g-poly (acrylic acid) hydrogels

Formulation	KG (mg)	Acrylic acid (mg)	APS (mg)	MBA (mg)	TEMED (mg)
KGA1	40	100	7.5	10	0.2
KGA2	40	100	15	10	0.2
KGA3	40	100	7.5	20	0.2
KGA4	60	150	7.5	10	0.2

3.4 Characterization of the Hydrogels

This section describes the techniques used for the analysis of raw materials, synthesized materials, and fabricated hydrogels.

3.4.1 Fourier Transform Infrared (FTIR) Analysis

FTIR spectroscopy deals with the absorption of radiations by sample in the infrared region of electromagnetic spectrum. This radiation has longer wavelength and lower frequency than visible light. The absorption of this radiation occurs correspond to each specific bond as well as specific functional group which present in a molecule. This absorption of radiations at specific frequencies helps to evaluate the interaction between the components and identification of chemical structure of the materials. Usually, the

frequency is measured in wavenumbers ranges from 4000 - 500 cm^{-1} . FTIR- ATR is a non-destructive technique in which small quantity of sample present in the form of powder, liquid or paste is required. The testing material is put on the top of glass. Then, the sample is compressed with the torque wrench to obtain proper contact between sample and refractive crystal. The proper contact between these gives reliable scanned images and maximum signal to noise ratio. In FTIR- ATR, infrared light is focused through the refractive crystal which is internally reflected at the interface between crystal and the testing material. The electric field of infrared light passes into the testing material as transitory wave that causes the attenuation effect on the incident wave. The attenuated radiations scanned in the form of IR spectrum which is generally known as FTIR-ATR spectrum. In this work, FTIR-ATR analysis of chitosan, N-succinyl chitosan, karaya gum, poly (acrylamide-co- acrylic acid), acrylic acid, methacrylic acid, acrylamide, theophylline, 5- fluorouracil, quercetin, and synthesized hydrogels was carried out using FTIR (PerkinElmer Spectrum 400) spectrometer in transmittance mode from 4000 to 500 cm^{-1} at resolution of 12 cm^{-1} at 25 °C.

3.4.2 X-ray Diffraction (XRD) Analysis

X-ray diffraction presents the dual (particles/ waves) nature of X- rays which is used to attain information regarding crystallinity of the material. This technique is mainly used to identify and characterize the materials based on the diffraction pattern. However, it does not provide information about chemical composition of the testing material. In X-ray diffraction, monochromatic X- ray beam when falls on the testing materials, undergo scattering and the constructive and destructive interference occur which is known as diffraction. The diffraction of X- rays is briefly explained by Bragg's law which is, $n\lambda = 2d \sin\theta$. The directions of diffracted X- rays are dependent on the size and shape of the unit cell while the intensity of the diffracted X-rays depends on the type and arrangement of atoms in a crystal structure of the testing material. However, most of the materials are

not single crystal but composed of small crystallites called powder samples. These small crystallites are randomly oriented in different directions. When X-ray beam is passed through this powder sample, it investigates maximum probable interatomic planes. X-ray diffraction is a non-destructive technique, small quantity of sample is required. This technique is used for qualitative as well as quantitative analysis. The information about crystallinity or amorphous nature of sample material can be compared with the reference material. The presence of some specific elements can be obtained by comparing the attained spectrum with the internationally distinguished databases. In this work, powder X-ray diffraction analysis of chitosan, N-succinyl chitosan, karaya gum, poly (acrylamide-co- acrylic acid), and all synthesized hydrogels were performed by X-ray diffractometer (Empyrean diffractometer). Samples were exposed to an accelerating voltage of 40 kV and current of 40 mA using Cu K α radiation at a scan rate of 1° min⁻¹. The diffraction angle was varied from 5- 50° at 2 θ at a temperature of 25 °C.

3.4.3 Differential Scanning Calorimetry (DSC) Analysis

Differential scanning calorimetry (DSC) is a thermoanalytical technique used to measure the thermal properties of the samples through the study of heat flow into or out of the samples as compared to reference material. DSC analysis can be done under different heating and cooling rates. The reference is typically taken as empty pan which is similar to the sample pan. The obtained data of heat flow into or out of samples is plotted against temperature and numerous thermal properties such as glass transition temperature, melting point, crystallization, enthalpies, and polymer degradation can be determined from the thermogram. DSC analysis is performed under inert conditions of nitrogen gas. The purpose of using nitrogen gas is to eliminate corrosive gases during analysis and to reduce the condensation risk within the instrument. The heating and cooling rates are imperative characteristics and generally limited to 40 °C per minutes. The variation in heating rates affects the required thermal properties. The low rate of heating present

superior resolution but high heating rate provide intrinsic sensitivity. Superior resolution means the clear separation of numerous thermal measures. However, intrinsic sensitivity refers to the ability to detect weak events (Verdonck et al., 1999).

The tested materials is weighed in the hermetic aluminum pan and put in the calorimeter. The supply of nitrogen gas switch on and start heating sample at a constant heating rate which was already fixed before analysis. The thermogram obtained usually consists of either endothermic or exothermic peak or both the peaks in single thermogram. Each sample has different heat absorption and evolution property which record as a thermogram. Different thermal events can be obtained from the thermogram as well as enthalpy of the specific peak which is directly proportional to area under curve. Moreover, the direction of peaks confirms the endothermic and exothermic nature.

Furthermore, temperature of the curve can be divided into three categories which are; a) starting temperature, b) peak temperature, c) ending temperature. The peak temperature is very easy to find and temperature of peak point of the curve is known as peak temperature. However, determination of starting and ending temperatures are bit tricky. In order to determine the starting and ending temperature, first of all it is required to draw baseline of the curve, then mark inflection points to the left and right side of the peak point. The tangents drawn at the inflection points intersect at the baseline. The lower temperature is known as starting temperature while the higher temperature represents the ending temperature. The enthalpy change can also be calculated by this method but this enthalpy change, starting temperature and ending temperature can be calculated using software. It is also necessary to mention that different types of baselines can be drawn such as linear, sigmoidal tangent, sigmoidal horizontal, and extrapolated to measure the above mentioned thermal properties.

In this work, thermal behavior of chitosan, N-succinyl chitosan, karaya gum, and synthesized N-succinyl chitosan/ poly (acrylamide-co-acrylic acid), N-succinyl chitosan-g-poly (acrylamide-co-acrylic acid), N-succinyl chitosan-g-poly (acrylic acid), N-succinyl chitosan-g-poly (methacrylic acid), and karaya gum-g-poly (acrylic acid) hydrogels was observed using differential scanning calorimeter (Perkin Elmer) within a temperature range of 25 – 350 °C at a scan rate of 10 °C per minute under inert nitrogen atmosphere. About 8-15 mg of each sample was weighed in an aluminum pan and empty pan was used as a reference.

3.4.4 Field Emission Scanning Electron Microscopy (FESEM) Analysis

Scanning electron microscope (SEM) and field emission scanning electron microscope are non-destructive and versatile techniques used to observe the morphology, size of nanoparticles, and composition of the synthesized materials. This technique capture the image of samples by scanning over with high energy electrons. The high energy electrons interact with atoms in the analyzed material to generate signals which restrain information about the surface, composition, and other properties of the material. The high energy electron beam is generated from the electron gun to produce stable current. Mainly, there are two types of electrons emission sources; a) thermionic emitter; b) field emitter. The difference between SEM and FESEM is the source of emission of electrons. Thermionic emitters are used in SEM as a source of electron emission while field emitter is the source of electron emission in FESEM.

Thermionic emitters consist of heating filament made up of Tungsten (W) and Lanthanum hexaboride (LaBF_6). When the filament is heated by electric current, it emits electrons. These emitters have low evaporation of cathode, glowing property and thermal drift during function. However, field emission is the source of electrons known as cold cathode emitter source. It avoids the problems occur with the former. Heating of the filament is

not required in this emitter. This emitter comprised of tungsten or zirconium oxide wire fashioned into sharp tip. The radius of this small tip is around 100 nm. The emission of electrons occurs by placing the small tip in huge electrical potential gradient. This field emission source is combined with the scanning electron microscope. The accelerating voltage between anode and cathode is between 0.5 to 30 kV and the apparatus requires very high vacuum around 10^{-6} Pa for the electron beam produced by field emission source is 1000 times smaller than thermionic emitter which improves the quality of the images. Objective lenses are used to deflect the electron beam to a point about 0.4 to 5 nm in diameter. The electron beam crosses scanning coils and deflector plates in the column. The deflector plates deflect the beam in the axes to raster scanning over rectangular area. In the present work, the surface morphology of the N-succinyl chitosan/ poly (acrylamide-co-acrylic acid), N-succinyl chitosan-g-poly (acrylamide-co-acrylic acid), N-succinyl chitosan-g-poly (acrylic acid), N-succinyl chitosan-g-poly (methacrylic acid), and karaya gum-g-poly (acrylic acid) hydrogels was examined using field emission scanning electron microscope (FESEM), Quanta FEG 450. The hydrogels were swelled, cut into small pieces to expose inner surface, then freeze-dried for 24 hours using freeze dryer (Supermodulyo Freeze dryer from Thermo) to remove water without disturbing the morphology. Dried samples were then coated with gold in order to prevent the charging effects. Beam voltage was 5 kV for magnifications up to 50,000.

3.4.5 Determination of Yield (%), Gel contents (%), and Gel time of the Hydrogels

In order to determine yield (%) and gel content (%) of the synthesized N-succinyl chitosan-g-poly (acrylamide-co-acrylic acid), N-succinyl chitosan-g-poly (acrylic acid), N-succinyl chitosan-g-poly (methacrylic acid), and karaya gum-g-poly (acrylic acid) hydrogels, the hydrogels were first dried to constant weight W_c . Then, the hydrogels were immersed in excess distilled water for 48 hours to remove water soluble parts of unreacted

monomers. The water insoluble gel samples were further kept in methanol for 3 hours followed by drying in vacuum oven to a constant weight W_f . The yield (%) and gel contents (%) were calculated according to equations 3.2 and 3.3, respectively.

$$\text{Yield (\%)} = \frac{W_c}{W_i} \times 100 \quad (\text{Equation 3.2})$$

$$\text{Gel contents (\%)} = \frac{W_f}{W_c} \times 100 \quad (\text{Equation 3.3})$$

Where, W_i is the total weight of N-succinyl chitosan, monomers, and MBA used for synthesis of the gel.

Gel time was measured using stop watch. Initially, mixture of monomers and initiator was heated and stirred at 1000 rpm for specific time. After that time, crosslinking agent was added and stirring was stopped to form thick hydrogels. The gel time was recorded after addition of crosslinking agent and kept the mixture at heating without stirring until hydrogels were formed.

3.5 Properties of Hydrogels

3.5.1 Mechanical Properties

Rheometry is a technique used to determine the rheological and mechanical properties of a material. Rheometer is an instrument used to measure these properties under fixed parameters such as deformation and shear stress. In this technique, liquids, solids, and viscoelastic materials can be investigated using oscillatory and rotational rheometer. Oscillatory tests are exploited to observe the viscoelastic materials from low viscosity liquids, polymer melts, gels, and rigid solids. The oscillatory tests are performed using two plate models. These plate models include coaxial cylindrical measuring plate systems, cone and plate measuring systems, and parallel plate measuring systems. The upper plate moves up and down during the analysis, while the lower plate is always

stationary. Sample holds firmly within the plates so that it cannot slip. Oscillatory tests are performed to observe the rheological properties of the materials against amplitude, time, frequency, and temperature. In case of the hydrogels, amplitude sweep test is performed prior to frequency sweep test to ensure the selected strain within the linear viscoelastic region (LVR) of the hydrogels. The time and frequency sweep tests are performed within the LVR to obtain storage modulus, loss modulus, complex shear modulus, and complex viscosity.

In this work, the viscoelastic properties of the N-succinyl chitosan/ poly (acrylamide-co-acrylic acid), N-succinyl chitosan-g-poly (acrylamide-co-acrylic acid), N-succinyl chitosan-g-poly (acrylic acid), N-succinyl chitosan-g-poly (methacrylic acid), and karaya gum -g-poly (acrylic acid) hydrogels were obtained using oscillatory MCR 301 rheometer (Paar-Physica) at 25 °C with 25 mm in diameter parallel plate geometry at 0.5 mm gap. The amplitude sweep test was conducted with the applied strain ranging from 0.01-25 % at a constant angular frequency of 10 rad/s. The linear viscoelasticity region (LVR) was determined in terms of elasticity modulus G' (storage modulus) and viscosity modulus G'' (loss modulus). The frequency sweep test was performed at a constant strain of 1% and varying the angular frequency from 0-100 rad/s using 25 mm parallel plate geometry at 0.5 mm gap between the two plates.

3.5.2 Swelling Ratio

Swelling ratio of synthesized N-succinyl chitosan/ poly (acrylamide-co-acrylic acid), N-succinyl chitosan-g-poly (acrylamide-co-acrylic acid), N-succinyl chitosan-g-poly (acrylic acid), N-succinyl chitosan-g-poly (methacrylic acid), and karaya gum-g-poly (acrylic acid) hydrogels was observed in water and buffer solutions. For this purpose, weighted amount of dried gels were kept in buffer solutions separately. The hydrogels were removed at specific time intervals and the surface water was wiped off. The weight

of hydrogels was measured and returned into the same medium. This process was continued until a constant weight was achieved. Swelling ratio was calculated by the following equation 3.4.

$$SR = \frac{W_t - W_0}{W_0} \quad (\text{Equation 3.4})$$

Where, W_0 is the initial weight of hydrogel and W_t is the weight of the hydrogel at time 't'.

3.5.2.1 Swelling Kinetics

The swelling ratio of the N-succinyl chitosan/ poly (acrylamide-co-acrylic acid), N-succinyl chitosan-g-poly (acrylamide-co-acrylic acid), N-succinyl chitosan-g-poly (acrylic acid), N-succinyl chitosan-g-poly (methacrylic acid), and karaya gum-g-poly (acrylic acid) hydrogels was measured at different time intervals and fitted into non-linear second order rate equations 3.5, 3.6, and 3.7 using Origin Pro-9 software (Mall et al., 2006b).

$$\frac{t}{SR_t} = \frac{1}{m_e} t + \frac{1}{m_e^2 k_{s2}} \quad (\text{Equation 3.5})$$

$$SR_t = \frac{m_e^2 k_{s2} t}{1 + m_e k_{s2} t} = \frac{r_0 t}{1 + m_e k_{s2} t} \quad (\text{Equation 3.6})$$

$$r_0 = m_e^2 k_{s2} \quad (\text{Equation 3.7})$$

SR_t is swelling ratio at time "t", m_e is mass of hydrogel at swelling equilibrium, r_0 is initial rate of swelling, and k_{s2} is a rate constant.

3.5.2.2 Salinity and Swelling Ratio

In this study, the effect of ionic strength on N-succinyl chitosan/ poly (acrylamide-co-acrylic acid), N-succinyl chitosan-g-poly (acrylamide-co-acrylic acid), N-succinyl chitosan-g-poly (acrylic acid), N-succinyl chitosan-g-poly (methacrylic acid), and karaya

gum-g-poly (acrylic acid) hydrogels swelling was studied by exposure of the hydrogels in monovalent NaCl, bivalent CaCl₂, and trivalent AlCl₃ aqueous solution of concentration ranging from 0.05 to 0.2 M. Specific weight of each hydrogel was immersed in each solution at constant pH and temperature and swelling behavior was calculated using equation 3.4.

3.6 Encapsulation Efficiency

Drug can be entrapped into the hydrogels through two methods. First method of drug entrapment is swelling method. In this method, hydrogels prepare first then washed, dried, and immersed in drug solution. Secondly, drug can be entrapped during the synthesis of hydrogels. In this work, both methods were adopted to entrap drugs through these methods.

a) Swelling method

5-Fluorouracil was entrapped into networks of N-succinyl chitosan/ poly (acrylamide-co-acrylic acid) hydrogels by swelling equilibrium method. Specified amount of hydrogels were immersed in 5-Fluorouracil and theophylline solution for 72 hours at 25 °C. Theophylline was entrapped into N-succinyl chitosan-g-poly (acrylic acid), and N-succinyl chitosan-g-poly (methacrylic acid) hydrogels through this method. These hydrogels were immersed in theophylline solution for 72 hours at 25 °C. 5-Fluorouracil and theophylline loaded hydrogels were washed with distilled water to remove adhered 5-Fluorouracil from N-succinyl chitosan/ poly (acrylamide-co-acrylic acid) hydrogels and theophylline from N-succinyl chitosan-g-poly (acrylic acid), and N-succinyl chitosan-g-poly (methacrylic acid) hydrogels on the surface and the washing was collected. 5-Fluorouracil and theophylline concentration in the solution was measured using UV-Vis spectrophotometer (UV-2600, Shimadzu, Japan) at 266 nm and 272 nm, respectively.

b) Direct method

Theophylline was entrapped into N-succinyl chitosan-g-poly (acrylamide-co-acrylic acid) hydrogels and quercetin was loaded into karaya gum-g-poly (acrylic acid). These drugs were entrapped during the synthesis of these hydrogels. Initially, mixtures of monomers and initiator was stirred for specific time. After specific time drug, MBA, and TEMED were added in the mixtures under continuous stirring. The stirring was stopped after specific time and gelation occurred. During the gelation, drug was entrapped. Drug entrapped hydrogels were washed. The amount of free drug was determined using UV-Vis spectrophotometer (UV-2600, Shimadzu, Japan) at 272 nm and 256 nm, respectively.

The encapsulation efficiency were determined by calculating the difference in concentration of total drug and drug entrapped into the hydrogels. The experiments were repeated three times and average values were taken (Mishra et al., 2014). The encapsulation efficiency were determined using the equation 3.8.

$$\text{Encapsulation efficiency (\%)} = \frac{\text{Amount of drug in the hydrogel}}{\text{Total amount of drug in the solution and in the hydrogel}} \times 100$$

(Equation 3.8)

3.7 In Vitro Drug Release

In vitro drug release from copolymer hydrogel networks with different drug loading contents, monomers concentration, crosslinking agent concentration, and initiator concentration was investigated in physiological mediums (pH 7.4 and pH 1.2) at 37 °C. A specific amount of drug loaded hydrogel was immersed in buffer solutions of pH 7.4 and pH 1.2, respectively. In order to study the drug release, 3 ml solution containing released drug was withdrew at predetermined time intervals. The concentration of 5-FU, theophylline and quercetin was measured at 266 nm, 272 nm and 256 nm using UV-Vis

spectrophotometer (UV-2600, Shimadzu, Japan), respectively. The drug release experiments were performed triplicates and the results were averaged.

3.7.1 Drug Release Kinetics

Drug release kinetics was investigated using Ritger-Peppas model as stated in equation 3.9 (Ritger & Peppas, 1987). The kinetics was determined by using Origin Pro software.

$$F_D = \frac{M_t}{M_\infty} = kt^n \quad (\text{Equation 3.9})$$

$\frac{M_t}{M_\infty}$ is a ratio of drug release at time 't' to the equilibrium swollen state. k is a constant to measure velocity of release and geometrical parameters analogous to drug-polymer system.

3.7.2 Chemical Activity of the Drugs

The chemical activity of the 5-FU, theophylline, and quercetin was observed in pure solution and after in vitro release. The chemical activity of 5-FU and theophylline was observed in water and water + ethanol mixture, respectively. However, the chemical activity of quercetin was observed in ethanol solution. Moreover, it was examined after in vitro release in buffer solution of pH 7.4. The UV spectra of pure 5-FU, theophylline, and quercetin before drug loading and after in vitro release in buffer solution were recorded using UV-Vis spectrophotometer (UV-2600, Shimadzu, Japan) at wavelength of 266 nm, 272 nm, and 256 nm.

CHAPTER 4: RESULTS AND DISCUSSION

This section comprehensively described the detailed findings of the research work which are mentioned in the given sections.

4.1 Synthesis

4.1.1 Synthesis of N-succinyl chitosan and Degree of Substitution

N-succinyl chitosan was synthesized successfully from chitosan and degree of substitution was also determined via potentiometric titration. The degree of substitution refers to the extent of average number of functional group replacement by another functional group per repeating unit. In this study, chitosan was modified via N-acylation using succinic anhydride, whereby the amino group of chitosan was substituted by succinyl group. The degree of substitution was found to be 0.48. The introduction of –COOH into the chitosan via succinyl group enhances the hydrophilicity and pH sensitivity. It was reported elsewhere that increase in hydrophilicity may enhance the mucoadhesive properties via hydrogen bond formation with tissues (Mura et al., 2011). Synthesis mechanism of N-succinyl chitosan from chitosan is shown in Figure 4.1.

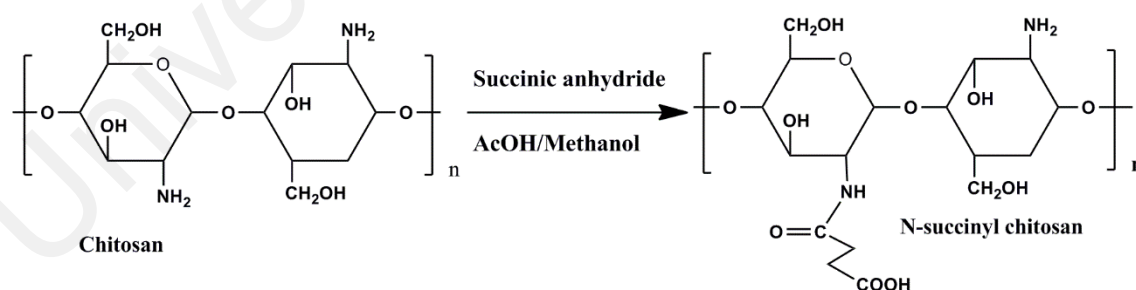


Figure 4.1: Synthesis of N-succinyl chitosan from chitosan

4.1.2 Synthesis of N-succinyl chitosan/ poly (acrylamide-co-acrylic acid) Hydrogels

N-succinyl chitosan/ poly (acrylamide-co-acrylic acid) hydrogels were synthesized. The proposed reaction mechanism is shown in Figure 4.2. This mechanism shows that amino

groups of N-succinyl chitosan crosslinked through glutaraldehyde. Amino groups reacts with the aldehyde group to form N=C, known as Schiff base. This mechanism is known as Schiff base mechanism due to formation of Schiff base.

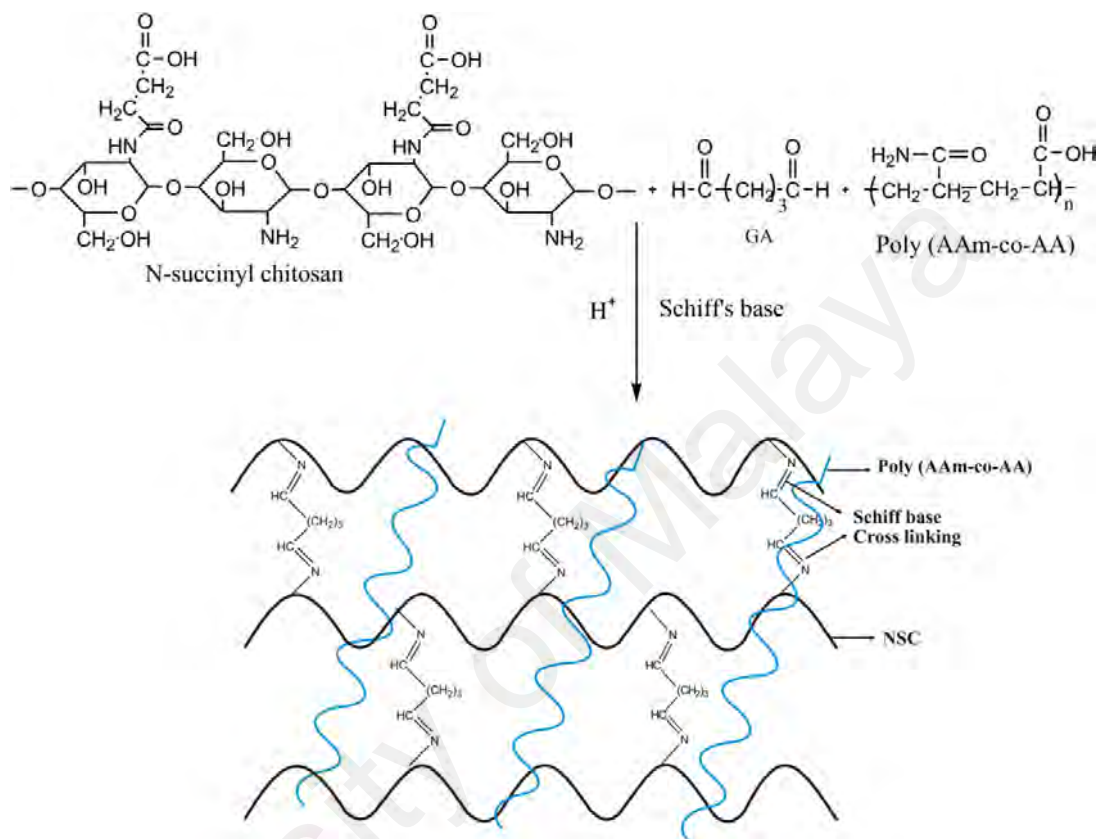


Figure 4.2: The proposed reaction mechanism of Schiff base crosslinking of N-succinyl chitosan and formation of semi-IPN through embedding of poly (acrylamide-co-acrylic acid) in N-succinyl chitosan network

4.1.3 Synthesis of N-succinyl chitosan-g-poly (acrylamide-co-acrylic acid)

Hydrogels

N-succinyl chitosan-g-poly (acrylamide-co-acrylic acid) hydrogels were prepared via free radical polymerization. In this mechanism, sulfate anion radicals were generated from APS under heating condition. Then, these radicals abstracted protons from water molecules and generated hydroxyl free radicals. These hydroxyl free radicals further abstract protons from active sites of N-succinyl chitosan, acrylamide, and acrylic acid to form active centers that can initiate the process of polymerization (Mahdavinia et al., 2004). In the polymerization process, polymer chains comprises a chemical crosslinked

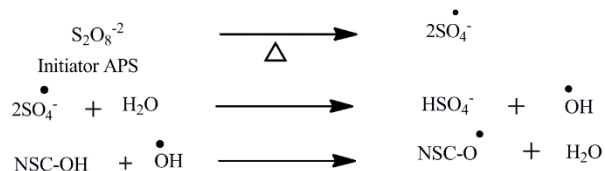
structure in the presence of crosslinking agent MBA and catalyst TEMED. The proposed reaction mechanism is shown in Figure 4.3.

4.1.4 Synthesis of N-succinyl chitosan-g-poly (acrylic acid) Hydrogels

N-succinyl chitosan-g-poly (acrylic acid) hydrogels were synthesized by free radical polymerization of N-succinyl chitosan and acrylic acid in the presence of initiator. The initiator produced sulfate anion radical and removed proton from one of the highly reactive functional groups of N-succinyl chitosan (i.e. OH, NH₂, or COOH) and mono-functional acrylic acid to form the corresponding free radicals (Pourjavadi et al., 2007). These radicals initiate polymerization in the presence of bifunctional monomer MBA and catalyst TEMED. The reaction mechanism is shown in Figure 4.4.

University of Malaya

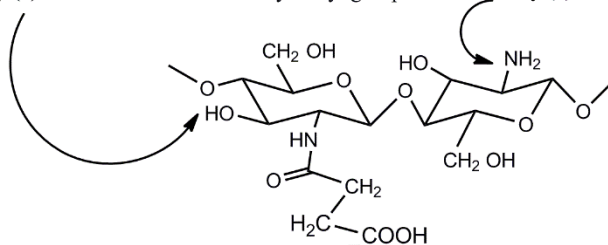
(a) **Initiation step**



Possibilities of generation of free radicals on NSC

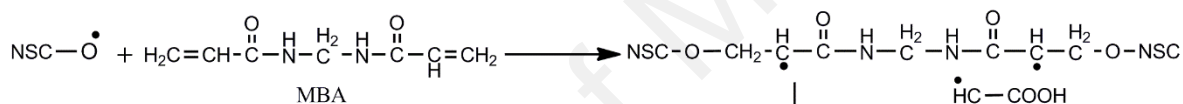
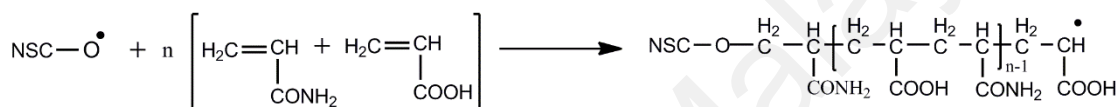
Possibility (2) : Abstraction of H from hydroxyl group

Possibility (1) : Abstraction of H from amino group



(b) **Propagation step**

Possibility (3) : Abstraction of H from carboxylic group



(c) **Termination step**

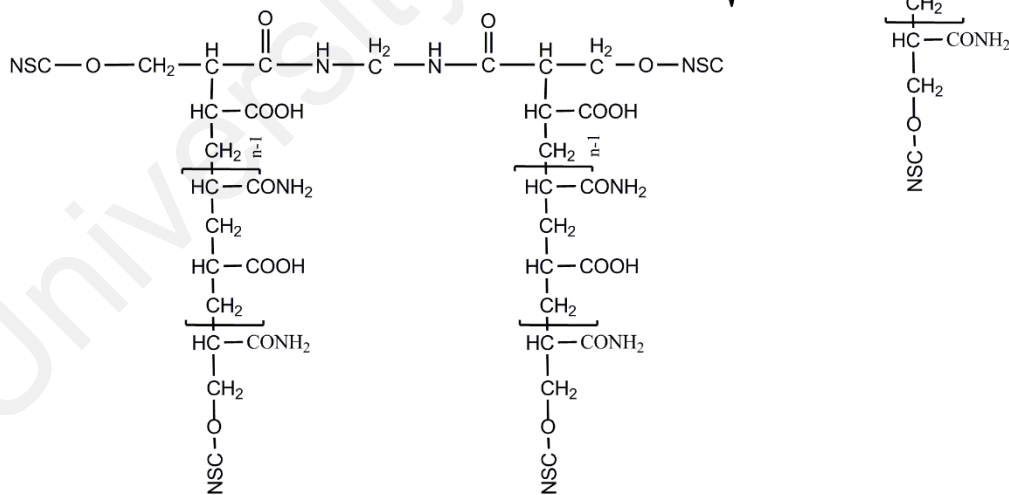
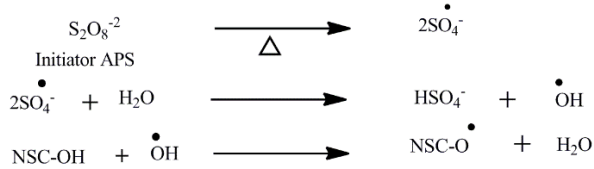


Figure 4.3: The proposed reaction mechanism of N-succinyl chitosan-g-poly (acrylamide-co-acrylic acid)

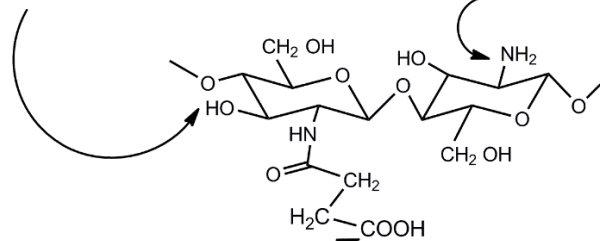
(a) Initiation step



Possibilities of generation of free radicals on NSC

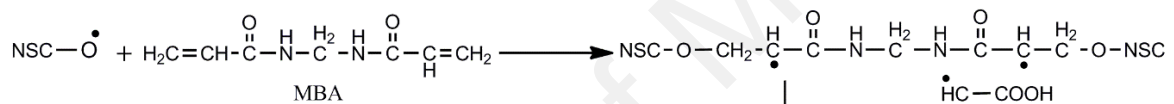
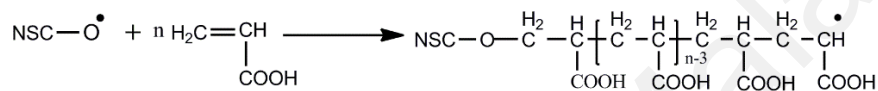
Possibility (2) : Abstraction of H from hydroxyl group

Possibility (1) : Abstraction of H from amino group



(b) Propagation step

Possibility (3) : Abstraction of H from carboxylic group



(c) Termination step

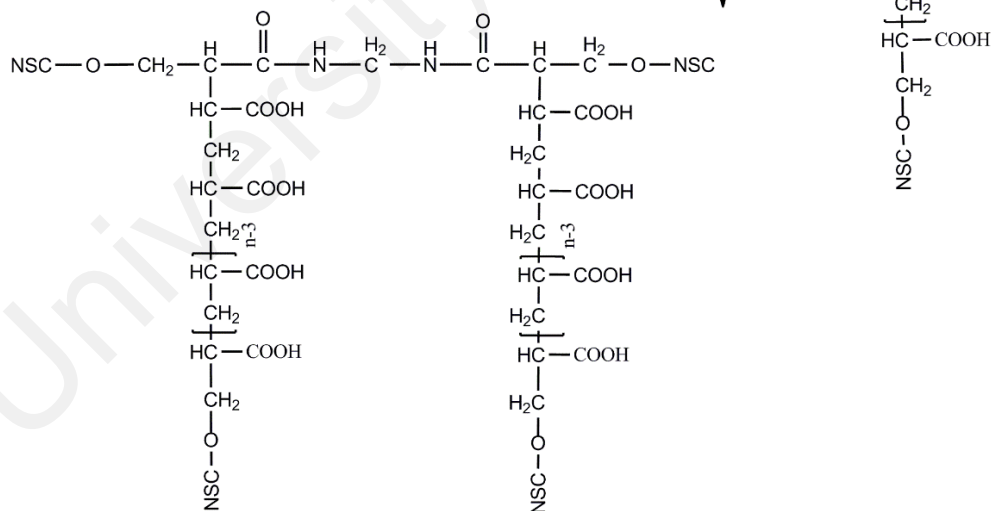


Figure 4.4: The proposed reaction mechanism of synthesis of N-succinyl chitosan-g-poly (acrylic acid)

4.1.5 Synthesis of N-succinyl chitosan-g-poly (methacrylic acid) Hydrogels

N-succinyl chitosan-g-poly (methacrylic acid) hydrogels were prepared by free radical polymerization. In this polymerization, the ammonium persulfate/sodium metabisulfite acted as redox pair free radical initiator. Metabisulfite as well as bisulfite anions can couple with traces of oxygen to form redox pair initiator and generate free radicals (Orakdogan & Okay, 2007). These free radicals initiate the process of polymerization. The formation of redox couple with oxygen prevents the oxidation of monomers. However, the mechanism of radical formation has not been established using sodium metabisulfite as a free radical initiator. Hence, we can also say that sodium metabisulfite might be act as a preservative because it protects reaction of free oxygen with monomer radicals. This redox couple also generate free radicals of methacrylic acid and N-succinyl chitosan (-COOH, NH₂, and OH) (Pourjavadi et al., 2007). These free radicals further propagated copolymerization in the presence of MBA and TEMED. The plausible reaction mechanism is shown in Figure 4.5.

4.1.6 Synthesis of Karaya gum-g-poly (acrylic acid) Hydrogels

Free radical polymerization method was adopted to synthesize karaya gum-g-poly (acrylic acid) hydrogels. In this free radical approach, sulfate anion free radicals from APS were generated due to heating of reaction mixture at 70 °C. This anion radical generated hydroxyl free radical which further produced free radicals of active sites of karaya gum and acrylic acid. The free radicals of acrylic acid initiated grafting over karaya gum. Furthermore, polymerization through crosslinking occurred due to presence of MBA. The grafting and polymerization was accelerated using TEMED. The proposed reaction mechanism is shown in Figure 4.6.

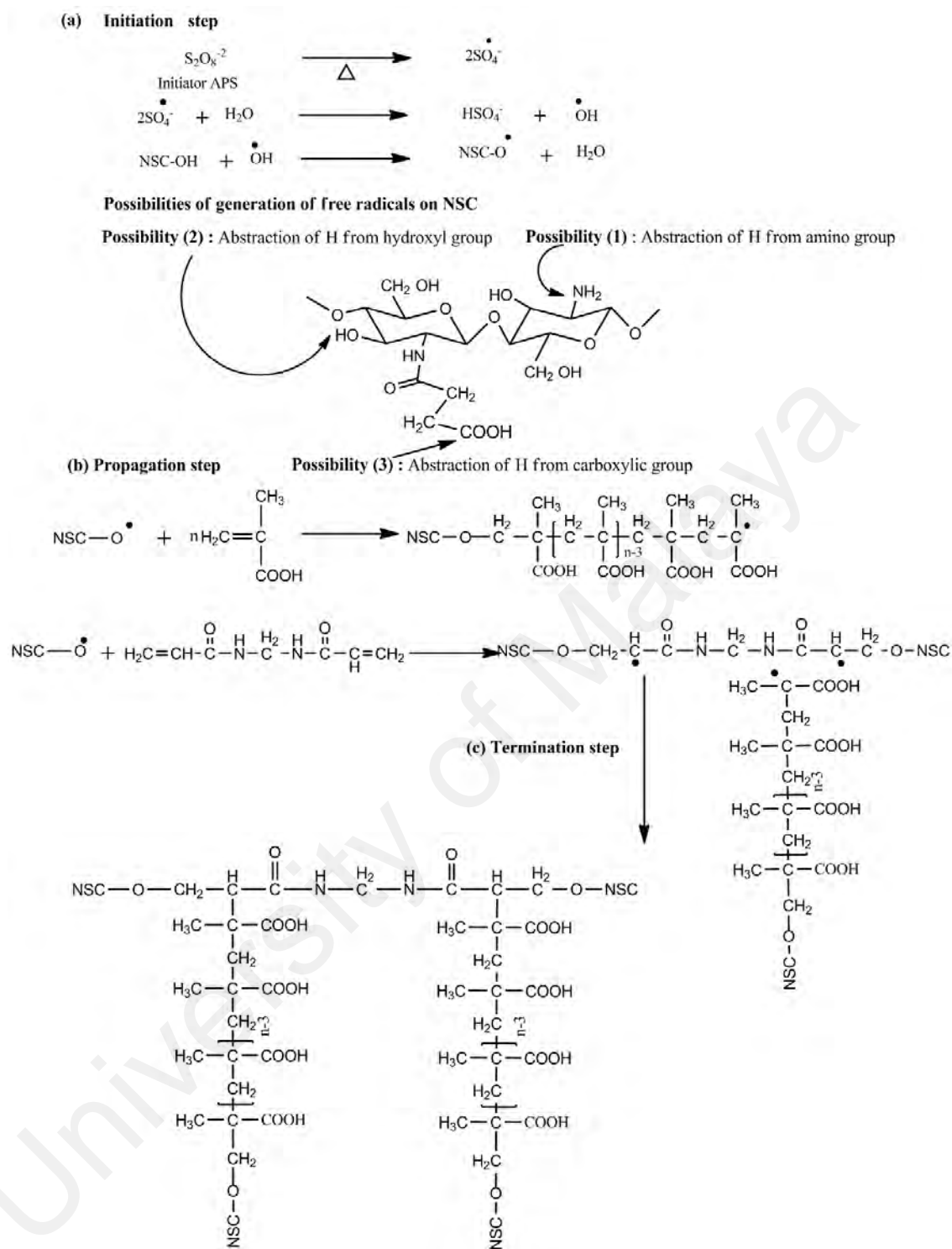
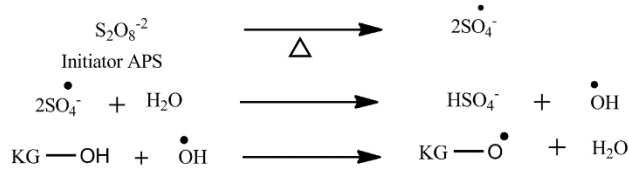


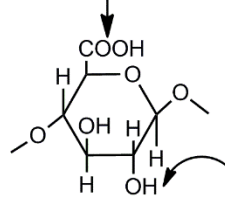
Figure 4.5: The proposed reaction mechanism of synthesis of N-succinyl chitosan-g-poly (methacrylic acid)

(a) **Initiation step**



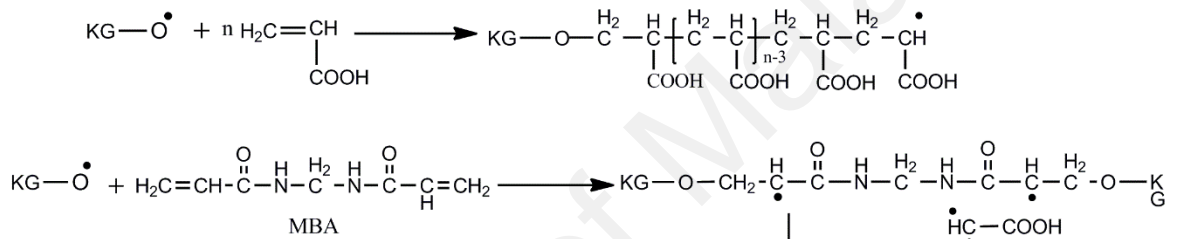
Possibilities of generation of free radicals on karaya gum (KG)

Possibility (1) : Abstraction of H from carboxylic group



Possibility (2) : Abstraction of H from hydroxyl group

(b) **Propagation step**



(c) **Termination step**

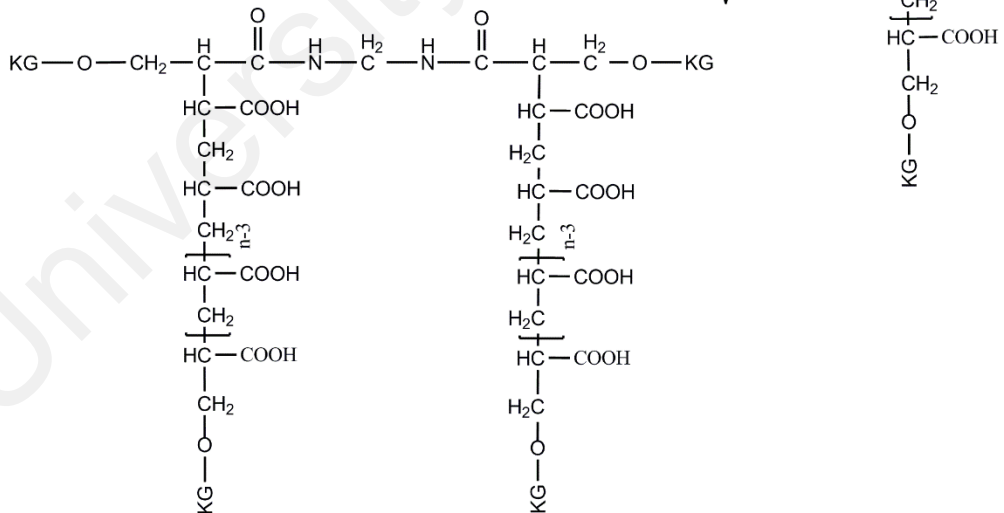


Figure 4.6: The proposed reaction mechanism of karaya gum-g-poly (acrylic acid)

4.2 Characterization

This section describes the findings of synthesized hydrogels through important characterization techniques. These findings will be discussed one by one in the given sections.

4.2.1 Fourier Transform Infrared Analysis

This section describes the FTIR analysis of raw materials as well as the synthesized hydrogels.

4.2.1.1 Starting Materials

a) Chitosan

Figure 4.7 (a & b) shows FTIR spectra of chitosan and N-succinyl chitosan, respectively. The FTIR spectrum of chitosan shows characteristic absorption peak at 3388 cm^{-1} which is assigned to stretching vibration of OH and NH_2 groups. The peak at 2926 cm^{-1} corresponds to C-H stretching vibration. The presence of primary amide can be clearly observed from absorption band at 1644 cm^{-1} . The absorption band at 1591 cm^{-1} is due to presence of protonated amino group. Furthermore, characteristic peak at 1151 cm^{-1} represents the saccharide unit of chitosan. The absorption peaks at 1070 cm^{-1} and 1027 cm^{-1} indicate the presence of C-N and C-O stretching vibration, respectively. The peak at 887 cm^{-1} indicates the presence of pyranoid ring (Cui et al., 2014).

b) N-Succinyl chitosan

In N-succinyl chitosan spectrum, the characteristic absorption peak at 3280 cm^{-1} is due to the combination of stretching of OH and NH, while the peak at 2960 cm^{-1} represents C-H stretching vibration. The presence of primary amide can be clearly observed from absorption band at 1641 cm^{-1} . However, the vanishing of peak at 1591 cm^{-1} and emergence of new absorption band at 1551 cm^{-1} provides evidence of chitosan

modification. Moreover, the prominent peaks at 1434 cm^{-1} and 1404 cm^{-1} attributes to the presence of carboxylate ions and confirms the formation of N-succinyl chitosan. Furthermore, absorption peaks at 1154 cm^{-1} , 1068 cm^{-1} , and 1020 cm^{-1} are due to presence of saccharide unit, C-N, and C-O stretching vibration, respectively. The peak at 884 cm^{-1} indicates the presence of pyranoid ring. Hence, FTIR of the synthesized N-succinyl chitosan is in good agreement with those already reported data (Mura et al., 2012).

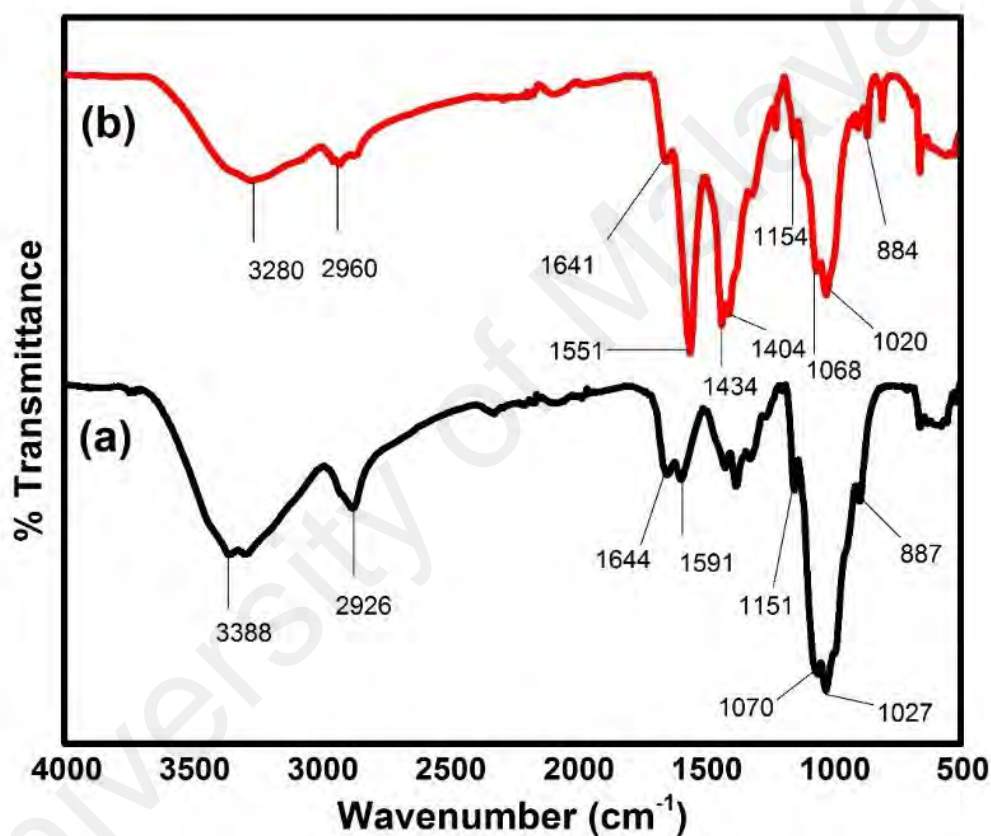


Figure 4.7: FTIR spectra of a) Chitosan, b) N-succinyl chitosan
c) Poly (acrylamide-co-acrylic acid)

FTIR spectrum of poly (acrylamide-co-acrylic acid) is shown in Figure 4.8 (a). This spectrum shows several peaks. The first peak at 3350 cm^{-1} corresponds to the N-H stretching vibration of acrylamide. The peaks at 3182 cm^{-1} and 2950 cm^{-1} represent the stretching vibration of O-H and C-H, respectively. The absorbance at 1650 cm^{-1} shows the presence of amide group. The peak at 1444 cm^{-1} is due to $-\text{CH}_2$ of acrylate chain. The

peaks at 1331 cm^{-1} and 1103 cm^{-1} are attributed to stretching vibration of C-N and -CO-O- respectively.

d) Acrylic acid

Figure 4.8 (b) represents the spectrum of acrylic acid. In this spectrum, the peak at 2983 cm^{-1} shows the presence of C-H stretching vibration. The main peak at 1702 cm^{-1} attributes to the -COOH group. Moreover, the peaks at 1634 cm^{-1} , 1437 cm^{-1} , 1237 cm^{-1} , correspond to stretching of C=C, -CH₂, and C-O, respectively.

e) Acrylamide

Figure 4.8 (c) represents the spectrum of acrylamide. In this spectrum, the peaks at 3335 cm^{-1} and 3162 cm^{-1} correspond to the asymmetric and symmetric stretching of N-H, respectively. The absorbance at 1673 cm^{-1} attributes to the amide group. The peaks at 1620 cm^{-1} , 1431 cm^{-1} and 1276 cm^{-1} represents the C=C, -CH₂ stretching and C-O stretching, respectively (Marques et al., 2000).

f) Methacrylic acid

The spectrum of methacrylic acid is shown in Figure 4.8 (d). In this spectrum, the peaks at 2968 cm^{-1} , 1701 cm^{-1} , 1620 cm^{-1} , 1434 cm^{-1} , 1303 cm^{-1} , and 1202 cm^{-1} correspond to the presence of C-H stretching vibration, COOH group, C=C, -CH₂ stretching, -CH₃ group and C-O stretching, respectively.

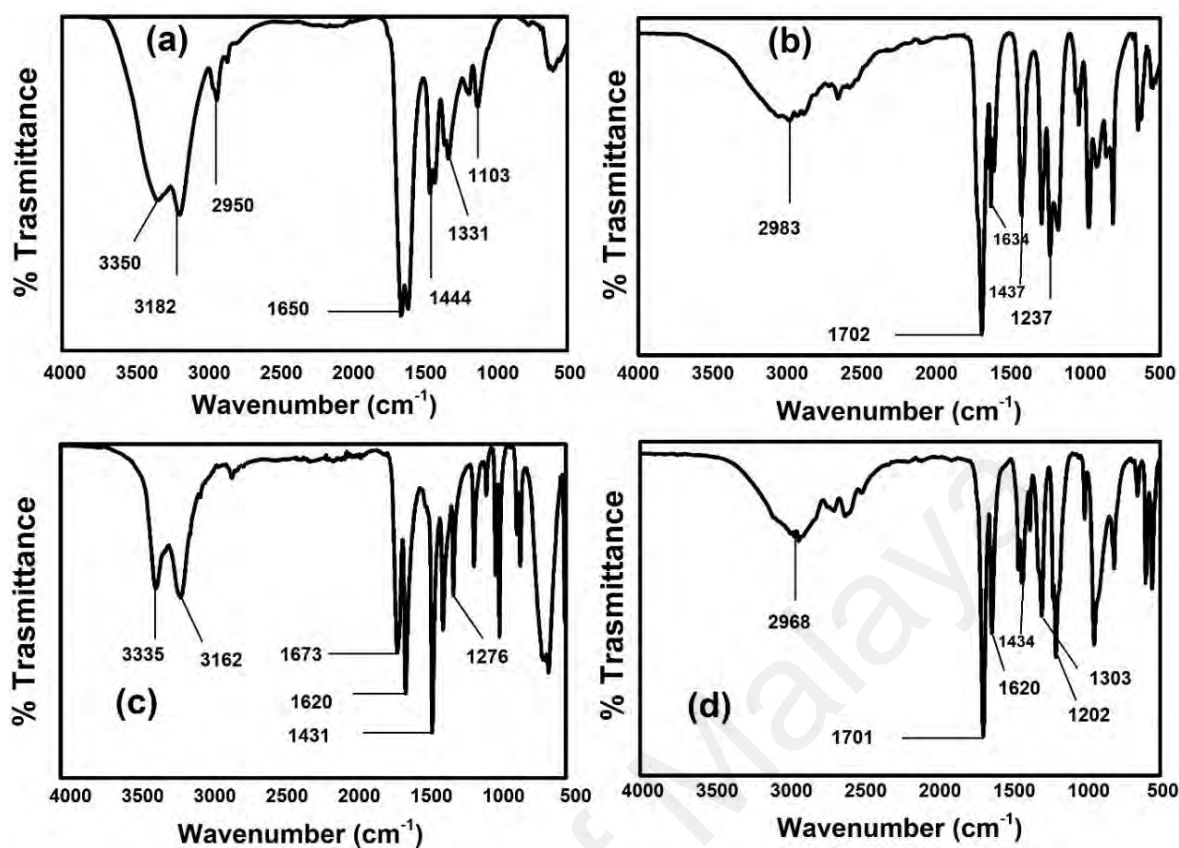


Figure 4.8: FTIR spectra of a) poly (acrylamide-co-acrylic acid), b) acrylic acid, c) acrylamide, and d) methacrylic acid

g) Karaya gum (KG)

Figure 4.9 shows the FTIR spectrum of karaya gum. In this spectrum, the peak at 3410 cm^{-1} assigned to the stretching vibration of OH group. The peak at 2930 cm^{-1} is attributed to the presence of C-H stretching vibration. Moreover, the peak at 1721 cm^{-1} correspond to the COOH group and the peak at 1604 cm^{-1} represents the presence of methylated galacturonic acid ester. The absorption band at 1410 cm^{-1} is owing to the $-\text{COO}^-$ and $-\text{CH}_2$ groups. The absorption peak at 1380 cm^{-1} reflects the bending vibrations of CH_2 and O-H groups. The characteristic peak at 1220 cm^{-1} corresponds to $-\text{CH}_3\text{CO}$ group and the peak at 1028 cm^{-1} shows the presence of C-O-C bond which is a characteristic of polysaccharide (Mittal et al., 2015; Singh et al., 2011).

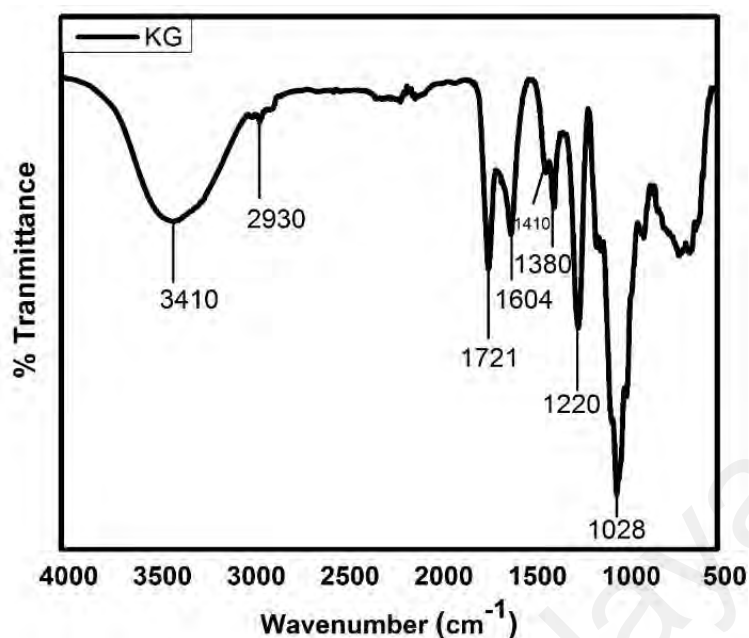


Figure 4.9: FTIR spectrum of karaya gum

h) 5-Fluorouracil (5-FU)

Figure 4.10 (a) shows the FTIR spectrum of 5-FU. In the spectrum of pure 5-FU, the absorption band at 3222 cm⁻¹ and 2933 cm⁻¹ correspond to N-H and C-H stretching vibration, respectively. The peaks at 1731 cm⁻¹, 1648 cm⁻¹, and 1251 cm⁻¹ represent the cyclic imide (CO-NH-CO), primary imide, and tertiary imide, respectively. The peak at 1428 cm⁻¹ is responsible for CH₂ stretching (Lin et al., 2002).

i) Theophylline

The spectrum of the pure theophylline is shown in Figure 4.10 (b), some intense major bands are observed. The absorption bands at 3123 cm⁻¹ and 2980 cm⁻¹ are due to N-H and C-H stretching vibration, respectively. However, the peak at 1670 cm⁻¹ corresponds to the presence of imide group of the heterocyclic ring and peak at 1236 cm⁻¹ also presents the C-N stretching vibration of theophylline. The absorption band at 1556 cm⁻¹ is due to bending vibration of N-H (Samanta & Ray, 2014a).

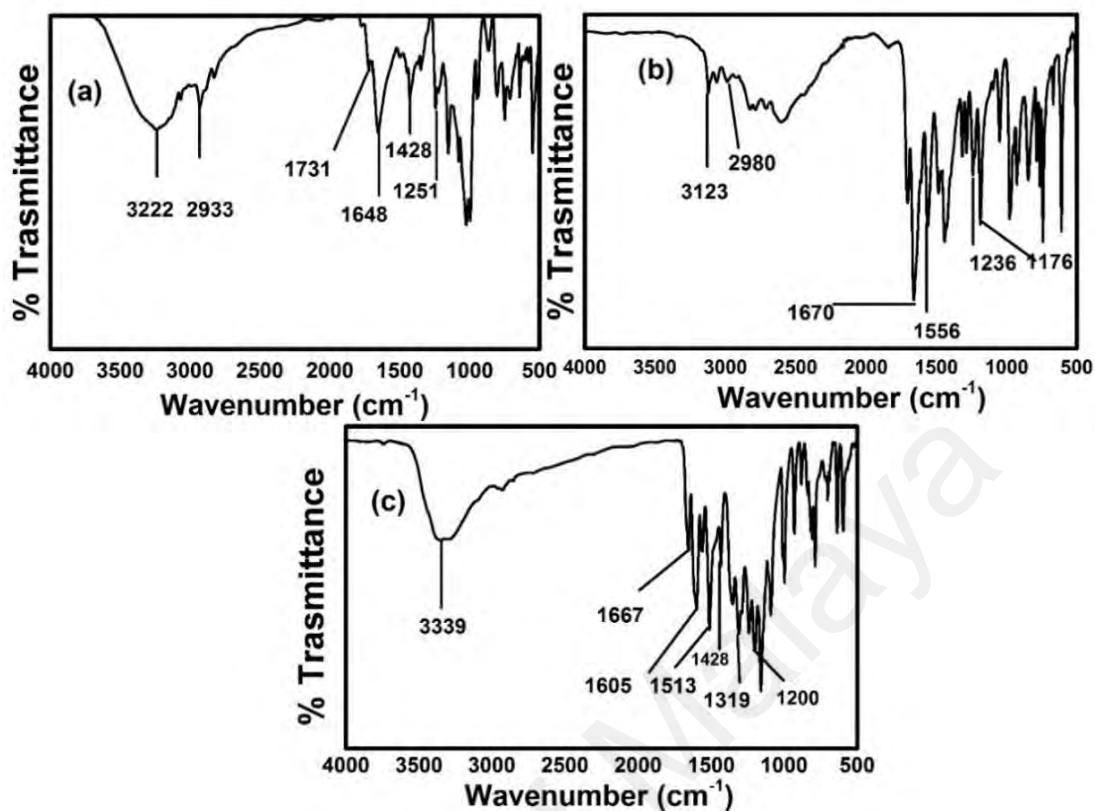


Figure 4.10: FTIR spectra of a) 5-Fluorouracil, b) theophylline, and c) quercetin

j) Quercetin (QRT)

Figure 4.10 (c) shows the spectrum of quercetin. In this spectrum, the broad band appeared at 3339 cm^{-1} shows the presence of phenolic OH group. The peak at 1667 cm^{-1} attribute to C=O stretching. Furthermore, the characteristic stretching vibration of cyclohexene skeleton can be observed at 1605 cm^{-1} , 1513 cm^{-1} and 1428 cm^{-1} respectively. The absorption band at $1400\text{-}1200\text{ cm}^{-1}$ correspond to bending of phenolic OH group (Song et al., 2009).

4.2.1.2 Hydrogels

(a) *N*-succinyl chitosan/ poly (acrylamide-co-acrylic acid) Hydrogel

The spectrum of *N*-succinyl chitosan/ poly (acrylamide-co-acrylic acid) hydrogel is shown in Figure 4.11. This spectrum showed appearance of some new peaks at 3350 cm^{-1} (O-H stretching), 3195 cm^{-1} ($-\text{NH}_2$), 2950 cm^{-1} (C-H stretching), 1646 cm^{-1} ($-\text{C}=\text{N}-$),

1444 cm^{-1} (symmetric stretching of $-\text{COO}^-$), 1404 cm^{-1} (asymmetric stretching of $-\text{COO}^-$), and 1329 cm^{-1} (imide). The absorption peak at 1030 cm^{-1} indicate the presence of C-N and C-O stretching vibration. The peaks at 1646 cm^{-1} and 1329 cm^{-1} provide strong evidence on the Schiff base formation between amino groups of N-succinyl chitosan. The presence of carboxylate ions and amide group in the semi-IPN hydrogel confirm the Schiff base formation and embedding of poly (acrylamide-co-acrylic acid) within the hydrogel

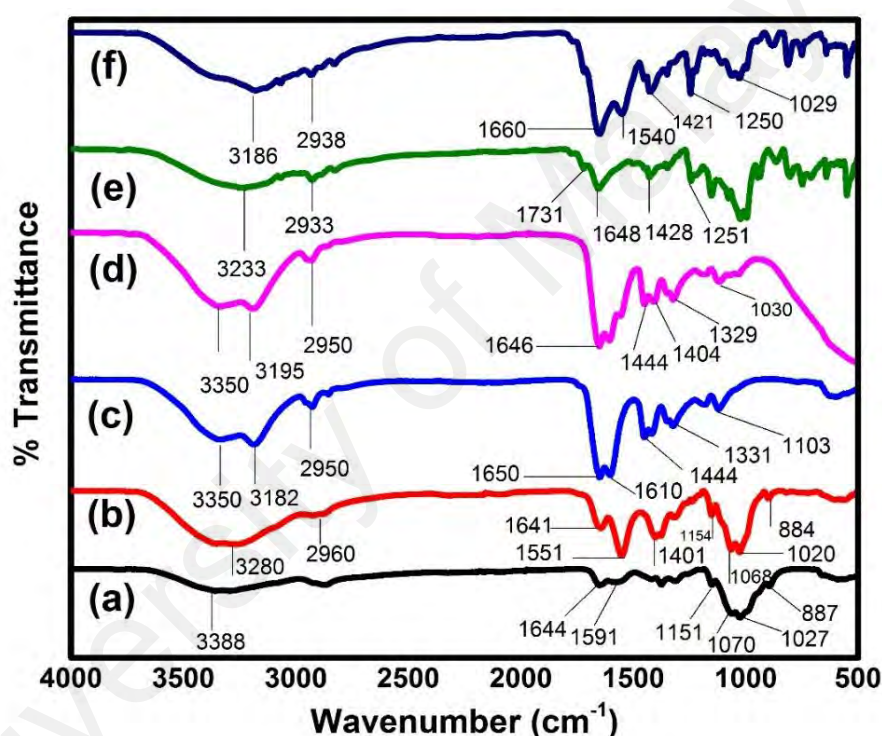


Figure 4.11: FTIR spectra of a) Chitosan, b) N-succinyl chitosan, c) poly (acrylamide-co-acrylic acid), d) SP2 formulation of N-succinyl chitosan/ poly (acrylamide-co-acrylic acid) hydrogel, e) 5-FU, and f) 5-FU loaded N-succinyl chitosan/ poly (acrylamide-co-acrylic acid) hydrogel

Furthermore, 5-FU loaded hydrogel spectrum shows the presence of 5-FU as all the bands present in 5-FU spectrum were found in the spectrum of 5-FU loaded hydrogel. Hence, FTIR analysis provides significant evidence for the formation of semi-IPN and successfully 5-FU loading in hydrogel. Moreover, it also confirms that there is no chemical interaction between 5-FU and hydrogel as there is no new peak representing the new chemical linkage between 5-FU and hydrogel.

(b) N-succinyl chitosan-g-poly (acrylamide-co-acrylic acid) Hydrogel

FTIR spectra of chitosan, N-succinyl chitosan, poly (acrylamide-co-acrylic acid), N-succinyl chitosan-g-poly (acrylamide-co-acrylic acid) hydrogel, theophylline and theophylline loaded N-succinyl chitosan-g-poly (acrylamide-co-acrylic acid) hydrogel are shown in Figure 4.12 (a, b, c, d, e & f). Figure 4.12 (d) shows the spectrum of N-succinyl chitosan-g-poly (acrylamide-co-acrylic acid) hydrogel. The absorption bands at 3339 cm^{-1} and 2955 cm^{-1} corresponds to OH and C-H stretching vibration, respectively. The characteristic intense peak at 1713 cm^{-1} shows the presence of COOH of acrylic acid group while the peak at 1643 cm^{-1} is due to the presence of carboxamide group of acrylamide. The peaks at 1455 cm^{-1} and 1413 cm^{-1} show N-H in plane bending of secondary amide and symmetric stretching vibration of carboxylate anion, respectively.

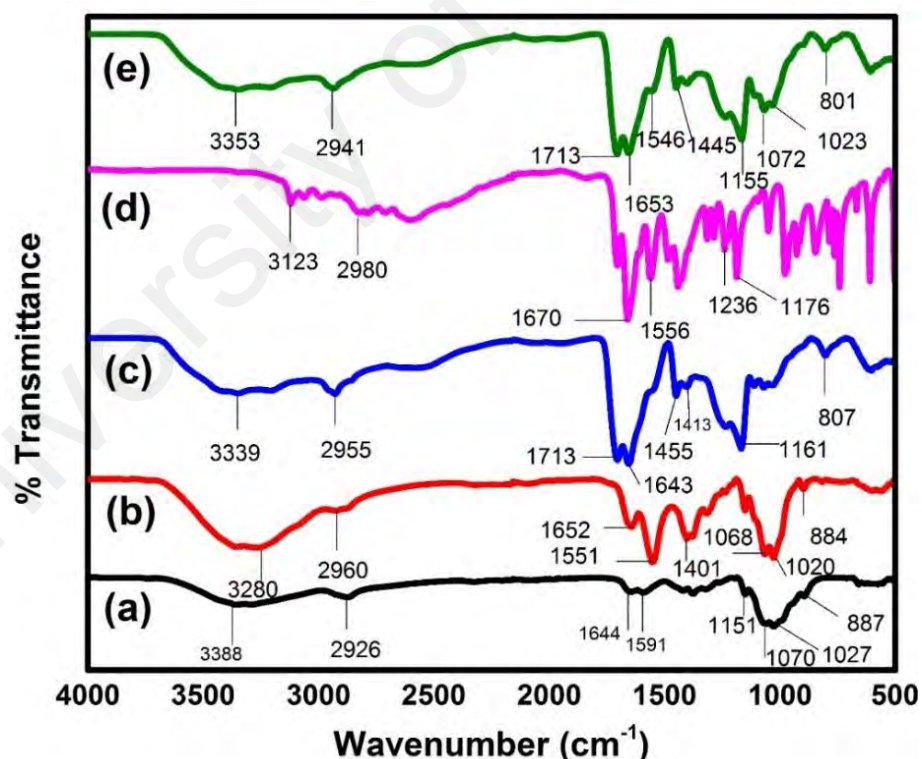


Figure 4.12: FTIR spectra of a) Chitosan, b) N-succinyl chitosan, c) NAA1 formulation of N-succinyl chitosan-g-poly (acrylamide-co-acrylic acid) hydrogel, d) theophylline, and e) theophylline loaded N-succinyl chitosan-g-poly (acrylamide-co-acrylic acid) hydrogel

Furthermore, absorption peaks at 1161 cm^{-1} and 807 cm^{-1} indicate presence of the saccharide unit of N-succinyl chitosan. Figure 4.12 (f) represents the spectrum of theophylline loaded N-succinyl chitosan-g-poly (acrylamide-co-acrylic acid) hydrogel. It can be seen that the peaks of theophylline are present in this spectrum which confirms the theophylline loading. Hence, FTIR analysis provides significant evidence of new formulation of gel and presence of theophylline in the drug loaded gel. This analysis also confirms that there is no significant interaction between theophylline and the gel.

(c) N-succinyl chitosan-g-poly (acrylic acid) Hydrogel

FTIR spectra of chitosan, N-succinyl chitosan, acrylic acid, N-succinyl chitosan -g-poly (acrylic acid) hydrogel, theophylline and theophylline loaded N-succinyl chitosan-g-poly (acrylic acid) hydrogel are shown in Figure 4.13 (a, b, c, d, e, & f).

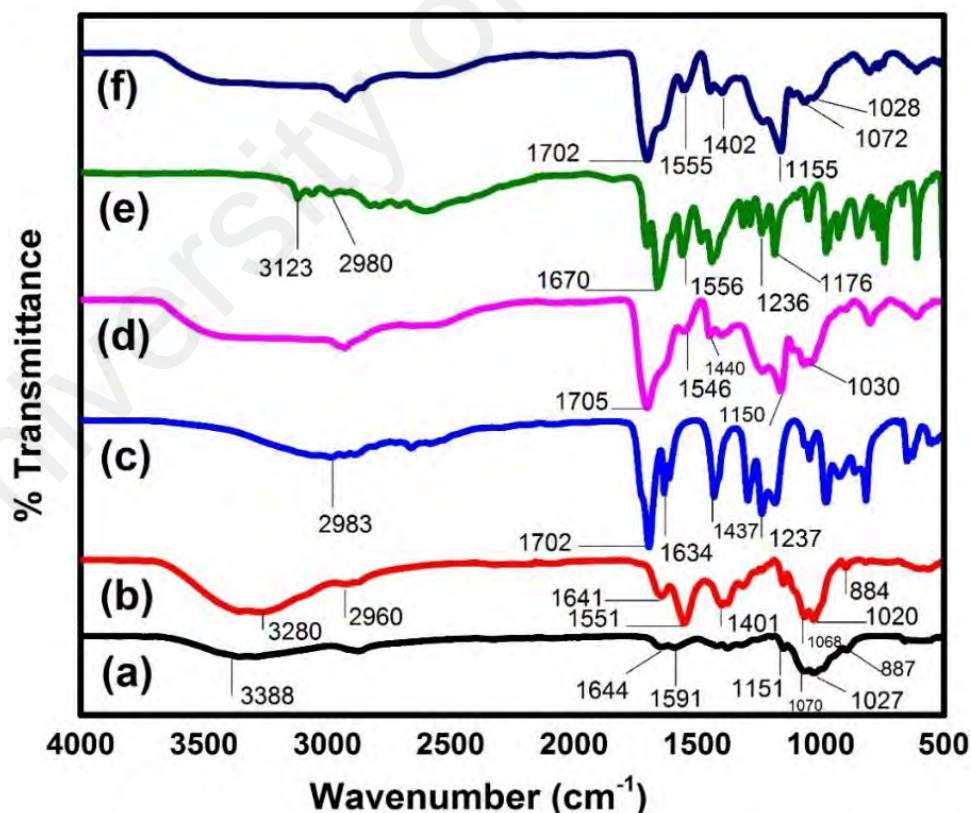


Figure 4.13: FTIR spectra of a) Chitosan, b) N-succinyl chitosan, c) acrylic acid, d) NSA1 formulation of N-succinyl chitosan-g-poly (acrylic acid) hydrogel, e) theophylline, and f) theophylline loaded N-succinyl chitosan-g-poly (acrylic acid) hydrogel

Figure 4.13 (d) shows the spectrum of N-succinyl chitosan-g-poly (acrylic acid) hydrogel. In this spectrum, some characteristic peaks of N-succinyl chitosan and acrylic acid have been found. The appearance of peak at 1702 cm^{-1} (-COOH) corresponds to the presence of COOH group from acrylic acid in the hydrogel. In the case of theophylline loaded N-succinyl chitosan-g-poly (acrylic acid) hydrogel, as shown in Figure 4.13 (f), all bands that were observed in pure theophylline are present, indicating the successful drug loading, no chemical interaction between drug and gel was observed as there is no new peak representing the new functional group. Moreover, the intensity of the bands in pure theophylline and theophylline loaded gels are not same. The peak intensity in IR spectrum is always relative. The decrease in peak intensity is due to less concentration of theophylline in the hydrogel (Rokhade et al., 2007; Samanta & Ray, 2014a).

(d) N-succinyl chitosan-g-poly (methacrylic acid) Hydrogel

The FTIR spectra of chitosan, N-succinyl chitosan, methacrylic acid, N-succinyl chitosan-g-poly (methacrylic acid) hydrogel, theophylline and theophylline loaded N-succinyl chitosan-g-poly (methacrylic acid) hydrogel are shown in Figure 4.14 (a, b, c, d, e, & f).

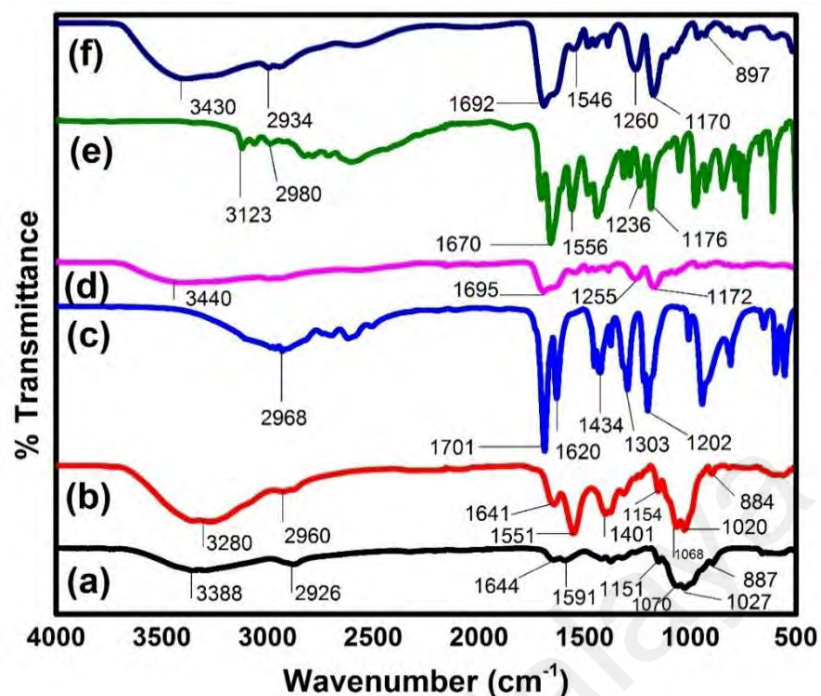


Figure 4.14: FTIR spectra of a) Chitosan, b) N-succinyl chitosan, c) methacrylic acid, d) NSM1 formulation of N-succinyl chitosan-g-poly (methacrylic acid) hydrogel, e) theophylline, and f) theophylline loaded N-succinyl chitosan-g-poly (methacrylic acid) hydrogel

In the FTIR spectrum of N-succinyl chitosan-g-poly (methacrylic acid) hydrogel which is shown in Figure 4.14 (d), the peak at 3440 cm^{-1} represents the presence of OH and N-H stretching vibration. Moreover, the strong absorption bands at 1695 cm^{-1} correspond to presence of methacrylic acid and N-succinyl chitosan was confirmed by the peak appeared at 1172 cm^{-1} . Furthermore, the spectrum of theophylline loaded hydrogel is shown in Figure 14.4 (f). It can be observed that the absorption bands present in the theophylline are also present in the theophylline loaded hydrogel spectrum. Hence, FTIR analysis provides significant evidence of new formulation of gel and presence of theophylline in the drug loaded hydrogel.

(e) Karaya gum-g-poly (acrylic acid) Hydrogel

The FTIR spectra of karaya gum, acrylic acid, karaya gum-g-poly (acrylic acid) hydrogel, quercetin and quercetin loaded karaya gum-g-poly (acrylic acid) hydrogel are shown in Figure 4.15 (a, b, c, d, & e). In spectrum of karaya gum-g-poly (acrylic acid) hydrogel,

as shown in Figure 4.15 (c), in spite of presence of OH, NH and C-H stretching vibrations, some specific functional groups which represent the karaya gum and acrylic acid are indicated. In this spectrum, the characteristic peak at 1700 cm^{-1} correspond to the presence of COOH group of karaya gum and acrylic acid. The absorption bands at 1444 cm^{-1} and 1410 cm^{-1} are owing to symmetric and asymmetric stretching of $-\text{COO}^-$ ions of karaya gum and acrylic acid, respectively. Moreover, the peak at 1410 cm^{-1} also represent the $-\text{CH}_2$ of karaya gum and acrylic acid. The peak at 1150 cm^{-1} correspond to saccharide unit of karaya gum and the peak at 1029 cm^{-1} shows the presence of C-O-C bond. Furthermore, the spectrum of quercetin loaded hydrogel has been shown in Figure 4.15 (e). It can be observed from the quercetin loaded hydrogel spectrum, the new peaks at 1602 cm^{-1} and 1520 cm^{-1} which show the presence of cyclobenzene skeleton confirm the successful loading of the drug in the hydrogel. Consequently, FTIR study reveals the successful synthesis of hydrogel and successful quercetin loading in the hydrogel.

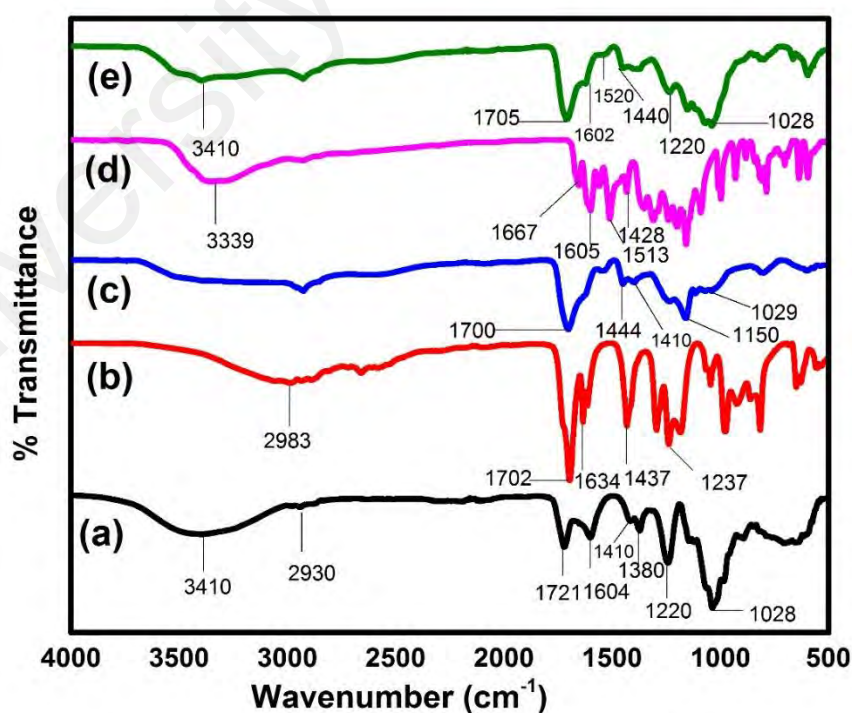


Figure 4.15: FTIR spectra of a) karaya gum, b) acrylic acid, c) KGA1 formulation of karaya gum-g-poly (acrylic acid) hydrogel, d) quercetin, and e) quercetin loaded karaya gum-g-poly (acrylic acid) hydrogel

4.2.2 X-ray Diffraction Analysis

This section describes the XRD analysis of reactants as well as the synthesized hydrogels.

4.2.2.1 Chitosan and N-succinyl chitosan

The change of chitosan structure after chemical modification was investigated by means of powder X-ray diffraction. Figure 4.16 shows the XRD pattern of chitosan and N-succinyl chitosan. Chitosan spectrum shows two distinct crystalline peaks at $2\theta = 10^\circ$ and $2\theta = 20^\circ$. According to Samuel's observations, the peaks at $2\theta = 10^\circ$ and $2\theta = 20^\circ$ represent the crystalline form I and II, respectively (Samuels, 1981). It might be owing to the formation of intermolecular and intramolecular hydrogen bonds between hydroxyl and amino groups of chitosan. Furthermore, there is a regularity in the structure of chitosan molecules which makes it crystalline (Ge & Wang, 2014). However, chemical modification of chitosan via N-succinylation changed the XRD pattern of chitosan. N-succinyl chitosan spectrum shows that the distinctive peak at $2\theta = 10^\circ$ disappeared while the broad peak at $2\theta = 20^\circ$ is retained with weak intensity. This decrease in the intensity might be owing to the destruction of chitosan structure and reduction in the ability to form hydrogen bonds between hydroxyl and amino groups after successful modification. This change in XRD pattern also explains the predominant amorphous nature of N-succinyl chitosan (Zhang et al., 2003).

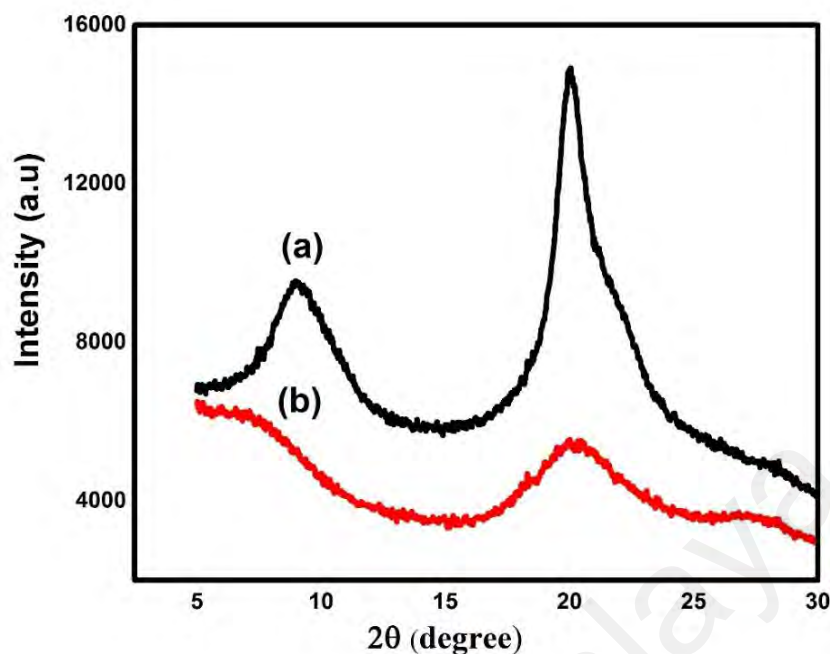


Figure 4.16: XRD spectra of a) Chitosan, b) N-succinyl chitosan

4.2.2.2 N-succinyl chitosan/ poly (acrylamide-co-acrylic acid) Hydrogel

Figure 4.17 (a) shows the XRD spectrum of N-succinyl chitosan/ poly (acrylamide-co-acrylic acid) hydrogel. XRD analysis showed that the intensity of reflection peak at $2\theta = 20^\circ$ of hydrogel further decreased as compared to N-succinyl chitosan and marginal shifting of peak at $2\theta = 20^\circ$ to $2\theta = 21.6^\circ$ occurred. The decreased in intensity and marginal shifting of peak strongly indicates the breakage of intermolecular hydrogen bonds between hydroxyl and amino groups of the parent N-succinyl chitosan. All these findings evidently verified that the modification of chitosan reduced the crystallinity due to reduction in the ordered structure and Schiff base formation further destroyed the ordered structure of N-succinyl chitosan and ultimately resulted in an increase of the amorphous nature in the hydrogel (Mukhopadhyay et al., 2014).

4.2.2.3 N-succinyl chitosan-g-poly (acrylamide-co-acrylic acid) Hydrogel

Figure 4.17 (b) shows the XRD pattern of N-succinyl chitosan-g-poly (acrylamide-co-acrylic acid) hydrogel. This pattern reveals that N-succinyl chitosan spectrum changed significantly after chemical crosslinking with poly (acrylamide-co-acrylic acid). The area

under the peak of crystalline form II decreased significantly after chemical crosslinking. Furthermore, the average crystallinity index (ratio of the area of peak at $2\theta = 20^\circ$) of N-succinyl chitosan was reduced when the poly (acrylamide-co-acrylic acid) was grafted over N-succinyl chitosan. So, crosslinking inhibits the close packing of polymer network chains by reducing the degree of freedom in the 3-D conformation and the formation of crystalline region. This reduction in crystallinity would play a crucial role on influencing hydrogel degradability, water absorption, and swelling ratio, as it is endorsed by results of the swelling ratio (Costa-Júnior et al., 2009).

4.2.2.4 N-succinyl chitosan-g-poly (acrylic acid) Hydrogel

Figure 4.17 (c) illustrates the spectrum of N-succinyl chitosan-g-poly (acrylic acid) hydrogel. According to this spectrum, hydrogel is more amorphous in nature owing to grafting of acrylic acid over N-succinyl chitosan. This grafting over N-succinyl chitosan reduces the intermolecular H-bonding and presence of acrylic acid destroyed the ordered structure of N-succinyl chitosan. Amorphous hydrogel has enhanced water absorption property and more water molecules bound to polysaccharide matrix.

4.2.2.5 N-succinyl chitosan-g-poly (methacrylic acid) Hydrogel

Figure 4.17 (d) shows the presence of N-succinyl chitosan-g-poly (methacrylic acid) hydrogel. Spectrum of hydrogel shows further decrease in crystallinity as compared to chitosan and N-succinyl chitosan. It might be due to the presence of methacrylic acid resulting in the conjugation of bulky poly (methacrylic acid) and MBA. The presence of bulky group caused increase in fraction of amorphous phase (Huang et al., 2006).

If we compare XRD results of above mentioned N-succinyl chitosan hydrogels, it can be said that N-succinyl chitosan/ poly (acrylamide-co-acrylic acid) hydrogel formed through Schiff base has less amorphous nature in comparison to N-succinyl chitosan-g-poly (acrylamide-co-acrylic acid), N-succinyl chitosan-g-poly (acrylic acid), and N-succinyl

chitosan-g-poly (methacrylic acid) hydrogels. It is already mentioned in the synthesis, poly (acrylamide-co-acrylic acid) was embedded in the N-succinyl chitosan hydrogel during synthesis and chemical interactions were not involved between N-succinyl chitosan hydrogel and poly (acrylamide-co-acrylic acid) while there were only physical interactions. However, chemical bonding as well as physical interaction existed in N-succinyl chitosan-g-poly (acrylamide-co-acrylic acid), N-succinyl chitosan-g-poly (acrylic acid), and N-succinyl chitosan-g-poly (methacrylic acid) hydrogels. Chemical interaction means the grafting of acrylamide-co-acrylic acid, acrylic acid, and methacrylic acid on N-succinyl chitosan.

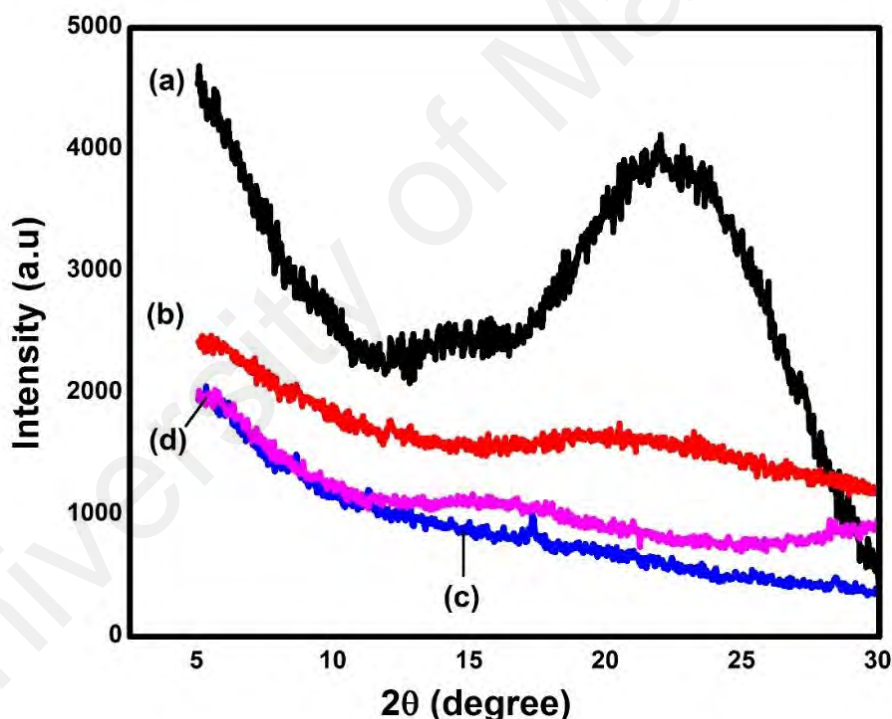


Figure 4.17: XRD spectra of a) SP2 formulation of N-succinyl chitosan/ poly (acrylamide-co-acrylic acid) hydrogel, b) NAA1 formulation of N-succinyl chitosan-g-poly (acrylamide-co-acrylic acid) hydrogel, c) NSA1 formulation of N-succinyl chitosan-g-poly (acrylic acid) hydrogel, and d) NSM1 formulation of N-succinyl chitosan-g-poly (methacrylic acid) hydrogel

The poly electrolyte complexes also formed between amino groups of N-succinyl chitosan and carboxylic groups of acrylic acid. The poly electrolyte complexes broke the

intermolecular forces and destroyed the ordered structure of N-succinyl chitosan whereas no poly electrolyte complex formation took place in the case of N-succinyl chitosan/ poly (acrylamide-co-acrylic acid) hydrogel. Consequently, crystallinity of grafted hydrogels is low as compared to N-succinyl chitosan/ poly (acrylamide-co-acrylic acid).

4.2.2.6 Karaya gum-g-poly (acrylic acid) Hydrogel

Figure 4.18 (a & b) shows the XRD spectra of karaya gum and karaya gum-g-poly (acrylic acid) hydrogel. The spectrum of pure karaya gum shows one peak at $2\theta = 25^\circ$ which reveals the highly ordered structure and crystalline nature of karaya gum. This crystalline nature is owing to the presence of regular arrangement of saccharide units as a result of intermolecular H-bonding. However, the grafting of acrylic acid over karaya gum results in the destruction in ordered structure and crosslinking inhibits the close packing of polymer which decreased the crystallinity of parent karaya gum (Mittal et al., 2015).

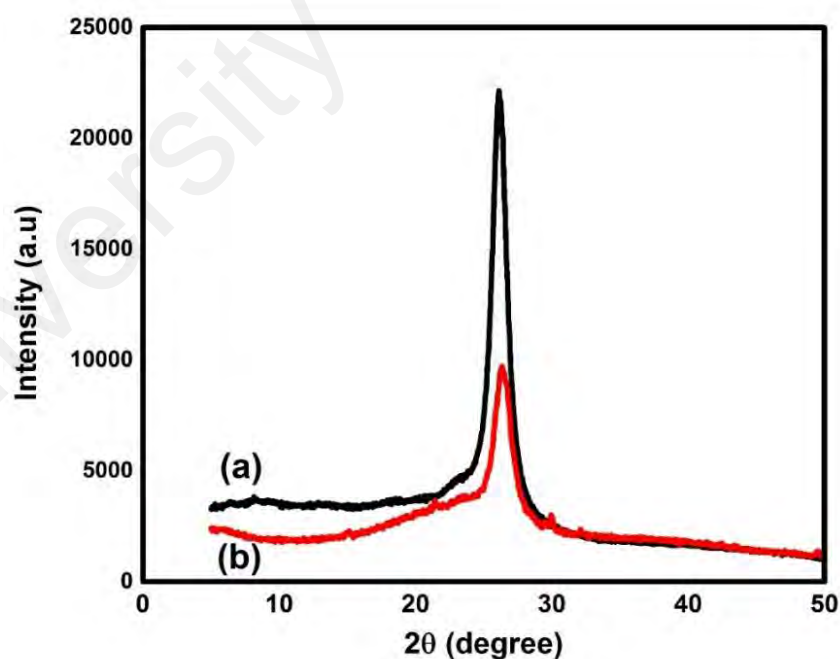


Figure 4.18: XRD spectra of a) karaya gum, b) KGA1 formulation of karaya gum-g-poly (acrylic acid) hydrogel

4.2.3 Differential Scanning Calorimetry Analysis

This section describes the differential scanning calorimetry analysis of chitosan, N-succinyl chitosan, and N-succinyl chitosan-g-poly (acrylamide-co-acrylic acid), N-succinyl chitosan-g-poly (acrylic acid), N-succinyl chitosan-g-poly (methacrylic acid), and karaya gum-g-poly (acrylic acid) hydrogels.

4.2.3.1 Chitosan and N-succinyl chitosan

The phase transitions detected in DSC thermograms of chitosan and N-succinyl chitosan are shown in Figure 4.20 (a & b). DSC thermogram of chitosan shows two curves, one endotherm ranged between 113-206 °C with a crystalline melting temperature (T_m) of 152 °C. The appearance of endotherm might be due to the evaporation of bound water and melting of chitosan (Zhang et al., 2003). The hydration properties depend on the supramolecular structures of polysaccharide. Macromolecules may have disordered structures in solid state and can absorb water easily (Phillips et al., 1996; Sakurai et al., 2000). However, exothermic peak was found at 300 °C which corresponds to decomposition of chitosan polysaccharide. On the other hand, N-succinyl chitosan showed deep endothermic peak centered between 109-187 °C with a crystalline melting temperature (T_m) of 144 °C. This endotherm represents shift of onset melting temperature might be due to decrease in degree of polymerization during N-succinylation under alkaline condition (Mourya et al., 2010, Hwang et al., 2002). Chitosan modification under alkaline conditions causes substantial depolymerization due to glycosidic bond cleavage (Kittur et al., 2002). However, close examination of endotherms of chitosan and N-succinyl chitosan reveals the difference in peak area might be due to different water holding capacity and strength of water-polymer interaction (Mourya et al., 2010, Kittur et al., 2002). Furthermore, increase in enthalpy change (ΔH) value with N-succinylation indicates that a definite correlation exists between supramolecular structure of polymer and water holding capacity. As succinylation proceeds, newly introduced succinyl group

at the chitosan will bind with more water molecules owing to hydrophilic nature and hence increase the content of bound water. Moreover, the decrease in ordered structure due to chemical modification may contribute towards the increase in the content of bound water. However, the second exothermic peak expressing thermal decomposition was found at 275 °C, at temperature lower than pure chitosan which shows less stability. This is also probably might be due to decrease in degree of polymerization. The difference in peak area, peak position, and ΔH suggests the chemical modification of chitosan. Furthermore, N-succinyl chitosan thermogram is distinctly different from the chitosan thermogram which assure their unequivocal identification (Zhang et al., 2003).

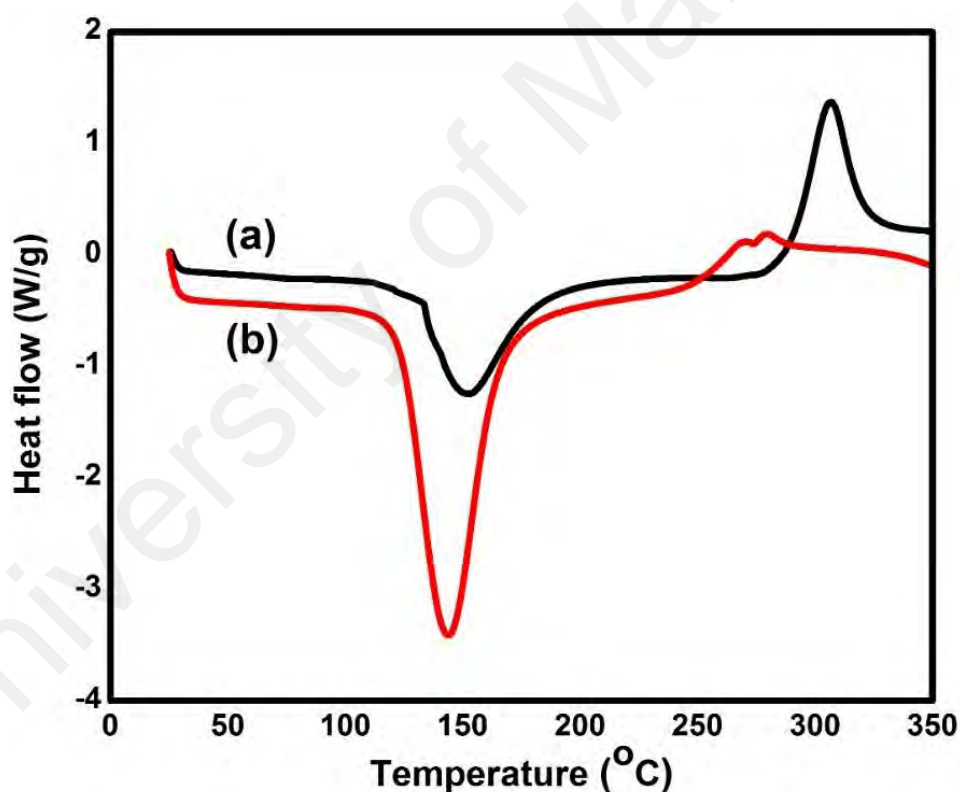


Figure 4.19: DSC thermograms of a) Chitosan and b) N-succinyl chitosan

4.2.3.2 N-succinyl chitosan/ poly (acrylamide-co-acrylic acid) Hydrogel

Figure 4.20 (a) shows the DSC thermogram of N-succinyl chitosan/ poly (acrylamide-co-acrylic acid) hydrogel. This thermogram illustrates two endothermic curves. First deep endothermic curve represents the removal of bound water and phase change with a crystalline melting temperature (T_m) of 172 °C from solid to liquid state. Crystalline

melting temperature (T_m) of pure N-succinyl chitosan was found to be 152 °C. However, it is 172 °C in the case of N-succinyl chitosan/ poly (acrylamide-co-acrylic acid) hydrogel, higher than pure N-succinyl chitosan. It might be owing to stability of hydrogel network due to Schiff base formation and physical interaction between N-succinyl chitosan and poly (acrylamide-co-acrylic acid). The second endothermic curve at a temperature of 233 °C characterized as breakage of crosslinking of N-succinyl chitosan.

4.2.3.3 N-succinyl chitosan-g-poly (acrylamide-co-acrylic acid) Hydrogel

Figure 4.20 (b) shows the DSC thermogram of N-succinyl chitosan-g-poly (acrylamide-co-acrylic acid) hydrogel. This thermogram shows phase change with a crystalline melting temperature (T_m) of 168 °C. The crystalline melting temperature as compared to N-succinyl chitosan might be due to increase in stability of gel network as compared to pure N-succinyl chitosan after crosslinking. The crosslinked network reduces the polymer chain flexibility which increases the crystalline melting temperature (Saboktakin et al., 2011). This endotherm shows the ΔH value of 54.8 J/g. It can be observed that thermograms of chitosan and N-succinyl chitosan showed only one endothermic peak while the N-succinyl chitosan-g-poly (acrylamide-co-acrylic acid) gel shows two endothermic peaks. The second endothermic curve with peak temperature (T_p) of 217 °C is indicating the breakage of crosslinking. Therefore, the gel formed is expected to be stable at physiological temperature of 37 °C.

4.2.3.4 N-succinyl chitosan-g-poly (acrylic acid) Hydrogel

Figure 4.20 (c) shows the DSC thermogram of N-succinyl chitosan-g-poly (acrylic acid) hydrogel. This thermogram reveals two endothermic curves. First endothermic curve with a crystalline melting temperature (T_m) of 204 °C. This endothermic curve represents the melting of the hydrogel. The increase in T_m as compared to pure N-succinyl chitosan might be owing to stable gel network. The hydrogel network seems to be stable due to

crosslinking. The second endothermic curve with a peak temperature of 270 °C represents the breakage of crosslinking (Saboktakin et al., 2011).

4.2.3.5 N-succinyl chitosan-g-poly (methacrylic acid) Hydrogel

Figure 4.20 (d) shows the thermogram of N-succinyl chitosan-g-poly (methacrylic acid) hydrogel. According to this thermogram, first endothermic curve with a peak temperature of 150 °C represents the loss of bound water and crystalline melting temperature (T_m) of N-succinyl chitosan-g-poly (methacrylic acid) hydrogel. The higher crystalline melting temperature (T_m) of hydrogel as compared to N-succinyl chitosan is due to crosslinking of N-succinyl chitosan and methacrylic acid (Saboktakin et al., 2011). In addition, the single T_m value and difference in ΔH of N-succinyl chitosan and gel indicate the crosslinking of N-succinyl chitosan and methacrylic acid. However, the other wide endothermic curve with peak temperature (T_p) of 235 °C is indicating the breakage of crosslinking.

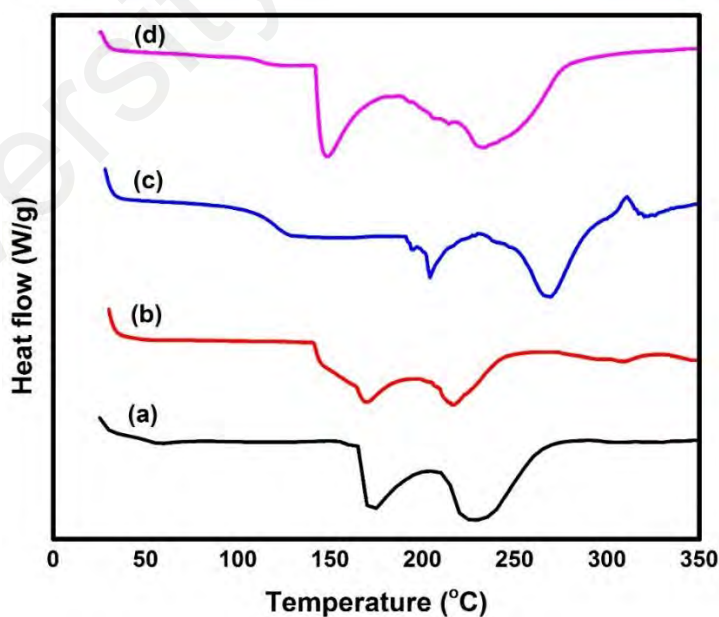


Figure 4.20: DSC thermograms of a) SP2 formulation of N-succinyl chitosan/ poly (acrylamide-co-acrylic acid), b) NAA1 formulation of N-succinyl chitosan-g-poly (acrylamide-co-acrylic acid), c) NSA1 formulation of N-succinyl chitosan-g-poly (acrylic acid), d) NSM1 formulation of N-succinyl chitosan-g-poly (methacrylic acid) hydrogels

Table 4.1: Crystalline melting temperature (T_m) of endothermic curves, peak temperature (T_p) of exothermic curves, and enthalpy change (ΔH) of chitosan, N-succinyl chitosan, karaya gum and N-succinyl chitosan-g-poly (acrylamide-co-acrylic acid), N-succinyl chitosan-g-poly (acrylic acid), N-succinyl chitosan-g-poly (methacrylic acid), and karaya gum-g-poly (acrylic acid) hydrogels

Formulation	Endotherm m T_m (°C)	ΔH (J/g)	Exotherm Tp (°C)	ΔH (J/g)	Endotherm (II) Tp (°C)	ΔH (J/g)
Chitosan	152	204.3	300	- 178.7		
NSC	144	469.3	268	-27.6		
NSC/ poly(AAm-co-AA)	172	76.0			233	123.7
NSC-g-poly(AAm-co-AA)	168	54.8			217	52.3
NSC-g-poly(AA)	204	21.3			269	96.6
NSC-g-poly(MAA)	150	112.8			234	253.9
KG	168	261.0	280	-81.9		
KG-g-poly(AA)	182	74.8			288	92.2

4.2.3.6 Karaya gum-g-poly (acrylic acid) Hydrogel

Figure 4.21 (a & b) shows the DSC thermogram of karaya gum and karaya gum-g-poly (acrylic acid) hydrogels. Karaya gum thermogram shows two curves. First is the endothermic curve with a crystalline melting temperature (T_m) of 168 °C. This endothermic curve shows phase change from solid state to liquid state and loss of water of crystallization. The crystalline melting temperature is very high which shows higher stability of the structure and resistant to heat. The endothermic curve seems to be very sharp which shows the crystal uniformity (Daoub et al., 2016). This higher crystalline nature was also observed in XRD analysis. Moreover, there is another exothermic curve with peak temperature of 280 °C. This exothermic curve shows the decomposition of karaya gum. Furthermore, thermogram of karaya gum-g-poly (acrylic acid) hydrogel shows two endothermic curves. First broad endothermic curve with a crystalline melting temperature 182 °C higher than pure karaya gum. This higher T_m value indicates the higher stability of hydrogel as compared to the pure karaya gum. Moreover, second endothermic curve with peak temperature of 288 °C shows the breakage of crosslinking.

Crystalline melting temperature (T_m) of endothermic curves, peak temperature (T_p) of exothermic curves, and enthalpy change (ΔH) of chitosan, N-succinyl chitosan, karaya gum and N-succinyl chitosan-g-poly (acrylamide-co-acrylic acid), N-succinyl chitosan-g-poly (acrylic acid), N-succinyl chitosan-g-poly (methacrylic acid), and karaya gum-g-poly (acrylic acid) hydrogels are given in Table 4.1.

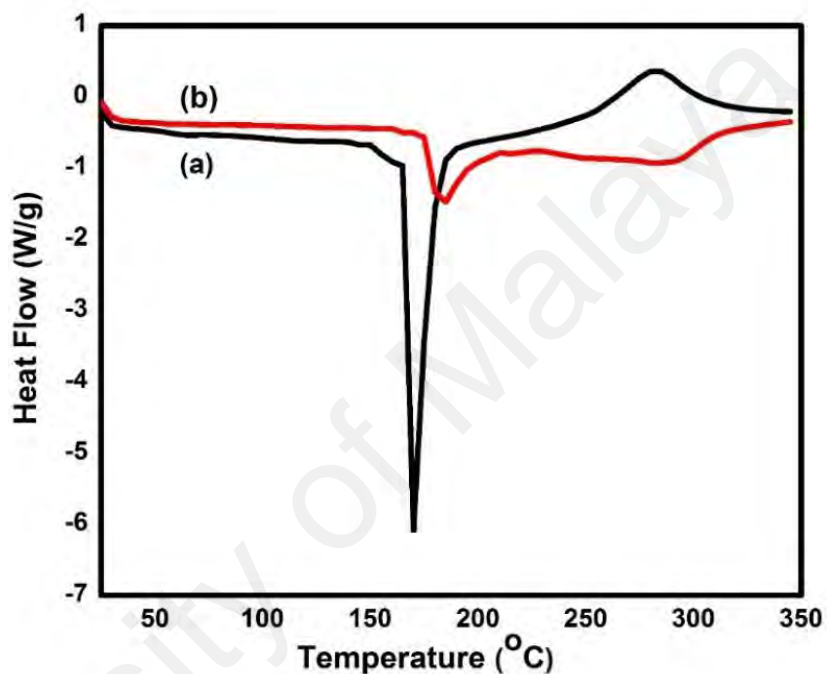


Figure 4.21: DSC thermograms of a) karaya gum, and b) KGA1 formulation of karaya gum-g-poly (acrylic acid) hydrogel

4.2.4 Morphology

The attained hydrogels were intended for drug delivery application. In this application, surface morphology and interior geometry play imperative role which affect the swelling properties and drug release behavior, so it was of great interest to explore these properties (Chen et al., 2009). FESEM is a very practical technique to analyze three-dimensional network structure and the matrix morphology of the gels. FESEM images were investigated to observe the microstructural morphology of freeze-dried hydrogels.

4.2.4.1 N-succinyl chitosan/ poly (acrylamide-co-acrylic acid) Hydrogels

The micrographs of freeze dried hydrogels crosslinked with GA are shown in Figure 4.22 (a, b, c & d). These micrographs show the high micro porosity structure of hydrogels. The porosity of hydrogels arose from evaporation of water during the process of freeze drying without affecting the morphology of hydrogels (Zhang et al., 2010). The porous construction of hydrogels enables them to swell, reduces flow resistance of water and enhances the rate to entrap drug. These hydrogels show different surface morphology due to change in concentration of polymers and crosslinking agent in the hydrogels. The change in the composition changed the network structure of the hydrogels. Figure 4.22 (a) shows highly porous network structure of the hydrogel. This porous network is owing to higher hydrophilicity of N-succinyl chitosan because it is present in larger amount. Moreover, Figure 4.22 (b) represents the surface morphology of SP2 hydrogels in which poly (acrylamide-co-acrylic acid) is embedded in large amount as compared to SP1. The embedding of this polymer resulted in apparently reduction in pore size (Lee & Chen, 2001). Besides, the pore size is more uniform as compared to SP1. Moreover, Figure 4.22 (c) illustrates the dense network structure of the hydrogel. This dense network might be due to embedment of larger amount of poly (acrylamide-co-acrylic acid) and lower amount of N-succinyl chitosan. Furthermore, pore walls of this hydrogels become thicker than those of SP1 and SP2 (Lee & Chen, 2001). Moreover, Figure 4.22 (d) demonstrates

the surface morphology of SP7 which contained greater amount of crosslinking agent. The enhanced crosslinking agent decreased the swelling ratio and water diffusion. The pore size reduced significantly due to formation of tightly packed network structure.

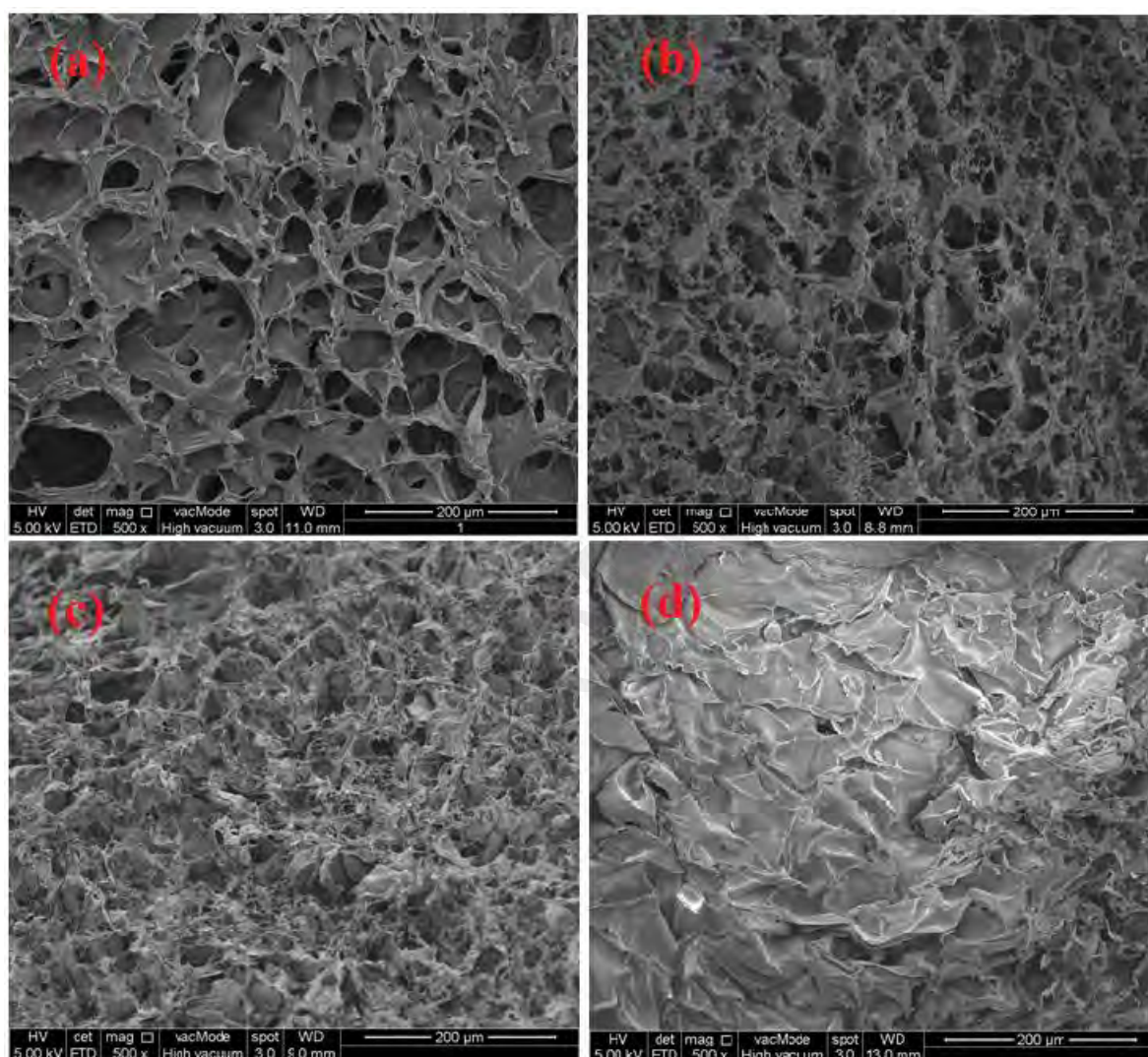


Figure 4.22: Micrographs of a) SP1, b) SP2, c) SP3, and d) SP7 hydrogel

4.2.4.2 N-succinyl chitosan-g-poly (acrylamide-co-acrylic acid) Hydrogels

Figure 4.23 (a & b) shows the micrographs of freeze-dried gel networks of NAA1 and NAA3, respectively. The effect of crosslinker concentration on morphology of the formulated hydrogels was observed. It is evident that the formulated hydrogels exhibit porous surface. However, variation in the crosslinker concentration results in different porous surface. A honeycomb-like loose structure is formed in NAA1 gel (Figure 4.23

(a) which was prepared with low concentration of crosslinking agent. The NAA1 gel also exhibits highly interconnected porous structure with uniform pore size distribution. However, pore size and uniformity of NAA3 gel (Figure 4.23 (b)) decreased with increase in the concentration of crosslinking agent. The increase in concentration of crosslinking agent decreased the swelling ratio, and migration of water. The results illustrate that pore size of the gels can be tailored by changing the composition of the hydrogels.

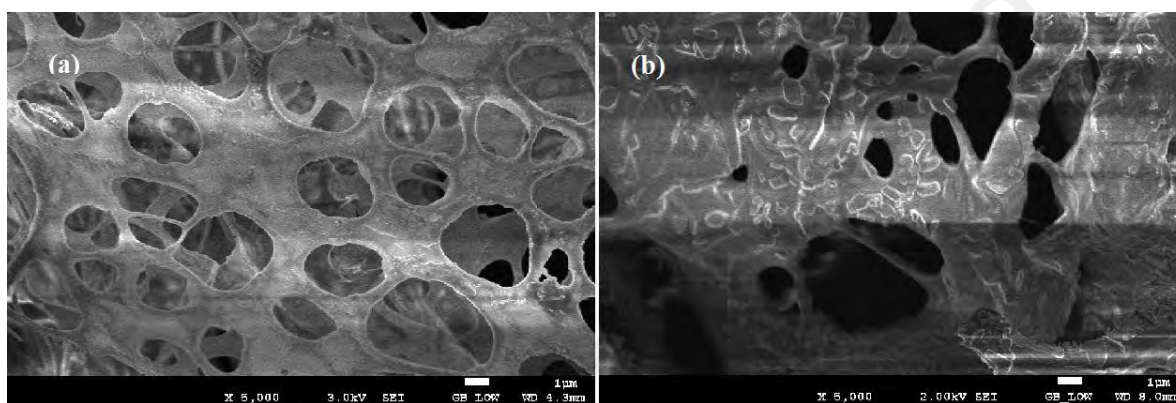


Figure 4.23: Micrographs of a) NAA1 and b) NAA3 hydrogels

4.2.4.3 N-succinyl chitosan-g-poly (acrylic acid) Hydrogels

Figure 4.24 (a & b) shows the micrographs of NSA1 and NSA3 gels with different crosslinking density, respectively. In this study, honeycomb-like structures of hard, rigid and strong hydrogel networks were found. These micrographs show the porous network structure of the hydrogels which can absorb water or physiological solution due to sorption capacity. It was also confirmed from measurement of swelling ratio. Moreover, the uniformity and homogeneity of the structures appears to be better porous network. Morphology study reveals that the porosity depends on the crosslinking density. Hydrogel consisted lower amount of crosslinking agent produced lower crosslinking density and hence loose network structure as compared to hydrogel with greater amount of crosslinking agent in the formulation. NSA3 hydrogel has tight network structure and small pores as compared to NSA1. NSA3 hydrogel shows compact structure as compared

to NSA1. Moreover, NSA1 prepared from lower amount of crosslinking agent compared to NSA3 is lower in crosslinking density, greater porosity, higher swelling ratio, drug entrapment, and drug release than NSA3.

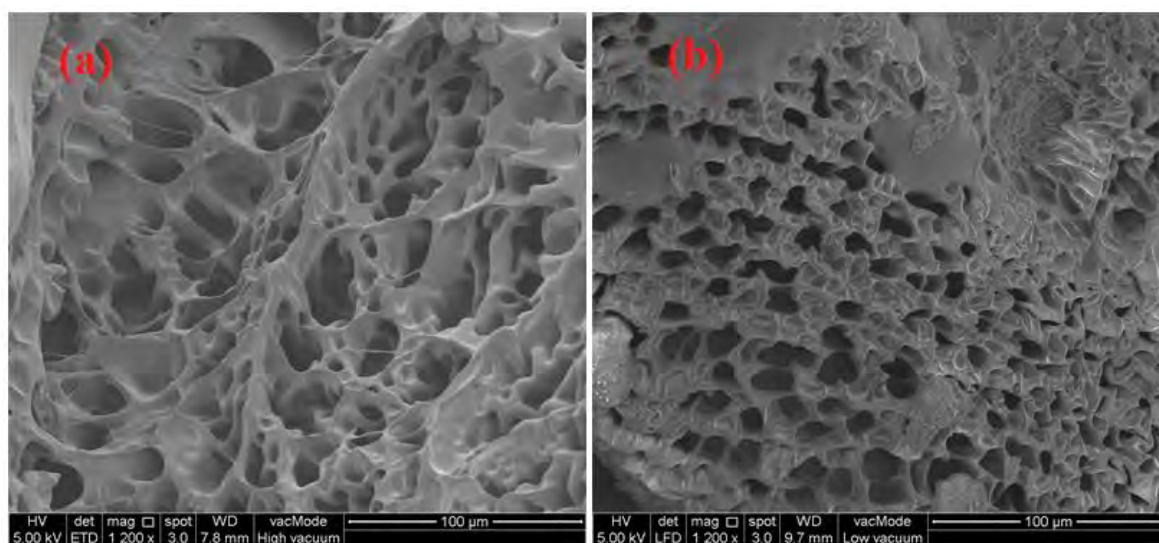


Figure 4.24: Micrographs of a) NSA1) and b) NSA3 hydrogels

4.2.4.4 N-succinyl chitosan-g-poly (methacrylic acid) Hydrogels

The surface morphology of NSM1 and NSM3 freeze-dried gels was observed. Hydrogels were crosslinked with different amounts of MBA. The micrographs of NSM1 and NSM3 are shown in Figure 4.25 (a & b). The micrographs clearly show the porous network of the hydrogels. This porous network was responsible for maximum swelling ratio, drug loading, and release as all these factors are sorption dependent. It can also be observed that morphology of the gels is dependent on the crosslinking concentration. Figure 4.25 (a) shows that NSM1 gel is more porous as compared to NSM3 which contains greater concentration of MBA (Figure 4.25 (b)).

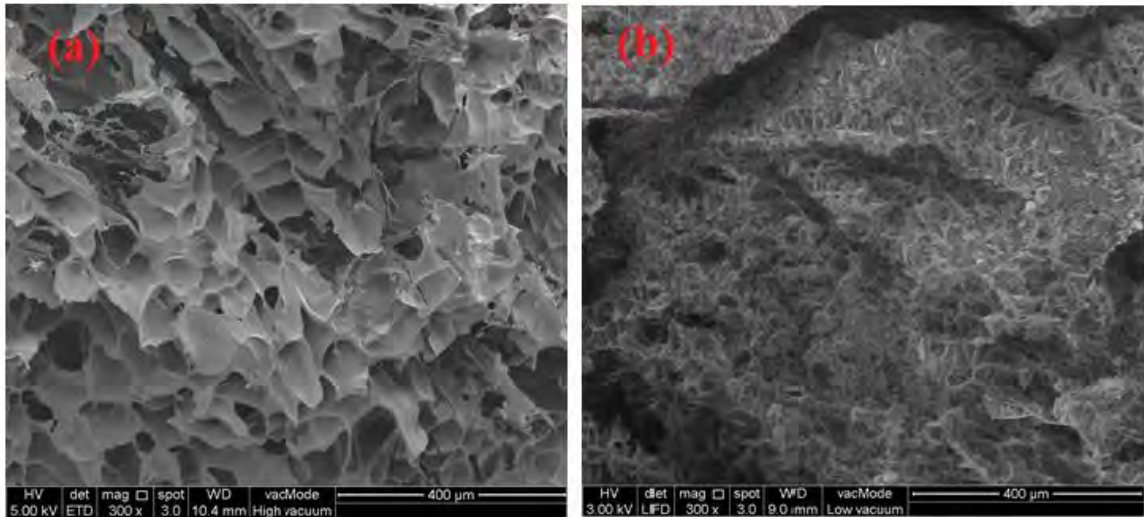


Figure 4.25: Micrographs of a) NSM1 and b) NSM3 hydrogels

4.2.4.5 Karaya gum-g-poly (acrylic acid) Hydrogels

The micrographs of karaya gum-g-poly (acrylic acid) are presented in Figure 4.26 (a & b). These micrographs show the porosity of two hydrogels having different composition. Figure 4.26 (a) reveals the skin layer morphology of KGA1 hydrogel retaining uniform pores throughout the hydrogel. These pores were retained during freeze-drying of the hydrogel. This image of the hydrogel confirms the reported literature that hydrogels form skin layer due to dehydration during gelation and freeze-drying. Moreover, Figure 4.26 (b) represents the morphology of KGA2 hydrogel containing greater amount of crosslinking agent (Crompton et al., 2005). Figure 4.26 (b) shows the fracture surface of

hydrogel with minimal microchannels which reveals the compact structure during water loss. This compact structure might be owing to the greater crosslinking concentration.

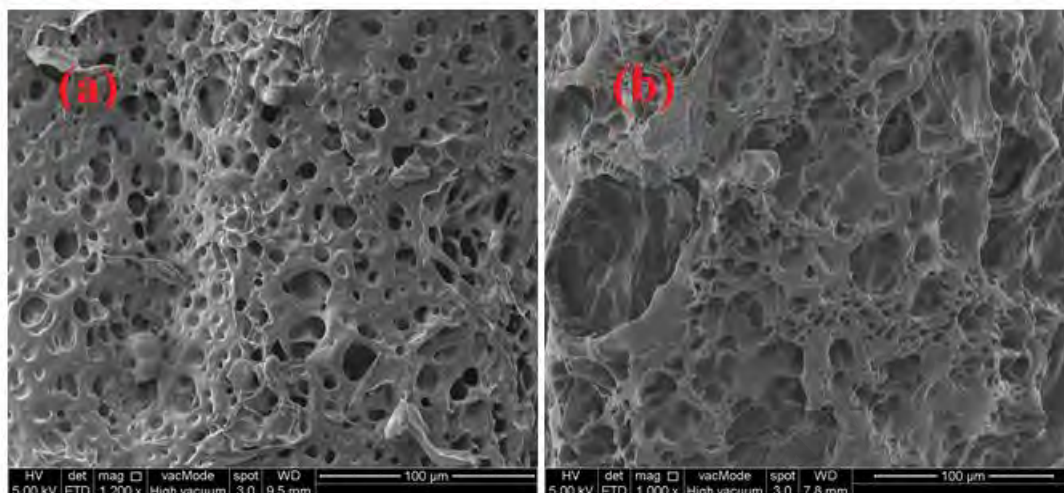


Figure 4.26: Micrographs of a) KGA1 and b) KGA3 hydrogels

4.2.5 Yield (%), Gel contents (%), and Gel time of the Hydrogels

N-succinyl chitosan-g-poly (acrylamide-co-acrylic acid), N-succinyl chitosan-g-poly (acrylic acid), N-succinyl chitosan-g-poly (methacrylic acid), and karaya gum-g-poly (acrylic acid) hydrogels were synthesized by varying the concentration of reaction variables such as initiator, crosslinker, and monomers. The variation of yield (%), gel contents (%) and gel time were observed during the synthesis of the hydrogels and discussed.

i) Effect of initiator concentration

Figures 4.27, 4.28, 4.29, and 4.30 (NAA1, NAA2, NSA1, NSA2, NSM1, NSM2, KGA1, KGA2) show the effect of concentration of initiator on yield (%), gel contents (%), and gel time. With the increase in concentration of initiator, yield (%) increased but gel contents (%) decreased and gel time decreased. The increase in yield (%) was due to maximum grafting of polymers in a limited time but decrease in gel contents (%) was owing to the termination of growing chains by excessive free radicals. The soluble part increased due to formation of short chain polymers, ultimately resulted in reduction of

gel contents (%). This short chain polymerization occurred at a faster rate and gel time decreased (Mall et al., 2006a; Mandal & Ray, 2013).

ii) Effect of crosslinker concentration

Figures 4.27, 4.28, 4.29, and 4.30 (NAA1, NAA3, NSA1, NSA3, NSM1, NSM3, KGA1, KGA3) show the effect of concentration of crosslinking agent on yield (%), gel contents (%), and gel time. Crosslinking agent had a significant effect on the yield (%), gel contents (%), and gel time. The increase in concentration of crosslinking agent increased yield (%) and gel contents (%) while gel time decreased. The increase in yield (%) and gel contents (%) is due to participation of maximum number of molecules in the polymerization and the reactant molecules hold firmly which ultimately increased the yield (%) and gel contents (%). However, gel time decreased due to increase in the rate of polymerization (Bhattacharya et al., 2009; Wang, & Chen, 2004).

iii) Effect of monomers concentration

Figures 4.27, 4.28, 4.29, and 4.30 (NAA1, NAA4, NSA1, NSA4, NSM1, NSM4, KGA1, KGA4) show the effect of concentration of monomers on yield (%), gel contents (%), and gel time. The increase in monomers concentration increased the gel time. It is obvious that it becomes difficult for the same amount of initiator to generate free radicals to large extent and also for same amount of crosslinker to crosslink all the molecules during grafting in a short time. There is no significant increase in yield (%) and gel contents (%) due to increase in concentration of monomers at pre-fixed concentration of initiator and crosslinker. This insignificant increase in the yield (%) and gel contents (%) is owing to

incomplete polymerization of monomers because of insufficient amount of initiator and crosslinker.

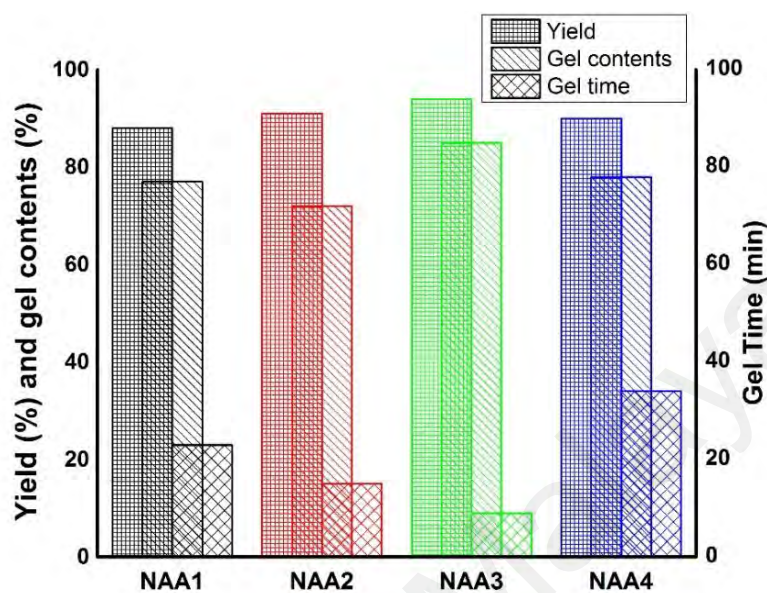


Figure 4.27: Yield (%), gel contents (%), and gel time of synthesized N-succinyl chitosan-g-poly (acrylamide-co-acrylic acid) hydrogels

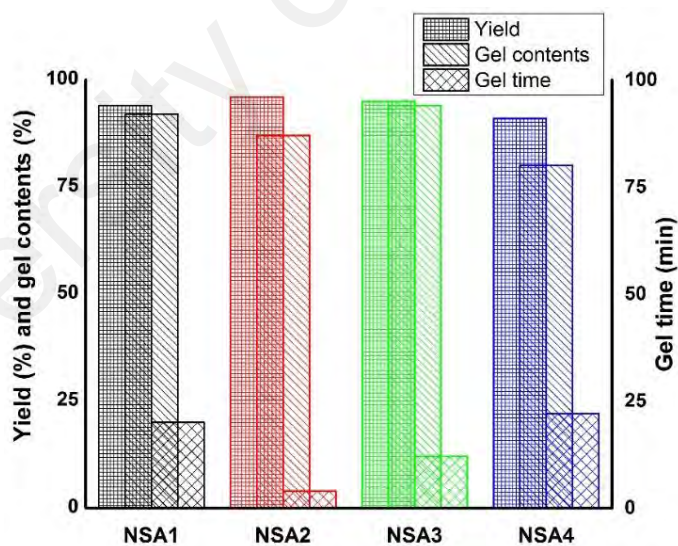


Figure 4.28: Yield (%), gel contents (%), and gel time of synthesized N-succinyl chitosan-g-poly (acrylic acid) hydrogels

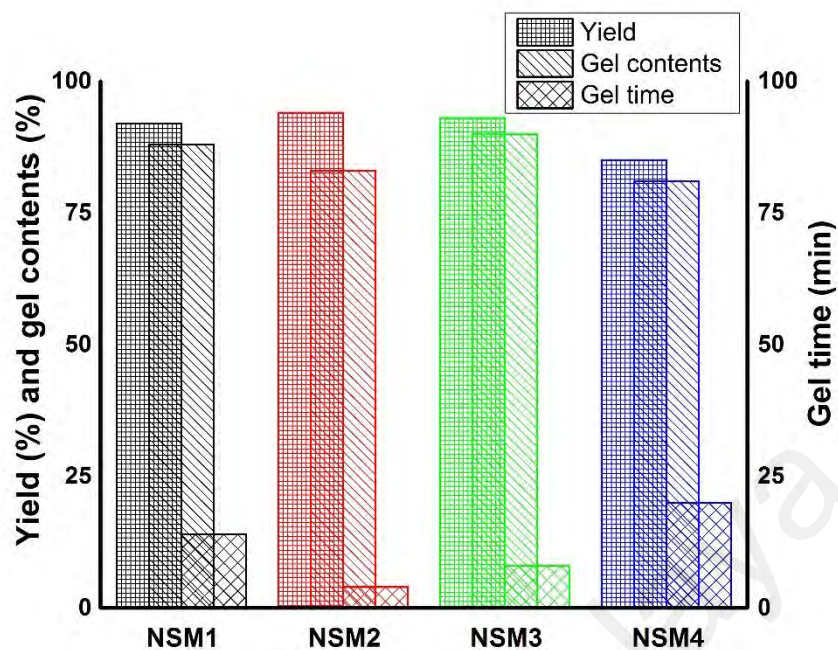


Figure 4.29: Yield (%), gel contents (%), and gel time of synthesized N-succinyl chitosan-g-poly (methacrylic acid) hydrogels

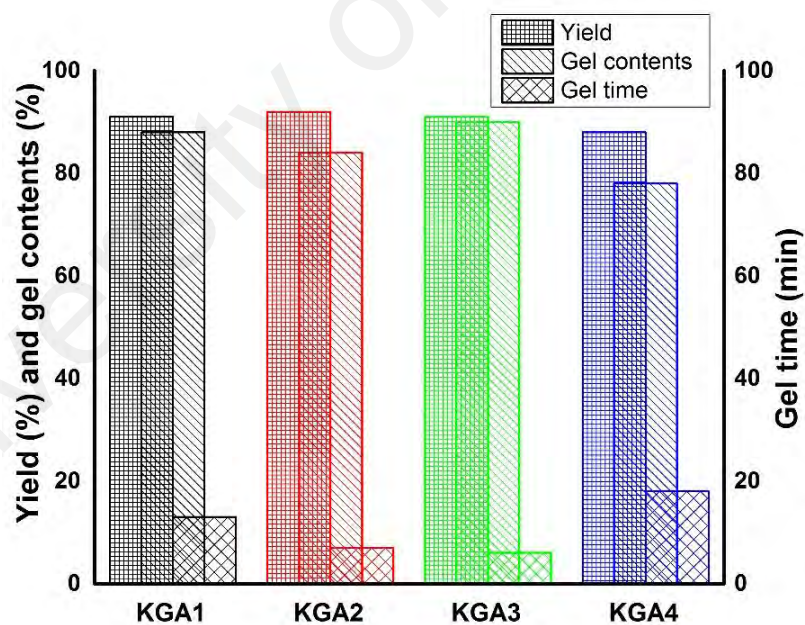


Figure 4.30: Yield (%), gel contents (%), and gel time of synthesized karaya gum-g-poly (acrylic acid) hydrogels

4.3 Properties of Hydrogels

4.3.1 Mechanical Properties

4.3.1.1 Mechanical Properties of N-succinyl chitosan/ poly (acrylamide-co-acrylic acid) Hydrogels

(a) *Strain Amplitude Test*

The amplitude sweep test is usually performed to determine the linear viscoelastic region (LVR) and critical strain of the hydrogels. Usually, the hydrogels show constant or linear response at low strain value while different response at higher strain values and become strain dependent. The hydrogels lose their non-destructive nature at higher strain values. This is due to the complex viscoelastic response of the gels at large amplitude and linear viscoelasticity analysis loses its validity at this amplitude. Furthermore, these parameters are used to investigate the rigidity or flexibility of the gels. In this work, the amplitude test was performed for all hydrogels having different compositions in the strain range 0-25 % to evaluate the LVR. The results of all the hydrogels revealed the linear response of the hydrogels in this range. The results of amplitude test are shown in Figure 4.31. Elastic and storage modulus of the hydrogels have been observed against strain in amplitude sweep test. The results of amplitude sweep test revealed the higher elastic modulus as compared to storage modulus. The higher elastic modulus indicated the strong network structure of the gels. The higher elastic modulus also showed the resistivity of the gels to deformation. The resistance against deformation of the gels was owing to formation of stable network through glutaraldehyde crosslinking. Moreover, random-coil chains of N-succinyl chitosan polysaccharide and synthetic polymer, poly (acrylamide-co-acrylic acid) entangled with each other to form stable and more flexible gels. Moreover, the higher elastic modulus than viscous modulus indicated the dominant solid-like nature of the hydrogels.

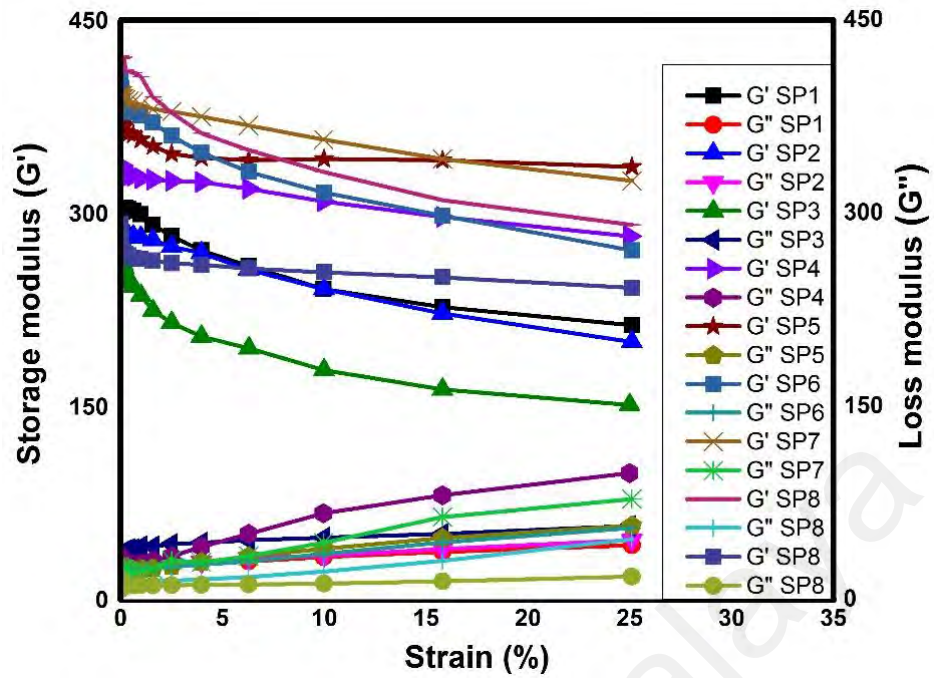


Figure 4.31: Strain amplitude test of all SP hydrogels (N-succinyl chitosan/ poly (acrylamide-co-acrylic acid) hydrogels)

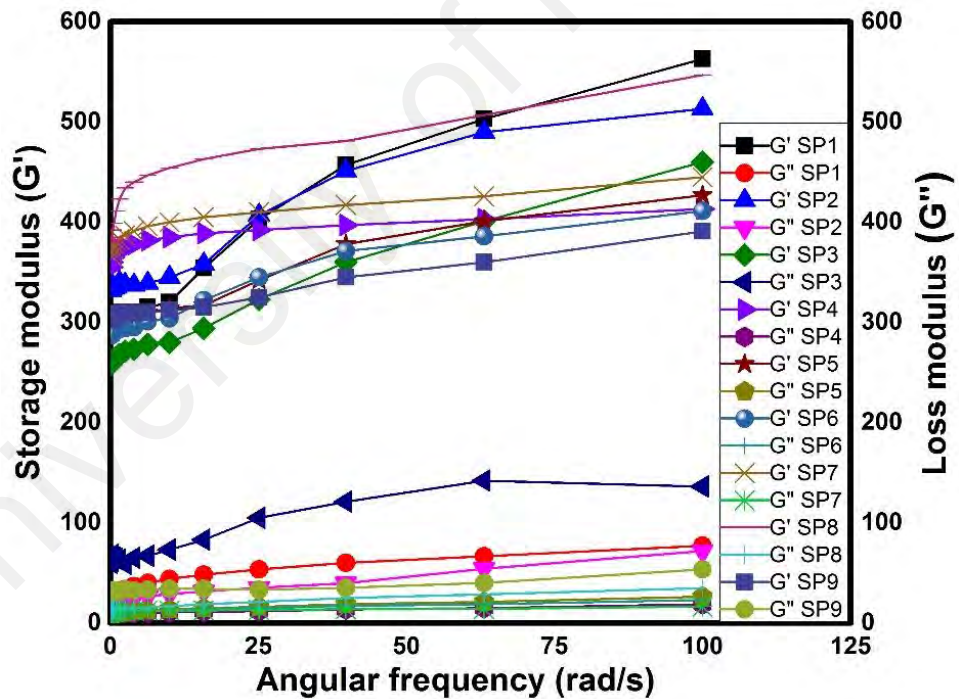


Figure 4.32: Frequency sweep test of all SP hydrogels (N-succinyl chitosan/ poly (acrylamide-co-acrylic acid) hydrogels)

(b) Frequency Sweep Test

Oscillatory linear frequency sweep test can be conducted to evaluate the dynamic gel properties, namely, the stability of three-dimensional crosslinked network of hydrogels at constant strain within the linear viscoelastic region. Ideal hydrogels show elastic behavior and higher elastic modulus than viscous modulus. The hydrogels were subjected to angular frequency from 1 rad/s to 100 rad/s. The frequency sweep profile of elastic modulus (G') and viscous modulus (G'') is shown in Figure 4.32. From the results, it can be observed that elastic behavior (G') is dominated over viscous property (G'') of the systems. These properties indicate the characteristics of solid-like network structure (Hu et al., 2014). Moreover, the magnitude of the elastic and viscous responses are dependent on the composition of the gels. In this work, the effect of different amounts of N-succinyl chitosan, poly (acrylamide-co-acrylic acid), and crosslinking agent (GA) on the rheological properties of gels were studied. The results revealed the gel (SP1) containing higher N-succinyl chitosan amount has relatively weak mechanical strength. It is owing to the inherent weak mechanical strength of the natural polysaccharide hydrogels. However, the gel (SP2) having higher amount of polymer possessed higher mechanical strength. This might be owing to enhance physical interaction between natural and synthetic polymers. Moreover, the mechanical strength of the SP3 gel containing lower amount of natural polymer N-succinyl chitosan and higher amount of synthetic polymer is low as compared to SP1 and SP2. The weak mechanical strength of the SP3 hydrogel might be due to two reasons. This gel contained lower crosslinked N-succinyl chitosan and greater amount of uncrosslinked poly (acrylamide-co-acrylic acid). Hence, the low value of elastic modulus is due to the presence of lower amount of crosslinked N-succinyl chitosan while the higher viscous modulus as compared to SP1 and SP2 might be due to greater amount of uncrosslinked poly (acrylamide-co-acrylic acid) (Barbucci et al., 2000). The increase in amount of poly (acrylamide-co-acrylic acid) indicated a decrease in the

elasticity and rigidity of the gel. Furthermore, the effect of crosslinking agent (GA) on the mechanical strength of the hydrogels was investigated and results revealed the higher mechanical strength as compared to hydrogels containing less amount of GA. SP4, SP5, and SP6 contained greater amount of GA and higher mechanical strength as compared to SP1, SP2, and SP3. The higher mechanical strength is owing to formation of stronger gel network. Similarly, SP7, SP8, and SP9 contained even greater amount of GA and showed greater mechanical strength as compared to already described hydrogels (Moura et al., 2007). From all these results of elastic and loss moduli, it can be concluded that stable networks were formed. The magnitude of moduli varied with the composition but almost independent of frequency. There was no abrupt change in the elastic and loss moduli with change in frequency. Moreover, storage and loss moduli of hydrogels containing less amount of GA showed slightly loose gel network and showed slight frequency dependency which can be easily observed from the moduli of SP1, SP2, and SP3. However, hydrogels containing larger amount of GA had higher elastic moduli which are frequency independent.

4.3.2 Mechanical Properties of Hydrogels Formed through Free radical Mechanism

This section describes the strain amplitude and frequency sweep tests of N-succinyl chitosan-g-poly (acrylamide-co-acrylic acid), N-succinyl chitosan-g-poly (acrylic acid), N-succinyl chitosan-g-poly (methacrylic acid), and karaya gum-g-poly (acrylic acid) hydrogels.

(a) Amplitude Sweep Test

N-succinyl chitosan-g-poly (acrylamide-co-acrylic acid), N-succinyl chitosan-g-poly (acrylic acid), N-succinyl chitosan-g-poly (methacrylic acid), and karaya gum-g-poly (acrylic acid) hydrogels were subjected to amplitude sweep test at constant angular frequency of 10 rad/sec in strain range of 0-25 %. The results of amplitude sweep test

revealed the linear response against strain which show the linear viscoelastic region (LVR) and stability of the hydrogel in this range. Moreover, the G' of the hydrogels were found to be greater than its G'' over the studied frequency range which indicated its solid-like behaviour. The results of amplitude test of all these hydrogels are shown in Figure 4.33, 4.34, 4.35, and 4.36.

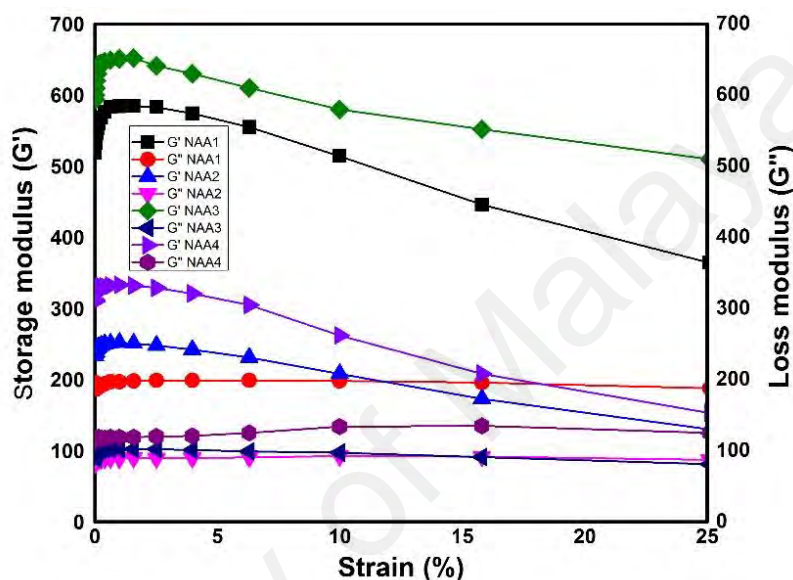


Figure 4.33: Strain amplitude test of N-succinyl chitosan-g-poly (acrylamide-co-acrylic acid) hydrogels

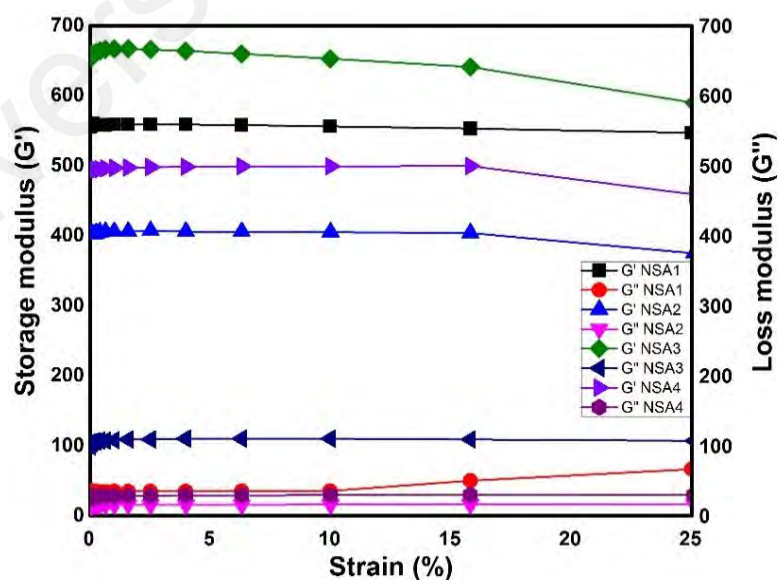


Figure 4.34: Strain amplitude test of N-succinyl chitosan-g-poly (acrylic acid) hydrogels

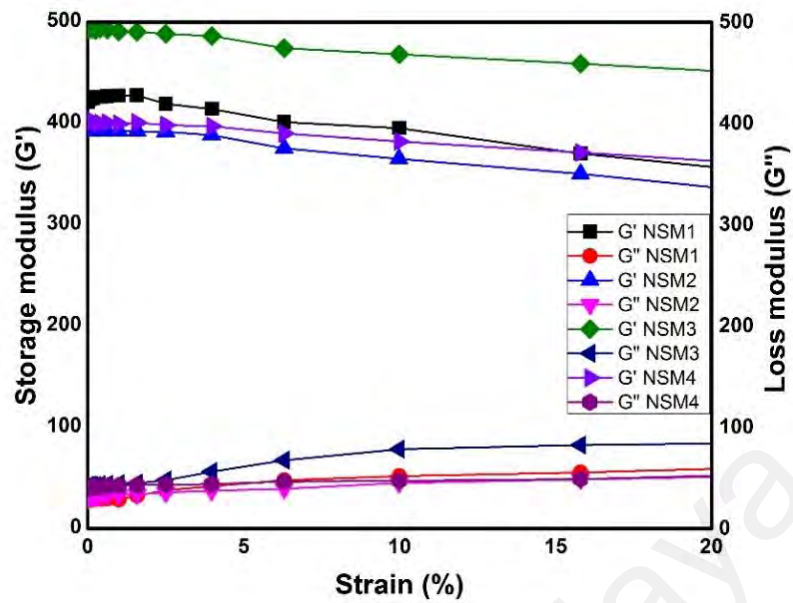


Figure 4.35: Strain amplitude test of N-succinyl chitosan-g-poly (methacrylic acid) hydrogels

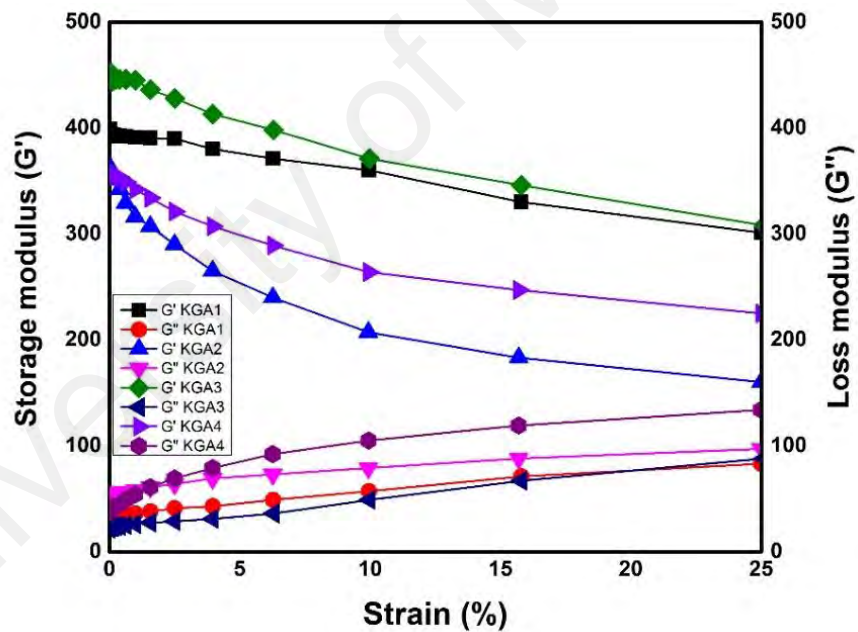


Figure 4.36: Strain amplitude test of karaya gum-g-poly (acrylic acid) hydrogels

(b) Frequency Sweep Test

Oscillatory linear frequency sweep test was conducted to evaluate the dynamic properties of gel, namely, the stability of three-dimensional crosslinked network of hydrogels at constant strain. The hydrogels were subjected to angular frequency from 1 rad/s to 100 rad/s. The frequency sweep profiles of elastic modulus (G') and viscous modulus (G'')

are shown in Figures 4.37, 4.38, 4.39, and 4.40. From the results, it can be observed that elastic behavior (G') is dominated over viscous property (G'') of the systems. These properties indicate the solid-like network structure of hydrogels (Hu et al., 2014). The mechanical strength of the hydrogels depended on the nature of materials involved in the synthesis of the hydrogels and the composition of the hydrogels. The crosslinking density has significant effect on the mechanical strength of the hydrogels. In this section, viscoelastic behaviors of four different types of hydrogels varying in the nature of materials have been investigated. These four types of hydrogels are N-succinyl chitosan-g-poly (acrylamide-co-acrylic acid), N-succinyl chitosan-g-poly (acrylic acid), N-succinyl chitosan-g-poly (methacrylic acid), and karaya gum-g-poly (acrylic acid) hydrogels.

This trend of mechanical strength can be seen from NAA1, NSA1, NSM1, and KGA1 from Figures 4.37, 4.38, 4.39, and 4.40.

i) Effect of initiator concentration

Initiator is necessary to start the polymerization reaction. The concentration of initiator is one of the variables affecting the gel properties. In this part of work, the effect of initiator APS was investigated. The samples were prepared using various concentrations of initiator. The rheology results revealed the effect of initiator concentration on mechanical strength. The modulus decreases with increasing initiator concentration. This observation can be explained based on more network defects induced at higher initiator concentration. According to the free-radical polymerization concepts, increasing the initiator concentration results in decreasing the kinetic chain length (lower molecular weight) and, consequently, enhancing chain ends, which are known as defects in the gel network. The imperfections are developed by the chain end enhancement originated from the collision of the additional initiating free-radicals. It means that fewer junctions form between the

chains and consequently the crosslink density and gel content are diminished. Decreased crosslink density leads to an enhanced swelling and the swollen gel appears to be softer, quantified as the decreasing dynamic elastic modulus (Ramazani-Harandi et al., 2009). The effect of initiator concentration on the mechanical strength can be observed by comparing the elastic modulus of NAA2 with NAA1, NSA2 with NSA1, NSM2 with NSM1, and KGA2 with KGA1 as shown in Figures 4.37, 4.38, 4.39, and 4.40. The elastic modulus is in the order of NAA1, NSA1, NSM1, and KGA1 > NAA2, NSA2, NSM2, and KGA2.

ii) Effect of concentration of crosslinking agent

The effect of crosslinking concentration on the polymer network was revealed by the elastic modulus (G') and viscous modulus (G''). The data obtained for NAA1, NSA1, NSM1, and KGA1 hydrogel revealed the frequency dependent viscoelastic response of polymer network. This behavior was expected because the magnitude of viscoelastic response is governed by the length of flexible polymer chains and the nature of imposed mechanical motion (Anseth et al., 1996). Long chain polymer has the characteristic of long relaxation times. The polymer chain segments between crosslinks are longer for the less crosslinked networks, thus, it will give origin to a lower molecular motion frequencies. However, at higher frequencies, long chains fail to rearrange themselves in the time scale of the imposed motion and, therefore, stiffen up, assuming a more “solid-like” behavior that is characterized by slight increase in G' , as observed in Figures 4.37, 4.38, 4.39, and 4.40. However, highly crosslinked NAA3, NSA3, NSM3, and KGA3 hydrogel showed different result from NAA1, NSA1, NSM1, and KGA1. G' for NAA3, NSA3, NSM3, and KGA3 was found higher which showed dominant solid-like behavior as compared to NAA1, NSA1, NSM1, and KGA1. However, elastic modulus of NAA3, NSA3, NSM3, and KGA3 increased gradually as compared to NAA1, NSA1, NSM1, and

KGA1 because shorter polymer chains resulting from highly crosslinked networks exhibit smaller relaxation times. They require higher applied frequencies to obtain a similar response, leading to a gradual rise in G' (Moura et al., 2007).

iii) Effect of concentration of monomers

The stable hydrogels will only be formed if the ratio of each component is appropriate. If the ratio of component changes, the properties of the hydrogels vary significantly. In this work, hydrogels were synthesized by varying the concentration of monomers, crosslinking agent and initiator. The concentration of monomers plays a significant role in the stability, flexibility and rigidity of the hydrogels. The effect of change in the concentration of monomers on the mechanical properties has been investigated which can be observed from Figures 4.37, 4.38, 4.39, and 4.40. NAA4, NSA4, NSM4, and KGA4 contain higher concentration of monomers as compared to NAA1, NSA1, NSM1, and KGA1. The results revealed that hydrogels NAA4, NSA4, NSM4, and KGA4 containing higher concentration of monomers have lower elastic modulus and large viscous modulus as compared to NAA1, NSA1, NSM1, and KGA1. It might be owing to the formation of loosely bound network in the presence of more monomers. It is obvious that it becomes difficult for the same amount of initiator to generate free radicals to large extent and also for the same amount of crosslinker to crosslink all the molecules during grafting and polymerization. Hence, incomplete polymerization of monomers occurs which results in the reduction of elastic modulus and increase in the viscous modulus.

The difference in the mechanical strength of the hydrogels is owing to the difference of materials. The acrylic acid and methacrylic acid containing hydrogels had higher mechanical strength. Carboxylic groups in ionized state form polyelectrolyte complexes and strong interpolymer hydrogen bonding. Polyelectrolyte complex and strong

interpolymer hydrogen bonding increase the viscoelastic behavior of the hydrogels (Li & Kwak, 2004).

However, acrylamide containing hydrogels showed slightly weak mechanical strength. Acrylamide has less tendency to form interpolymer hydrogen bonding as compared to acrylic acid while no propensity to form polyelectrolyte complex. That's the reason of weak mechanical strength of hydrogels containing acrylamide.

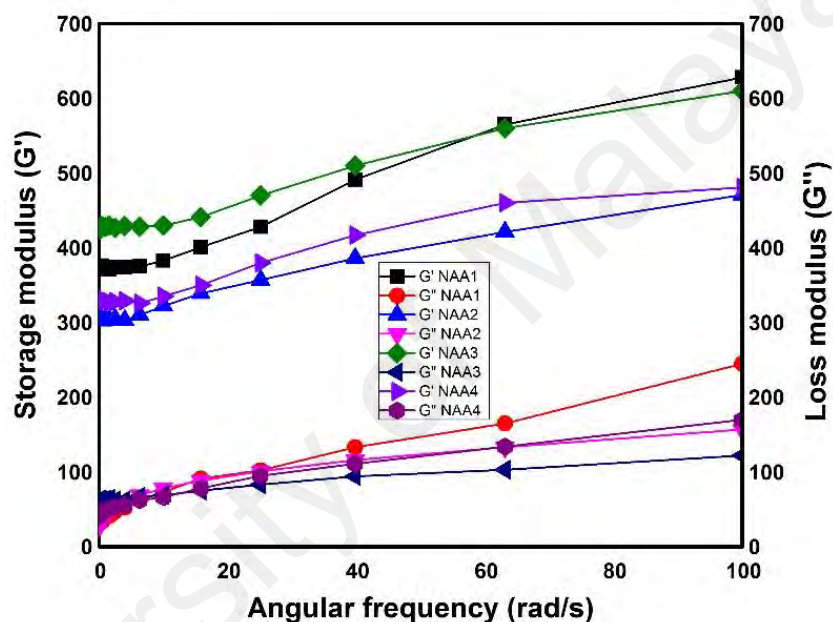


Figure 4.37: Frequency sweep test of N-succinyl chitosan-g-poly (acrylamide-co-acrylic acid) hydrogels

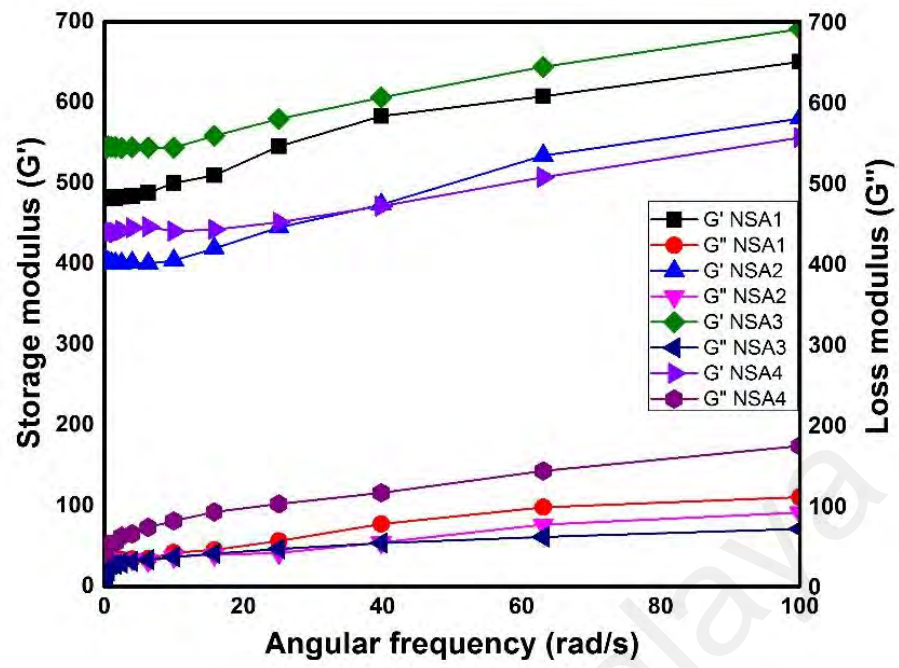


Figure 4.38: Frequency sweep test of N-succinyl chitosan-g-poly (acrylic acid) hydrogels

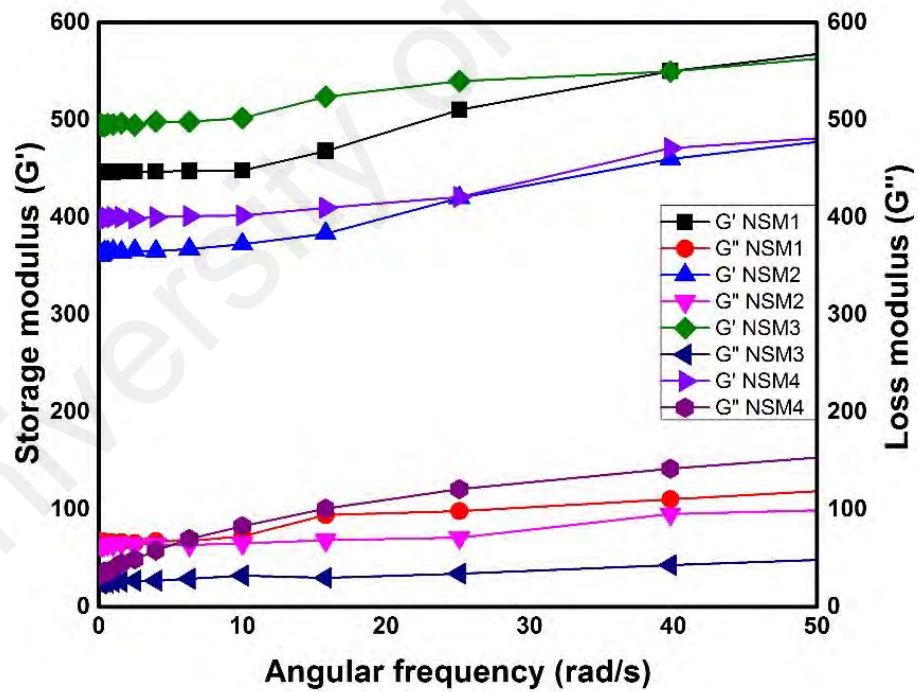


Figure 4.39: Frequency sweep test of N-succinyl chitosan-g-poly (methacrylic acid) hydrogels

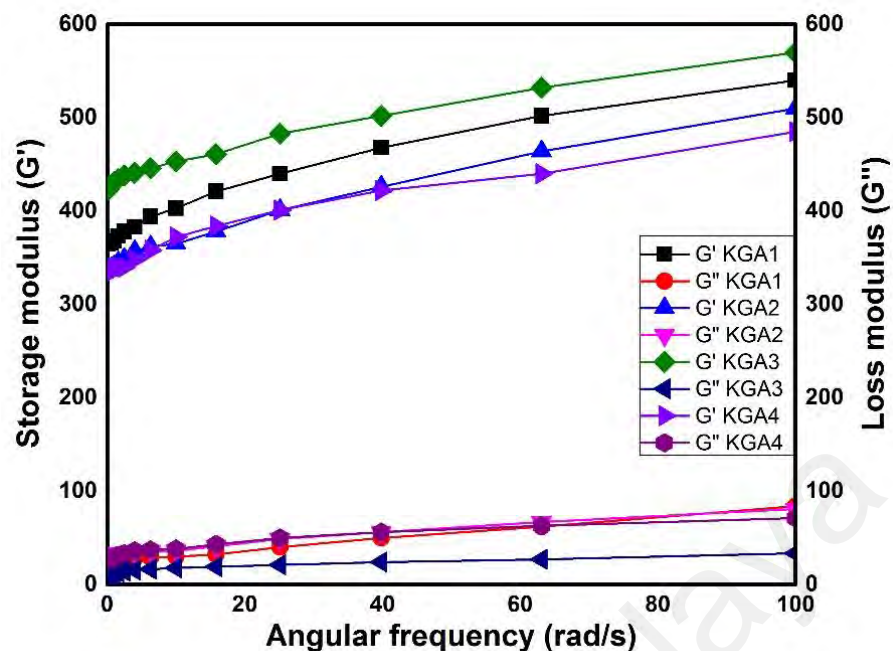


Figure 4.40: Frequency sweep test of karaya gum-g-poly (acrylic acid) hydrogels

4.3.3 Swelling Ratio

Swelling property of the hydrogels is very imperative and is widely used as preliminary assessment for prospective evaluation of hydrogels.

4.3.3.1 Swelling Ratio of N-succinyl chitosan/ poly (acrylamide-co-acrylic acid) Hydrogels

Several hydrogels were synthesized using different concentrations of N-succinyl chitosan, poly (acrylamide-co-acrylic acid) and crosslinking agent GA. These hydrogels were immersed in buffer solutions of pH 7.4 and pH 1.2. The swelling results demonstrate that swelling of hydrogel depends on the pH of swelling medium, amount of N-succinyl chitosan and poly (acrylamide-co-acrylic acid), and crosslinking agent concentration (Mirzaei et al., 2013). The results of swelling ratio at pH 7.4 and pH 1.2 are shown in Figure 4.41. It can be seen that hydrogels showed higher swelling at pH 7.4 and lower swelling ratio at pH 1.2. The higher swelling at pH 7.4 might be due to presence of greater number of carboxylic groups. The carboxylic groups changed into carboxylate ions due to deprotonation. The carboxylate ions caused repulsion and swelling ratio increased (Li

et al., 2007). However, swelling ratio of hydrogels at pH 1.2 might be due to protonation of amino groups and carboxylate ions present in the N-succinyl chitosan. These amino groups were less in number and swelling ratio was low. The composition of hydrogels had also influence on the swelling ratio. SP1, SP2, and SP3 hydrogels showed higher swelling due to less concentration of GA. Swelling ratio decreased with the increase in the concentration of GA. It can be observed from SP4, SP5, and SP6 hydrogels comprising higher concentration of GA. Furthermore, SP7, SP8, and SP9 showed lower swelling ratio due to higher concentration of GA as compared to the already described. Low concentration of GA resulted in higher swelling ratio due to looser network of hydrogels while increase in concentration of GA resulted in denser and tighter network of hydrogels (Samanta & Ray, 2014a) and hence lower the value of swelling ratio. The concentration of N-succinyl chitosan and poly (acrylamide-co-acrylic acid) also influenced the swelling ratio of hydrogels. Hydrogels having higher concentration of N-succinyl chitosan had greater swelling ratio as compared to the hydrogels containing less concentration of swelling ratio. This is due to the high hydrophilicity of polysaccharide backbone and presence of hydrophilic groups such as $-NH_2$, $-COOH$, and $-OH$ groups. Furthermore, swelling ratio also affected with the change in concentration of poly (acrylamide-co-acrylic acid). The swelling ratio increased with the increase in concentration of poly (acrylamide-co-acrylic acid).

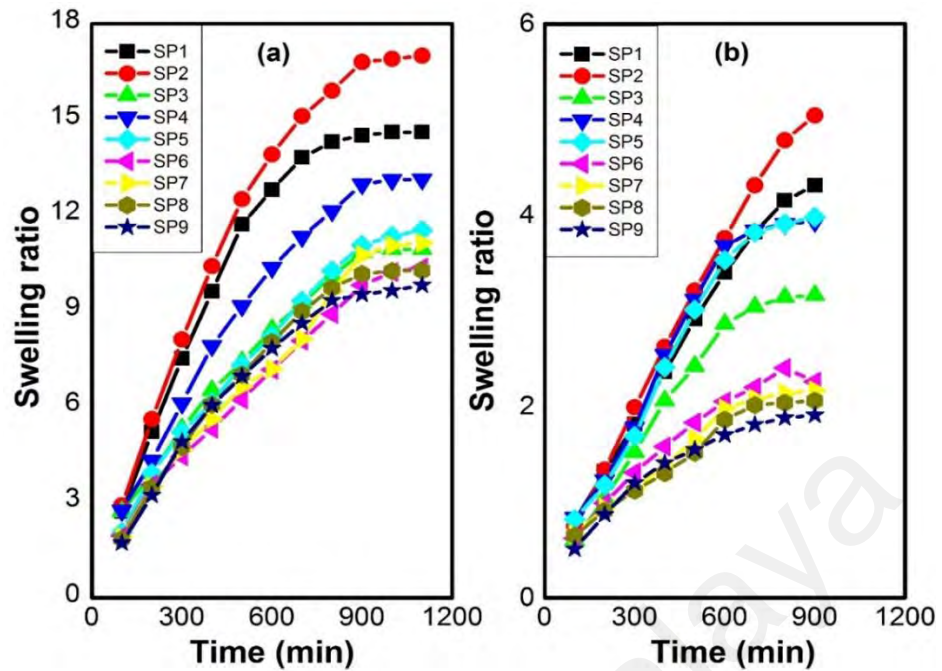


Figure 4.41: Swelling ratios of N-succinyl chitosan/ poly (acrylamide-co-acrylic acid) hydrogels at a) pH 7.4, b) pH 1.2

4.3.3.2 Swelling Ratio of Hydrogels Formed through Free radical Mechanism

The swelling characteristics of the N-succinyl chitosan-g-poly (acrylamide-co-acrylic acid), N-succinyl chitosan-g-poly (acrylic acid), N-succinyl chitosan-g-poly (methacrylic acid), and karaya gum-g-poly (acrylic acid) hydrogels varying in concentration of initiator, crosslinker, and monomers were evaluated in water, pH 7.4 and pH 1.2.

(a) Swelling Ratio of Hydrogels in Water

Figures 4.42 (a), 4.43 (a), 4.44 (a), 4.45 (a), respectively shown the swelling ratio of N-succinyl chitosan-g-poly (acrylamide-co-acrylic acid), N-succinyl chitosan-g-poly (acrylic acid), N-succinyl chitosan-g-poly (methacrylic acid), and karaya gum-g-poly (acrylic acid) hydrogels in water at 37 °C. The effect of initiator, crosslinker, and monomers concentration on swelling ratio of the hydrogels were also included. All these curves show an increase in swelling ratio with time and level off at equilibrium.

i) Effect of initiator concentration

The effect of initiator concentration on the change in swelling ratio of the hydrogels can be seen from Figures 4.42 (a), 4.43 (a), 4.44 (a), 4.45 (a) for NAA2, NSA2, NSM2, and KGA2 with higher amount of initiator concentration as compared to swelling ratio of NAA1, NSA1, NSM1, and KGA1 with less amount of initiator concentration, respectively. It can be observed that swelling ratio increases with the increase in initiator concentration. At high initiator concentration, the rate of polymerization increased which consume shorter time to form the gel completely as compared to formation of hydrogel with low initiator concentration. It is found that increase in initiator concentration increases low molecular weight gels formation with more chain ends. The gels with more chain ends possess imperfect network. Furthermore, the short chain polymer molecules have more interaction with water and absorption phenomenon enhanced because shorter polymer chains have less entanglement, more exposure of hydrophilic groups to interact with water and subsequently increased in the swelling ratio (Chang et al., 2010).

ii) Effect of concentration of crosslinking agent

The presence of crosslinker is significant in preparation of polymer hydrogels to evade the dissolution of hydrophilic polymers in an aqueous environment. The effect of crosslinking agent concentration on equilibrium swelling ratio can be observed from NAA3, NSA3, NSM3, and KGA3 hydrogels having higher concentration of crosslinking agent as compared to NAA1, NSA1, NSM1, and KGA1 hydrogels and results can be seen in Figures 4.42 (a), 4.43 (a), 4.44 (a), 4.45 (a). The results indicate strong influence of crosslinking agent concentration on the swelling ratio. This study revealed inverse relation between swelling ratio and crosslinker concentration. At low concentration of crosslinking agent, the network density was low while the swelling ratio was high. This might be due to increase in availability of hydrodynamic free volume which promotes the

gels to accommodate more solvent molecules. On the contrary, as the concentration of crosslinking agent used in the preparation of gel is high, the swelling ratio is found low. The increase in the crosslinking agent concentration increases the crosslinking points in the polymeric chain and extent of crosslinking increases in the polymer network, consequently, less swelling when brought into contact with water (Wu et al., 2001). Hence, increase in crosslinking agent concentration, encourage formation of tightly packed network which hindered the mobility and relaxation of polymer chain and reduced the availability of free volume and ultimately the equilibrium swelling ratio decreased.

iii) Effect of concentration of monomers

The effect of monomers concentration on swelling ratio can be seen from Figures 4.42 (a), 4.43 (a), 4.44 (a), 4.45 (a). NAA4, NSA4, NSM4, and KGA4 possessed higher amount of monomers as compared to NAA1, NSA1, NSM1, and KGA1. The equilibrium swelling ratio of hydrogels changed with concentration of monomers. The swelling ability of N-succinyl chitosan-g-poly (acrylamide-co-acrylic acid) hydrogels is owing to the presence of both functional groups such as carboxylate ions of N-succinyl chitosan and acrylic acid and non-ionic carboxamide group. However, the presence of ionic groups enhances the swelling ratio because ions can be highly solvated compared to non-ionic groups in aqueous medium. The swelling ratio increased with increase in concentration of monomers due to increase in hydrophilicity of monomers. Moreover, further increase in the concentration of monomers results in poor mechanical strength of the hydrogels network due to insufficient initiator and crosslinker, ultimately makes the gel useless for controlled drug delivery application.

(b) Swelling Ratio of Hydrogels in Buffer Solutions

The swelling ratio was investigated in buffer solutions of pH 7.4 and pH 1.2 with a constant ionic strength (0.1 molL^{-1}) at 37°C . The results of this study are summarized in

Figures 4.42 (b & c), 4.43 (b & c), 4.44 (b & c), 4.45 (b & c). The swelling behavior of polymer hydrogels in buffer solution depends on the gel composition, particularly when ionizable groups are present. The swelling ability of polymer gels is owing to chain relaxation, osmotic swelling pressure and interaction between functional groups (Nesrinne & Djamel, 2013). The ionic monomers in polymer hydrogels cause chain relaxation with the change in pH. It is well known that N-succinyl chitosan, karaya gum and acrylic acid are highly pH-sensitive due to deprotonation phenomenon of COOH groups. Both N-succinyl chitosan-g-poly (acrylic acid) and karaya gum-g-poly (acrylic acid) hydrogels showed higher swelling ratio and longer time to achieve equilibrium in swelling might be due to higher mechanical strength and higher swelling ratio of these hydrogels as a result of higher hydrophilicity and strong repulsion between carboxylate ions of acrylic acid (pKa 4.25) at pH 7.4. This deprotonation caused breakage of interaction among COOH groups as well as interaction between COOH and CONH₂ groups. Furthermore, the electrostatic repulsion increased among negatively charged ions (Turan & Caykara, 2007). This electrostatic repulsion caused significant expansion of gel network, which attracted more water molecules into the gel network and consequently, increase in swelling ratio. On the other hand, the lower swelling ratio of N-succinyl chitosan-g-poly (acrylamide-co-acrylic acid) and N-succinyl chitosan-g-poly (methacrylic acid) hydrogels might be due to the presence of acrylamide containing neutral carboxamide and presence of hydrophobic -CH₃ group in the methacrylic acid. There is no significant influence of pH on the neutral and hydrophobic groups, hence could not play their role in expansion of hydrogel networks and swelling ratio. However, carboxamide is neutral in nature and hydrophilic. It can cause increase in swelling of hydrogels irrespective of pH. Furthermore, equilibrium in swelling ratio attained in short time as compared to N-succinyl chitosan-g-poly (acrylic acid) and karaya gum-g-poly (acrylic acid) hydrogels. This might be owing to weak mechanical strength of the

hydrogels. On the contrary, the swelling ratio of hydrogels at pH 1.2 was low. This might be owing to protonation of carboxylic groups. Hydrogen bonding occurred among carboxylic groups of N-succinyl chitosan, karaya gum, and acrylic acid. The hydrogen bonding also occurred between COOH, OH, and NH₂ groups of N-succinyl chitosan and COOH of acrylic acid. This polymer-polymer interaction is predominant over polymer-water interaction. Moreover, interaction among COO⁻ is restricted due to protonation of the carboxylate ions at pH 1.2. The hydrogels shrank significantly and ultimately showed less swelling.

University of Malaya

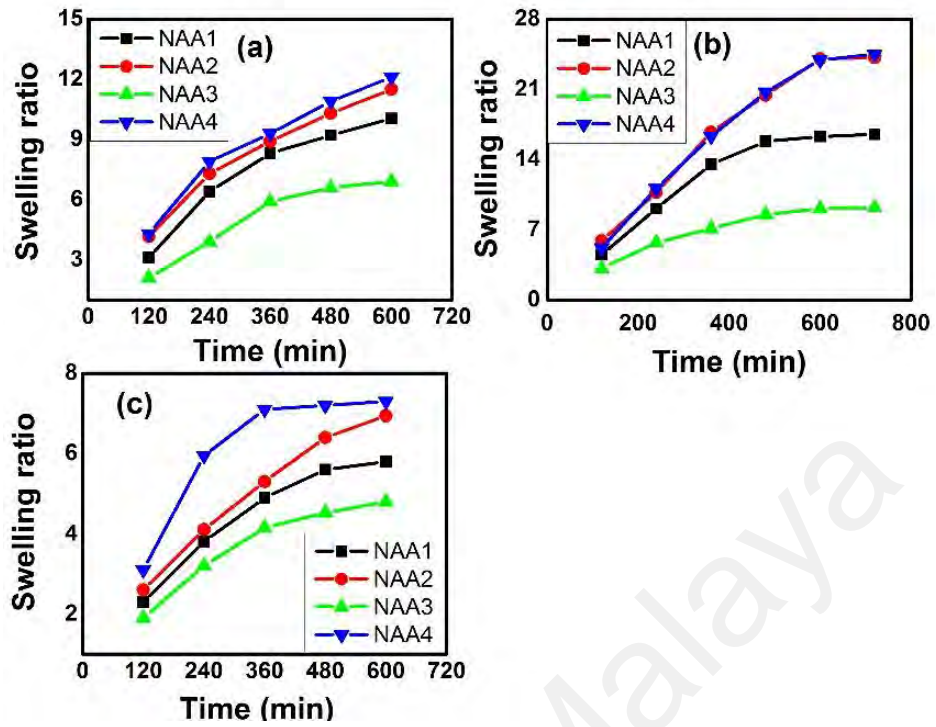


Figure 4.42: Swelling ratio of N-succinyl chitosan-g-poly (acrylamide-co-acrylic acid) hydrogels in a) water, b) pH 7.4, and c) pH 1.2

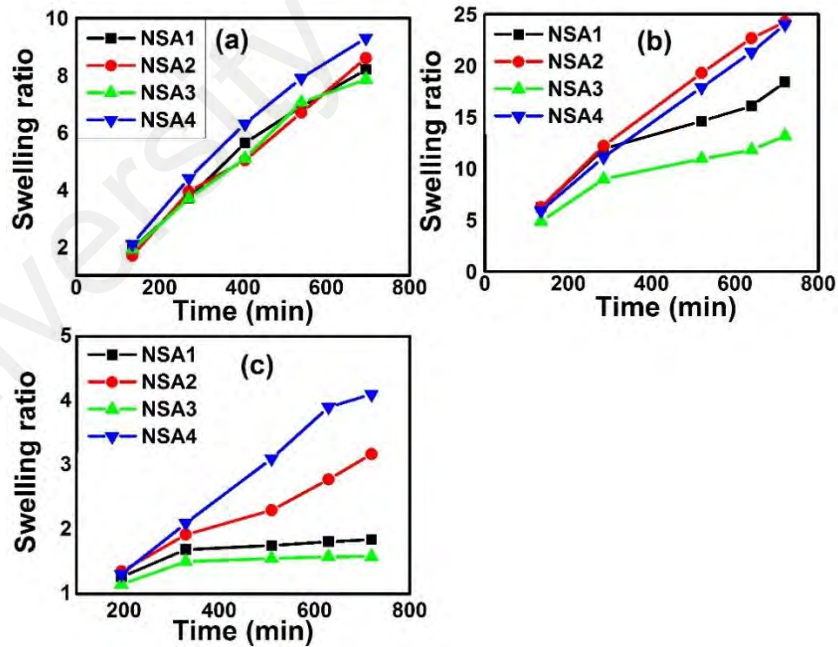


Figure 4.43: Swelling ratio of N-succinyl chitosan-g-poly (acrylic acid) hydrogels in a) water, b) pH 7.4, and c) pH 1.2

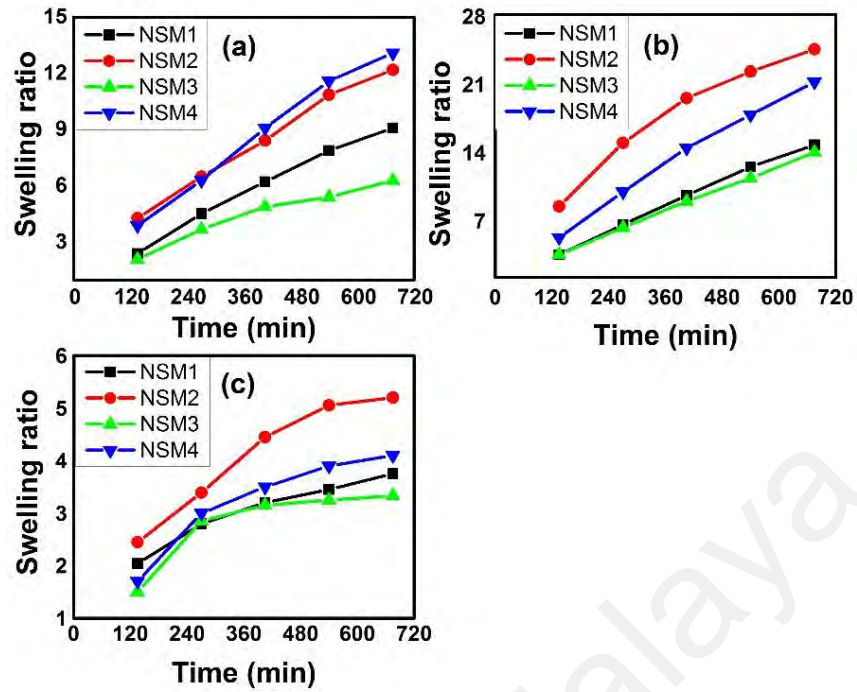


Figure 4.44: Swelling ratio of N-succinyl chitosan-g-poly (methacrylic acid) hydrogels in a) water, b) pH 7.4, and c) pH 1.2

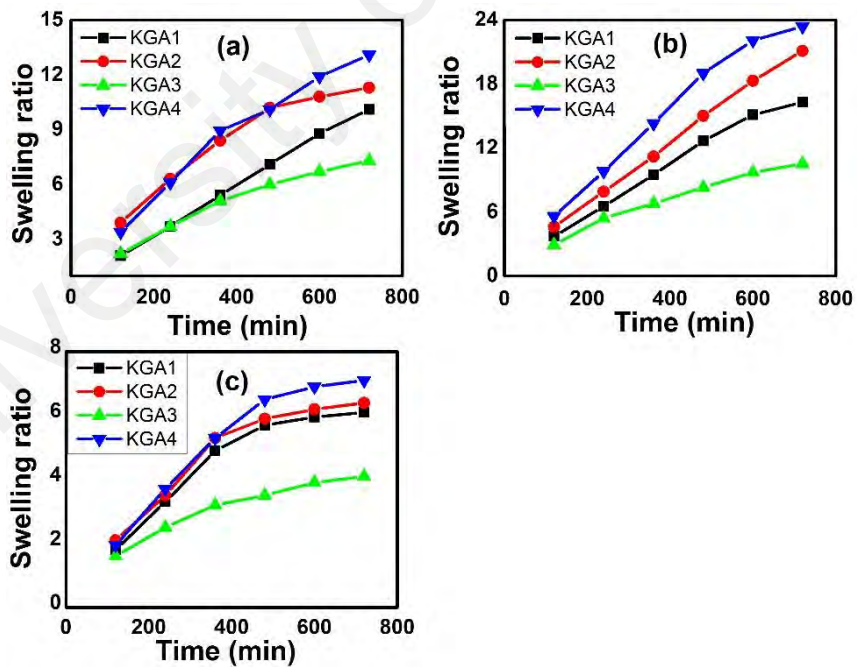


Figure 4.45: Swelling ratio of karaya gum-g-poly (acrylic acid) hydrogels in a) water, b) pH 7.4, and c) pH 1.2

4.3.3.3 Swelling Ratio of Hydrogels in Salt Solutions

The swelling ratio varies with the change in ionic strength of salt solution. Hydrogels do not swell in the presence of electrolyte salt solutions. Besides that, the swollen hydrogels shrink dramatically in the presence of salt solution. This is due to the process of ex-osmosis. Actually, hydrogel shriveling occurs due to loss of hydrophobic-hydrophilic balance of network in the presence of electrolyte (Nesrinne & Djamel, 2013). In the present study, the effect of ionic strength of NaCl, CaCl₂, and AlCl₃ on swelling ratio of hydrogels was investigated. The swelling ratio was calculated according to equation 3.4. The effect of ionic strength of salt solution can be seen from Figures 4.46, 4.47, 4.48, 4.49, and 4.50. The salt solutions contain monovalent Na⁺, bivalent Ca²⁺, and trivalent Al³⁺ ions in the concentration range of 0.05 - 0.2 M. According to this study, swelling ratio of the hydrogels varied with the change in salt concentration. It was found that swelling ratio of the hydrogels decreased drastically with increasing the concentration of salt solutions. This phenomenon is commonly observed in the hydrogels containing ionizable groups such as carboxylate ions as in the synthesized hydrogels. This decrease in swelling tendency is owing to shielding effect caused by the presence of cation in the salt solution. Cations from the salt solutions surrounded the negatively charged ions present in the polymer chain. The swelling ability decreased with the increase in concentration of salt solution. The order of the swelling ratio of hydrogels in salt solution with different concentration is as follows: 0.05 M > 0.1 M > 0.15 M > 0.2 M. When the concentration of salt solution increased, the number of cations surrounds the negatively charged ions increases and consequently minimizes the repulsion between negatively charged ions in the polymer and hence reduced the swelling ratio. The swelling ratio is also affected by the charge of cation. The order of swelling ratio of the hydrogel in different salt solution is as follow: swelling ratio of hydrogel in NaCl > swelling ratio of hydrogel in CaCl₂ > swelling ratio of hydrogel in AlCl₃. It might be due to increase in the

complexing ability of the multivalent cations with the negatively charged groups from the hydrogels. The complexing ability of the cations is as follows: $\text{Al}^{3+} > \text{Ca}^{2+} > \text{Na}^+$. Moreover, the complexation between cations and anions occurs at the surface of the hydrogels and increase the hardness of hydrogel (Mahdavinia et al., 2004).

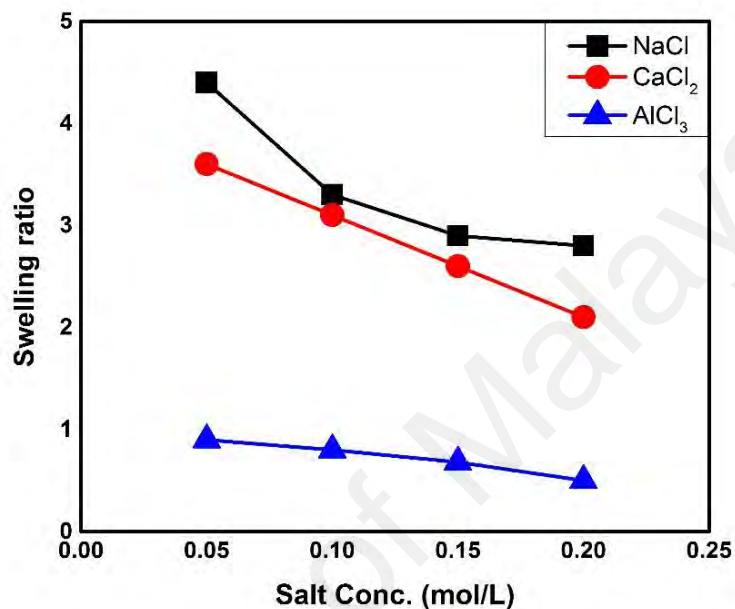


Figure 4.46: Effect of ionic strength of salt solutions on swelling ratio of SP1 (N-succinyl chitosan/ poly (acrylamide-co-acrylic acid) hydrogel)

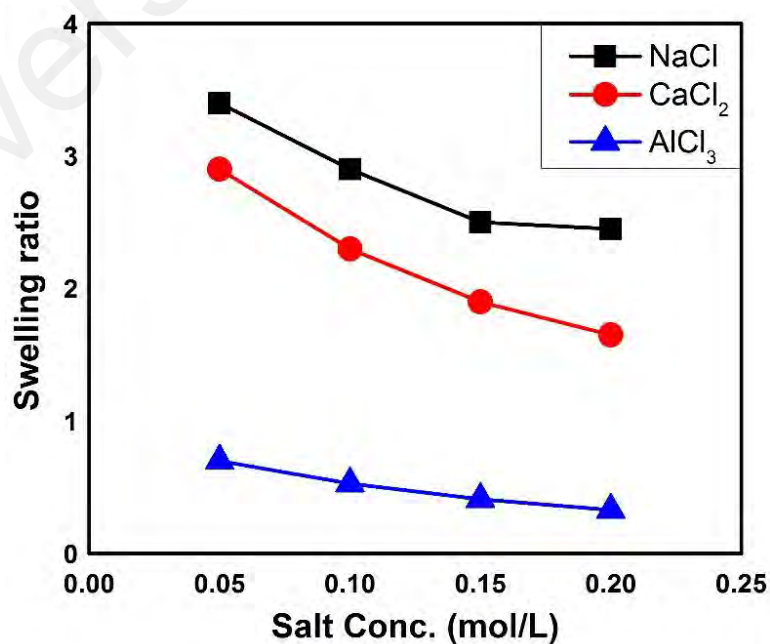


Figure 4.47: Effect of ionic strength of salt solutions on swelling ratio of NAA1 (N-succinyl chitosan-g-poly (acrylamide-co-acrylic acid) hydrogel)

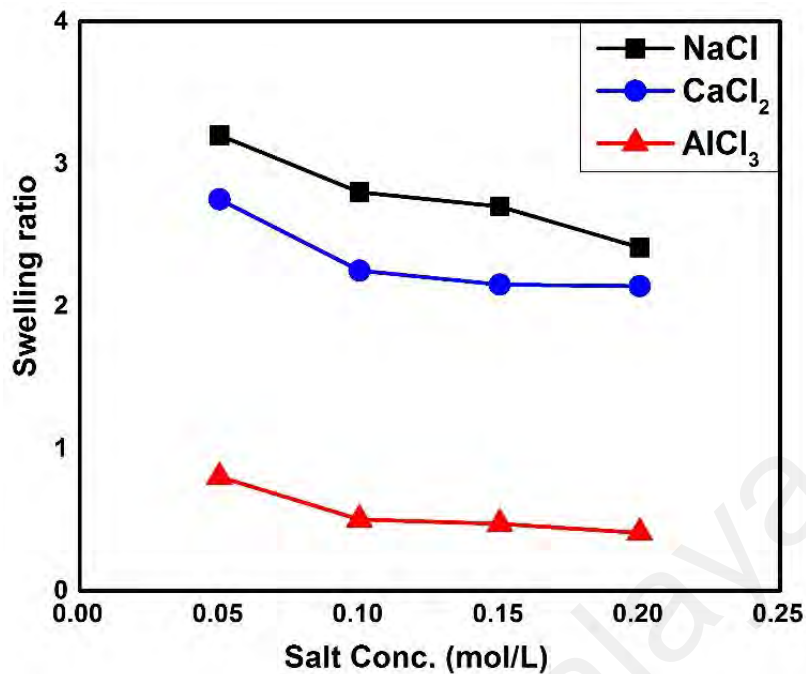


Figure 4.48: Effect of ionic strength of salt solutions on swelling ratio of NSA1 (N-succinyl chitosan-g-poly (acrylic acid) hydrogel)

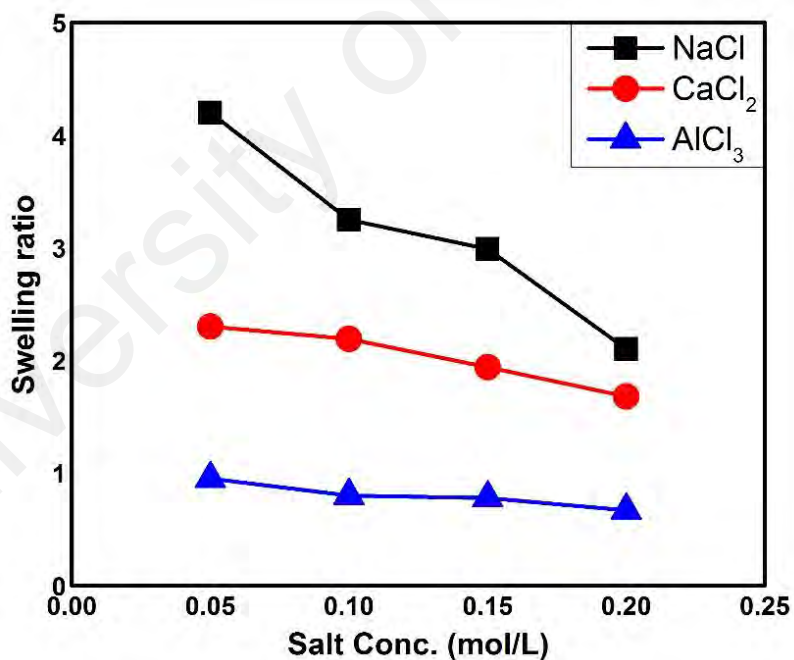


Figure 4.49: Effect of ionic strength of salt solutions on swelling ratio of NSM1 (N-succinyl chitosan-g-poly (methacrylic acid) hydrogel)

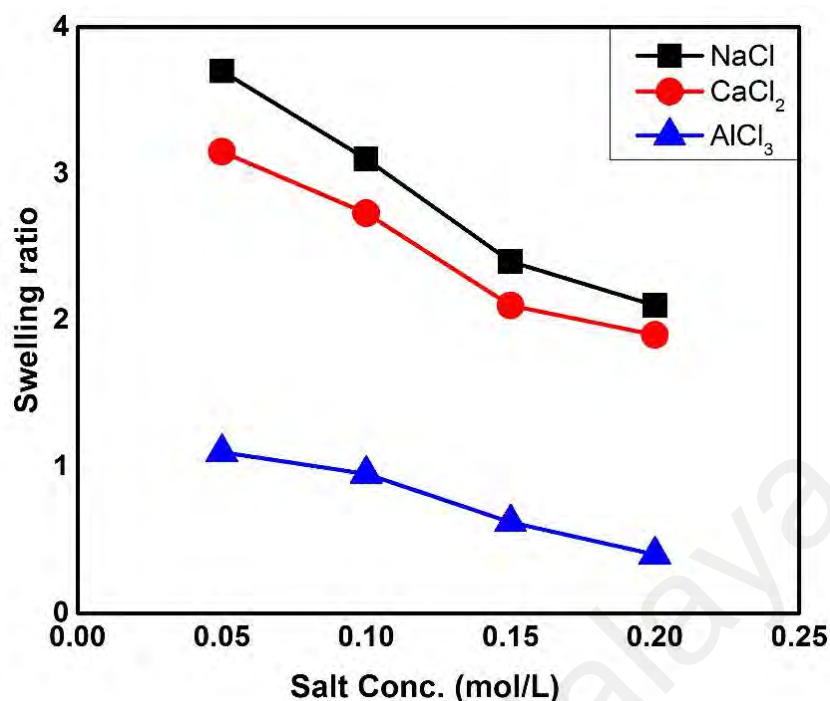


Figure 4.50: Effect of ionic strength of salt solutions on swelling ratio of KGA1 (Karaya gum-g-poly (acrylic acid) hydrogel)

4.3.3.4 Swelling Kinetics

(a) *Swelling Kinetics of N-succinyl chitosan/ poly (acrylamide-co-acrylic acid) Hydrogels*

Water permeation through hydrogel depends on the functional groups and the interaction between polymer and water (Bashir et al., 2016). The swelling results of hydrogels obtained from experimental observation were fitted in non-linear second order kinetic equation. The trend lines of non-linear fittings were obtained using Origin Pro Software. From these graphs, swelling ratio at time “t”, SR_t was calculated for each hydrogel using non-linear second order equation. The calculated swelling ratios are very close to the experimental swelling ratios. The regression coefficients (R^2) of all these hydrogels are close to unity, while regressions show higher F values. The experimental and calculated swelling ratio, r_0 , k_{s2} , and statistical parameters (R^2 & F) are shown in Table 4.2. For a good fitting of data to second order kinetic equation, R^2 should be close to unity and with greater F value. Moreover, rate constant and initial rate of swelling should be comparable. The experimental and calculated swelling ratio of each formulation is also very close to

each other. From the Table 4.2, it can be observed that with change in amount of N-succinyl chitosan, poly (acrylamide-co-acrylic acid) and crosslinking agent, there is a significant change in swelling parameters. It means these parameters are dependent on swelling of the gel and swelling depends on the crosslinking agent concentration and polymers amount. It might be owing to structural changes in the hydrogels and interactions between solvent and polymers. From the results, it can be clearly observed that all these values are according to literature reported. Hence, swelling data has significant fitting in second order rate equation (Samanta & Ray, 2014b).

University of Malaya

Table 4.2: Swelling kinetics at pH 7.4 and pH 1.2 ((N-succinyl chitosan/ poly (acrylamide-co-acrylic acid) hydrogels)

Hydrogels	$K_{S2} \times 10^{-6}$	r_0	ESR_{exp}	ESR_{cal}	R^2	F
SP1	4.0/77.3	0.031/0.008	14.6/4.4	15.8/4.6	0.97/0.96	390/545
SP2	5.9/17.7	0.033/0.008	17.0/5.0	117.4/5.1	0.99/0.96	930/1035
SP3	73.3/128.6	0.026/0.007	10.92/3.2	10.94/3.4	0.97/0.98	684/954
SP4	49.1/144.8	0.029/0.009	13.12/3.9	13.75/4.2	0.97/0.98	1210/1342
SP5	48.4/115.6	0.022/0.008	11.65/3.9	12.09/4.2	0.98/0.96	1139/1018
SP6	53.4/470.9	0.020/0.007	10.41/2.3	10.71/2.4	0.96/0.97	482/982
SP7	32.6/550.3	0.019/0.007	11.12/2.2	11.33/2.2	0.96/0.97	1090/1234
SP8	50.7/643.5	0.021/0.007	10.26/2.0	10.88/2.0	0.98/0.97	1102/1165
SP9	59.5/739.6	0.021/0.006	9.8/1.9	10.36/2.0	0.99/0.99	1254/344

(b) Swelling Kinetics of Hydrogels Formed through Free radical Mechanism

Swelling kinetics of N-succinyl chitosan-g-poly (acrylamide-co-acrylic acid), N-succinyl chitosan-g-poly (acrylic acid), N-succinyl chitosan-g-poly (methacrylic acid), and karaya gum-g-poly (acrylic acid) hydrogels are given in Tables 4.3, 4.4, 4.5, and 4.6. The data of swelling ratio obtained from second order kinetic equation of various synthesized hydrogels with different amounts of monomers, initiator, and crosslinking agent are summarized. It includes r_0 , k_{S2} , and calculated swelling ratio along with statistical parameters (R^2 , χ^2 , and F). These statistical parameters revealed well-fitting of the data to second order rate equation as indicated by the value of R^2 which is very close to unity, very small value of χ^2 and high F value. The calculated swelling ratio values are also very close to experimental swelling ratio, significant evidence of data fitting to second order equation. The variation in r_0 and k_{S2} is due to different composition of hydrogels. The change in composition caused structural changes and water-polymer interaction.

Table 4.3: Swelling kinetics in water, pH 7.4 and pH 1.2 (N-succinyl chitosan-g-poly (acrylamide-co-acrylic acid) hydrogels)

Gel	r_0	$k_{S2} \times 10^{-6}$	ESR _{cal}	ESR _{exp}	R ²	$\chi^2 \times 10^{-3}$	F
NAA1	0.03/0.05/0.02	66.2/38.6/284	10.4/17.8/6.0	10.0/16.5/5.8	0.92/0.92/0.98	13.1/93.5/4.8	825/940/1045
NAA2	0.05/0.05/0.02	112.9/9.2/170	11.5/26.0/7.0	11.5/24.1/6.9	0.99/0.85/0.99	0.008/123.5/0.5	890/870/1103
NAA3	0.02/0.04/0.02	73.6/159/372	7.2/9.6/4.9	6.9/9.2/4.8	0.9/0.97/0.98	16.0/16.7/2.5	860/932/1070
NAA4	0.05/0.05/0.04	105.1/6.2/413	12.2/26.4/7.7	12.1/24.5/7.3	0.98/0.84/0.93	0.8/136.7/21.8	895/865/1022

Table 4.4: Swelling kinetics in water, pH 7.4 and pH 1.2 (N-succinyl chitosan-g-poly (acrylic acid) hydrogels)

Gel	r_0	$k_{S2} \times 10^{-6}$	ESR _{cal}	ESR _{exp}	R ²	$\chi^2 \times 10^{-3}$	F
NSA1	0.02/0.06/0.02	10.0/66.0/3900	8.4/17.9/1.9	8.2/18.4/1.8	0.96/0.96/0.99	4.4/15.3/0.01	2530/4780/2345
NSA2	0.01/0.05/0.01	1.9/9.7/58	8.0/24.3/3.1	8.6/24.2/3.17	0.97/0.99/0.96	34.1/0.37/2.3	2517/3451/2987
NSA3	0.01/0.06/0.02	0.1/198/6200	7.8/12.5/1.6	7.9/13.2/1.5	0.95/0.99/0.99	0.3/31.8/0.02	3316/4232/2873
NSA4	0.01/0.04/0.007	9.3/7.7/13.6	9.6/23.1/4.1	9.3/23.9/4.1	0.91/0.96/0.94	7.0/21.0/0.6/	3070/3840/2780

Table 4.5: Swelling kinetics in water, pH 7.4 and pH 1.2 (N-succinyl chitosan-g-poly (methacrylic acid) hydrogels)

Gel	r_0	$k_{s2} \times 10^{-6}$	ESR _{cal}	ESR _{exp}	R ²	$\chi^2 \times 10^{-3}$	F
NSM1	0.02/0.03/ 0.03	0.2/2.2/1168	9.2/14.8/3.7	9.1/14.6/3.8	0.99/0.97/0.99	0.77/1.3/ 7.7	560/745/932
NSM2	0.04/0.08/ 0.03	0.6/3.6/435	12.0/24.8/5.3	12.2/24.5/5.2	0.97/0.99/0.98	4.7/3.9/ 1.2	332/702/870
NSM3	0.02/0.03/ 0.02	133/5.7/ 1012	6.3/13.6/3.5	6.3/13.8/3.3	0.98/0.99/0.98	0.12/4.5/ 4.7	340/699/977
NSM4	0.03/0.04/ 0.01	0.2/4.0/492	13.0/21.4/4.2	13.1/21.1/4.1	0.92/0.97/0.98	0.06/4.4/ 3.4	430/750/890

Gel	r_0	$k_{s2} \times 10^{-6}$	ESR _{cal}	ESR _{exp}	R ²	$\chi^2 \times 10^{-3}$	F
KGA1	0.02/0.03/0.02	0.8/8/138	10.0/16.8/6.5	10.1/16.3/6.1	0.9/0.88/0.9	1/13.7/2.22	2504/2675/1820
KGA2	0.04/0.04/0.02	114/4.7/178	11.6/20.8/6.7	11.3/21.1/6.4	0.98/0.81/0.95	7.2/4.3/ 11.7	2560/2770/1865
KGA3	0.02/0.03/0.02	113/59.8/507	7.3/10.6/4.1	7.3/10.5/4.1	0.99/0.98/0.99	0.21/0.23/2.43	2612/2710/1890
KGA4	0.03/0.05/0.02	35.4/8.3/85	13.2/24.3/ 7.5	13.1/23.4/7.1	0.97/0.89/0.9	0.7/34.8/25.7	2670/2695/1813

4.4 Drug Encapsulation Efficiency of Hydrogels

4.4.1 Encapsulation Efficiency of N-succinyl chitosan/ poly (acrylamide-co-acrylic acid) Hydrogels

In vitro encapsulation efficiency of 5-FU was observed by UV-Vis spectrophotometer and results are shown in Table 4.7. The encapsulation efficiency in various formulation of N-succinyl chitosan and poly (acrylamide-co-acrylic acid) in the gel was studied. The 5-FU encapsulation efficiency of the hydrogels were found to be changed slightly with change in the amount of N-succinyl chitosan and poly (acrylamide-co-acrylic acid) and the encapsulation efficiency might increase due to the increase in the amount of N-succinyl chitosan and poly (acrylamide-co-acrylic acid). This might be due to the increased active sites of interaction of N-succinyl chitosan and acrylic acid with the drug molecules. 5-FU being a pyrimidine analog able to interact with active sites of hydrogels via hydrogen bonding. It was also observed that decrease in crosslinking agent amount increased in encapsulation efficiency as a result of significant increase in swelling of hydrogels. Swelling promotes exposure of large surface area of hydrogel to drug and hence cause enhanced penetration and entanglement of the drug within the polymers.

Table 4.6: 5-FU encapsulation efficiency of N-succinyl chitosan/ poly (acrylamide-co-acrylic acid) hydrogels

Hydrogels	EE%
SP1	58.16 ± 0.04
SP2	72.45 ± 0.06
SP3	65.21 ± 0.3
SP4	30.4 ± 0.07
SP5	28.3 ± 0.06
SP6	21.85 ± 0.04
SP7	15.3 ± 0.09
SP8	15.9 ± 0.09
SP9	10.7 ± 0.07

4.4.2 Encapsulation Efficiency of Hydrogels Formed through Free radical Mechanism

The EE % of formulations NAA1, NSA1, NSM1 was found to be 80.0 ± 0.3 %, 84.0 ± 0.1 %, and 84.0 ± 0.1 %, respectively. After that, the composition was varied with the above mentioned factors. With the increase in the concentration of initiator (NAA2, NSA2, NSM2), EE % increased to 83.0 ± 0.2 %, 86.0 ± 0.1 %, and 88.0 ± 0.2 %, respectively. The increase in encapsulation efficiency for formulation with higher amount of initiator might be due to formation of short chain polymer network. The short chain network possessed greater surface area exposure for polymer-drug molecules interaction. The effect of crosslinking agent on the encapsulation efficiency was observed when comparing the formulation of NAA3, NSA3, and NSM3 with NAA1, NSA1, and NSM1. It was noticed that EE % of NAA3, NSA3, and NSA4 decreased to 59.0 ± 0.1 %, 76.0 ± 0.1 %, and 68.0 ± 0.1 % with the increase in concentration of MBA. It might be due to formation of tightly packed rigid network structure in the polymer and hence less availability of surface within the hydrogel in order to interact with the drug (Babu et al., 2008). Furthermore, the effect of monomers concentration on the EE % was investigated and found that EE % increased with increasing amount of monomers. The EE % in NAA4, NSA4, and NSM4 was found to be 88.0 ± 0.2 %, 88.0 ± 0.2 %, and 90.0 ± 0.2 %, respectively. This might be due to greater availability of active sites within the hydrogel and more interaction with the polymer network. Besides, theophylline being a methyl xanthine molecule could interact with the active sites of polymer network via hydrogen bonding (Menon et al., 2015).

Furthermore the quercetin encapsulation were investigated in karaya gum-g-poly (acrylic acid) hydrogels. The same trends were observed as mentioned above. However, quercetin being hydrophobic drug was loaded in small amount. The quercetin encapsulation is owing to hydrophobic association with the hydrophobic sites of the polymers and

hydrogen bonding between hydroxyl groups of quercetin and hydroxyl, carboxyl and amino groups of polymers.

Furthermore encapsulation of quercetin in karaya gum-g-poly (acrylic acid) hydrogels were investigated. Same trends of encapsulation efficiency were observed as in the hydrogel formed from N-succinyl chitosan-g-poly (acrylamide-co-acrylic acid), N-succinyl chitosan-g-poly (acrylic acid), and N-succinyl chitosan-g-poly (methacrylic acid). However, quercetin being hydrophobic drug was encapsulated in small amount as compared to 5-Fu and theophylline. The successful of quercetin encapsulated in hydrogel is owing to hydrophobic association with the hydrophobic sites of the polymers and formation of hydrogen bonding between hydroxyl groups of quercetin and hydroxyl, carboxyl and amino groups of polymers. (Tan et al., 2011). Basically, there were appropriate crosslink in the attained networks where quercetin molecules accommodated inside the loops. The encapsulation efficiency was slightly affected by hydrogel composition due to difference in network formation. KGA1 hydrogel has encapsulation efficiency of $80.0 \pm 0.03 \%$, while KGA2 hydrogel having loose network structure as compared to KGA1 has encapsulation efficiency of $84.0 \pm 0.07 \%$. This might be owing to greater exposure of hydrophobic sites of hydrogels and interaction of drug with the hydrogels. The encapsulation efficiency of KGA3 is $76.0 \pm 0.09 \%$. This slightly less encapsulation efficiency is owing to tight network structure of the hydrogels and greater gel contents (%) of the hydrogel while KGA4 has attained maximum encapsulation efficiency of $88.0 \pm 0.03 \%$ which is due to greater amount of karaya gum and acrylic acid.

4.5 In Vitro Drug Release

4.5.1 In Vitro Drug Release from N-succinyl chitosan/ poly (acrylamide-co-acrylic acid) Hydrogels

It is a well-known fact that release of drug from hydrogels usually follow three types of mechanism: a) drug release from the surface of the hydrogel, b) drug diffusion through the swollen rubbery hydrogel, and c) drug release owing to erosion of hydrogel network in external environment. In our work, 5-FU loaded hydrogels were evaluated through in vitro release in buffer solutions of pH 1.2 and pH 7.4 and the results are shown in Figure 4.51. The results of 5-FU release % were drawn against time. 5-FU release was observed to be dependent on N-succinyl chitosan and poly (acrylamide-co-acrylic acid) amount, crosslinking concentration, and pH of physiological medium. The maximum release of encapsulated 5-FU was observed to be 15-20 % at pH 1.2. This insignificant small release of drug at pH 1.2 was due to the protonation of carboxylate ions of N-succinyl chitosan and acrylic acid. The protonation of carboxylate ions resulted in shrinkage of the N-succinyl chitosan/ poly (acrylamide-co-acrylic acid) hydrogels. This shrinkage of hydrogels caused low swelling. The higher amount of 5-FU released at pH 7.4 from hydrogel might be due to significant swelling of hydrogel. This remarkable drug release was owing to higher electrostatic repulsion of $-\text{COO}^-$ ions of N-succinyl chitosan and acrylic acid. The initial burst release from hydrogels was observed followed by sustained release. This burst release might show the presence of 5-FU on the surface of hydrogels and high concentration gradient between 5-FU and buffer solution (Patil et al., 1996). Moreover, release profile followed the swelling trend of the hydrogels (Kulkarni et al., 2012). The increased concentration of N-succinyl chitosan and poly (acrylamide-co-acrylic acid) resulted in maximum release of drug. SP2, SP5, and SP8 contained same amount of N-succinyl chitosan and poly (acrylamide-co-acrylic acid) but different GA while SP1, SP4, and SP7 also possessed same amount of N-succinyl chitosan and poly

(acrylamide-co-acrylic acid) but different GA. Similarly, SP3, SP6, and SP9 formulations contained same amount of N-succinyl chitosan and poly (acrylamide-co-acrylic acid) but different GA. The 5-FU release (%) in case of SP2, SP5, and SP8 formulations was $85.9 \pm 0.2 \%$, $79.2 \pm 0.06 \%$, and $67.0 \pm 0.09 \%$, respectively. Furthermore, release (%) was $85.0 \pm 0.1 \%$, $79.1 \pm 0.07 \%$, and $67.3 \pm 0.09 \%$ in the case of SP1, SP4, and SP7 formulations. Similarly, SP3, SP6, and SP9 showed $82.5 \pm 0.1 \%$, $76.3 \pm 0.07 \%$, and $66.4 \pm 0.08 \%$ drug release. Hence, from the above mentioned results, it can be concluded that SP2, SP5, and SP8 showed higher release rates as compared to rest formulations which attributes to the existence of greater hydrophilic moieties and higher swelling nature. The crosslinking agent also affected the release rate of 5-FU. SP1, SP2, and SP3 were crosslinked with 1mg GA, SP4, SP5, and SP6 were crosslinked with 2mg GA while SP7, SP8, and SP9 were crosslinked with 3mg GA. The highest drug release (%) was observed from SP1, SP2, and SP3. If we further investigate the drug release profile of SP1, SP2, and SP3, it can be seen that $85.9 \pm 0.2 \%$ drug was released from SP2 which is highest among all the hydrogels. Furthermore, least drug release (%) was found from SP7, SP8, and SP9 formulations due to higher GA concentration. This was due to the fact that higher crosslinking concentration, free volume as well as swelling of hydrogels decreased significantly, thereby hindered the transport of drug molecules through the gel matrix into the release medium. Thus, N-succinyl chitosan/ poly (acrylamide-co-acrylic acid) gels found to be efficient in 5-FU release in a controlled manner at pH 7.4 while protected its release at pH 1.2, which is pH of stomach. The release profile of 5-FU fulfilled the basic requirement of US pharmacopeia (USP XXIV). According to this, minimum of 80 % drug release at pH 7.4 is the standard for oral drug delivery (Zeitoun, 2003).

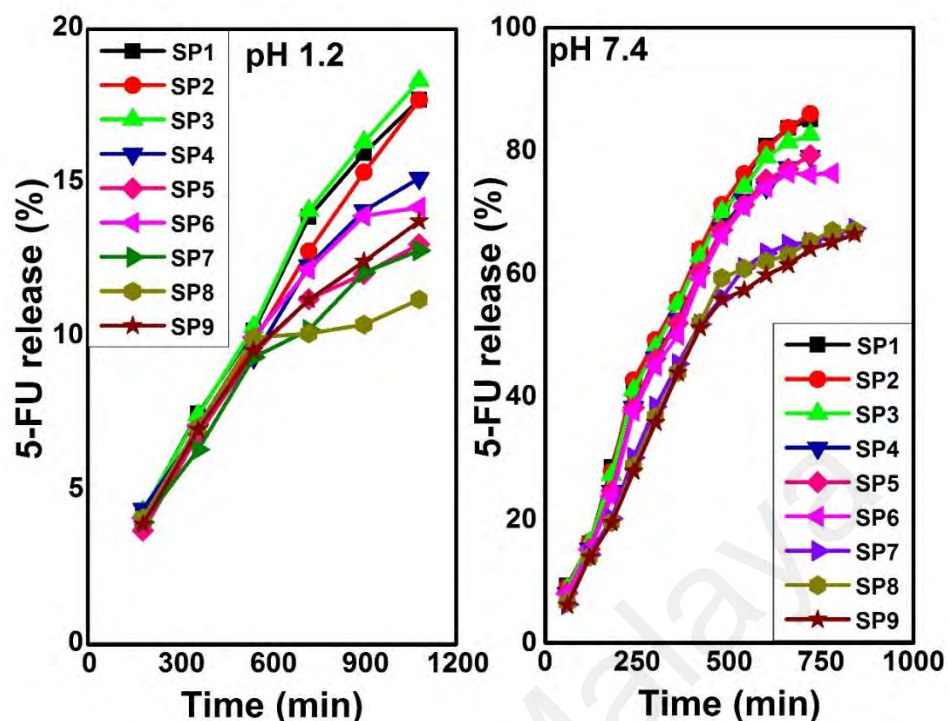


Figure 4.51: Drug release of 5-Fu from N-succinyl chitosan/ poly (acrylamide-co-acrylic acid) hydrogels at pH 7.4 and pH 1.2

4.5.2 In Vitro Drug Release from Hydrogels Formed through Free radical Mechanism

This section describes the in vitro release of theophylline from N-succinyl chitosan-g-poly (acrylamide-co-acrylic acid), N-succinyl chitosan-g-poly (acrylic acid), N-succinyl chitosan-g-poly (methacrylic acid) hydrogels and quercetin release from karaya gum-g-poly (acrylic acid) hydrogels. The residence time for drug in different part of GI system after oral administration varies. The average residence time is approximately 1 - 3 hours in stomach, 3 - 5 hours in intestine, and 30 - 50 hours in the colon. Minimum drug should be released during the first 3 hours of consumption in order to overcome the undesirable side effects and pass through the stomach safely and then maintain the sustain release in the small intestine and colon (Garcia et al., 2004). In vitro drug release from polymer hydrogel is intimately related to numerous factors such as composition, swelling behavior of hydrogel, drug affinity towards polymer gel matrix (amount of drug encapsulated), and release media. In this study, the release behavior of theophylline was observed in physiological media of pH 7.4 and pH 1.2 at 37 °C. In addition, the effect of gel

composition on the release behavior was also investigated. The release of theophylline is plotted against time. The drug was released in small amount at pH 1.2 while in large amount at pH 7.4. In all of the investigated systems, it was observed that the amount and behavior of drug release was dependent on the physiological media and composition of the hydrogels. The drug release from the all the hydrogels can be observed from Figures 4.52, 4.53, 4.54, and 4.55.

i) Effect of initiator concentration

The results show that 86.0 ± 0.09 %, 77.0 ± 0.1 % and 76.0 ± 0.2 % theophylline was released from NAA1, NSA1 and NSM1 at pH 7.4, respectively. However, 16.0 ± 0.14 %, 11.1 ± 0.06 %, and 11.1 ± 0.09 % theophylline release at pH 1.2 from NAA1, NSA1 and NSM1 at pH 1.2, respectively. The small amount of drug release at pH 1.2 was owing to the low swelling ratio and less interaction between the solvent and drug. The small amount of drug release from NAA2, NSA2, and NSM2 at pH 1.2 was owing to the low swelling ratio and large amount of drug release from NAA2, NSA2, and NSM2 at pH 7.4 was due to high swelling ratio. Furthermore, NAA2, NSA2, and NSM2 showed 93.0 ± 0.03 %, 83.0 ± 0.3 %, and 78.0 ± 0.12 % theophylline release at pH 7.4 while 21.0 ± 0.09 %, 12.3 ± 0.09 % and 12.1 ± 0.1 % drug release at pH 1.2, respectively. Higher amount of drug release from NAA2, NSA2, and NSM2 than NAA1, NSA1, and NSM1, might be due to greater amount of initiator used in this formulation that encourage formation of short chain polymer network. This short chain polymer network interacted with physiological medium in large extent. Besides, greater percentage of drug encapsulated in short chain polymer network as discussed in section 4.4.2. Hence, large amount of drug was released. It was also observed that the release rate of NAA2, NSA2, and NSM2 was higher than NAA1, NSA1, and NSM1. The initial burst release of drug occurred due to

high swelling ratio of NAA2, NSA2, and NSM2, therefore maximum drug release in short time.

ii) Effect of concentration of crosslinking agent

In case of NAA3, NSA3, and NSM3, 67.0 ± 0.09 %, 69.0 ± 0.1 %, and 63.0 ± 0.3 % and 14.0 ± 0.09 %, 9.2 ± 0.07 %, and 9.9 ± 0.07 % drug was released at pH 7.4 and pH 1.2, respectively. NAA3, NSA3, and NSM3 composed greater amount of crosslinking agent than NAA1, NSA1, and NSM1 formulations. Drug was released in small amount from NAA3, NSA3, and NSM3 due to tightly packed network, less available free volume to interact with physiological media and small amount of encapsulated drug. It was also observed that drug was released at a slower rate from NAA3, NSA3, and NSM3 as compared to NAA1, NSA1, and NSM1.

iii) Effect of monomers concentration

The effect of monomers ratio on release profile was also investigated at pH 1.2 and pH 7.4. In this study, NAA4, NSA4, and NSM4 possessed greater amount of monomers as compared to NAA1, NSA1, and NSM1. NAA4, NSA4, and NSM4 showed 88.0 ± 0.1 %, 87.3 ± 0.09 %, and 89.5 ± 0.15 % and 24.0 ± 0.1 %, 12.5 ± 0.09 %, and 13.2 ± 0.18 % drug released at pH 7.4 and pH 1.2, respectively. The higher percentage of released drug might be due to higher hydrophilicity and greater amount of monomers N-succinyl chitosan, acrylic acid, and acrylamide in NAA4, greater amount of N-succinyl chitosan and acrylic acid in NSA4 and greater amount of N-succinyl chitosan and methacrylic acid in NSM4 than in NAA1, NSA1, and NSM1. NAA4, NSA4, and NSM4 also contained greater amount of encapsulated drug than NAA1, NSA1, and NSM1. The higher encapsulation efficiency of the NAA4, NSA4, and NSM4 as compared to NAA1, NSA1, and NSM1 was due to the increased number of hydrophilic groups. The increased

hydrophilic groups was owing to presence of greater amount of monomers. However, the initial burst release of drug occurred at pH 7.4 might be due to greater interaction of hydrophilic groups of polymer network due to weak mechanical strength of the hydrogels with buffer solution. Moreover, the drug release was occurred in short time as compared to NAA1, NSA1, and NSM1.

iv) In vitro release of quercetin from karaya gum-g-poly (acrylic acid) hydrogels

In vitro release of quercetin as a hydrophobic drug was studied in buffer solutions of pH 7.4 and pH 1.2. The results of this investigation are presented in Figure 4.56. Figure 4.56 (a & b) presents the release profile of quercetin in buffer solution of pH 7.4 and pH 1.2 for 12 hours. The release results show comparatively high initial release rates due to loosely attached quercetin molecules on the surface of the hydrogels. At the initial stage, high release rates were observed due to the dissolution of quercetin molecules which were attached loosely on the surface of hydrogels, the release occurred to the surrounding medium. For a prolong period, drug release becomes much slower because the drug release is controlled by diffusion rather than erosion of the hydrogels (Amin et al., 2012). Moreover, the quercetin release was also dependent on the composition of hydrogels. KGA1 showed maximum release of $77.0 \pm 0.2 \%$, and $17.0 \pm 0.15 \%$ in buffer solutions of pH 7.4 and pH 1.2, respectively. However, KGA2 displayed total $80.0 \pm 0.3 \%$ and $18.0 \pm 0.15 \%$ drug release in buffer solutions of pH 7.4 and pH 1.2. This large release from KGA2 as compared to KGA1 is owing to greater exposed area of KGA2 hydrogel due to short chain polymer network. Furthermore, $73.0 \pm 0.1 \%$ and $15.0 \pm 0.2 \%$ drug released from KGA3 in buffer solutions of pH 7.4 and pH 1.2. This low amount of drug release was owing to the low encapsulation efficiency and tight network structure of the KGA3. Moreover, KGA4 showed highest drug release of $83.0 \pm 0.15 \%$ and $19.0 \pm 0.15 \%$ in buffer solutions of pH 7.4 and pH 1.2. This large release as compared to the other

formulation of karaya gum hydrogels is owing to the presence of greater amount of karaya gum and acrylic acid in the hydrogel, slightly loose network structure of the hydrogel (due to large amount of karaya gum and acrylic acid) and greater amount of encapsulated quercetin. All these results clearly indicated the large amount of quercetin release at pH 7.4 compared to the medium of pH 1.2. It is evident that quercetin release can be explained based on the influence of pH on the release profile from the hydrogels. The quercetin release from the hydrogels increased with the increase in pH, just because of carboxylic groups' dissociation and repulsion between carboxylate anions swelled hydrogels enough to release quercetin expeditiously (Hemmati et al., 2015).

University of Malaya

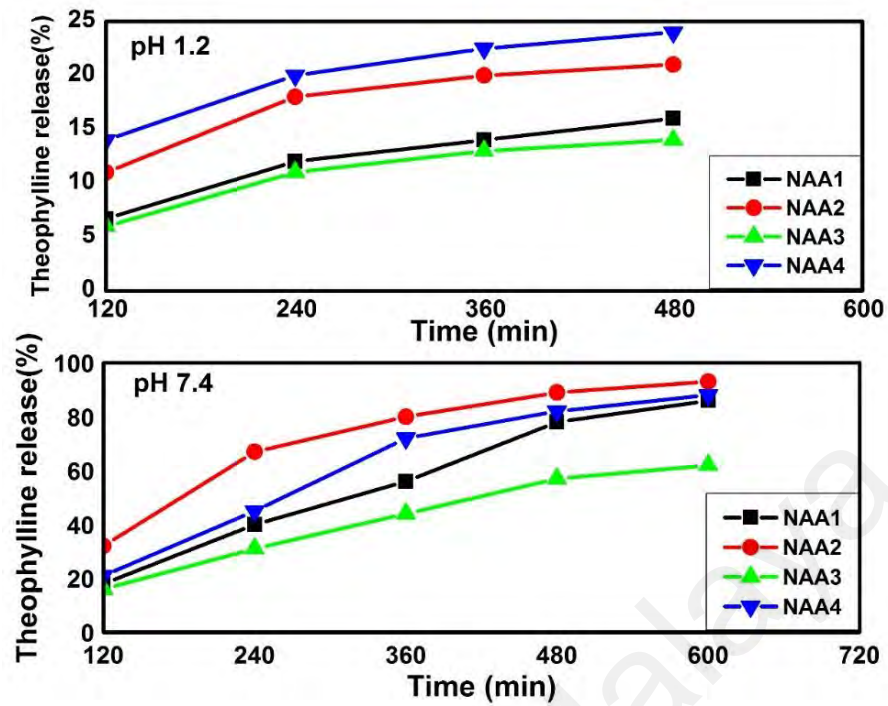


Figure 4.52: In vitro release of theophylline from N-succinyl chitosan-g-poly (acrylamide-co-acrylic acid) hydrogels at pH 7.4 and pH 1.2

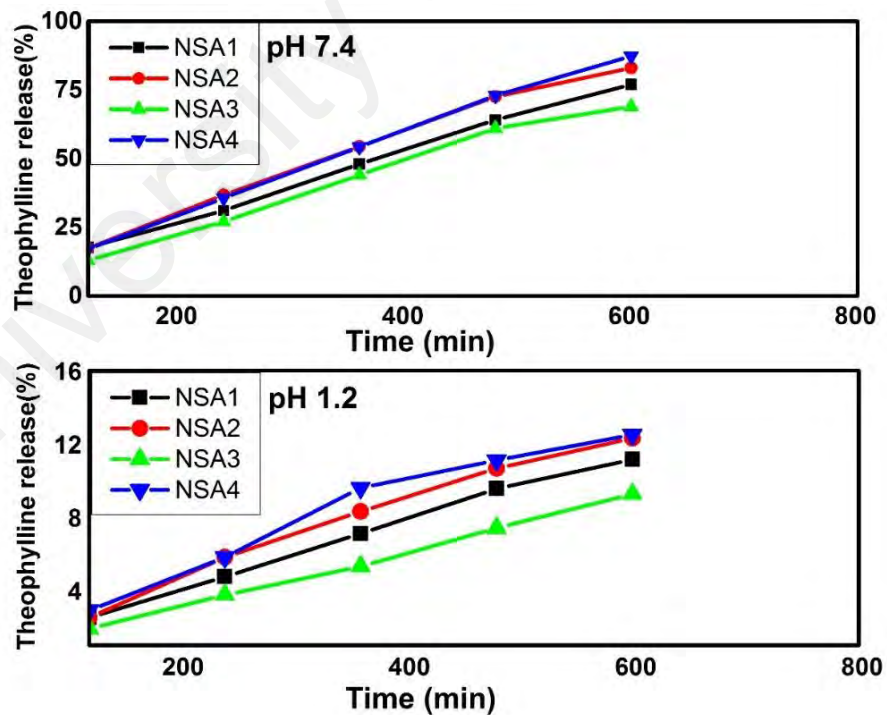


Figure 4.53: In vitro release of theophylline from N-succinyl chitosan-g-poly (acrylic acid) hydrogels at pH 7.4 and pH 1.2

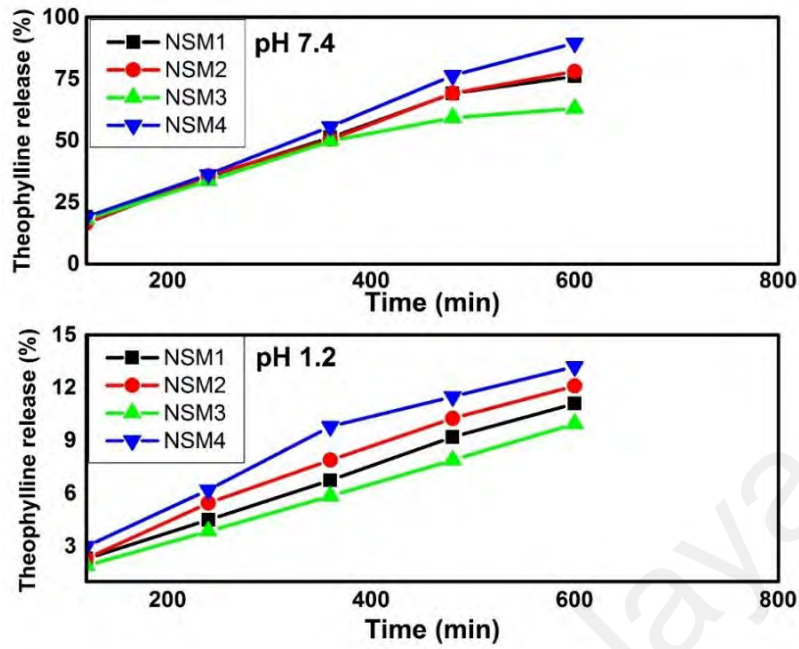


Figure 4.54: In vitro release of theophylline from N-succinyl chitosan-g-poly (methacrylic acid) hydrogels at pH 7.4 and pH 1.2

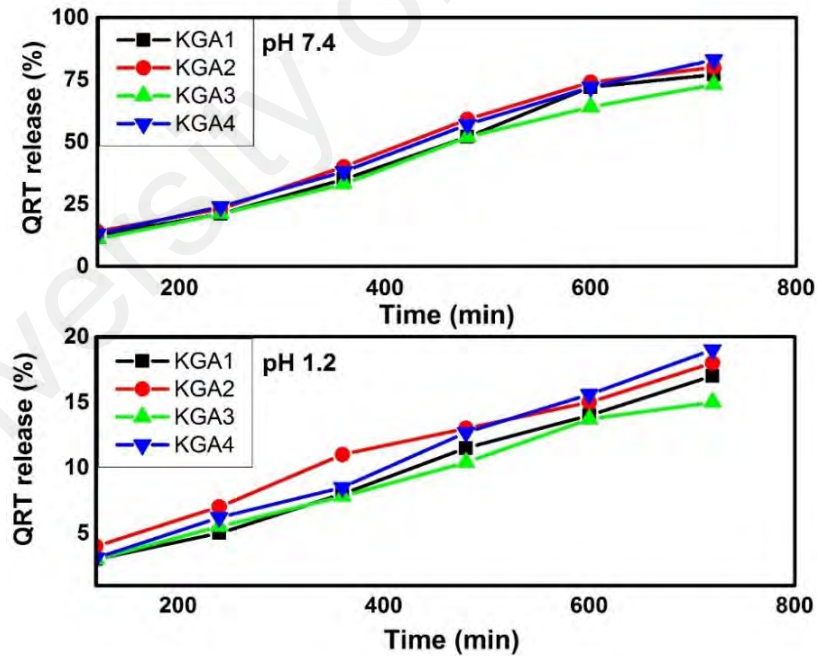


Figure 4.55: In vitro release of quercetin from karaya gum-g-poly (acrylic acid) hydrogels at pH 7.4 and pH 1.2

4.5.3 Drug Release Kinetics

4.5.3.1 Drug Release Kinetics of N-succinyl chitosan/ poly (acrylamide-co-acrylic acid) Hydrogels

Drug release data of the hydrogels were fitted into the Ritger-Peppas model shown in the equation 4.1 to evaluate drug release kinetics (Ritger & Peppas, 1987). Origin Pro software was used to determine the release kinetics.

$$F_D = \frac{M_t}{M_\infty} = kt^n \quad (4.1)$$

Where, $\frac{M_t}{M_\infty}$ is a ratio of theophylline release at time “t” to the equilibrium swollen state.

k is a constant to measure release velocity and geometrical parameters analogous to drug-polymer system. It also describes the effect of chemical functionality of carrier on drug release system, while n is a diffusional exponent and explains the drug release mechanism. The release kinetic results showed the statistical parameter such as R² was very close to unity, while F values were also very high for this release data. However, the drug release data showed close fitting to Ritger-Peppas model. The n and k values of different formulations were obtained from this model and are shown in Table 4.8. It is already described that n value suggests the drug release mechanism. If n < 0.45, drug release follows Fickian diffusion behavior, n < 0.89 elucidates anomalous transport (non-Fickian), and n ≥ 0.9 explain the drug release dependent on relaxation or swelling of system (Case-II transport) (Brannon-Peppas & Peppas, 1990). In this study, n values range from 0.49 to 0.84 when drug release occurred at pH 1.2. On the other hand, n values range from 0.90-0.95 when drug release occurred at pH 7.4. Hence, it is suggested that drug release followed non-Fickian diffusion controlled release of drug at pH 1.2 while Case-II transport of drug at pH 7.4.

The drug release followed non-Fickian transport and was dependent on the crosslinking agent concentration. The n values are slightly greater at low concentration of GA while small at high concentration of GA. The higher n values at lower GA concentration describes the loose gel network and greater swelling ratio. Unlike, high n values attribute to tight network of gel matrices at higher concentration of GA, thereby leading to least swelling of hydrogels and diffusion of drug adsorbed on the surface of the hydrogels. Similarly, k values range between 0.002-0.027 for all formulations. The smaller values of k indicate the lesser interactions between the gel matrices and drug. The statistical parameters such as R^2 and F values highly indicated close fitting of drug release data to this model and strongly sports the accuracy of results. Hence, it can be concluded that drug release rate is dependent on the swelling and relaxation of polymer system.

Table 4.7: 5-FU release kinetics at pH 7.4/ pH 1.2

Hydrogels	$k \times 10^{-3}$	n	R^2	F
SP1	6.0/3.0	0.92/0.79	0.99/0.99	2302/1230
SP2	4.0/2.0	0.93/0.84	0.99/0.99	2427/1090
SP3	5.0/3.0	0.94/0.80	0.99/0.99	2346/1706
SP4	2.0/7.0	0.95/0.69	0.99/0.99	2267/1675
SP5	2.0/9.0	0.92/0.69	0.99/0.99	2163/1534
SP6	7.0/7.0	0.92/0.70	0.98/0.99	2278/1589
SP7	3.0/11.0	0.90/0.62	0.99/0.99	2304/1633
SP8	3.0/27.0	0.90/0.49	0.98/0.98	2416/1677
SP9	27.0/14.0	0.90/0.59	0.99/0.99	2356/1548

4.5.3.2 Drug Release Kinetics of Hydrogels Formed through Free radical Mechanism

Theophylline release kinetics from N-succinyl chitosan-g-poly (acrylamide-co-acrylic acid), N-succinyl chitosan-g-poly (acrylic acid), and N-succinyl chitosan-g-poly

(methacrylic acid), while quercetin release kinetics from karaya gum-g-poly (acrylic acid) hydrogels was investigated using equation 4.1. Drug release kinetics of these hydrogels are presented in Tables 4.9, 4.10, 4.11, and 4.12. The results revealed different n value for each hydrogel system. The value of n for NAA1, NSA1, NSM1, and KGA1 is 0.98, 0.93, 0.88, and 1.04 in buffer solution of pH 7.4 and 0.63, 0.94, 0.98, and 0.99 in buffer solution of pH 1.2. The drug release followed complete non-Fickian or case-II transport mechanism at pH 7.4 and pH 1.2. However, the drug release from NAA1 in buffer solution of pH 1.2 was owing to diffusion and polymer relaxation (non-Fickian) at pH 1.2. This difference in drug release mechanism of NAA1 at pH 7.4 and pH 1.2 might be due to difference in structure of the hydrogels. NAA1 contained acrylamide having neutral carboxamide group which is pH independent. The drug release from NAA1 was comparatively faster than other hydrogels due to carboxamide group of acrylamide. However, other hydrogels possessed anionic groups, drug release significantly affected by the ionization of functional groups. The ionization contributes the electrostatic repulsion leading to chain expansion which, in turn, affects macromolecular chain relaxation. Therefore, the swelling mechanism becomes more relaxation-controlled as gel ionization becomes prominent.

In the case of NAA2, NSA2, NSM2, and KGA2 values of n are 0.66, 0.99, 0.98, and 0.94 at pH 7.4 and 0.47, 0.99, 1.0, and 0.84 at pH 1.2, respectively. Mechanism of drug release from NAA2 is according to diffusion and polymer relaxation controlled at pH 7.4 and pH 1.2, while NSA2, NSM2, and KGA2 followed only swelling controlled drug release (complete non-Fickian) in buffer solutions of pH 7.4 and pH 1.2. These hydrogels were synthesized with higher concentration of initiator as compared to NAA1, NSA1, NSM1, and KGA1. Short chain polymer gel system exists in these hydrogels. The values of n also represents penetration of solvent, n value were found slightly different due to difference in structure of the hydrogels.

Furthermore, values of n are 0.81, 1.0, 0.8, and 1.1 in buffer solution of pH 7.4 while 0.62, 0.97, 1.0, and 1.0 in buffer solution of pH 1.2 for NAA3, NSA3, NSM3, and KGA3, respectively. These hydrogels contained greater concentration of crosslinking agent which significantly restricts the molecular chain movement leads to the decreasing of solvent diffusion and the slower of chain relaxation which results in the increase in the value of n (Agnihotri & Aminabhavi, 2006; Guilherme et al., 2010). Drug release followed complete non-Fickian trend in case of these hydrogels. The drug release from these hydrogels was more swelling controlled due to presence of acrylic acid having high mechanical strength as compared to methacrylic acid and acrylamide. However, value of n decreased in the case of NAA3 and NSM3 compared to NSA3, and KGA3. The decrease in the value of n showed the swelling controlled as well as diffusion controlled. The decrease in the value of n might be owing to higher drug release which was adsorbed at the surface of NAA3 and NSM3 hydrogels.

The values of values of n are 0.92, 0.91, 0.98, and 0.90 in buffer solution of pH 7.4 while 0.45, 0.88, 0.93, and 0.92 in buffer solution of pH 1.2 for NAA4, NSA4, NSM4, and KGA4 and drug release followed complete non-Fickian at pH 7.4. Same trends were observed for NSA4, NSM4, and KGA4 at pH 1.2. However, value of n for NAA4 at pH 1.2 found to be very low which showed non-Fickian trend which is a border line of Fickian and non-Fickian trends of drug release. This non-Fickian trend might be owing to the initial fast release of drug adsorbed at the surface of the NAA4 hydrogel. The other hydrogels found to be stable and showed swelling controlled drug release even at high concentration of monomers. In addition, k values are very small at pH 1.2 and pH 7.4 which illustrate the less interaction between the drug and polymer network. Statistical parameters (R^2 (high), χ^2 (low), and F (high)) suggested the best fitting of data to Ritger-Peppas model.

Table 4.8: Theophylline release kinetics at pH 7.4 and pH 1.2 (N-succinyl chitosan-g-poly (acrylamide-co-acrylic acid) hydrogels)

Gel	n	$k \times 10^{-3}$	R^2	$\chi^2 \times 10^{-2}$	F
NAA1	0.98/0.63	1.9/22	0.98/0.99	1.3/1.1	980/760
NAA2	0.66/0.47	16/57	0.96/0.97	1.5/1.4	780/680
NAA3	0.81/0.62	5.1/23	0.99/0.98	1.1/1.9	1040/675
NAA4	0.92/0.45	3.1/91	0.98/0.96	1.1/1.8	930/715

Table 4.9: Theophylline release kinetics at pH 7.4 and pH 1.2 (N-succinyl chitosan-g-poly (acrylic acid) hydrogels)

Gel	n	$k \times 10^{-3}$	R^2	$\chi^2 \times 10^{-2}$	F
NSA1	0.93/0.94	2.5/2.4	0.97/0.97	3.1/1.7	1431/2543
NSA2	0.99//0.99	1.87/1.85	0.98/0.98	1.54/1.4	1345/2342
NSA3	1.0/0.97	1.1/1.83	0.97/0.99	4.7/0.9	1475/2746
NSA4	0.91/0.88	3.4/2.4	0.98/0.91	2.1/1.3	1278/2550

Table 4.10: Theophylline release kinetics at pH 7.4/pH 1.2 (N-succinyl chitosan-g-poly (methacrylic acid) hydrogels)

Gel	n	$k \times 10^{-3}$	R^2	$\chi^2 \times 10^{-2}$	F
NSM1	0.88/0.98	3.6/1.8	0.98/0.98	8/1	598/1011
NSM2	0.98/1.0	2/1.4	0.96/0.98	0.8/1	521/1231
NSM3	0.8/1.0	6.3/1.4	0.97/0.97	7/1	499/1432
NSM4	0.98/0.93	2.6/1.5	0.95/93	4/1	634/1088

Table 4.11: Quercetin release kinetics in pH 7.4/pH 1.2 (Karaya gum-g-poly (acrylic acid) hydrogels)

Gel	n	$k \times 10^{-3}$	R^2	$\chi^2 \times 10^{-2}$	F
KGA1	1.04/0.99	0.79/1.4	0.98/0.99	2/0.5	1025/1452
KGA2	0.94/0.84	1.1/4	0.98/0.99	1.5/1	1040/1470
KGA3	1.1/1.0	0.7/2	0.99/0.99	2.3/0.7	1034/1455
KGA4	0.90/0.92	0.9/1.2	0.99/0.99	1.6/0.9	1018/1427

4.5.4 Chemical Activity of Drugs

In drug delivery systems, the chemical and biological activity of drug after release into the body is the most critical parameter. Most often, drugs denature occur due to chemical reaction with carrier and cause some detrimental outcomes after release. In order to avoid this upshot, the carrier should not react with the drug and able to be delivered into the body without any chemical transformation.

Chemical activity of pure 5-FU and 5-FU after release from semi-IPN N-succinyl chitosan/ poly (acrylamide-co-acrylic acid) hydrogels was studied using UV-Vis spectrophotometer (UV-2600, Shimadzu, Japan). The spectra were recorded at wavelength of 266 nm. The spectra of pure 5-FU and in the release medium were recorded. The spectra are shown in the Figure 4.56.

Chemical activity of theophylline before loading and after release from N-succinyl chitosan-g-poly (acrylamide-co-acrylic acid), N-succinyl chitosan-g-poly (acrylic acid), and N-succinyl chitosan-g-poly (methacrylic acid) hydrogels was observed using UV-Vis spectrophotometer (UV-2600, Shimadzu, Japan) at wavelength of 272 nm. The spectra of pure theophylline and theophylline in the release medium were recorded. The spectra are shown in the Figures 4.57, 4.58, and 4.59.

Furthermore, chemical activity of pure quercetin and quercetin after release was observed before and after drug loading from karaya gum-g-poly (acrylic acid) hydrogel using UV-Vis spectrophotometer (UV-2600, Shimadzu, Japan) at wavelength of 256 nm. The spectra of pure quercetin and quercetin in the release medium were recorded. The spectra are shown in the Figure 4.60.

It can be observed that there is no significant difference in spectra of drugs before drug loading and after release. This shows that the drugs maintained their chemical structure after release from hydrogels.

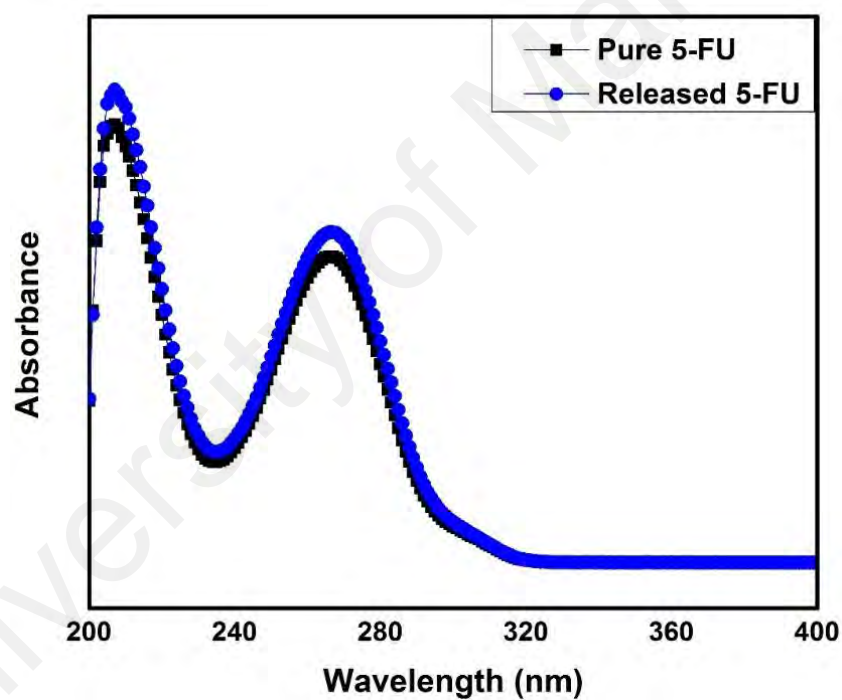


Figure 4.56: Chemical activity of pure 5-FU and 5-FU after release from N-succinyl chitosan/ poly (acrylamide-co-acrylic acid) hydrogel

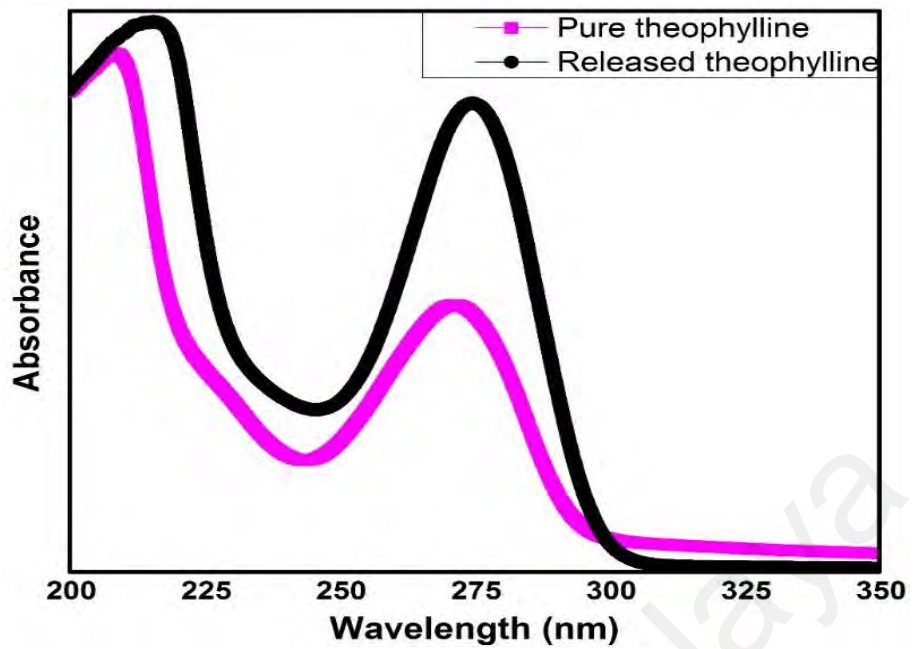


Figure 4.57: Chemical activity of pure theophylline and theophylline after release from N-succinyl chitosan-g-poly (acrylamide-co-acrylic acid) hydrogel

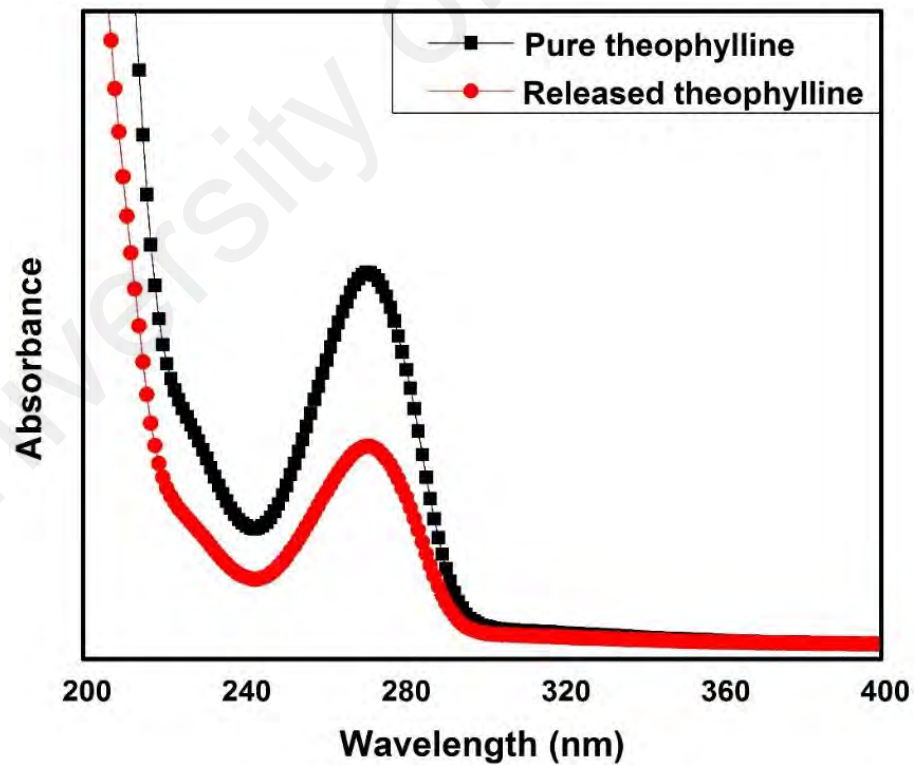


Figure 4.58: Chemical activity of pure theophylline and theophylline after release from N-succinyl chitosan-g-poly (acrylic acid) hydrogel

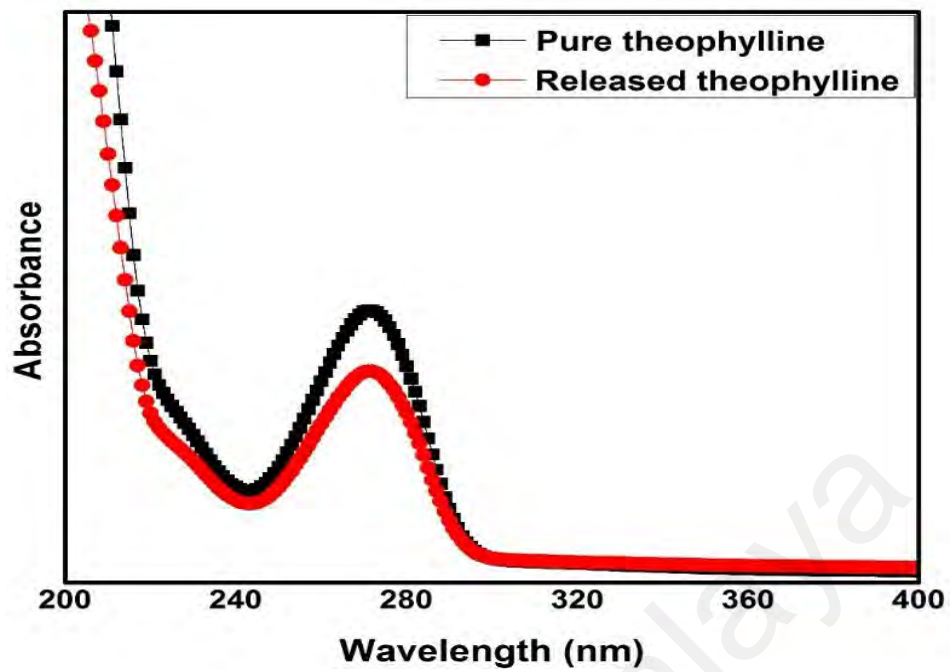


Figure 4.59: Chemical activity of pure theophylline and theophylline after release from N-succinyl chitosan-g-poly (methacrylic acid) hydrogel

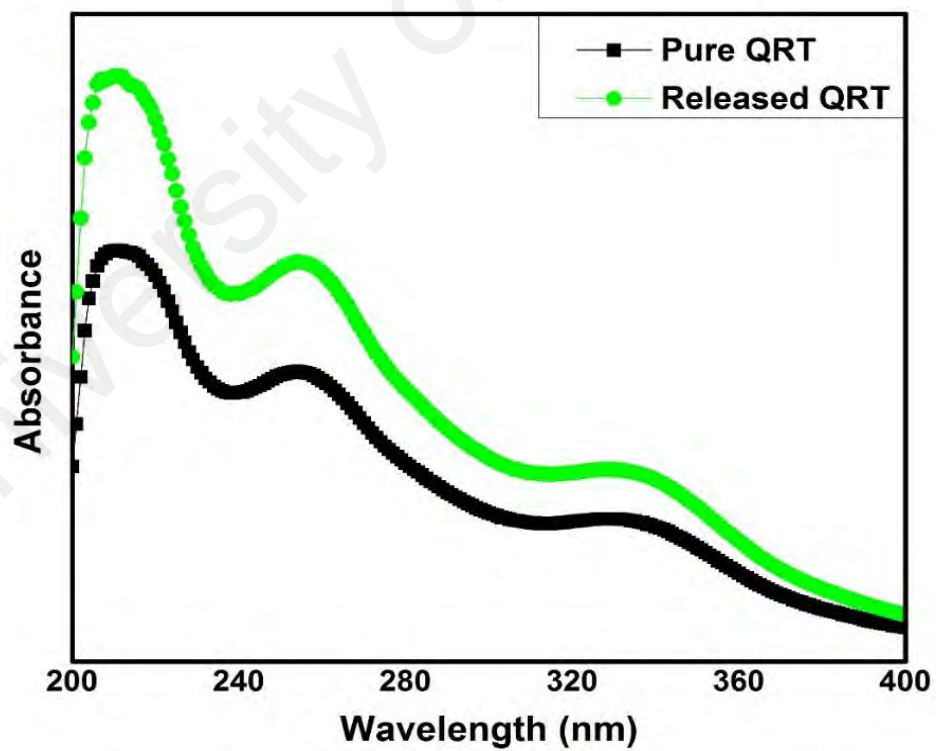


Figure 4.60: Chemical activity of pure quercetin and quercetin after release from karaya gum-g-poly (acrylic acid) hydrogel

CHAPTER 5: CONCLUSION AND FUTURE WORK

5.1 Conclusion

Polysaccharides represent a large and various class of biopolymers with a broad range of physico-chemical properties, which explain their extensive use in pharmacy and medicine for different applications, such as ophthalmology, dentistry, orthopedic surgery (implantation of medical devices and artificial organs), tissue engineering and drug delivery. Polysaccharides unmodified or after appropriate derivatizations, are able to form three dimensional hydrogels that create a suitable environment for embedding drugs. Polysaccharide hydrogels can be composed of two or more different polymers, combined in the form of IPNs or graft copolymers. Polysaccharide hydrogels are relatively deformable and can be formulated in a variety of physical forms, including macroscopic networks such as cylindrical, beads, blends, films and slabs. IPNs and graft copolymers are particularly interesting because they allow to exploit and improve the physico-chemical properties of each component. Polysaccharide hydrogels possess potential advantages in the biomedical field. However, polysaccharides have several limitations such as weak mechanical strength and uncontrolled drug release characteristics. Synthetic polymers having high mechanical strength and controlled drug release properties can compensate these drawbacks. A diverse range of polymer compositions have been used to fabricate hydrogels. The compositions can be divided into natural, synthetic or combination of two classes. Combination of natural and synthetic polymers has great significance because it improves the physical, chemical and biological properties and balances the mechanical properties which make them appropriate for complex biological system. Furthermore, biodegradable nature of polysaccharides and excellent mechanical strength of synthetic polymers can make the hydrogels highly suitable for controlled drug delivery systems.

In this work, chitosan was modified using succinic anhydride to synthesize pH-sensitive derivative which is N-succinyl chitosan. The synthesized derivative was characterized using Fourier transform Infrared (FTIR), X-ray diffraction (XRD), and differential scanning calorimetric (DSC) analysis. All these characterization techniques proof the successful synthesis of N-succinyl chitosan. This pH-sensitive derivative was used in the synthesis of hydrogels.

After successful synthesis of N-succinyl chitosan, semi-IPN of N-succinyl chitosan/ poly (acrylamide-co-acrylic acid) hydrogels were synthesized by crosslinking of N-succinyl chitosan using glutaraldehyde as a cross-linking agent in the presence of poly (acrylamide-co-acrylic acid). Poly (acrylamide-co-acrylic acid) was embedded during the formation of Schiff base between the amino groups of N-succinyl chitosan. These hydrogels were prepared by varying amounts of N-succinyl chitosan, poly (acrylamide-co-acrylic acid), and glutaraldehyde. Hydrogels were characterized by FTIR, XRD, DSC, and FESEM. FTIR, XRD, and DSC data confirmed the successful synthesis of hydrogel while FESEM showed porous morphology of hydrogels. The swelling characteristics were highly dependent on the amount of N-succinyl chitosan, poly (acrylamide-co-acrylic acid), glutaraldehyde and pH of the medium. Swelling kinetics was studied using Origin Pro Software. Maximum encapsulation efficiency of 5-FU was found to be 72.4 ± 0.06 %. In vitro release of 5-FU was observed at pH 7.4 and pH 1.2 and drug release studies showed the significant effect of pH, polymers amount and concentration of glutaraldehyde on release profile. Hydrogels showed 5-FU release in the range of 64.0 % to 85.9 % at pH 7.4 while 13.3 % to 19.6 % at pH 1.2. Among all these hydrogels, SP2 showed higher encapsulation efficiency and drug release. Drug release kinetics and statistical parameters showed non-Fickian diffusion controlled release of 5-FU and closely fitted to Ritger-Peppas model. Furthermore, 5-FU maintained its chemical activity after in vitro release.

In other work, synthetic polymerizable monomers such as acrylic acid, methacrylic acid, and acrylamide were grafted over N-succinyl chitosan through free radical polymerization. Similarly, polymerizable monomer acrylic acid was grafted over karaya gum. These synthesized hydrogels were N-succinyl chitosan-g-poly (acrylamide-co-acrylic acid), N-succinyl chitosan-g-poly (acrylic acid), N-succinyl chitosan-g-poly (methacrylic acid), and karaya gum-g-poly (acrylic acid).

Several hydrogels were synthesized by varying the concentration of monomers, initiator, and crosslinking agent. These hydrogels were characterized using FTIR, XRD, and DSC to confirm the successful synthesis of hydrogels. The porous morphology of hydrogels were observed through FESEM. Moreover, yield (%), gel contents (%) and gel time were found significantly affected by varying the concentration of monomers, initiator, and crosslinking agent.

The rheology study revealed the significant mechanical strength of the hydrogels and it was dependent on the amount of initiator, crosslinking agent, and monomers. Besides, swelling ratio results revealed strong influence of pH and gel composition on swelling behavior. Additionally, ionic strength of NaCl, CaCl₂, and AlCl₃ also affected the swelling response of hydrogels significantly. The swelling data showed close fitting to second order rate equation and swelling kinetics revealed the non-Fickian anomalous transport mechanism.

The amount of drug entrapped in hydrogels was dependent on the nature of the drug. The results revealed large amount of hydrophilic theophylline being encapsulated in the hydrogel. However, only very small amount of quercetin as hydrophobic drug encapsulated in the hydrogels.

In vitro release of hydrophilic theophylline indicated that release behavior was dependent on pH of the medium. Small amount of drug released at pH 1.2 while large theophylline release occurred at pH 7.4. The release of theophylline was also dependent on the materials involved in synthesis of hydrogels and composition of hydrogels.

In vitro release of hydrophobic quercetin from karaya gum-g-poly (acrylic acid) hydrogels was studied. The release of quercetin from karaya gum-g-poly (acrylic acid) hydrogels was dependent on the hydrogels composition. Furthermore, small amount of quercetin release at pH 1.2 and large release at pH 7.4. Slow release of quercetin was found which might be owing to controlled release characteristics of hydrogels and solubility of quercetin in the physiological medium. The release profile of quercetin from hydrogels showed fitting to Ritger-Peppas model. The kinetic parameters indicated the drug diffusion through the hydrogels were non-Fickian to non-Fickian anomalous (case-II) transport. Theophylline and quercetin retained their structural integrity after release from hydrogel which is a critical requirement for preserving drug activity.

In conclusion, among all formulated hydrogels, SP2, NAA1, NSA1, NSM1, and KGA1 formulations found to be highly pH sensitive and exhibited efficient drug carrier properties as candidates for colon specific controlled release of drug.

5.2 Future Work

In the future, N-succinyl chitosan and karaya gum formulations should be tested in the biological environment. Formulations of N-succinyl chitosan and karaya gum are still not commercialized clinically for drug delivery applications. These formulations should be commercialized after successful evaluation of in vivo analysis. Moreover, applications such as tissue engineering and wound dressing applications of N-succinyl chitosan and karaya hydrogels formed through free radical approach should be investigated. Other

hydrophilic and pH-sensitive chitosan derivatives should be synthesized to improve the drug delivery systems.

University of Malaya

REFERENCES

- Abad, L. V., Relleve, L. S., Aranilla, C. T., & Dela Rosa, A. M. (2003). Properties of radiation synthesized PVP-kappa carrageenan hydrogel blends. *Radiation Physics and Chemistry*, 68(5), 901-908.
- Abdelaal, M., Abdel-Razik, E., Abdel-Bary, E., & El-Sherbiny, I. (2007). Chitosan-based interpolymeric pH-responsive hydrogels for in vitro drug release. *Journal of Applied Polymer Science*, 103(5), 2864-2874.
- Agnihotri, S. A., & Aminabhavi, T. M. (2006). Novel interpenetrating network chitosan-poly (ethylene oxide-g-acrylamide) hydrogel microspheres for the controlled release of capecitabine. *International Journal of Pharmaceutics*, 324(2), 103-115.
- Ahmed, A. A.-K., Naik, H. B., & Sherigara, B. (2009). Synthesis and characterization of chitosan-based pH-sensitive semi-interpenetrating network microspheres for controlled release of diclofenac sodium. *Carbohydrate Research*, 344(5), 699-706.
- Ahmed, E. M. (2015). Hydrogel: Preparation, characterization, and applications: A review. *Journal of Advanced Research*, 6(2), 105-121.
- Aiedeh, K., & Taha, M. O. (2001). Synthesis of iron-crosslinked chitosan succinate and iron-crosslinked hydroxamated chitosan succinate and their in vitro evaluation as potential matrix materials for oral theophylline sustained-release beads. *European Journal of Pharmaceutical Sciences*, 13(2), 159-168.
- Aiping, Z., Tian, C., Lanhua, Y., Hao, W., & Ping, L. (2006). Synthesis and characterization of N-succinyl-chitosan and its self-assembly of nanospheres. *Carbohydrate Polymers*, 66(2), 274-279.
- Ali, S. W., & Zaidi, S. A. R. (2005). Synthesis of copolymeric acrylamide/potassium acrylate hydrogels blended with poly (vinyl alcohol): Effect of crosslinking and the amount of poly (vinyl alcohol) on swelling behavior. *Journal of Applied Polymer Science*, 98(5), 1927-1931.
- Amin, M. C. I. M., Ahmad, N., Halib, N., & Ahmad, I. (2012). Synthesis and characterization of thermo-and pH-responsive bacterial cellulose/acrylic acid hydrogels for drug delivery. *Carbohydrate Polymers*, 88(2), 465-473.
- Angadi, S. C., Manjeshwar, L. S., & Aminabhavi, T. M. (2010). Interpenetrating polymer network blend microspheres of chitosan and hydroxyethyl cellulose for controlled release of isoniazid. *International Journal of Biological Macromolecules*, 47(2), 171-179.
- Anitha, A., Rani, V. D., Krishna, R., Sreeja, V., Selvamurugan, N., Nair, S., Jayakumar, R. (2009). Synthesis, characterization, cytotoxicity and antibacterial studies of chitosan, O-carboxymethyl and N, O-carboxymethyl chitosan nanoparticles. *Carbohydrate Polymers*, 78(4), 672-677.

- Anseth, K. S., Bowman, C. N., & Brannon-Peppas, L. (1996). Mechanical properties of hydrogels and their experimental determination. *Biomaterials*, *17*(17), 1647-1657.
- Ao, H., Huang, M., Wu, J., Lin, J., Tang, Q., & Sun, H. (2009). Synthesis and properties of poly (acrylamide-co-acrylic acid)/polyacrylamide superporous IPN hydrogels. *Polymers for Advanced Technologies*, *20*(12), 1044-1049.
- Arifin, D. Y., Lee, L. Y., & Wang, C.-H. (2006). Mathematical modeling and simulation of drug release from microspheres: Implications to drug delivery systems. *Advanced Drug Delivery Reviews*, *58*(12), 1274-1325.
- Atta, A. M., & Arndt, K. F. (2004). Swelling behavior of pH-and temperature-sensitive copolymers containing 2-hydroxy-ethyl methacrylate and N-vinyl-2-pyrrolidone crosslinked with new crosslinkers. *Polymer International*, *53*(11), 1870-1881.
- Atta, S., Khaliq, S., Islam, A., Javeria, I., Jamil, T., Athar, M. M., Ghaffar, A. (2015). Injectable biopolymer based hydrogels for drug delivery applications. *International Journal of Biological Macromolecules*, *80*, 240-245.
- Aziz, M. A., Cabral, J. D., Brooks, H. J., Moratti, S. C., & Hanton, L. R. (2012). Antimicrobial properties of a chitosan dextran-based hydrogel for surgical use. *Antimicrobial Agents and Chemotherapy*, *56*(1), 280-287.
- Babu, V. R., Hosamani, K., & Aminabhavi, T. (2008). Preparation and in-vitro release of chlorothiazide novel pH-sensitive chitosan-N, N'-dimethylacrylamide semi-interpenetrating network microspheres. *Carbohydrate Polymers*, *71*(2), 208-217.
- Babu, V. R., Sairam, M., Hosamani, K. M., & Aminabhavi, T. M. (2006). Development of 5-fluorouracil loaded poly (acrylamide-co-methylmethacrylate) novel core-shell microspheres: In vitro release studies. *International Journal Pharmaceutics*, *325*(1), 55-62.
- Bao, Y., Ma, J., & Li, N. (2011). Synthesis and swelling behaviors of sodium carboxymethyl cellulose-g-poly (AA-co-AM-co-AMPS)/MMT superabsorbent hydrogel. *Carbohydrate Polymers*, *84*(1), 76-82.
- Barbucci, R., Magnani, A., & Consumi, M. (2000). Swelling behavior of carboxymethylcellulose hydrogels in relation to cross-linking, pH, and charge density. *Macromolecules*, *33*(20), 7475-7480.
- Barnes, H. A., Hutton, J. F., & Walters, K. (1989). An introduction to rheology, (Vol. 3). Elsevier, Netherlands.
- Bashir, S., Teo, Y. Y., Ramesh, S., & Ramesh, K. (2016). Synthesis, characterization, properties of N-Succinyl chitosan-g-Poly (methacrylic acid) hydrogels and In vitro release of theophylline. *Polymer*, *92*, 36-49.
- Berger, J., Reist, M., Mayer, J. M., Felt, O., & Gurny, R. (2004). Structure and interactions in chitosan hydrogels formed by complexation or aggregation for biomedical applications. *European Journal of Pharmaceutics and Biopharmaceutics*, *57*(1), 35-52.

- Berger, J., Reist, M., Mayer, J. M., Felt, O., Peppas, N., & Gurny, R. (2004). Structure and interactions in covalently and ionically crosslinked chitosan hydrogels for biomedical applications. *European Journal of Pharmaceutics and Biopharmaceutics*, 57(1), 19-34.
- Bhattacharya, A., Rawlins, J. W., & Ray, P. (2009). Polymer grafting and crosslinking. Wiley Online Library, New Jersey.
- Bhattarai, N., Gunn, J., & Zhang, M. (2010). Chitosan-based hydrogels for controlled, localized drug delivery. *Advanced Drug Delivery Reviews*, 62(1), 83-99.
- Bhattarai, N., Matsen, F. A., & Zhang, M. (2005). PEG-Grafted Chitosan as an Injectable Thermoreversible Hydrogel. *Macromolecular Bioscience*, 5(2), 107-111.
- Bilia, A., Carelli, V., Di Colo, G., & Nannipieri, E. (1996). In vitro evaluation of a pH-sensitive hydrogel for control of GI drug delivery from silicone-based matrices. *International Journal of Pharmaceutics*, 130(1), 83-92.
- Bordi, F., Paradossi, G., Rinaldi, C., & Ruzicka, B. (2002). Chemical and physical hydrogels: two casesystems studied by quasi elastic light scattering. *Physica A: Statistical Mechanics and Its Applications*, 304(1), 119-128.
- Boucard, N., Viton, C., & Domard, A. (2005). New aspects of the formation of physical hydrogels of chitosan in a hydroalcoholic medium. *Biomacromolecules*, 6(6), 3227-3237.
- Brack, H., Tirmizi, S., & Risen, W. (1997). A spectroscopic and viscometric study of the metal ion-induced gelation of the biopolymer chitosan. *Polymer*, 38(10), 2351-2362.
- Brannon-Peppas, L. (1997). Polymers in controlled drug delivery. *Medical Plastic and Biomaterials*, 4, 34-45.
- Brannon-Peppas, L., & Peppas, N. A. (1990). Dynamic and equilibrium swelling behaviour of pH-sensitive hydrogels containing 2-hydroxyethyl methacrylate. *Biomaterials*, 11(9), 635-644.
- Brazel, C. S., & Peppas, N. A. (1996). Pulsatile local delivery of thrombolytic and antithrombotic agents using poly (N-isopropylacrylamide-co-methacrylic acid) hydrogels. *Journal of Controlled Release*, 39(1), 57-64.
- Buenger, D., Topuz, F., & Groll, J. (2012). Hydrogels in sensing applications. *Progress in Polymer Science*, 37(12), 1678-1719.
- Cai, Z., & Kim, J. (2009). Cellulose–chitosan interpenetrating polymer network for electro-active paper actuator. *Journal of Applied Polymer Science*, 114(1), 288-297.
- Caló, E., & Khutoryanskiy, V. V. (2015). Biomedical applications of hydrogels: A review of patents and commercial products. *European Polymer Journal*, 65, 252-267.
- Campoccia, D., Doherty, P., Radice, M., Brun, P., Abatangelo, G., & Williams, D. F. (1998). Semisynthetic resorbable materials from hyaluronan esterification. *Biomaterials*, 19(23), 2101-2127.

- Cascone, M., Maltinti, S., Barbani, N., & Laus, M. (1999). Effect of chitosan and dextran on the properties of poly (vinyl alcohol) hydrogels. *Journal of Materials Science; Materials in Medicine*, 10(7), 431-435.
- Champagne, L. M. (2008). The synthesis of water soluble N-acyl chitosan derivatives for characterization as antibacterial agents. Xavier University of Louisiana, Louisiana. <http://etd.lsu.edu/docs/available/etd-12052007-130029/>
- Chan, P., Kurisawa, M., Chung, J. E., & Yang, Y.-Y. (2007). Synthesis and characterization of chitosan-g-poly (ethylene glycol)-folate as a non-viral carrier for tumor-targeted gene delivery. *Biomaterials*, 28(3), 540-549.
- Chang, C., Duan, B., Cai, J., & Zhang, L. (2010). Superabsorbent hydrogels based on cellulose for smart swelling and controllable delivery. *European Polymer Journal*, 46(1), 92-100.
- Chen, H., Gu, Y., Hu, Y., & Qian, Z. (2007). Characterization of pH-and temperature-sensitive hydrogel nanoparticles for controlled drug release. *PDA Journal of Pharmaceutical Science and Technology*, 61(4), 303-313.
- Chen, J., Liu, M., Jin, S., & Liu, H. (2008). Synthesis and characterization of κ -carrageenan/poly (N, N-diethylacrylamide) semi-interpenetrating polymer network hydrogels with rapid response to temperature. *Polymers for Advanced Technologies*, 19(11), 1656-1663.
- Chen, J., Liu, M., Liu, H., & Ma, L. (2009). Synthesis, swelling and drug release behavior of poly (N, N-diethylacrylamide-co-N-hydroxymethyl acrylamide) hydrogel. *Materials Science and Engineering: C*, 29(7), 2116-2123.
- Chen, S.-C., Wu, Y.-C., Mi, F.-L., Lin, Y.-H., Yu, L.-C., & Sung, H.-W. (2004). A novel pH-sensitive hydrogel composed of N, O-carboxymethyl chitosan and alginate cross-linked by genipin for protein drug delivery. *Journal of Controlled Release*, 96(2), 285-300.
- Chen, S., Liu, M., Jin, S., & Chen, Y. (2005). Synthesis and swelling properties of pH-sensitive hydrogels based on chitosan and poly (methacrylic acid) semi-interpenetrating polymer network. *Journal of Applied Polymer Science*, 98(4), 1720-1726.
- Costa-Júnior, E. S., Barbosa-Stancioli, E. F., Mansur, A. A., Vasconcelos, W. L., & Mansur, H. S. (2009). Preparation and characterization of chitosan/poly (vinyl alcohol) chemically crosslinked blends for biomedical applications. *Carbohydrate Polymers*, 76(3), 472-481.
- Costa-Júnior, E. S., Barbosa-Stancioli, E. F., Mansur, A. A. P., Vasconcelos, W. L., & Mansur, H. S. (2009). Preparation and characterization of chitosan/poly(vinyl alcohol) chemically crosslinked blends for biomedical applications. *Carbohydrate Polymers*, 76(3), 472-481.
- Crompton, K., Pranker, R., Paganin, D., Scott, T., Horne, M., Finkelstein, D., Forsythe, J. (2005). Morphology and gelation of thermosensitive chitosan hydrogels. *Biophysical Chemistry*, 117(1), 47-53.

- Cui, L., Jia, J., Guo, Y., Liu, Y., & Zhu, P. (2014). Preparation and characterization of IPN hydrogels composed of chitosan and gelatin cross-linked by genipin. *Carbohydrate Polymers*, 99, 31-38.
- Dai, Y. N., Li, P., Zhang, J. P., Wang, A. Q., & Wei, Q. (2008). A novel pH sensitive N-succinyl chitosan/alginate hydrogel bead for nifedipine delivery. *Biopharmaceutics & Drug Disposition*, 29(3), 173-184.
- Daoub, R. M., Elmubarak, A. H., Misran, M., Hassan, E. A., & Osman, M. E. (2016). Characterization and functional properties of some natural Acacia gums. *Journal of the Saudi Society of Agricultural Sciences*. DOI.org/10.1016/j.jssas.2016.05.002
- Das, N. (2013). Preparation methods and properties of hydrogel: a review. *International Journal of Pharmacy and Pharmaceutical Sciences*, 5, 112-117.
- Das, R., Panda, A., & Pal, S. (2012). Synthesis and characterization of a novel polymeric hydrogel based on hydroxypropyl methyl cellulose grafted with polyacrylamide. *Cellulose*, 19(3), 933-945.
- Oliveira, H. P., Albuquerque Jr, J. J. F., Nogueiras, C., & Rieumont, J. (2009). Physical chemistry behavior of enteric polymer in drug release systems. *International Journal of Pharmaceutics*, 366(1-2), 185-189.
- Dos Santos, K., Coelho, J., Ferreira, P., Pinto, I., Lorenzetti, S. G., Ferreira, E., Gil, M. (2006). Synthesis and characterization of membranes obtained by graft copolymerization of 2-hydroxyethyl methacrylate and acrylic acid onto chitosan. *International Journal of Pharmaceutics*, 310(1), 37-45.
- Dragan, E. S. (2014). Design and applications of interpenetrating polymer network hydrogels. A review. *Chemical Engineering Journal*, 243, 572-590.
- Dragan, E. S., Perju, M. M., & Dinu, M. V. (2012). Preparation and characterization of IPN composite hydrogels based on polyacrylamide and chitosan and their interaction with ionic dyes. *Carbohydrate Polymers*, 88(1), 270-281.
- Drury, J. L., & Mooney, D. J. (2003). Hydrogels for tissue engineering: scaffold design variables and applications. *Biomaterials*, 24(24), 4337-4351.
- Duan, H., Lü, S., Qin, H., Gao, C., Bai, X., Wei, Y., Liu, Z. (2016). Co-delivery of zinc and 5-aminosalicylic acid from alginate/N-succinyl-chitosan blend microspheres for synergistic therapy of colitis. *International Journal of Pharmaceutics*, 516(1-2), 214-224.
- El-Sherbiny, I., Lins, R., Abdel-Bary, E., & Harding, D. (2005). Preparation, characterization, swelling and in vitro drug release behaviour of poly [N-acryloylglycine-chitosan] interpolymeric pH and thermally-responsive hydrogels. *European Polymer Journal*, 41(11), 2584-2591.
- Elvira, C., Mano, J., San Roman, J., & Reis, R. (2002). Starch-based biodegradable hydrogels with potential biomedical applications as drug delivery systems. *Biomaterials*, 23(9), 1955-1966.

- Eweis, M., Elkholy, S., & Elsabee, M. (2006). Antifungal efficacy of chitosan and its thiourea derivatives upon the growth of some sugar-beet pathogens. *International Journal of Biological Macromolecules*, 38(1), 1-8.
- Fan, L., Yu, L., Xu, Y., Yi, C., Cai, J., Li, M., & Huang, J. (2010). The novel alginate/N-succinyl-chitosan antibacterial blend fibers. *Journal of Applied Polymer Science*, 116(4), 2151-2156.
- Fan, M., Hu, Q., & Shen, K. (2009). Preparation and structure of chitosan soluble in wide pH range. *Carbohydrate Polymers*, 78(1), 66-71.
- Ferreira, L., Vidal, M. M., & Gil, M. H. (2000). Evaluation of poly(2-hydroxyethyl methacrylate) gels as drug delivery systems at different pH values. *International Journal of Pharmaceutics*, 194(2), 169-180.
- Fischer, C., Speth, V., Fleig-Eberenz, S., & Neuhaus, G. (1997). Induction of zygotic polyembryos in wheat: influence of auxin polar transport. *The Plant Cell*, 9(10), 1767-1780.
- Formica, J., & Regelson, W. (1995). Review of the biology of quercetin and related bioflavonoids. *Food and Chemical Toxicology*, 33(12), 1061-1080.
- Fournier, E., Passirani, C., Vonarbourg, A., Lemaire, L., Colin, N., Sagodira, S., Benoit, J.-P. (2003). Therapeutic efficacy study of novel 5-FU-loaded PMM 2.1. 2-based microspheres on C6 glioma. *International Journal of Pharmaceutics*, 268(1), 31-35.
- Gacesa, P. (1988). Alginates. *Carbohydrate Polymers*, 8(3), 161-182.
- Gao, X., He, C., Xiao, C., Zhuang, X., & Chen, X. (2013). Biodegradable pH-responsive polyacrylic acid derivative hydrogels with tunable swelling behavior for oral delivery of insulin. *Polymer*, 54(7), 1786-1793.
- García, D., Escobar, J., Bada, N., Casquero, J., Hernández, E., & Katime, I. (2004). Synthesis and characterization of poly (methacrylic acid) hydrogels for metoclopramide delivery. *European Polymer Journal*, 40(8), 1637-1643.
- Ge, H., & Wang, S. (2014). Thermal preparation of chitosan–acrylic acid superabsorbent: Optimization, characteristic and water absorbency. *Carbohydrate Polymers*, 113, 296-303.
- Gong, C., Qian, Z., Liu, C., Huang, M., Gu, Y., Wen, Y., Li, X. (2007). A thermosensitive hydrogel based on biodegradable amphiphilic poly (ethylene glycol)–polycaprolactone–poly (ethylene glycol) block copolymers. *Smart Materials and Structures*, 16(3), 927.
- Goodwin, J. W., & Hughes, R. W. (2008). Rheology for chemists: an introduction: *Royal Society of Chemistry*. <http://dx.doi.org/10.1039/9781847558046>
- Green, R. A., Baek, S., Poole-Warren, L. A., & Martens, P. J. (2010). Conducting polymer-hydrogels for medical electrode applications. *Science and Technology of Advanced Materials*, 11(1), 014107.

- Guilherme, M. R., Fajardo, A. R., Moia, T. A., Kunita, M. H., do Carmo Gonçalves, M., Rubira, A. F., & Tambourgi, E. B. (2010). Porous nanocomposite hydrogel of vinylated montmorillonite-crosslinked maltodextrin-co-dimethylacrylamide as a highly stable polymer carrier for controlled release systems. *European Polymer Journal*, 46(7), 1465-1474.
- Guimard, N. K., Gomez, N., & Schmidt, C. E. (2007). Conducting polymers in biomedical engineering. *Progress in Polymer Science*, 32(8-9), 876-921.
- Guo, B., Yuan, J., Yao, L., & Gao, Q. (2007). Preparation and release profiles of pH/temperature-responsive carboxymethyl chitosan/P (2-(dimethylamino) ethyl methacrylate) semi-IPN amphoteric hydrogel. *Colloid and Polymer Science*, 285(6), 665-671.
- Guo, W., Lu, C. H., Orbach, R., Wang, F., Qi, X. J., Ceconello, A., Willner, I. (2015). pH-Stimulated DNA Hydrogels Exhibiting Shape-Memory Properties. *Advanced Materials*, 27(1), 73-78.
- Han, Y. A., Lee, E. M., & Ji, B. C. (2008). Mechanical properties of semi-interpenetrating polymer network hydrogels based on poly (2-hydroxyethyl methacrylate) copolymer and chitosan. *Fibers and Polymers*, 9(4), 393-399.
- Harris, I. R., Harmon, A. M., Brown, L. J., & Gosiewska, A. (2011). Tissue-engineering scaffolds containing self-assembled-peptide hydrogels: Google Patents. Publication Number US8039258 B2
- Hassan, C. M., Doyle, F. J., & Peppas, N. A. (1997). Dynamic behavior of glucose-responsive poly (methacrylic acid-g-ethylene glycol) hydrogels. *Macromolecules*, 30(20), 6166-6173.
- Hemmati, K., Masoumi, A., & Ghaemy, M. (2015). Synthesis and characterization of pH-responsive nanohydrogels as biocompatible drug carriers based on chemically modified tragacanth gum polysaccharide. *RSC Advances*, 5(104), 85310-85318.
- Hennink, W. E., & van Nostrum, C. F. (2012). Novel crosslinking methods to design hydrogels. *Advanced Drug Delivery Reviews*, 64, Supplement, 223-236.
- Hirano, S., Yamaguchi, Y., & Kamiya, M. (2002a). Novel N-saturated-fatty-acyl derivatives of chitosan soluble in water and in aqueous acid and alkaline solutions. *Carbohydrate Polymers*, 48(2), 203-207.
- Hirano, S., Yamaguchi, Y., & Kamiya, M. (2002b). Novel N-saturated-fatty-acyl derivatives of chitosan soluble in water and in aqueous acid and alkaline solutions. *Carbohydrate Polymers*, 48(2), 203-207.
- Hirotsu, S., Hirokawa, Y., & Tanaka, T. (1987). Volume-phase transitions of ionized N-isopropylacrylamide gels. *The Journal of Chemical Physics*, 87(2), 1392-1395.
- Hoffman, A., Chen, G., Wu, X., & Ding, Z. (1997). Graft copolymers of PEO-PPO-PEO triblock polyethers on bioadhesive polymer backbones: Synthesis and properties. Paper presented at the Abstracts of Papers of the American Chemical Society.

- Hoffman, A. S. (2012). Hydrogels for biomedical applications. *Advanced Drug Delivery Reviews*, 64, 18-23.
- Hossain, K. S., Miyanaga, K., Maeda, H., & Nemoto, N. (2001). Sol-gel transition behavior of pure ι-carrageenan in both salt-free and added salt states. *Biomacromolecules*, 2(2), 442-449.
- Hu, X., Feng, L., Wei, W., Xie, A., Wang, S., Zhang, J., & Dong, W. (2014). Synthesis and characterization of a novel semi-IPN hydrogel based on Salecan and poly (N, N-dimethylacrylamide-co-2-hydroxyethyl methacrylate). *Carbohydrate Polymers*, 105, 135-144.
- Huang, M., Jin, X., Li, Y., & Fang, Y. e. (2006). Syntheses and characterization of novel pH-sensitive graft copolymers of maleoylchitosan and poly (acrylic acid). *Reactive and Functional Polymers*, 66(10), 1041-1046.
- Hui, H.-W., & Robinson, J. R. (1985). Ocular delivery of progesterone using a bioadhesive polymer. *International Journal of Pharmaceutics*, 26(3), 203-213.
- Hwang, K. T., Jung, S. T., Lee, G. D., Chinnan, M. S., Park, Y. S., & Park, H. J. (2002). Controlling molecular weight and degree of deacetylation of chitosan by response surface methodology. *Journal of Agricultural and Food Chemistry*, 50(7), 1876-1882.
- Islam, A., Yasin, T., Bano, I., & Riaz, M. (2012). Controlled release of aspirin from pH-sensitive chitosan/poly (vinyl alcohol) hydrogel. *Journal of Applied Polymer Science*, 124(5), 4184-4192.
- Ito, T., Yeo, Y., Highley, C. B., Bellas, E., Benitez, C. A., & Kohane, D. S. (2007). The prevention of peritoneal adhesions by in situ cross-linking hydrogels of hyaluronic acid and cellulose derivatives. *Biomaterials*, 28(6), 975-983.
- Ito, T., Yeo, Y., Highley, C. B., Bellas, E., & Kohane, D. S. (2007). Dextran-based in situ cross-linked injectable hydrogels to prevent peritoneal adhesions. *Biomaterials*, 28(23), 3418-3426.
- Jain, N., Rajoriya, V., Jain, P. K., & Jain, A. K. (2014). Lactosaminated-N-succinyl chitosan nanoparticles for hepatocyte-targeted delivery of acyclovir. *Journal of Nanoparticle Research*, 16(1), 1-14.
- Janes, K. A., Fresneau, M. P., Marazuela, A., Fabra, A., & Alonso, M. a. J. (2001). Chitosan nanoparticles as delivery systems for doxorubicin. *Journal of Controlled Release*, 73(2), 255-267.
- Jayakumar, R., Nwe, N., Tokura, S., & Tamura, H. (2007). Sulfated chitin and chitosan as novel biomaterials. *International Journal of Biological Macromolecules*, 40(3), 175-181.
- Kajjari, P. B., Manjeshwar, L. S., & Aminabhavi, T. M. (2013). Novel blend microspheres of poly (vinyl alcohol) and succinyl chitosan for controlled release of nifedipine. *Polymer Bulletin*, 70(12), 3387-3406.

- Kang, E. Y., Moon, H. J., Joo, M. K., & Jeong, B. (2012). Thermogelling chitosan-g-(PAF-PEG) aqueous solution as an injectable scaffold. *Biomacromolecules*, *13*(6), 1750-1757.
- Karadeniz, F., Karagozlu, M. Z., Pyun, S.-Y., & Kim, S.-K. (2011). Sulfation of chitosan oligomers enhances their anti-adipogenic effect in 3T3-L1 adipocytes. *Carbohydrate Polymers*, *86*(2), 666-671.
- Karimi, M., Ghasemi, A., Sahandi Zangabad, P., Rahighi, R., Moosavi Basri, S. M., Mirshekari, H., Hamblin, M. R. (2016). Smart micro/nanoparticles in stimulus-responsive drug/gene delivery systems. *Chemical Society Reviews*, *45*(5), 1457-1501.
- Karlsson, J., & Gatenholm, P. (1997). Preparation and characterization of cellulose-supported HEMA hydrogels. *Polymer*, *38*(18), 4727-4731.
- Kato, Y., Onishi, H., & Machida, Y. (2000). Evaluation of N-succinyl-chitosan as a systemic long-circulating polymer. *Biomaterials*, *21*(15), 1579-1585.
- Katono, H., Maruyama, A., Sanui, K., Ogata, N., Okano, T., & Sakurai, Y. (1991). Thermo-responsive swelling and drug release switching of interpenetrating polymer networks composed of poly (acrylamide-co-butyl methacrylate) and poly (acrylic acid). *Journal of Controlled Release*, *16*(1-2), 215-227.
- Kim, I.-S., & Oh, I.-J. (2005). Drug release from the enzyme-degradable and pH-sensitive hydrogel composed of glycidyl methacrylate dextran and poly (acrylic acid). *Archives of Pharmacal Research*, *28*(8), 983-987.
- Kim, M. S., Choi, Y. J., Noh, I., & Tae, G. (2007). Synthesis and characterization of in situ chitosan-based hydrogel via grafting of carboxyethyl acrylate. *Journal of Biomedical Materials Research Part A*, *83*(3), 674-682.
- Kim, S. J., Lee, K. J., Kim, I. Y., & Kim, S. I. (2003). Swelling Kinetics of Interpenetrating Polymer Hydrogels Composed of Poly(Vinyl Alcohol)/Chitosan. *Journal of Macromolecular Science, Part A*, *40*(5), 501-510.
- Kim, S. J., Park, S. J., Kim, I. Y., Shin, M.-S., & Kim, S. I. (2002). Electric stimuli responses to poly(vinyl alcohol)/chitosan interpenetrating polymer network hydrogel in NaCl solutions. *Journal of Applied Polymer Science*, *86*(9), 2285-2289.
- Kim, S. J., Park, S. J., & Kim, S. I. (2003). Swelling behavior of interpenetrating polymer network hydrogels composed of poly (vinyl alcohol) and chitosan. *Reactive and Functional Polymers*, *55*(1), 53-59.
- Kim, S. J., Shin, S. R., Lee, S. M., Kim, I. Y., & Kim, S. I. (2004). Electromechanical properties of hydrogels based on chitosan and poly (hydroxyethyl methacrylate) in NaCl solution. *Smart Materials and Structures*, *13*(5), 1036.
- Kim, S. J., Shin, S. R., Spinks, G. M., Kim, I. Y., & Kim, S. I. (2005). Synthesis and characteristics of a semi-interpenetrating polymer network based on chitosan/polyaniline under different pH conditions. *Journal of Applied Polymer Science*, *96*(3), 867-873.

- Kim, S. J., Yoon, S. G., Kim, I. Y., & Kim, S. I. (2004). Swelling characterization of the semiinterpenetrating polymer network hydrogels composed of chitosan and poly (diallyldimethylammonium chloride). *Journal of Applied Polymer Science*, 91(5), 2876-2880.
- Kim, S. J., Yoon, S. G., Lee, Y. H., & Kim, S. I. (2004). Bending behavior of hydrogels composed of poly (methacrylic acid) and alginate by electrical stimulus. *Polymer International*, 53(10), 1456-1460.
- Kim, S. W. (1996). Temperature Sensitive Polymers for Delivery of Macromolecular Drugs. In N. Ogata, S. W. Kim, J. Feijen, & T. Okano (Eds.), *Advanced Biomaterials in Biomedical Engineering and Drug Delivery Systems* (126-133). Tokyo: Springer Japan.
- Kirschner, C. M., & Anseth, K. S. (2013). Hydrogels in healthcare: From static to dynamic material microenvironments. *Acta Materialia*, 61(3), 931-944.
- Kittur, F., Prashanth, K. H., Sankar, K. U., & Tharanathan, R. (2002). Characterization of chitin, chitosan and their carboxymethyl derivatives by differential scanning calorimetry. *Carbohydrate Polymers*, 49(2), 185-193.
- Kou, J. H., Amidon, G. L., & Lee, P. I. (1988). pH-Dependent Swelling and Solute Diffusion Characteristics of Poly (Hydroxyethyl Methacrylate–CO–Methacrylic Acid) Hydrogels. *Pharmaceutical Research*, 5(9), 592-597.
- Kulkarni, R. V., Boppana, R., Mohan, G. K., Mutalik, S., & Kalyane, N. V. (2012). pH-responsive interpenetrating network hydrogel beads of poly (acrylamide)-g-carrageenan and sodium alginate for intestinal targeted drug delivery: Synthesis, in vitro and in vivo evaluation. *Journal of Colloid Interface Science*, 367(1), 509-517.
- Kumari, A., Yadav, S. K., Pakade, Y. B., Singh, B., & Yadav, S. C. (2010). Development of biodegradable nanoparticles for delivery of quercetin. *Colloids and Surfaces B: Biointerfaces*, 80(2), 184-192.
- Kurita, K. (1986). Chemical modifications of chitin and chitosan Chitin in nature and technology (287-293). Tokyo: Springer Japan.
- Kwei, T., & Zupko, H. (1969). Diffusion in glassy polymers. I. *Journal of Polymer Science Part A-2: Polymer Physics*, 7(5), 867-877.
- Lee, A. L. S., Ordeñez, G., & Chakraborty, S. (2011). Novel glycerol cross-linked poly (acrylic acid) hydrogel for encapsulation and release of benzocaine. *Philippino Science Letters*, 4(2), 81-87.
- Lee, D.-H., Sim, G.-S., Kim, J.-H., Lee, G.-S., Pyo, H.-B., & Lee, B.-C. (2007). Preparation and characterization of quercetin-loaded polymethyl methacrylate microcapsules using a polyol-in-oil-in-polyol emulsion solvent evaporation method. *Journal of Pharmacy and Pharmacology*, 59(12), 1611-1620.
- Lee, K. Y., Alsberg, E., & Mooney, D. J. (2001). Degradable and injectable poly (aldehyde guluronate) hydrogels for bone tissue engineering. *Journal of Biomedical Materials Research*, 56(2), 228-233.

- Lee, P. I., & Peppas, N. A. (1987). Prediction of polymer dissolution in swellable controlled-release systems. *Journal of Controlled Release*, 6(1), 207-215.
- Lee, S. B., Park, E. K., Lim, Y. M., Cho, S. K., Kim, S. Y., Lee, Y. M., & Nho, Y. C. (2006). Preparation of alginate/poly (N-isopropylacrylamide) semi-interpenetrating and fully interpenetrating polymer network hydrogels with γ -ray irradiation and their swelling behaviors. *Journal of Applied Polymer Science*, 100(6), 4439-4446.
- Lee, W. F., & Chen, Y. J. (2001). Studies on preparation and swelling properties of the N-isopropylacrylamide/chitosan semi-IPN and IPN hydrogels. *Journal of Applied Polymer Science*, 82(10), 2487-2496.
- Lejardi, A., Hernández, R., Criado, M., Santos, J. I., Etxeberria, A., Sarasua, J., & Mijangos, C. (2014). Novel hydrogels of chitosan and poly (vinyl alcohol)-glycolic acid copolymer with enhanced rheological properties. *Carbohydrate Polymers*, 103, 267-273.
- Li, A., Wang, A., & Chen, J. (2004). Studies on poly(acrylic acid)/attapulgit superabsorbent composite. I. Synthesis and characterization. *Journal of Applied Polymer Science*, 92(3), 1596-1603.
- Li, J., Cai, J., Zhong, L., & Du, Y. (2012). Immobilization of a protease on modified chitosan beads for the depolymerization of chitosan. *Carbohydrate Polymers*, 87(4), 2697-2705.
- Li, P., Zhang, J., & Wang, A. (2007). A Novel N-Succinylchitosan-graft-Polyacrylamide/Attapulgit Composite Hydrogel Prepared through Inverse Suspension Polymerization. *Macromolecular Materials and Engineering*, 292(8), 962-969.
- Li, X., Xu, S., Wang, J., Chen, X., & Feng, S. (2009). Structure and characterization of amphoteric semi-IPN hydrogel based on cationic starch. *Carbohydrate Polymers*, 75(4), 688-693.
- Li, Y., & Kwak, J. C. (2004). Rheology of hydrophobically modified polyacrylamide-copoly (acrylic acid) on addition of surfactant and variation of solution pH. *Langmuir*, 20(12), 4859-4866.
- Lin, F.-H., Lee, Y.-H., Jian, C.-H., Wong, J.-M., Shieh, M.-J., & Wang, C.-Y. (2002). A study of purified montmorillonite intercalated with 5-fluorouracil as drug carrier. *Biomaterials*, 23(9), 1981-1987.
- Liu, J., Lin, S., Li, L., & Liu, E. (2005). Release of theophylline from polymer blend hydrogels. *International Journal of Pharmaceutics*, 298(1), 117-125.
- Liu, X., Peng, W., Wang, Y., Zhu, M., Sun, T., Peng, Q., Weng, J. (2013). Synthesis of an RGD-grafted oxidized sodium alginate-N-succinyl chitosan hydrogel and an in vitro study of endothelial and osteogenic differentiation. *Journal of Materials Chemistry B*, 1(35), 4484-4492.

- Lu, B., Sun, Y.-X., Li, Y.-Q., Zhang, X.-Z., & Zhuo, R.-X. (2009). N-Succinyl-chitosan grafted with low molecular weight polyethylenimine as a serum-resistant gene vector. *Molecular Biosystems*, 5(6), 629-637.
- Lu, B., Wu, D.-Q., Zheng, H., Quan, C.-Y., Zhang, X.-Z., & Zhuo, R.-X. (2010). Galactosyl conjugated N-succinyl-chitosan-graft-polyethylenimine for targeting gene transfer. *Molecular Biosystems*, 6(12), 2529-2538.
- Lü, S., Liu, M., & Ni, B. (2010). An injectable oxidized carboxymethylcellulose/N-succinyl-chitosan hydrogel system for protein delivery. *Chemical Engineering Journal*, 160(2), 779-787.
- Madgulkar, A., Kadam, S., & Pokharkar, V. (2009). Development of buccal adhesive tablet with prolonged antifungal activity: Optimization and ex vivo deposition studies. *Indian Journal of Pharmaceutical Sciences*, 71(3), 290.
- Magami, S. M., Oldring, P. K. T., Castle, L., & Guthrie, J. T. (2015). The physical-chemical behaviour of amino cross-linkers and the effect of their chemistry on selected epoxy can coatings' hydrolysis to melamine and to formaldehyde into aqueous food simulants. *Progress in Organic Coatings*, 78, 325-333.
- Mahdavinia, G., Pourjavadi, A., Hosseinzadeh, H., & Zohuriaan, M. (2004). Modified chitosan 4. Superabsorbent hydrogels from poly (acrylic acid-co-acrylamide) grafted chitosan with salt-and pH-responsiveness properties. *European Polymer Journal*, 40(7), 1399-1407.
- Majzoob, S., Atyabi, F., Dorkoosh, F., Kafedjiiski, K., Loretz, B., & Bernkop-Schnürch, A. (2006). Pectin-cysteine conjugate: synthesis and in-vitro evaluation of its potential for drug delivery. *Journal of Pharmacy and Pharmacology*, 58(12), 1601-1610.
- Mall, I., Srivastava, V., Kumar, G., & Mishra, I. (2006a). Characterization and utilization of mesoporous fertilizer plant waste carbon for adsorptive removal of dyes from aqueous solution. *Colloids and Surfaces A: Physicochemical and Engineering Aspects*, 278(1), 175-187.
- Mall, I., Srivastava, V., Kumar, G., & Mishra, I. (2006b). Characterization and utilization of mesoporous fertilizer plant waste carbon for adsorptive removal of dyes from aqueous solution. *Colloids and Surfaces A*, 278(1), 175-187.
- Mandal, B., & Ray, S. K. (2013). Synthesis of interpenetrating network hydrogel from poly (acrylic acid-co-hydroxyethyl methacrylate) and sodium alginate: modeling and kinetics study for removal of synthetic dyes from water. *Carbohydrate Polymers*, 98(1), 257-269.
- Marques, M. M., Fernandes, S., Correia, S. G., Ascenso, J. R., Caroço, S., Gomes, P. T., Dias, A. R. (2000). Synthesis of acrylamide/olefin copolymers by a diimine nickel catalyst. *Macromolecular Chemistry and Physics*, 201(17), 2464-2468.
- Martinez-Ruvalcaba, A., Sanchez-Diaz, J., Becerra, F., Cruz-Barba, L., & Gonzalez-Alvarez, A. (2009). Swelling characterization and drug delivery kinetics of polyacrylamide-co-itaconic acid/chitosan hydrogels. *Express Polymer Letters*, 3(1), 25-32.

- Mashkevich, B. O. (2007). Drug Delivery Research Advances: Nova Science Publishers United States of America.
- Matevosyan, G., Yukha, Y. S., & Zavlin, P. (2003). Phosphorylation of chitosan. *Russian Journal of General Chemistry*, 73(11), 1725-1728.
- Matricardi, P., Di Meo, C., Coviello, T., Hennink, W. E., & Alhaique, F. (2013). Interpenetrating polymer networks polysaccharide hydrogels for drug delivery and tissue engineering. *Advanced Drug Delivery Reviews*, 65(9), 1172-1187.
- Matzelle, T., Geuskens, G., & Kruse, N. (2003). Elastic properties of poly (N-isopropylacrylamide) and poly (acrylamide) hydrogels studied by scanning force microscopy. *Macromolecules*, 36(8), 2926-2931.
- McBath, R. A., & Shipp, D. A. (2010). Swelling and degradation of hydrogels synthesized with degradable poly([small beta]-amino ester) crosslinkers. *Polymer Chemistry*, 1(6), 860-865.
- Menon, P., Yin, T. Y., & Misran, M. (2015). Preparation and characterization of liposomes coated with DEAE-Dextran. *Colloids and Surfaces A: Physicochemical and Engineering Aspects*, 481, 345-350.
- Mi, F.-L., Wu, Y.-B., Shyu, S.-S., Schoung, J.-Y., Huang, Y.-B., Tsai, Y.-H., & Hao, J.-Y. (2002). Control of wound infections using a bilayer chitosan wound dressing with sustainable antibiotic delivery. *Journal of Biomedical Materials Research*, 59(3), 438-449.
- Milosavljević, N. B., Milašinović, N. Z., Popović, I. G., Filipović, J. M., & Kalagasidis Krušić, M. T. (2011). Preparation and characterization of pH-sensitive hydrogels based on chitosan, itaconic acid and methacrylic acid. *Polymer International*, 60(3), 443-452.
- Mima, S., Miya, M., Iwamoto, R., & Yoshikawa, S. (1983). Highly deacetylated chitosan and its properties. *Journal of Applied Polymer Science*, 28(6), 1909-1917.
- Mirzaei B, E., Ramazani SA, A., Shafiee, M., & Danaei, M. (2013). Studies on glutaraldehyde crosslinked chitosan hydrogel properties for drug delivery systems. *International Journal of Polymeric Materials and Polymeric Biomaterials*, 62(11), 605-611.
- Mishra, R., Ramasamy, K., Ahmad, N., Eshak, Z., & Majeed, A. (2014). pH dependent poly [2-(methacryloyloxyethyl) trimethylammonium chloride-co-methacrylic acid] hydrogels for enhanced targeted delivery of 5-fluorouracil in colon cancer cells. *Journal of Materials Science: Materials in Medicine*, 25(4), 999-1012.
- Mishra, R. K., Datt, M., & Banthia, A. K. (2008). Synthesis and characterization of pectin/PVP hydrogel membranes for drug delivery system. *Aaps PharmSciTech*, 9(2), 395-403.
- Mittal, H., Maity, A., & Ray, S. S. (2015). Synthesis of co-polymer-grafted gum karaya and silica hybrid organic-inorganic hydrogel nanocomposite for the highly effective removal of methylene blue. *Chemical Engineering Journal*, 279, 166-179.

- Miyata, T., Uragami, T., & Nakamae, K. (2002). Biomolecule-sensitive hydrogels. *Advanced Drug Delivery Reviews*, 54(1), 79-98.
- Moura, M. J., Figueiredo, M. M., & Gil, M. H. (2007). Rheological study of genipin cross-linked chitosan hydrogels. *Biomacromolecules*, 8(12), 3823-3829.
- Mourya, V., Inamdar, N. N., & Tiwari, A. (2010). Carboxymethyl chitosan and its applications. *Advanced Materials Letters*, 1(1), 11-33.
- Mukhopadhyay, P., Sarkar, K., Bhattacharya, S., Bhattacharyya, A., Mishra, R., & Kundu, P. (2014). pH sensitive N-succinyl chitosan grafted polyacrylamide hydrogel for oral insulin delivery. *Carbohydrate Polymers*, 112, 627-637.
- Mukhopadhyay, P., Sarkar, K., Soam, S., & Kundu, P. (2013). Formulation of pH-responsive carboxymethyl chitosan and alginate beads for the oral delivery of insulin. *Journal of Applied Polymer Science*, 129(2), 835-845.
- Mundargi, R., Patil, S., Kulkarni, P., Mallikarjuna, N., & Aminabhavi, T. (2008). Sequential interpenetrating polymer network hydrogel microspheres of poly (methacrylic acid) and poly (vinyl alcohol) for oral controlled drug delivery to intestine. *Journal of Microencapsulation*, 25(4), 228-240.
- Mura, C., Manconi, M., Valenti, D., Manca, M. L., Díez-Sales, O., Loy, G., & Fadda, A. M. (2011). In vitro study of N-succinyl chitosan for targeted delivery of 5-aminosalicylic acid to colon. *Carbohydrate Polymers*, 85(3), 578-583.
- Mura, C., Nácher, A., Merino, V., Merino-Sanjuan, M., Carda, C., Ruiz, A., Díez-Sales, O. (2011). N-Succinyl-chitosan systems for 5-aminosalicylic acid colon delivery: in vivo study with TNBS-induced colitis model in rats. *International Journal of Pharmaceutics*, 416(1), 145-154.
- Mura, C., Nácher, A., Merino, V., Merino-Sanjuan, M., Manconi, M., Loy, G., Díez-Sales, O. (2012). Design, characterization and in vitro evaluation of 5-aminosalicylic acid loaded N-succinyl-chitosan microparticles for colon specific delivery. *Colloids and Surfaces B: Biointerfaces*, 94, 199-205.
- Mura, C., Nácher, A., Merino, V., Merino-Sanjuán, M., Manconi, M., Loy, G., Díez-Sales, O. (2012). Design, characterization and in vitro evaluation of 5-aminosalicylic acid loaded N-succinyl-chitosan microparticles for colon specific delivery. *Colloids and Surfaces B: Biointerfaces*, 94, 199-205.
- Muzzarelli, R. A. (2009). Genipin-crosslinked chitosan hydrogels as biomedical and pharmaceutical aids. *Carbohydrate Polymers*, 77(1), 1-9.
- Narasimhan, B. (2001). Mathematical models describing polymer dissolution: consequences for drug delivery. *Advanced Drug Delivery Reviews*, 48(2), 195-210.
- Nesrinne, S., & Djamel, A. (2013). Synthesis, characterization and rheological behavior of pH sensitive poly (acrylamide-co-acrylic acid) hydrogels. *Arabian Journal of Chemistry*. DOI.org/10.1016/j.arabjc.2013.11.027

- Nguyen, Q. V., Huynh, D. P., Park, J. H., & Lee, D. S. (2015). Injectable polymeric hydrogels for the delivery of therapeutic agents: A review. *European Polymer Journal*, 72, 602-619.
- Nho, Y.-C., Park, J.-S., & Lim, Y.-M. (2014). Preparation of poly (acrylic acid) hydrogel by radiation crosslinking and its application for mucoadhesives. *Polymers*, 6(3), 890-898.
- Omidian, H., & Park, K. (2008). Swelling agents and devices in oral drug delivery. *Journal of Drug Delivery Science and Technology*, 18(2), 83-93.
- Onishi, H., & Machida, Y. (1999). Biodegradation and distribution of water-soluble chitosan in mice. *Biomaterials*, 20(2), 175-182.
- Onishi, H., Takahashi, H., Yoshiyasu, M., & Machida, Y. (2001). Preparation and in vitro properties of N-succinylchitosan-or carboxymethylchitin-mitomycin C conjugate microparticles with specified size. *Drug Development and Industrial Pharmacy*, 27(7), 659-667.
- Ono, K., Saito, Y., Yura, H., Ishikawa, K., Kurita, A., Akaike, T., & Ishihara, M. (2000). Photocrosslinkable chitosan as a biological adhesive. *Journal of Biomedical Materials Research*, 49(2), 289-295.
- Orakdogan, N., & Okay, O. (2007). Influence of the initiator system on the spatial inhomogeneity in acrylamide-based hydrogels. *Journal of Applied Polymer Science*, 103(5), 3228-3237.
- Oyen, M. (2014). Mechanical characterisation of hydrogel materials. *International Materials Reviews*, 59(1), 44-59.
- P Pawar, R., U Tekale, S., U Shisodia, S., T Totre, J., & J Domb, A. (2014). Biomedical applications of poly (lactic acid). *Recent Patents on Regenerative Medicine*, 4(1), 40-51.
- Panayiotou, M., & Freitag, R. (2005). Synthesis and characterisation of stimuli-responsive poly (N, N'-diethylacrylamide) hydrogels. *Polymer*, 46(3), 615-621.
- Park, S. E., Nho, Y. C., Lim, Y. M., & Kim, H. I. (2004). Preparation of pH-sensitive poly (vinyl alcohol-g-methacrylic acid) and poly (vinyl alcohol-g-acrylic acid) hydrogels by gamma ray irradiation and their insulin release behavior. *Journal of Applied Polymer Science*, 91(1), 636-643.
- Patel, V. R., & Amiji, M. M. (1996). Preparation and characterization of freeze-dried chitosan-poly (ethylene oxide) hydrogels for site-specific antibiotic delivery in the stomach. *Pharmaceutical Research*, 13(4), 588-593.
- Patil, N. S., Dordick, J. S., & Rethwisch, D. G. (1996). Macroporous poly (sucrose acrylate) hydrogel for controlled release of macromolecules. *Biomaterials*, 17(24), 2343-2350.
- Pauliukaite, R., Ghica, M. E., Fatibello-Filho, O., & Brett, C. M. A. (2010). Electrochemical impedance studies of chitosan-modified electrodes for

application in electrochemical sensors and biosensors. *Electrochimica Acta*, 55(21), 6239-6247.

- Peppas, N., Bures, P., Leobandung, W., & Ichikawa, H. (2000). Hydrogels in pharmaceutical formulations. *European Journal of Pharmaceutics and Biopharmaceutics*, 50(1), 27-46.
- Peppas, N. A., Bures, P., Leobandung, W., & Ichikawa, H. (2000). Hydrogels in pharmaceutical formulations. *European Journal of Pharmaceutics and Biopharmaceutics*, 50(1), 27-46.
- Petelin, M., Šentjurc, M., Stolič, Z., & Skalerič, U. (1998). EPR study of mucoadhesive ointments for delivery of liposomes into the oral mucosa. *International Journal of Pharmaceutics*, 173(1-2), 193-202.
- Phillips, G., Takigami, S., & Takigami, M. (1996). Hydration characteristics of the gum exudate from *Acacia senegal*. *Food Hydrocolloids*, 10(1), 11-19.
- Pillai, C., Paul, W., & Sharma, C. P. (2009). Chitin and chitosan polymers: Chemistry, solubility and fiber formation. *Progress in Polymer Science*, 34(7), 641-678.
- Pillai, O., & Panchagnula, R. (2001). *Polymers in drug delivery*. *Current Opinion in Chemical Biology*, 5(4), 447-451.
- Piyakulawat, P., Praphairaksit, N., Chantarasiri, N., & Muangsin, N. (2007). Preparation and evaluation of chitosan/carrageenan beads for controlled release of sodium diclofenac. *Aaps PharmSciTech*, 8(4), 120-130.
- Polnok, A., Verhoef, J., Borchard, G., Sarisuta, N., & Junginger, H. E. (2004). In vitro evaluation of intestinal absorption of desmopressin using drug-delivery systems based on superporous hydrogels. *International Journal of Pharmaceutics*, 269(2), 303-310.
- Pourjavadi, A., Barzegar, S., & Zeidabadi, F. (2007). Synthesis and properties of biodegradable hydrogels of κ -carrageenan grafted acrylic acid-co-2-acrylamido-2-methylpropanesulfonic acid as candidates for drug delivery systems. *Reactive and Functional Polymers*, 67(7), 644-654.
- Pourjavadi, A., Harzandi, A., & Hosseinzadeh, H. (2004). Modified carrageenan 3. Synthesis of a novel polysaccharide-based superabsorbent hydrogel via graft copolymerization of acrylic acid onto kappa-carrageenan in air. *European Polymer Journal*, 40(7), 1363-1370.
- Pourjavadi, A., & Mahdavinia, G. R. (2006). Superabsorbency, pH-sensitivity and swelling kinetics of partially hydrolyzed chitosan-g-poly (acrylamide) hydrogels. *Turkish Journal of Chemistry*, 30(5), 595-608.
- Povea, M. B., Monal, W. A., Cauich-Rodríguez, J. V., Pat, A. M., Rivero, N. B., & Covas, C. P. (2011). Interpenetrated chitosan-poly (acrylic acid-co-acrylamide) hydrogels. Synthesis, characterization and sustained protein release studies. *Materials Sciences and Applications*, 2(06), 509.

- Prabaharan, M. (2011). Prospective of guar gum and its derivatives as controlled drug delivery systems. *International Journal of Biological Macromolecules*, 49(2), 117-124.
- Pulat, M., & Asil, D. (2009). Fluconazole release through semi-interpenetrating polymer network hydrogels based on chitosan, acrylic acid, and citraconic acid. *Journal of Applied Polymer Science*, 113(4), 2613-2619.
- Rafique, A., Mahmood Zia, K., Zuber, M., Tabasum, S., & Rehman, S. (2016). Chitosan functionalized poly(vinyl alcohol) for prospects biomedical and industrial applications: A review. *International Journal of Biological Macromolecules*, 87, 141-154.
- Rama, A. R., Hernandez, R., Perazzoli, G., Burgos, M., Melguizo, C., Vélez, C., & Prados, J. (2015). Specific colon cancer cell cytotoxicity induced by bacteriophage E gene expression under transcriptional control of carcinoembryonic antigen promoter. *International Journal of Molecular Sciences*, 16(6), 12601-12615.
- Ramazani-Harandi, M., Zohuriaan-Mehr, M., Yousefi, A., Ershad-Langroudi, A., & Kabiri, K. (2009). Effects of structural variables on AUL and rheological behavior of SAP gels. *Journal of Applied Polymer Science*, 113(6), 3676-3686.
- Rana, V., Rai, P., Tiwary, A. K., Singh, R. S., Kennedy, J. F., & Knill, C. J. (2011). Modified gums: Approaches and applications in drug delivery. *Carbohydrate Polymers*, 83(3), 1031-1047.
- Rao, K. K., Naidu, B. V. K., Subha, M., Sairam, M., & Aminabhavi, T. (2006). Novel chitosan-based pH-sensitive interpenetrating network microgels for the controlled release of cefadroxil. *Carbohydrate Polymers*, 66(3), 333-344.
- Rasool, N., Yasin, T., Heng, J. Y., & Akhter, Z. (2010). Synthesis and characterization of novel pH-, ionic strength and temperature-sensitive hydrogel for insulin delivery. *Polymer*, 51(8), 1687-1693.
- Ravichandran, P., Shantha, K., & Rao, K. P. (1997). Preparation, swelling characteristics and evaluation of hydrogels for stomach specific drug delivery. *International Journal of Pharmaceutics*, 154(1), 89-94.
- Reddy, N., Tan, Y., Li, Y., & Yang, Y. (2008). Effect of glutaraldehyde crosslinking conditions on the strength and water stability of wheat gluten fibers. *Macromolecular Materials and Engineering*, 293(7), 614-620.
- Reis, A. V., Guilherme, M. R., Moia, T. A., Mattoso, L. H., Muniz, E. C., & Tambourgi, E. B. (2008). Synthesis and characterization of a starch-modified hydrogel as potential carrier for drug delivery system. *Journal of Polymer Science Part A: Polymer Chemistry*, 46(7), 2567-2574.
- Rekha, M., & Sharma, C. P. (2008). pH sensitive succinyl chitosan microparticles: a preliminary investigation towards oral insulin delivery. *Trends in Biomaterials & Artificial Organs*, 21(2), 107-115.

- Remuñán-López, C., Lorenzo-Lamosa, M. L., Vila-Jato, J. L., & Alonso, M. J. (1998). Development of new chitosan–cellulose multicore microparticles for controlled drug delivery. *European Journal of Pharmaceutics and Biopharmaceutics*, *45*(1), 49-56.
- Richardson, S., & Gorton, L. (2003). Characterisation of the substituent distribution in starch and cellulose derivatives. *Analytica Chimica Acta*, *497*(1), 27-65.
- Ritger, P. L., & Peppas, N. A. (1987). A simple equation for description of solute release II. Fickian and anomalous release from swellable devices. *Journal of Controlled Release*, *5*(1), 37-42.
- Ritschel, W. A. (1989). Biopharmaceutic and pharmacokinetic aspects in the design of controlled release peroral drug delivery systems. *Drug Development and Industrial Pharmacy*, *15*(6-7), 1073-1103.
- Rodrigues, I. R., de Camargo Forte, M. M., Azambuja, D. S., & Castagno, K. R. L. (2007). Synthesis and characterization of hybrid polymeric networks (HPN) based on polyvinyl alcohol/chitosan. *Reactive and Functional Polymers*, *67*(8), 708-715.
- Rogalsky, A. D., Kwon, H., & Lee-Sullivan, P. (2011). Compressive stress–strain response of covalently crosslinked oxidized-alginate/N-succinyl-chitosan hydrogels. *Journal of Biomedical Materials Research Part A*, *99*(3), 367-375.
- Rokhade, A. P., Patil, S. A., & Aminabhavi, T. M. (2007). Synthesis and characterization of semi-interpenetrating polymer network microspheres of acrylamide grafted dextran and chitosan for controlled release of acyclovir. *Carbohydrate Polymers*, *67*(4), 605-613.
- Rokhade, A. P., Shelke, N. B., Patil, S. A., & Aminabhavi, T. M. (2007). Novel interpenetrating polymer network microspheres of chitosan and methylcellulose for controlled release of theophylline. *Carbohydrate Polymers*, *69*(4), 678-687.
- Saboktakin, M. R., Tabatabaie, R. M., Maharramov, A., & Ramazanov, M. A. (2011). Development and in vitro evaluation of thiolated chitosan—poly (methacrylic acid) nanoparticles as a local mucoadhesive delivery system. *International Journal of Biological Macromolecules*, *48*(3), 403-407.
- Sagara, A., Igarashi, K., Otsuka, M., Karasawa, T., Gotoh, N., Narita, M., Kato, Y. (2016). Intrinsic Resistance to 5-Fluorouracil in a Brain Metastatic Variant of Human Breast Cancer Cell Line, MDA-MB-231BR. *Plos One*, *11*(10), e0164250.
- Sakurai, K., Maegawa, T., & Takahashi, T. (2000). Glass transition temperature of chitosan and miscibility of chitosan/poly (N-vinyl pyrrolidone) blends. *Polymer*, *41*(19), 7051-7056.
- Samanta, H. S., & Ray, S. K. (2014a). Controlled release of tinidazole and theophylline from chitosan based composite hydrogels. *Carbohydrate Polymers*, *106*, 109-120.
- Samanta, H. S., & Ray, S. K. (2014b). Synthesis, characterization, swelling and drug release behavior of semi-interpenetrating network hydrogels of sodium alginate and polyacrylamide. *Carbohydrate Polymers*, *99*, 666-678.

- Samuels, R. J. (1981). Solid state characterization of the structure of chitosan films. *Journal of Polymer Science: Polymer Physics Edition*, 19(7), 1081-1105.
- Saraydın, D., Karadag, E., Işıkver, Y., Şahiner, N., & Güven, O. (2004). The influence of preparation methods on the swelling and network properties of acrylamide hydrogels with crosslinkers. *Journal of Macromolecular Science, Part A*, 41(4), 419-431.
- Sastre, R. L., Olmo, R., Teijón, C., Muñiz, E., Teijón, J. M., & Blanco, M. D. (2007). 5-Fluorouracil plasma levels and biodegradation of subcutaneously injected drug-loaded microspheres prepared by spray-drying poly (D, L-lactide) and poly (D, L-lactide-co-glycolide) polymers. *International Journal of Pharmaceutics*, 338(1), 180-190.
- Schmolka, I. R. (1972). Artificial skin I. Preparation and properties of pluronic F-127 gels for treatment of burns. *Journal of Biomedical Materials Research*, 6(6), 571-582.
- Schwoerer, A. D., Harling, S., Scheibe, K., Menzel, H., & Daniels, R. (2009). Influence of degree of substitution of HES–HEMA on the release of incorporated drug models from corresponding hydrogels. *European Journal of Pharmaceutics and Biopharmaceutics*, 73(3), 351-356.
- Shantha, K., & Harding, D. (2000). Preparation and in-vitro evaluation of poly [N-vinyl-2-pyrrolidone-polyethylene glycol diacrylate]-chitosan interpolymeric pH-responsive hydrogels for oral drug delivery. *International Journal of Pharmaceutics*, 207(1), 65-70.
- Sharma, C. P. (2006). Interpolymer complex microparticles based on polymethacrylic acid-chitosan for oral insulin delivery. *Journal of Applied Polymer Science*, 99(2), 506-512.
- Shim, J. W., & Nho, Y. C. (2003). γ -Irradiation preparation of poly (acrylic acid)–chitosan hydrogels for in vitro drug release. *Journal of Applied Polymer Science*, 90(12), 3270-3277.
- Siegel, R. A., Falamarzian, M., Firestone, B. A., & Moxley, B. C. (1988). pH-controlled release from hydrophobic/polyelectrolyte copolymer hydrogels. *Journal of Controlled Release*, 8(2), 179-182.
- Siepmann, J., Kranz, H., Bodmeier, R., & Peppas, N. (1999). HPMC-matrices for controlled drug delivery: a new model combining diffusion, swelling, and dissolution mechanisms and predicting the release kinetics. *Pharmaceutical Research*, 16(11), 1748-1756.
- Siepmann, J., & Peppas, N. (2000). Hydrophilic matrices for controlled drug delivery: an improved mathematical model to predict the resulting drug release kinetics (the “sequential layer” model). *Pharmaceutical Research*, 17(10), 1290-1298.
- Siepmann, J., Siegel, R. A., & Rathbone, M. J. (2011). Fundamentals and applications of controlled release drug delivery. Springer, United States. DOI:10.1007/978-1-4614-0881-9.

- Singh, A., Narvi, S., Dutta, P., & Pandey, N. (2006). External stimuli response on a novel chitosan hydrogel crosslinked with formaldehyde. *Bulletin of Materials Science*, 29(3), 233-238.
- Singh, B., & Pal, L. (2008). Development of sterculia gum based wound dressings for use in drug delivery. *European Polymer Journal*, 44(10), 3222-3230.
- Singh, B., & Sharma, N. (2008a). Development of novel hydrogels by functionalization of sterculia gum for use in anti-ulcer drug delivery. *Carbohydrate Polymers*, 74(3), 489-497.
- Singh, B., & Sharma, N. (2008b). Modification of sterculia gum with methacrylic acid to prepare a novel drug delivery system. *International Journal of Biological Macromolecules*, 43(2), 142-150.
- Singh, B., Sharma, V., & Pal, L. (2011). Formation of sterculia polysaccharide networks by gamma rays induced graft copolymerization for biomedical applications. *Carbohydrate Polymers*, 86(3), 1371-1380.
- Singh, B., & Vashishtha, M. (2008). Development of novel hydrogels by modification of sterculia gum through radiation cross-linking polymerization for use in drug delivery. *Nuclear Instruments and Methods in Physics Research Section B: Beam Interactions with Materials and Atoms*, 266(9), 2009-2020.
- Slamon, D. J., Leyland-Jones, B., Shak, S., Fuchs, H., Paton, V., Bajamonde, A., Pegram, M. (2001). Use of chemotherapy plus a monoclonal antibody against HER2 for metastatic breast cancer that overexpresses HER2. *New England Journal of Medicine*, 344(11), 783-792.
- Sohail, K., Khan, I. U., Shahzad, Y., Hussain, T., & Ranjha, N. M. (2014). pH-sensitive polyvinylpyrrolidone-acrylic acid hydrogels: Impact of material parameters on swelling and drug release. *Brazilian Journal of Pharmaceutical Sciences*, 50, 173-184.
- Sokker, H., Ghaffar, A. A., Gad, Y., & Aly, A. (2009). Synthesis and characterization of hydrogels based on grafted chitosan for the controlled drug release. *Carbohydrate Polymers*, 75(2), 222-229.
- Song, X., Li, J., Wang, J., & Chen, L. (2009). Quercetin molecularly imprinted polymers: Preparation, recognition characteristics and properties as sorbent for solid-phase extraction. *Talanta*, 80(2), 694-702.
- Soppimath, K. S., Kulkarni, A. R., & Aminabhavi, T. M. (2000). Controlled release of antihypertensive drug from the interpenetrating network poly (vinyl alcohol)–guar gum hydrogel microspheres. *Journal of Biomaterials Science, Polymer Edition*, 11(1), 27-43.
- Soppirnath, K. S., & Aminabhavi, T. M. (2002). Water transport and drug release study from cross-linked polyacrylamide grafted guar gum hydrogel microspheres for the controlled release application. *European Journal of Pharmaceutics and Biopharmaceutics*, 53(1), 87-98.

- Straccia, M. C., Romano, I., Oliva, A., Santagata, G., & Laurienzo, P. (2014). Crosslinker effects on functional properties of alginate/N-succinylchitosan based hydrogels. *Carbohydrate Polymers*, *108*, 321-330.
- Sun, J., Jiang, G., Wang, Y., & Ding, F. (2012). Thermosensitive chitosan hydrogel for implantable drug delivery: Blending PVA to mitigate body response and promote bioavailability. *Journal of Applied Polymer Science*, *125*(3), 2092-2101.
- Sun, J., Xiao, C., Tan, H., & Hu, X. (2013). Covalently crosslinked hyaluronic acid-chitosan hydrogel containing dexamethasone as an injectable scaffold for soft tissue engineering. *Journal of Applied Polymer Science*, *129*(2), 682-688.
- Sutar, P. B., Mishra, R. K., Pal, K., & Banthia, A. K. (2008). Development of pH sensitive polyacrylamide grafted pectin hydrogel for controlled drug delivery system. *Journal of Materials Science: Materials in Medicine*, *19*(6), 2247-2253.
- Takamura, A., Ishii, F., & Hidaka, H. (1992). Drug release from poly (vinyl alcohol) gel prepared by freeze-thaw procedure. *Journal of Controlled Release*, *20*(1), 21-27.
- Tan, H., Chu, C. R., Payne, K. A., & Marra, K. G. (2009a). Injectable in situ forming biodegradable chitosan-hyaluronic acid based hydrogels for cartilage tissue engineering. *Biomaterials*, *30*(13), 2499-2506.
- Tan, H., Chu, C. R., Payne, K. A., & Marra, K. G. (2009b). Injectable in situ forming biodegradable chitosan-hyaluronic acid based hydrogels for cartilage tissue engineering. *Biomaterials*, *30*(13), 2499-2506.
- Tan, H., Luan, H., Hu, Y., & Hu, X. (2013). Covalently crosslinked chitosan-poly (ethylene glycol) hybrid hydrogels to deliver insulin for adipose-derived stem cells encapsulation. *Macromolecular Research*, *21*(4), 392-399.
- Tan, H., & Marra, K. G. (2010). Injectable, biodegradable hydrogels for tissue engineering applications. *Materials*, *3*(3), 1746-1767.
- Tan, Q., Liu, W., Guo, C., & Zhai, G. (2011). Preparation and evaluation of quercetin-loaded lecithin-chitosan nanoparticles for topical delivery. *International Journal of Nanomedicine*, *6*, 1621-1630.
- Tang, F., Lv, L., Lu, F., Rong, B., Li, Z., Lu, B., Wu, D. (2016). Preparation and characterization of N-chitosan as a wound healing accelerator. *International Journal of Biological Macromolecules*, *93*, 1295-1303.
- Thanou, M., Verhoef, J., Marbach, P., & Junginger, H. (2000). Intestinal absorption of octreotide: N-trimethyl chitosan chloride (TMC) ameliorates the permeability and absorption properties of the somatostatin analogue in vitro and in vivo. *Journal of Pharmaceutical Sciences*, *89*(7), 951-957.
- Turan, E., & Caykara, T. (2007). Swelling and network parameters of pH-sensitive poly (acrylamide-co-acrylic acid) hydrogels. *Journal of Applied Polymer Science*, *106*(3), 2000-2007.

- Vaghani, S. S., Patel, M. M., & Satish, C. (2012). Synthesis and characterization of pH-sensitive hydrogel composed of carboxymethyl chitosan for colon targeted delivery of ornidazole. *Carbohydrate Research*, 347(1), 76-82.
- Vamshi Vishnu, Y., Chandrasekhar, K., Ramesh, G., & Madhusudan Rao, Y. (2007). Development of Mucoadhesive Patches for Buccal Administration of Carvedilol. *Current Drug Delivery*, 4(1), 27-39.
- van Dijk-Wolthuis, W., Hoogeboom, J., Van Steenberg, M., Tsang, S., & Hennink, W. (1997). Degradation and release behavior of dextran-based hydrogels. *Macromolecules*, 30(16), 4639-4645.
- Varghese, J. S., Chellappa, N., & Fathima, N. N. (2014). Gelatin–carrageenan hydrogels: role of pore size distribution on drug delivery process. *Colloids and Surfaces B: Biointerfaces*, 113, 346-351.
- Verdonck, E., Schaap, K., & Thomas, L. C. (1999). A discussion of the principles and applications of modulated temperature DSC (MTDSC). *International Journal of Pharmaceutics*, 192(1), 3-20.
- Verheul, R. J., Amidi, M., van Steenberg, M. J., van Riet, E., Jiskoot, W., & Hennink, W. E. (2009). Influence of the degree of acetylation on the enzymatic degradation and in vitro biological properties of trimethylated chitosans. *Biomaterials*, 30(18), 3129-3135.
- Wang, K., Xu, X., Wang, Y., Yan, X., Guo, G., Huang, M., Qian, Z. (2010). Synthesis and characterization of poly (methoxyl ethylene glycol-caprolactone-co-methacrylic acid-co-poly (ethylene glycol) methyl ether methacrylate) pH-sensitive hydrogel for delivery of dexamethasone. *International Journal of Pharmaceutics*, 389(1), 130-138.
- Wang, M., Fang, Y., & Hu, D. (2001). Preparation and properties of chitosan-poly (N-isopropylacrylamide) full-IPN hydrogels. *Reactive and Functional Polymers*, 48(1), 215-221.
- Wang, Y., Peng, W., Liu, X., Zhu, M., Sun, T., Peng, Q., Weng, J. (2014). Study of bilineage differentiation of human-bone-marrow-derived mesenchymal stem cells in oxidized sodium alginate/N-succinyl chitosan hydrogels and synergistic effects of RGD modification and low-intensity pulsed ultrasound. *Acta Biomaterialia*, 10(6), 2518-2528.
- Weng, L., Chen, X., & Chen, W. (2007). Rheological characterization of in situ crosslinkable hydrogels formulated from oxidized dextran and N-carboxyethyl chitosan. *Biomacromolecules*, 8(4), 1109-1115.
- Wongpanit, P., Sanchavanakit, N., Pavasant, P., Supaphol, P., Tokura, S., & Rujiravanit, R. (2005). Preparation and Characterization of Microwave-treated Carboxymethyl Chitin and Carboxymethyl Chitosan Films for Potential Use in Wound Care Application. *Macromolecular Bioscience*, 5(10), 1001-1012.
- Wu, C.-J., Gaharwar, A. K., Schexnailder, P. J., & Schmidt, G. (2010). Development of Biomedical Polymer-Silicate Nanocomposites: A Materials Science Perspective. *Materials*, 3(5), 2986.

- Wu, J., Lin, J., Li, G., & Wei, C. (2001). Influence of the COOH and COONa groups and crosslink density of poly (acrylic acid)/montmorillonite superabsorbent composite on water absorbency. *Polymer International*, 50(9), 1050-1053.
- Wu, Y., Seo, T., Sasaki, T., Irie, S., & Sakurai, K. (2006). Layered structures of hydrophobically modified chitosan derivatives. *Carbohydrate Polymers*, 63(4), 493-499.
- Xia, Y.-q., Guo, T.-y., Song, M.-d., Zhang, B.-h., & Zhang, B.-l. (2005). Hemoglobin recognition by imprinting in semi-interpenetrating polymer network hydrogel based on polyacrylamide and chitosan. *Biomacromolecules*, 6(5), 2601-2606.
- Yan, C., Chen, D., Gu, J., Hu, H., Zhao, X., & Qiao, M. (2006). Preparation of N-succinyl-chitosan and their physical-chemical properties as a novel excipient. *Yakugaku Zasshi*, 126(9), 789-793.
- Yang, J., Chen, J., Pan, D., Wan, Y., & Wang, Z. (2013). pH-sensitive interpenetrating network hydrogels based on chitosan derivatives and alginate for oral drug delivery. *Carbohydrate Polymers*, 92(1), 719-725.
- Yang, Z., Han, B., Fu, D., & Liu, W. (2012). Acute toxicity of high dosage carboxymethyl chitosan and its effect on the blood parameters in rats. *Journal of Materials Science: Materials in Medicine*, 23(2), 457-462.
- Yasin, T., Rasool, N., & Akhter, Z. (2008). Synthesis of carboxymethyl-chitosan/acrylic acid hydrogel using silane crosslinker. *e-Polymers*, 8(1), 1636-1646.
- Yin, L., Fei, L., Cui, F., Tang, C., & Yin, C. (2007). Superporous hydrogels containing poly (acrylic acid-co-acrylamide)/O-carboxymethyl chitosan interpenetrating polymer networks. *Biomaterials*, 28(6), 1258-1266.
- Yin, L., Fei, L., Tang, C., & Yin, C. (2007). Synthesis, characterization, mechanical properties and biocompatibility of interpenetrating polymer network–superporous hydrogel containing sodium alginate. *Polymer International*, 56(12), 1563-1571.
- Yin, L., Zhao, Z., Hu, Y., Ding, J., Cui, F., Tang, C., & Yin, C. (2008). Polymer–protein interaction, water retention, and biocompatibility of a stimuli-sensitive superporous hydrogel containing interpenetrating polymer networks. *Journal of Applied Polymer Science*, 108(2), 1238-1248.
- Yokoyama, F., Masada, I., Shimamura, K., Ikawa, T., & Monobe, K. (1986). Morphology and structure of highly elastic poly (vinyl alcohol) hydrogel prepared by repeated freezing-and-melting. *Colloid and Polymer Science*, 264(7), 595-601.
- Yoo, H. S. (2007). Photo-cross-linkable and thermo-responsive hydrogels containing chitosan and Pluronic for sustained release of human growth hormone (hGH). *Journal of Biomaterials Science, Polymer Edition*, 18(11), 1429-1441.
- Zadražil, A., & Štěpánek, F. (2010). Investigation of thermo-responsive optical properties of a composite hydrogel. *Colloids and Surfaces A: Physicochemical and Engineering Aspects*, 372(1), 115-119.

- Zeitoun, A. A. (2003). A comparative single-dose bioequivalence study of 'two enteric coated aspirin brands among healthy volunteers. Lebanese American University, Byblos, Lebanon.
- Zhang, C., Ping, Q., Zhang, H., & Shen, J. (2003). Synthesis and characterization of water-soluble O-succinyl-chitosan. *European Polymer Journal*, 39(8), 1629-1634.
- Zhang, J.-T., Petersen, S., Thunga, M., Leipold, E., Weidisch, R., Liu, X., Jandt, K. D. (2010). Micro-structured smart hydrogels with enhanced protein loading and release efficiency. *Acta Biomaterialia*, 6(4), 1297-1306.
- Zhang, X.-Z., Zhuo, R.-X., Cui, J.-Z., & Zhang, J.-T. (2002). A novel thermo-responsive drug delivery system with positive controlled release. *International Journal of Pharmaceutics*, 235(1), 43-50.
- Zhong, Z., Xing, R., Liu, S., Wang, L., Cai, S., & Li, P. (2008). Synthesis of acyl thiourea derivatives of chitosan and their antimicrobial activities in vitro. *Carbohydrate Research*, 343(3), 566-570.
- Zhou, Y., Yang, D., Ma, G., Tan, H., Jin, Y., & Nie, J. (2008). A pH-sensitive water-soluble N-carboxyethyl chitosan/poly (hydroxyethyl methacrylate) hydrogel as a potential drug sustained release matrix prepared by photopolymerization technique. *Polymers for Advanced Technologies*, 19(8), 1133-1141.

LIST OF PUBLICATIONS AND PAPERS PRESENTED

Journal Publication for Thesis

Bashir, S., Teo, Y. Y., Ramesh, S., & Ramesh, K. (2017). Physico-chemical characterization of pH-sensitive N-Succinyl chitosan-g-poly (acrylamide-co-acrylic acid) hydrogels and in vitro drug release studies. *Polymer Degradation and Stability*, 139, 38-54.

Bashir, S., Teo, Y. Y., Ramesh, S., & Ramesh, K. (2016). Synthesis, characterization, properties of N-Succinyl chitosan-g-Poly (methacrylic acid) hydrogels and In vitro release of theophylline. *Polymer*, 92, 36-49.

Bashir, S., Teo, Y. Y., Ramesh, S., Ramesh, K., & Khan, A. A. (2015). N-succinyl chitosan preparation, characterization, properties and biomedical applications: a state of the art review. *Reviews in Chemical Engineering* 31(6), 563-597.

Bashir, S., Teo, Y. Y., Naeem, S., Ramesh, S., & Ramesh, K. (2017). pH responsive N-succinyl chitosan/Poly (acrylamide-co-acrylic acid) hydrogels and in vitro release of 5-fluorouracil. *Plos One*, 12(7), e0179250.

Work presented in Conference

Bashir, S., Teo, Y. Y., Naeem, S., Ramesh, S., Ramesh, K. & Rizwan, M. (2016) Synthesis, characterization and properties of N-Succinyl chitosan hydrogel, presented in *2ND INTERNATIONAL CONGRESS ON TECHNOLOGY-ENGINEERING & SCIENCE (ICONTES)*, Kuala Lumpur, Malaysia.